# Assessing the role of JNK in Human Endothelial Cell Death Induced by Anti-Cancer Therapies.


**By**

**Ashley McCulloch**


A thesis submitted in the fulfilment of the requirements for the degree of Doctor of Philosophy

October 2024


Strathclyde Institute of Pharmacy and Biomedical Sciences (SIPBS)

Glasgow, UK

This thesis is the result of the author's original research. It has been composed by the author and had not been previously submitted for examination which has led to the award of a degree.



Signed:

Date:

# Abstract

Cardiovascular disease is a common side effect of cancer treatment, particularly in those who have been disease-free for over 10 years. Several studies have shown that radiation and chemotherapeutics, such as Doxorubicin and Cisplatin, can induce cardiovascular disease. Currently, little is understood about the mechanisms behind this phenomenon. The JNK pathway, a key intracellular signalling pathway, has been shown to be activated by both treatment options. Therefore, this could provide a novel target for treatment and prevention.

Human Umbilical Vein Endothelial Cells (HUVECs) were exposed to Sunitinib, Doxorubicin, Cisplatin and irradiation kinetic parameters and concentration response curves were established. The effect of these treatments on JNK activation was observed using western blots and cell viability assays. Doxorubicin and Cisplatin were shown to activate JNK, whilst radiation and Sunitinib were found to have no effect on the pathway. Phosphorylation of JNK by Doxorubicin and Cisplatin were found to be delayed and sustained, an observation linked to cell death. FACS analysis then indicated substantial cell damage with an increase in apoptosis and necrosis. Further investigation of the pathway utilised inhibitors, a pharmaceutical inhibitor SP600125, an adenovirus Adv.NLS-1 MKP-2 and CRISPR knockout cell lines. It was shown that the inhibitors did not affect cell viability. However, when investigating a novel cell death mechanism pyroptosis it was found that Adv.NLS-1 MKP-2 reduced LDH levels. It was also observed that this inhibitor reduced pCaspase-3 and GSDME levels, key proteins in pyroptosis. linking JNK to endothelial cell damage.

Here it has been observed that Doxorubicin and Cisplatin are linked to JNK activation and cell death. However, the inhibition of JNK did not reduce cell viability indicating further investigation is required to fully understand the phenomenon.

# Acknowledgements

First of all, I would like to thank my supervisor Robin not only for the opportunity to complete a PhD but also his support and expertise throughout. It's been hard work, but we got there in the end! I would also like to thank my second supervisor Marie Boyd.

I could have not got through this without the help and support of the people who makes SIPBS SIPBS. Thank you to the students of level 4 for all the support and good times along the way. To Anne and Chrisine, who made coming into the lab everyday more enjoyable from the laughs and stories to a shoulder to cry on. It would have been a much less friendly place without you and for that I'm forever grateful.

I would also like to thank the ladies on the train, who made the journey into the lab so enjoyable. A special mention to Lesley and Caren for being a very welcome distraction on the way to the lab every morning.

To my "Support group" Dr Rachel Craig and Dr Calum McMullen I don't even know where to start. I don't think I could have got through this without you, from help with techniques, analysis and thesis writing to support both for my PhD and in the real world I cannot thank you enough. Your friendship is what has got me through to the end and for that I could never repay you.

To Joanne for your mentorship without which I probably wouldn't be where I am. I can't tell you how grateful I am to have you or how thankful I am for everything you do. I would also like to thank Jean, Kathryn, C, Molly, Sara, Kathy, Sarah and the rest of the girls at Glasgow for your unwavering support for these last few months.

Finally, I want to thank my friends and family for your support for the last 4 years. In particular my Mum, sisters (Georgina and Samantha), Mama and Andrew (and little Midge!). It's been a tough few years for us all, but I couldn't have done this without you. Andrew, you have been my rock through everything and without your support this would not have been possible. Now it's time to start the next chapter!

# Abbreviations

| | |
|---|---|
| **Abl** | Tyrosine-Protein Kinase ABL1 |
| **APC1 AnV** | APC conjugated annexin V |
| **ATM** | Ataxia-telangiectasia mutated |
| **ATP** | Adenosine triphosphate |
| **ATR** | ATM-and-Rad3 related kinases |
| **AP-1** | Activator protein |
| **APS** | Ammonium persulfate |
| **ASK-1** | Apoptosis signal-regulating kinase |
| **BSA** | Bovine Serum Albumin |
| **Ca2+** | Calcium ion |
| **CCSS** | Childhood cancer survivor study |
| **Cisplatin** | cis-diamminedichloroplatinum(II) (CDDP) |
| **CPA** | Cyclophosphamide |
| **CRISPR** | Clustered regular interspaced palindromic repeats |
| **CVD** | Cardiovascular disease |
| **DMEM** | Dulbeccos Modified Eagle Medium |
| **DMSO** | Dimethyl sulfoxide |
| **DNA** | Deoxyribonucleic acid |
| **DSB** | Double stranded break |
| **DTT** | 1,4-Dithiothreitol |
| **DUSP** | Dual specificity phosphatase |
| **EA.hy926 cells** | Stable endothelial cell line established from HUVEC and A549 cells |
| **ECL** | Enhanced Chemiluminescence |
| **ED** | Endothelial dysfunction |
| **EDTA** | Ethylenediaminetetraacetic acid |
| **eNOS** | Endothelial nitric oxide synthase |
| **ERK** | extracellular signal- regulated kinases |
| **FAT** | FRAP-ATM-TRAPP |
| **FDA** | Food and drug administrations |
| **Fes** | Fes proto-oncogene, tyrosine kinase |
| **5-FU** | 5-Fluorouracil |

| | |
|---|---|
| **GSH** | Glutathione |
| **Gy** | Gray |
| **HAT** | Hypoxathine-Aminoptein-Thymidine |
| **HI-FCS** | Heat Inactivated fetal calf serum |
| **HMEC-1** | Human demal micro-vascular endothelial cell line |
| **HMG-CoA** | hydroxymethyl glutaryl coenzyme A reductase |
| **HRP** | Horseradish peroxidase |
| **HUVEC** | Human Umbilical Vein Endothelial Cells |
| **IMRT** | Intensity-modulated radiotherapy |
| **iNOS** | Inducible Nitric oxide synthase |
| **JNK** | c-Jun N-terminal kinase |
| **KIM** | Kinase interacting site |
| **LB broth** | Lysogeny Broth |
| **LSB** | Laemmli sample buffer |
| **LV** | Left ventricular dysfunction |
| **LVEF** | Left ventricular ejection fraction |
| **MKP** | Mitrogen-activated protein kinase |
| **MAPK** | Mitogen activated protein kinase |
| **MAPKK** | Mitogen activated protein kinase kinase |
| **MAPKKK** | Mitogen activated protein kinase kinase kinase |
| **MAPK8** | JNK1 |
| **MAPK9** | JNK2 |
| **MAPK10** | JNK3 |
| **MCF-7** | Michigan cancer foundation -7 |
| **MTT** | (3-(4,5-dimethylthiazol-2-yl)-2,5-diphenyltetrazolium bromide, a tetrazole) |
| **M.W** | Molecular Weight |
| **NADH** | nicotinamide adenine dinucleotide + hydrogen |
| **NATT** | Sodium Tris-Tween |
| **NES** | Nuclear export sequence |
| **NFAT** | Nuclear factor activated T-cell |
| **NLS** | Nuclear localization sequence |
| **NO** | Nitric oxide |
| **NOS** | Nitric oxide synthase |
| **nNOS** | Neuronal nitric oxide synthase |

| | |
|---|---|
| **P13K** | Phosphatidylinositol-3-OH-kinases |
| **PAM** | Protospacer adjacent motif |
| **PARP** | Poly(ADP-ribose) polymerase |
| **PCR** | Polymerase chain reaction |
| **PFU** | Plaque Forming Units |
| **PDGFR** | Platelet derived growth factor receptor |
| **PI** | Propridium Iodide |
| **PMSF** | phenylmethylsulfonyl fluoride |
| **PPAR** | Peroxisome proliferator-activated receptor |
| **Ras GTPase** | (RAS)Guanosine triphosphate Guanosine triphosphatases (GTPase) |
| **RelA** | P65 |
| **ROS** | Reactive oxygen species |
| **RNA** | Ribonucleic acid |
| **SAPK** | Stress activated protein kinase |
| **SDS** | Sodium dodecyl sulfate |
| **SDS-PAGE** | Sodium dodecyl sulfate Polyacrylamide gel electrophoresis |
| **SIPS** | Stress-induced premature senescence |
| **SOD** | Superoxide dismutase |
| **Src** | Cytoplasmic tyrosine kinases |
| **TBE** | Tris Borate buffer |
| **TE buffer** | Tris-EDTA Buffer |
| **TEMED** | tetramethylethylnediamine |
| **Thr** | Threonine |
| **Thr-X-Tyr** | Threonine-x-Tyrosine |
| **TKI** | Tyrosine Kinase Inhibitor |
| **TNFα** | Tumour necrosis factor |
| **TOP2** | Topoisomerase 2 |
| **TLRs** | Toll like receptor |
| **Tyr** | Tyrosine |
| **VEGF** | Vascular endothelial growth factor |
| **VEGFR** | Vascular endothelial growth factor receptor |

# Contents

# List of Figures

# List of Tables

# Chapter One

## Introduction

# 1. Introduction

Currently in the UK 1 in 2 people are expected to be diagnosed with cancer in their lifetime (Ahmad et al., 2015). Cancer can be defined as a genomic change to cells that allows them to overcome their own defence mechanisms (Hanahan and Robert, 2011). There are currently 6 hallmarks of cancer; sustaining proliferative signalling, evading growth suppressors, activating invasion and metastasis, enabling replicative immortality, inducing angiogenesis and resisting cell death (Hanahan and Weinberg, 2000). All these factors are required for the cancerous cells to thrive, with the resulting cells overcoming the body's internal defence mechanisms and culminating in tumour spread and metastases. This understanding has led to the development of effective treatments and early detection, which is thought to lead to over 5 million survivors in the UK alone by 2040 (Maddams et al., 2012). These advances have already shown a 27% drop in cancer associated deaths between 1991 and 2016 (Siegel et al., 2019). Therefore, more people are surviving cancer than ever before, and the long-term effects of cancer treatment are becoming more prevalent.

There are two main therapeutic approaches that can support surgical procedures. Excluding haematological cancers, these are the major treatment strategies, chemotherapy and radiotherapy (Debela et al., 2021). Chemotherapy usually involves a series of intermittent treatments often with 2 or 3 agents across a 3-to-6-month period which can abolish residual cancer cells (Ganai, 2017, Iveson et al., 2019).

Radiotherapy is an effective cytotoxic therapy used to treat solid tumours (Najafi et al., 2021). This is where energy, usually x-rays, is targeted at the tumour (Vaidya, 2021). Treatment is usually delivered externally and using improved targeted systems focused directly on the tumour, avoiding organs and important vessel (Vaidya, 2021). These beams are made up of photons allowing them to reach deep into the body, damaging the DNA in the cell preventing repair (Vaidya, 2021).

## 1.1. Cardiovascular problems due to cancer therapy

Unquestionably, a serious long-term effect of anti-cancer treatment is cardiovascular toxicities. The problem is evident in childhood cancer survivors, who are at 10 times greater risk of developing cardiovascular disease (CVD) including ischaemic heart disease and stroke (Chow et al., 2018). Furthermore, the incidence of cardiovascular toxicities occurrence has also been shown to vary depending on the treatment; anthracyclines >51%, cyclophosphamides >43%, and tyrosine kinase inhibitors (TKIs) >47% (Swain et al., 2003, Yeh and Bickford, 2009, Dempke et al., 2023, Wang et al., 2023, Iqubal et al., 2019). Other studies looking at the effect of radiation treatment have found that a third of all patients show signs of heart disease 10 years post treatment (Siaravas et al., 2023). This data highlights the potential severity of anti-cancer treatment on cardiovascular health and the importance of understanding the mechanism of such side effects. This will, in turn, enable the future development of preventative and effective treatments for this problem.

One of the world leading forms of cancer, particularly in women, is breast cancer with over 2 million new cases diagnosed in 2018 alone (Bray et al., 2018). Statistics show that in 2019 5-year survival rate for breast cancer was estimated to be 90% in the United States (Siegel et al., 2019). This significant improvement in survival rate allows studies to examine the effect of prolonged survival has on the development of CVD. In breast cancer, patients are susceptible to cardiovascular toxicities from both chemotherapeutic agents and radiotherapy (Darby et al., 2003). Patients who were treated for cancer of the left breast, with radiotherapy, have been shown to be at a significantly greater risk of myocardial infarction than those treated for cancer on the right (Darby et al., 2003).

Goody et al, 2013 have also shown that cardiovascular disease is more prominent in patients irradiated on the left side for breast cancer. It has also been shown that modern radiation techniques, whilst limiting damage to normal tissues, also result in such side effects (Demirci et al., 2009).

However, it has been shown that if radiation is given after breast conservation surgery at an early stage, there is no significant difference in cardiovascular toxicities between left and right sided tumours (Darby et al. 2003).

Aleman and colleagues found that on average CVDs were diagnosed 19 years after treatment (Aleman et al., 2007). They also found that 66-80% of cardiovascular disease cases in their cohort were caused by the anthracycline chemotherapy and radiation treatment of Hodgkin Lymphoma (Aleman et al., 2007). Though 78% of patients diagnosed with myocardial infarction were non-fatal, the risk of CVD was found to be 7 times higher with radiotherapy (Adams et al., 2003, Aleman et al., 2007). Van den Belt-Dusebout and co-researchers found similarly that 64% of patients treated for testicular cancer were diagnosed with myocardial infarction. Indicating that irradiation of the chest is not necessarily the cause of such damage, but further highlights how treatment induced cardiovascular toxicities is a systemic issue (van den Belt-Dusebout et al., 2006).

Interestingly, studies have shown the potential protective effect of statins. Statins are hydroxymethyl glutaryl coenzyme A reductase (HMG-CoA) inhibitors (Ramkumar et al., 2016). They are known clinically to reduce cardiovascular disease due to anti-oxidative, anti-inflammatory properties (Ramkumar et al., 2016). They have also been shown to inhibit Ras GTPases implicated in anthracycline treatment (Henninger and Fritz, 2017). It has therefore been suggested that statins may be used to reduce the side effects of radiotherapy and protect healthy tissue. Patients treated with statins have shown a reduction in cardiovascular toxicities by up to 50% (Obasi et al., 2021). This may reflect effects at a cellular level (see section 1.5), in particular Lovastatin has been shown to reduce the Doxorubicin stimulated stress responses, e.g. JNK and NFKappaB by reducing DNA strand breaks without effecting reactive oxygen species (ROS) formation (Damrot et al., 2006, Wojcik et al., 2015).

Taken together these studies show the potential damaging effects of anti-cancer therapies and radiotherapies with respect to the cardiovascular system and importantly, the effect of cardiovascular toxicities.

## 1.2. Cardiovascular toxicities

Cardiovascular toxicities is a prominent long term side effect of cancer treatment, that can develop up to 20 years post treatment (Clark et al., 2016). There are many definitions for Cardiovascular toxicities, however the American Society of Echocardiology and the European Association of Cardiovascular Imaging have both defined it as when the left ventricular ejection fraction (LVEF) is less than 53% (Plana et al., 2014). There are a number of methods used to diagnose and monitor cardiovascular toxicities which include LVEF, echocardiographic monitoring, nuclear imaging and endomyocardial biopsy (Ruggeri et al., 2018). Biopsies were once the gold standard for diagnosis, but their usage has declined with improvements in much less invasive methods, such as biomarkers, which includes troponin and brain natriuretic peptides (Ruggeri et al., 2018, Plana et al., 2014, Tan and Lyon, 2018).

The clinical focus of heart disease involves using the ejection fraction to determine left ventricular remodeling, this method however only determines heart failure that follows expected characteristics (McLean et al., 2019). McLean et al (2019) discuss how cancer therapy may not follow this pattern and therefore this method may not be effective in detecting heart failure as a result of anti-cancer treatment (McLean et al., 2019).

Cardiovascular toxic effects as a result of cancer treatment include heart failure, ischaemia, hypertension thrombosis and arrhythmias (Abdul-Rahman et al., 2023). Although there are other documented side effects that include thromboembolism and hypertension (Abdul-Rahman et al., 2023) Conditions such as cardiomyopathy are asymptomatic and can occur in up to 20% of cancer survivors 5-20 years post-treatment (Mulrooney et al., 2009).

Lubberts et al (2023) found that 64% of patients treated for testicular cancer were diagnosed with myocardial infarction, whilst 28% presented with coronary artery disease, after Cisplatin treatment (Lubberts et al., 2023).

As the incidence of cancer increases, with 5 million survivors predicted by 2040, it is vital that the mechanisms underpinning treatment induced cardiovascular toxicities are better understood to enable preventative and effective treatments (Maddams et al., 2012).

A number of chemotherapeutic agents have shown to directly impact the heart, due to the resultant cell death, which leads side effects such as angiogenesis and growth suppression (Florescu et al., 2013). Along with anthracyclines, platinum based and tyrosine kinase inhibitors, there are a number of other classes of chemotherapy known to have the same side effects (Abdul-Rahman et al., 2023). PARP inhibitors (poly(ADP-ribose) polymerase) mainly used for ovarian breast and prostate cancers the BRCA1/BRCA2 mutation (Palazzo et al., 2023). Palazzo et al (2023) have determined that the use of PARP inhibitors increases the risk of hypertension and thromboembolic events by 17.5% and 4.1% respectively. However, hypertension has been shown in 70% of patients treated with anti-VEGF drugs such as sunitinib (Abdul-Rahman et al., 2023) In one study of breast cancer patients, 63% of patients who were treated with 500mg/m2 of anthracyclines in a clinical study showed LV dysfunction 10 years post treatment (Cardinale et al., 2010). The main mechanism of chemotherapeutic agents is to prevent the proliferation of cancer cells; however, cancer cells require endothelial cells to do this (Wojcik et al., 2015). Therefore, it is hypothesised that endothelial cell damage may be contributing to the cardiovascular toxicities of chemotherapy. Wojcik et al (2015) have shown that cancer patients have poor endothelial function 20 years post treatment which has been linked to anthracycline use (Wojcik et al., 2015). Doxorubicin has also been shown to induce endothelial cell apoptosis which has been linked to increased production of ROS (Vásquez-Vivar et al., 1997, Wang et al., 2004).

Cisplatin has also been implicated with endothelial dysfunction, in testicular cancer patients where endothelial function and cardiovascular biomarkers were measured, such as triglycerides, low density lipoprotein and von Willebrand factor (Cameron et al., 2020). Endothelial damage was shown from 24 hours up to 7 years post treatment (Cameron et al., 2020). Cisplatin has been shown to cause cardiovascular toxicities that can go from asymptomatic arrhythmias to cardiomyopathy, and even paroxysmal supraventricular tachycardia, a rare form of arrhythmia (Raja et al., 2013). Yavaş et al (2008) have shown 66.7% of patients treated with Cisplatin showed acute arrhythmia. They also showed that this was independent of changes in electrolyte levels and may be due to the effect on cardiac sodium channels which increased the QT dispersion (Yavaş et al., 2008). In addition, Altena et al have shown in prostate cancer that 7 years post Cisplatin treatment patients presented with a decline in diastolic function (Altena et al., 2011).

Analysis of the Childhood Cancer Survivor Study (CCSS) has shown that radiation particularly to the chest elevates the risk for ischaemic heart disease, heart failure and stroke (Chow et al., 2018). As all the structures of the heart are subject to potential radiation damage, the myocardium, pericardium, valves and coronary arteries, the use of chemotherapeutics such as anthracyclines increases the risk of cardiomyopathy and heart failure (Chow et al. 2018). Whilst many studies have shown a decrease in heart mass due to cancer-induced cachexia (McLean et al., 2019, Tichy and Parry, 2023, Wiggs et al., 2022). Cancer cachexia results in progressive muscle wasting, this has also been linked to impaired cardiac contractility and relaxation (Von Haehling et al., 2017). However, there are few studies that have investigated cancer cachexia of the heart muscle (Wiggs et al., 2022).

In addition to direct cardiovascular toxicities, accumulating evidence indicates an increased incidence of CVD because of the anti-cancer treatments including both chemotherapy and radiotherapy. Radiotherapy, particularly in left breast cancer patients, has been found to cause an increase in cardiac problems more so than patients with cancer in the right breast (Stewart et al., 2013).

The left-hand side of the heart also presented severe damage compared to the right, due to increased pressure of systemic circulation (Stewart et al., 2013). Radiation damage can cause inflammation of the arteries which leads to the development of fibrosis (Adams et al., 2003, Yu et al., 2023). Such damage leads to obstruction of the lumen and thrombi of platelets and fibrin to the capillary endothelial cells. Healthy endothelial cells then replicate but cannot generate enough unobstructed capillaries (Yu et al., 2023). This leads to ischaemia and ultimately myocardial cell death (Yu et al., 2023). Therefore, it is believed such damage starts within the endothelium.

The endothelium lines the blood vessels and has many functions such as the regulation of vascular tone and maintaining homeostasis as well as controlling adhesion (Mailloux et al., 2001, Drożdż et al., 2023, Gimbrone and García-Cardeña, 2016). Cancer treatments are believed to induce endothelium dysfunction, where the endothelium has the inability to cope with changes in the functional phenotype of the endothelial cells (Gimbrone and García-Cardeña, 2016).

## 1.3. Pathogenesis of endothelial dysfunction

With respect to understanding the effect of anti-cancer therapies on the endothelium, it is essential to understand the normal physiology and pathology of this important cell type. The endothelium is the barrier between flowing blood, vessels, and organs, allowing the control of coagulation, adhesion, and invasion of immune cells (Mailloux et al, 2001). The vascular endothelium has many functions and is known as a paracrine, endocrine and autocrine organ that regulates vascular tone and maintains homeostasis (Hadi Ar et al., 2005). When healthy, the endothelium expresses very little proinflammatory factors and maintains a relaxed vascular tone, ensuring blood fluidity (Brouns et al., 2020, Huot et al., 1997). The endothelium prevents cell adhesion by maintaining blood flow and producing endothelium derived relaxing factors such as nitric oxide (NO).

NO prevents the activation of flowing platelets and subsequent adhesion of these and other white blood cell types (Brouns et al. 2020).

Only when the endothelial cell layer is disrupted due to tissue damage is the coagulation/adhesion process initiated, as shown in figure 1.1 (Noonan et al., 2022). This is largely temporary, but essential for wound healing and blood vessel reconstruction (Yau et al., 2015). However, due to risk factors that include; smoking, aging, genetic factors, diabetes, high blood pressure and high cholesterol, endothelial dysfunction can occur (Boueiz and Hassoun, 2009).

There is no standard definition for endothelial dysfunction (ED), however, it was described by Gimbrone and García-Cardeña (2016) as an inability to cope with changes in the functional phenotype of the endothelial cell (Gimbrone and García-Cardeña 2016). The dysfunction can be defined by a reduction in vasodilators, NO and increased endothelium derived contracting factors, such as endothelin which together impair the endothelium (John et al., 2020, Lüscher et al., 1992).

ED incorporates all changes whether acute or chronic, systemic or localized dysfunction of the cells (Gimbrone and García-Cardeña 2016). These changes result in damage, such as impaired barrier function, impaired antithrombogenic properties and inability to regulate vascular smooth muscle cell tonicity (Boueiz and Hassoun, 2009, Celermajer et al., 1992). Such changes lead to acute inflammation and chronic inflammatory diseases which include atherosclerosis, microangiopathies or pulmonary fibrosis (Boueiz and Hassoun, 2009). These are all linked with endothelial damage, and feature in many of the pathologies of chemotherapeutic agents and radiation (Mailloux et al. 2001; Vásquez-Vivar et al. 1997). ED results in a proinflammatory, proliferative and prothrombotic state, which are all factors of atherosclerosis, a well-defined disease of the endothelium that can ultimately be fatal (Qiao et al., 2020, Raitoharju et al., 2011).

ED is the first detectable sign of atherosclerosis, a disease of the vascular intima, known to follow the same pathogenesis as ED (Chatterjee et al., 2009). Initially the endothelium recruits monocytes from the circulating blood in the damaged areas, lesions and sites of inflammation as shown in figure 1.1 (Qiao et al. 2020).

These monocytes then differentiate into macrophages and internalise oxidised low-density lipoproteins becoming foam cells (Qiao et al. 2020). Foam cells then utilise different forms of programmed cell death including apoptosis, autophagy and pyroptosis, which aids the formation of necrotic cores of atherosclerotic plaques (Gui et al., 2022). Cytokines and growth factors are also secreted which accelerates inflammation (Raitoharju et al., 2011). This induces proliferation of vascular smooth muscle cells, and synthesis of extracellular matrix forming a fibrous plaque (Raitoharju et al. 2011). These plaques then line the endothelium narrowing the diameter of the vessel causing conditions such as angina, however due to the high pressure of the blood flow, these plaques can also breakaway and lead to cardiac infarction and strokes (Chatterjee et al. 2009; Raitoharju et al. 2011).

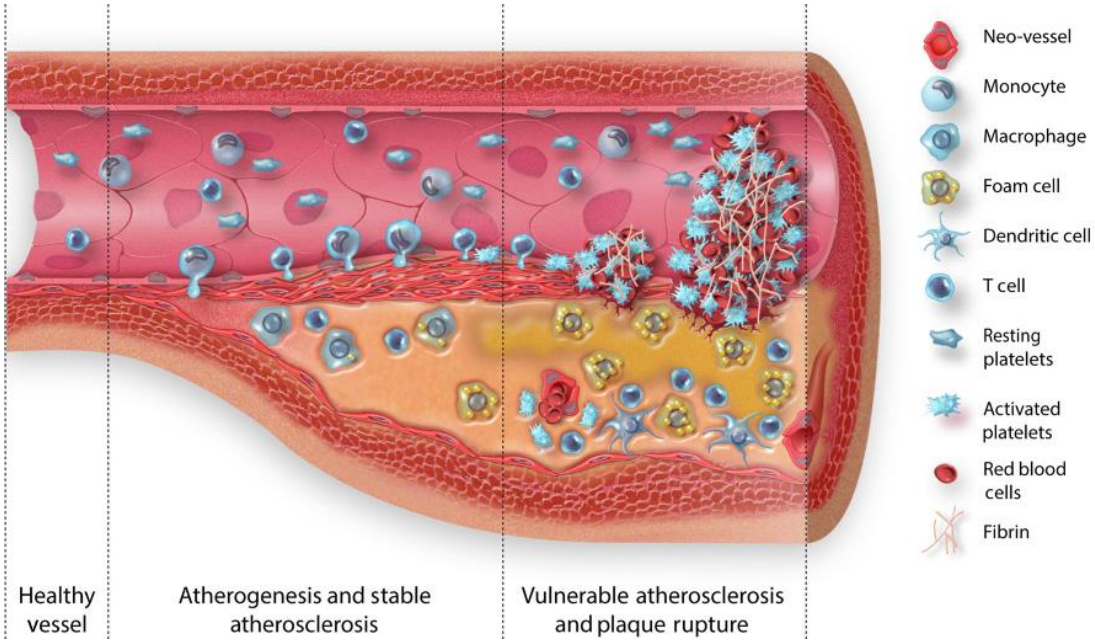


**Figure 1.1 Progression of atherosclerosis and endothelial dysfunction.**

Representation of differing stages of atherosclerosis from healthy to damaged vessel. Depicting the initiation of damage due to stimuli and mechanisms such as changes in shear stress and recruitment of immune cells. Resulting in the formation of atherosclerotic plaques due to recruitment of macrophages and formation foam cells. Ultimately leading to an cardiovascular event (Noonan et al., 2022).

ED is also known to cause oedemas and impact organ function by allowing water and proteins to move from the vascular system into tissues (Watanabe et al., 1991, Wolf and Baynes, 2006). A lack of NO, caused by free radicals, leads to such damage, causing the barrier between vessels to become more permeable which causes toxins to pass through to tissues and an accumulation of leukocytes (Rajendran et al., 2013, Rubanyi and Vanhoutte, 1986). A disruption of NO levels is one of the main features of ED (Ray et al., 2023).

NO is a signalling molecule formed from the guanidino nitrogen of L-arginine (Giroud et al., 2010). It has a number of important actions that include modulating blood flow and inhibiting adhesion to cellular immunity via macrophages (Kubes et al., 1991, Palmer et al., 1988, Takeuchi, 2004). It is synthesised in mammals by nitric oxide synthase (NOS) of which there are 3 isoforms, endothelial (eNOS), neuronal (nNOS) and inducible (iNOS) (Forstermann and Sessa, 2012). These are expressed by a number of cells including endothelial cells (Khatsenko et al., 1993, Lantoine et al., 1998). The level of NO is usually low, determined by its rate of formation and deactivation by superoxide (Kubes et al. 1991). A number of different cell types are able to produce NO including vascular endothelial cells, smooth muscle cells and macrophages (Khatsenko et al. 1993). Under normal conditions moderate levels of NO, formed in endothelial cells, are stimulated by shear stress which promotes an increase in intracellular $Ca^{2+}$ (Takeuchi, 2004). The activation of the $Ca^{2+}$-dependent eNOS isoform to enable a sustained activation of NO formation (Takeuchi et al. 2004).

The systemic concentration of NO can increase due to injury, either physical or biochemical, for example by acetylcholine or shear stress (Tran et al., 2022, Takeuchi, 2004). During ED a large increase of NOS results in inflammation and apoptosis (Takeuchi et al. 2004). This is because a decrease in NO synthesis or increase in its activation results in an increase in ROS leading to oxidative stress within the endothelium (O'Riordan et al., 2005).

Oxidative stress also increases the permeability of the endothelium and allows leukocyte adhesion (Hadi Ar et al. 2005). Oxidative stress is a common trigger and cause of endothelial dysfunction which is well-documented as a side effect to anti-cancer therapeutics (Scioli et al., 2020, Terwoord et al., 2022).

## 1.4. Anti-cancer drug effects on endothelial cell function

The main mechanism of an anti-cancer drug is to prevent proliferation of cancer cells, prevent DNA damage repair and promote cell death such as apoptosis (Tilsed et al., 2022). However, it has been shown that anti-cancer drugs are also toxic to endothelial cells as well as cancer cells themselves. Grant et al (2003) have shown HUVECs treated with taxanes, Paclitaxel and Docetaxel, cause significant damage both *in vivo* and *in vitro*. They used nude mice in *in vivo* and *ex vivo* assays, as well as *in vitro* cell death studies, to show that endothelial cells are up to 100-fold more sensitive to Paclitaxel and Docetaxel than tumour cells (Grant et al., 2003, Wolf and Baynes, 2006). Anthracyclines, alkylating agents, vascular endothelial growth inhibitors and radiation all result in cardiovascular toxicity and endothelial damage (Hsu et al., 2021). Endothelial damage is a result of inhibiting proliferation, survival and signalling resulting in conditions such as myocardial infarction, atherothrombosis and hypertension (Hsu et al, 2021). 25% of cancer patients treated with such agents presented with hypertension of which the pathophysiology is not understood (Hsu et al., 2021). A number of mechanisms have been proposed for this damage which include a reduction in vasodilator production and nitric oxide, an increase of vasoconstrictors, vascular tone and rarefaction (Hsu et al., 2021). A change in the balance between NO (vasorelaxant) and Endothelin-1 (vasoconstrictor) is a sign of endothelial dysfunction with an important role in vascular disease (Lim et al., 2009).

NO is known to be protective to the cardiovascular system, however, when combined with ROS peroxynitrite radicals are generated promoting inflammation and cell death mechanisms, such as apoptosis and necrosis (Lim et al., 2009). It is therefore believed that endothelial cell damage may contribute to the cardiovascular toxicities of chemotherapy.

Wojcik found that cancer patients have poor endothelial function 20 years post treatment which has been linked to anthracycline use (Wojcik et al., 2015). This research has been ongoing for many years with Vasquez-Vivar et al (1997) showing that Doxorubicin binds to the reductase domain of eNOS, causing the formation of superoxide and the decrease in NO (Vásquez-Vivar et al., 1997). Endothelial cell apoptosis has been linked to increased ROS production, in response to Doxorubicin (Clayton et al., 2020a). Clayton et al (2020a) found that excessive ROS mediated endothelial dysfunction in mice treated with Doxorubicin (10mg/kg) (Clayton et al., 2020a).

ROS are by products of metabolic reactions and generated by aerobic metabolism (Hadi Ar et al. 2005). ROS is generated at sites of inflammation or injury on the endothelium, which at low concentrations act as regulating signalling molecule that are fundamental in cell growth and response (Hadi Ar et al. 2005). However, at high concentrations ROS can cause cell injury and death(Villalpando-Rodriguez and Gibson, 2021, Lum and Roebuck, 2001). The vascular endothelium regulates the movement of macromolecules from the blood to tissue, which is a major target for oxidative stress (Lum and Roebuck 2001). Oxidative stress ultimately results in changes to endothelium signalling and redox regulated transcription factors (Lum and Roebuck 2001). These processes have also been linked to the MAPK pathways, ERK has been associated with endothelial cell survival, whereas inflammation and apoptosis of endothelial cells has been shown to be due to the P38 and JNK pathways (Pan, 2009).

## 1.5. Cellular mechanisms of anti-cancer treatments

Many underlying mechanisms have been linked to the use of anti-cancer treatments, some of which have already been mentioned. Therefore, it is important to understand their mechanism(s) of action and implications in cardiovascular toxicities.

### 1.5.1. Chemotherapy

Radiation aside, chemotherapy is one of the most versatile and utilised treatment options for eradicating cancer (Anand et al., 2024). There are many chemotherapeutic agents used currently, which can be administered independently or in combination with each other. For this thesis, Doxorubicin, Cisplatin and Sunitinib have been highlighted as chemotherapeutic agents used to treat solid tumours. However, they have been shown to mediate cardiovascular toxicities and endothelial damage side effects in surviving cancer patients, albeit with differing mechanisms of action.

#### 1.5.1.1. Sunitinib

Sunitinib malate (Sutent®) is a relatively new anti-cancer agent in comparison with the aforementioned compounds having been approved by the FDA in 2006 (figure 1.3) (Ebrahimi et al., 2023). Sunitinib is part of a targeted therapy approach that targets receptor tyrosine kinases, transmembrane receptors that promotes growth and proliferation (Ebrahimi et al., 2023). Tyrosine Kinase inhibitors ((TKIs) were invented in the early 2000s and are effective in the treatment of solid and haematological tumours (Shyam Sunder et al., 2023). The aim is for TKIs to influence pathways regulating malignant growth (Zhao et al., 2019).

TKIs such as Sunitinib have an immunosuppressive activity, which is well documented in the treatment of breast cancer amongst many others (Zhao et al., 2019). Tyrosine kinases can activate processes such as angiogenesis and cell proliferation (Bantscheff et al., 2007). This is by the transfer of phosphatase groups from adenosine triphosphate (ATP) to specific signalling proteins, which are part of growth factor and cytokine signalling pathways (Bantscheff et al., 2007). Sunitinib is known to have over 50 targets including growth factor receptors such as PDGFR (platelet derived growth factor receptor), VEGFR1 and 2 (vascular endothelial growth factor receptor) and cytosolic tyrosine kinases such as Abl, Src and Fes (Siveen et al., 2018, Wang et al., 2020, Li et al., 2024).

Over expression of these growth factors have been implicated in several cancers. For example an increase in VEGF is associated with several solid tumours such as breast cancer and colorectal cancer, whereas Abl is linked with leukaemia (Greuber et al., 2013, Hicklin and Ellis, 2005). TKIs are therefore an important class of anti-cancer agent and can be effectively used in combination with both traditional chemotherapies (Chatziathanasiadou et al., 2019). More recently, monoclonal antibodies such as anti-PD-1 and bevacizumab to prevent cellular activation (Bazarbashi et al., 2023, Chatziathanasiadou et al., 2019, Qi et al., 2020).

Sunitinib was initially approved for the treatment of renal cell carcinoma treatments and then gastrointestinal cancers (Chatziathanasiadou et al. 2019; Motzer et al. 2007). It inhibits many growth factor receptor kinases such as VEGF, PDGFR and EGF, which impairs angiogenesis tumour growth and metastasis formation (Chatziathanasiadou et al. 2019; Motzer et al. 2007; Paech et al. 2018; Truitt et al. 2018). It is well established that both VEGF and PDGFR are both expressed on endothelial cells (Huang et al., 2010). VEGF members are important for physiological angiogenic processes as well as conditions such as cancer (Nilsson and Heymach, 2006). VEGF ligands activate angiogenic programs for example VEGFR-1 binds VEGF, VEGF-B and PIGF-1,2 (Nilsson and Heymach, 2006).

This complex promotes endothelial progenitors and monocyte migration, whilst VEGFR2 is known to regulate endothelial cell proliferation and survival as shown in figure 1.2 (Nilsson and Heymach, 2006). Receptor tyrosine kinases are a vital part in pathogenesis of clear cell carcinoma through interactions with VHL (von Hippel-Lindau) tumour suppression genes (Motzer et al. 2007). This tumour suppressor gene encodes protein regulation in VEGF and PDGF stimulating angiogenesis and metastasis (Motzer et al. 2007). VEGF and VEGFR (VEGF receptor) regulate several functions including lymphangiogenic processes (Kodera et al., 2011). Kodera has shown that Sunitinib blocks VEGFR-3 and VEGFR-2 signalling in lymphatic endothelial cells, therefore suppressing lymph angiogenesis and inhibiting metastasis via the lymph nodes in breast cancer (Kodera et al., 2011).

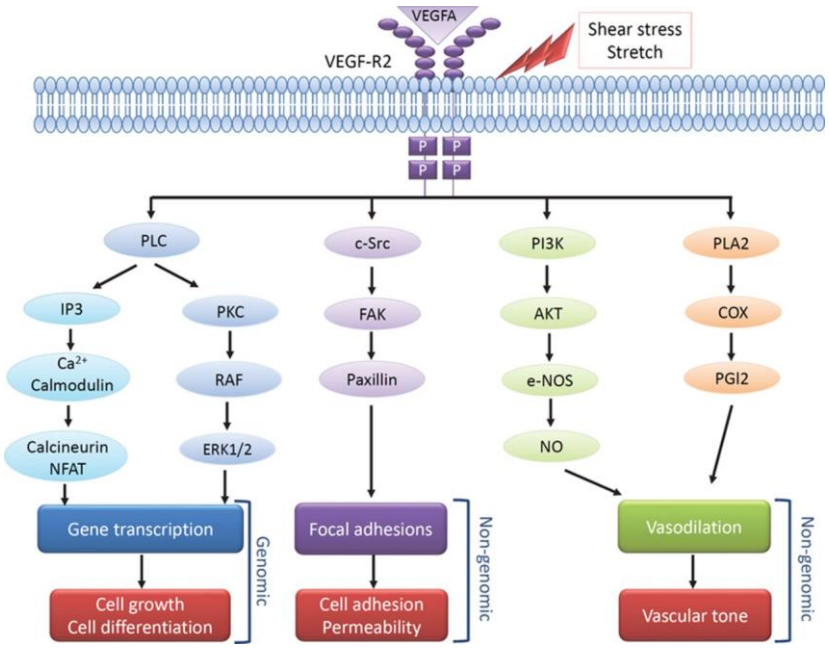


**Figure 1.2 Signalling pathways induced by VEGFR activation.**

VEGFR is activated by VEGF and mechanisms such as shear stress. This leads to processes such as endothelial cell growth, differentiation, adhesion and vasodilation (Touyz et al., 2017).

The principal action of Sunitinib is the inhibition of angiogenesis, by reducing VEGFR1, VEGFR2 and PDGFR beta signalling (Mena et al., 2010, Roskoski, 2007). These tumour vessels are unstable, leaky and inefficient in oxygen delivery, ultimately leading to hypoxia in the tumour (Hicklin and Ellis, 2005). This in turn promotes the formation of VEGF through the presence of HIF-1 binding sites on the VEGF promotor region (Schoch, 2002). As VEGF mediated endothelial proliferation and migration is a prime pathway for angiogenesis, the inhibition of these cellular outcomes underpins Sunitinibs' overall mechanism of action (Bantscheff et al., 2007) . At the molecular level, Sunitinib occupies the ATP binding pocket in the catalytic portion of the receptor tyrosine kinase preventing phosphorylation, and therefore inhibiting the activation of downstream substrates (Bantscheff et al., 2007). Sunitinib inhibits this mechanism by reducing signalling through VEGFR1, VEGFR2 and PDGFRβ (Roskoski 2007). VEGF inhibition increases mitochondrial superoxides and decreases nitric oxide production (Shyam Sunder et al., 2023). However, Sunitinib is susceptible to off target effects as the ATP binding site is shared between a number of different kinases and proteins, leading to side effects such as cardiovascular toxicities (Bantscheff et al. 2007).

Sunitinib is understood to be a relatively safe drug, although it is linked with cardiovascular toxicities and is associated with liver failure, causing fatalities in 0.3% of patients (Paech et al. 2018). Toxicities have been linked to both on and off target effects due to the inhibition of multiple other kinases due to selectivity (Shyam Sunder et al., 2023). These toxicities can be treated, however it can disrupt treatment and even necessitate a dose reduction (Truitt et al. 2018). It is believed that these toxicities are caused by the lack of specificity of Sunitinib, similar effects are also seen in a number of other chemotherapeutic agents (Cooper et al., 2018).

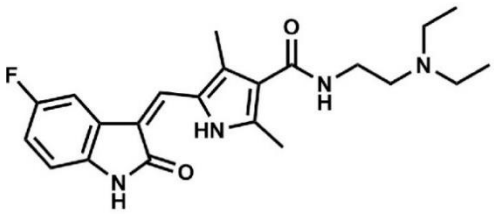


sunitinib

**Figure 1.3 Sunitinib**

Molecular structure of the tyrosine kinase inhibitor Sunitinib (Motzer et al., 2007, El-Awady et al., 2011).

Cardiovascular complications are thought to be the result of off target inhibition of receptor tyrosine kinases and mitochondrial function (Shah et al., 2013). TKIs such as Sunitinib affect vascular endothelial cells, cardiomyocyctes and post mitotic cells (Gomez, 2022{Wang, 2019 #672). Cardiovascular complications are thought to be the result of off target inhibition of tyrosine kinase activity and mitochondrial function (Wang et al., 2019). Off target effects include inhibition of AMP-activated protein kinase and activation of calcium/calmodulin dependent protein kinase, both linked to cardiac dysfunction (Mcmullen et al., 2021). It is also well documented that inhibiting VEGF leads to microvascular changes that reduce the myocardial capillary network which leads to rarefaction (Shyam Sunder et al., 2023). Rarefaction is the loss of capillary density, which has been linked to hypoperfusion and impaired contractility (Shyam Sunder et al., 2023, Karpurapu et al., 2024). VEGF inhibition has also resulted in increased atherosclerosis, where mice models have also shown reduced endothelial NO reduces vasorelaxation (Thijs et al., 2015)

Sunitinib is closely linked to hypertension, but it is still not understood whether it causes LV dysfunction or lowers the threshold for the drug (Truitt et al., 2018 ). Hypertension affects 8-47% of patients treated in this way, whilst 28% of which suffer from left ventricular dysfunction (Wang et al., 2019).

Not only this but endothelial dysfunction and cardiovascular damage has been seen as a long-term effect of treatment (Lai et al., 2020). Clinical studies looking at 20 patients have shown early signs of endothelial dysfunction, with a reduction in the flow-mediated vasodilation of the brachial artery (Lai et al., 2020). Reduced left ventricular ejection fraction and myocardial infarction have all be seen as a result of Sunitinib based treatments (Escalante et al., 2016)

There have been a number of studies trying to understand the mechanism underpinning the cellular and organ damage caused by Sunitinib. In mice models, it has been demonstrated that Sunitinib induces mitochondrial damage and cardiomyocyte apoptosis (Cooper et al., 2018). Other studies, for example, by Xu et al (2022b) have shown that autophagic degradation of cellular communication network factor 2 has been linked to the cardiotoxic effects of Sunitinib (Xu et al., 2022b). They found, using $Atg7^{-/+}$ heterozygous mice, resistant to Sunitinib, and human embryonic cardiac tissue-derived cell lines, that the autophagy induced by Sunitinib results in cardiomyocyte death (Xu et al., 2022b).

ROS is also known to be an important mediator in cardiovascular damage. Accumulation of ROS has resulted in functional effects such as hypertrophy and impaired contraction (Mcmullen et al., 2021). The increase of ROS triggers oxidative stress leading to cellular dysfunction (Mir et al., 2020, Li et al., 2024). ROS levels are controlled through antioxidants which can be both enzymatic and non-enzymatic such as GSH (glutathione) and SOD (superoxide dismutase) (Li et al., 2024). ROS is well established mechanism of endothelial damage as a result of TKI use, as its accumulation enables the production of toxic metabolites resulting in tumour lysis and cytokine release (Shyam Sunder et al., 2023). Li et al (2024) have also shown that ROS is linked a new regulated cell death ferroptosis, which together are implicated in sunitinib cardiovascular toxicities (Li et al., 2024). Using H9c2 cardiomycocytes and mouse models they were able to show Sunitinib caused an increase in ROS, impaired cardiac function and caused structural injuries to the heart (Li et al., 2024). They showed that increased levels of ROS reduced Nrf2 levels which activates ferroptosis (Li et al., 2024).

Indicating a link between oxidative stress and Nrf2-dependent ferroptosis cardiovascular toxicity caused by Sunitinib (Li et al., 2024). There are a number of factors linked to such damage, showing that more research is required to prevent the long-term effects found clinically for this treatment.

#### 1.5.1.2. Cisplatin

There are many drugs known to cause cardiovascular toxicities, Cisplatin (Cis-dichlorodiammine-platinum (II)/CDDP) is a major contributor to this effect (figure 1.4). Cisplatin is a well-established anti-cancer agent commonly used by the NHS that has shown cardiovascular toxicities in surviving patients. It is a small molecule platinum compound that was first discovered 40 years ago (El-Awady et al., 2011). The cytotoxic effect is thought to be through its interactions with DNA, as it forms covalent adducts between some bases and the platinum compound (Yousef et al., 2009). This well documented anti-tumour agent is prescribed in the treatment of solid tumours associated with advanced and reoccurring cancers such as breast, testicular and bladder (El-Awady et al. 2011). This potent drug has a 90% success rate in treating testicular cancer (El-Awady et al. 2011). Cisplatin is a chemotherapeutic agent that is widely used as a single chemotherapeutic or in combination therapy strategies (El-Awady et al. 2011). However, when combined with other cancer drugs such as Fluorouracil or Docetaxel it has been associated with lethal cardiomyopathy and nephrotoxicity, bone marrow suppression and many others (Tsvetkova and Ivanova, 2022, Yousef et al., 2009). Cisplatin is also widely known for its dose limiting factors nephrotoxicity and cardiovascular toxicities, with symptoms such as congestive heart failure (Lieberthal et al., 1996, Al-Majed et al., 2006). Combining this treatment with a number of other anti-cancer agents such as Doxorubicin and Methotrexate has resulted in lethal cardiomyopathy (Al-Majed et al., 2006).

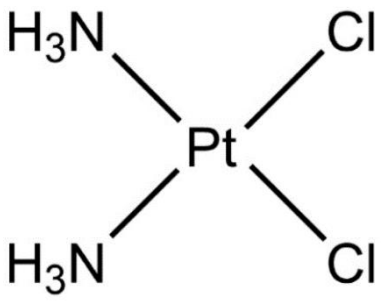


**Figure 1.4 Cisplatin**

The Molecular structure of Cisplatin Image modified from Kishimoto et al, 2019.

The prevalence of resistance however is a significant issue for Cisplatin treatment and increases with its use in combination therapies (Fuertes et al., 2003). One way involves the decreased uptake accelerated DNA repair and the inactivation of nucleophilic substances such as glutathione (El-Awady et al., 2011). However, inhibiting glutathione synthesis results in tumour cell death as well as increasing normal cell toxicity (El-Awady et al. 2011). This also generates ROS and has shown to lower antioxidants in plasma leading to antioxidative defense mechanism failure (El-Awady et al., 2011).

#### 1.5.1.2.1. Mechanism of action of Cisplatin

Cisplatin is activated once inside the cell, whilst in the cytoplasm Cisplatin chloride atoms are displaced (Dasari and Bernard Tchounwou, 2014). As shown in figure 1.5 , when Cisplatin enters the intracellular environment of the cancer cell, it hydrates due to the low chloride, becomes positively charged and then reacts with the nuclear DNA and nucleophilic species (Yang et al., 2006). This cellular uptake is mediated by copper transporters (Kiss et al., 2021). These include sulfhdryl groups on proteins and nitrogen donor on nucleic acids (Kiss et al., 2021). Cisplatin binds to N7 on the purine residues causing DNA damage in cancer cells preventing cell division and causing cell death (Dasari and Bernard Tchounwou 2014).

The cytotoxic effect is hypothesised to be through its interactions with DNA, as it forms covalent adducts between some bases and the platinum compound (Yousef et al., 2009). It was originally thought that this interaction caused cytotoxicity, however it has been shown that this is caused by apoptosis and not DNA interactions (Yang et al. 2006).. The mechanism of how the bonding of Cisplatin and DNA result in apoptosis is not widely understood (Yang et al. 2006). Apoptosis and necrosis have been seen to induce cell death once treated with Cisplatin (Dasari and Bernard Tchounwou 2014). However, it is also understood that Cisplatin induces oxidative stress and modulates calcium signalling (Dasari and Bernard Tchounwou 2014). The increase in ROS due to Cisplatin also aids its function by targeting the mitochondria reducing its function and triggering cell death (Saad et al., 2004). This increase in oxidative stress has shown to be linked with a decrease in mitochondrial gluthione (GSH) and Nicotinamide adenine dinucleotide (NADH) (Aggarwal, 1998). It is required to maintain mitochondrial function, this causes an influx of calcium from the mitochondria resulting in disrupted cell function (Aggarwal, 1998).

Apoptosis causes shrinkage of the cytosol and nucleus; and condensation of nuclear chromatin (Sánchez-Pérez et al., 2000). However, no impact on the plasma membrane or mitochondria has been shown (Lieberthal et al. 1996; Yousef et al. 2009). The condensed nuclei disintegrate into apoptotic bodies and are phagocytosed (Dursun et al., 2006). Caspases and calpain, intracellular cysteine proteases, have been found to induce Cisplatin-mediated cell death (Dursun et al., 2006). Dursun et al. (2006), found that caspase, a major apoptosis mediator can also cause necrosis, and that inhibiting calpain can protect from this. Calpain has also been shown to be implicated in endothelial injury caused by Cisplatin (Eguchi et al., 2010).

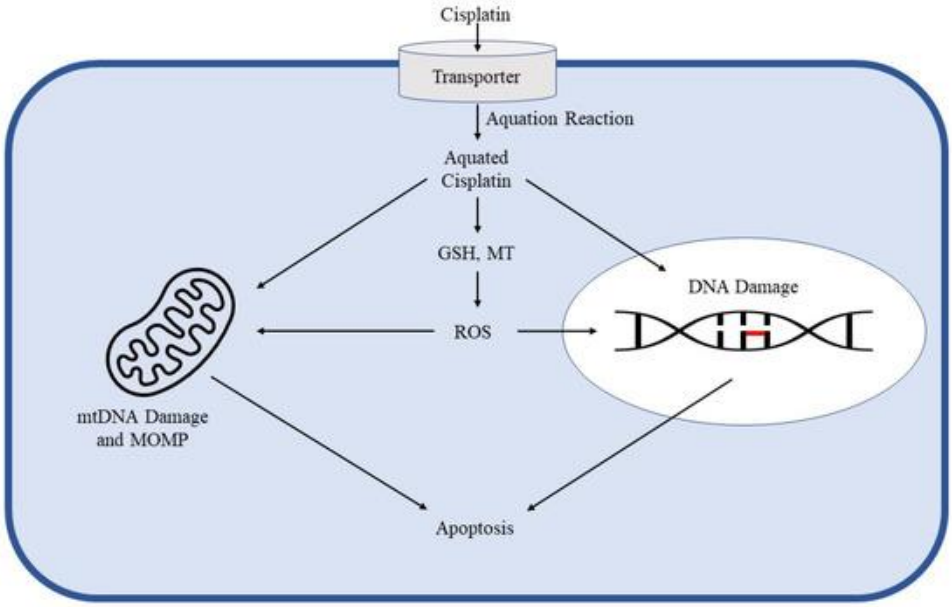


**Figure 1.5 Cisplatin Mechanism of Action**

Showing Cisplatin uptake via copper transporters and the activation in the cytoplasm that leads to nuclear damage and mitochondrial damage. Cisplatin binds to GSH reducing GSH levels. This leads to an increase in ROS inducing apoptosis (Kiss et al., 2021).

#### 1.5.1.2.2. Cisplatin effect on endothelial cells

Cisplatin has been shown to cause endothelial cell injury and even death (Eguchi et al. 2010). Interestingly, they did Eguchi et al (2010) show using both three-dimensional blood vessels lined with HUVECs, and monolayer cell culture, two differing results. In 3-D cultures calpain was involved in endothelial injury, and the breakdown of the tube (Eguchi et al., 2010). However, they did not show any evidence of DNA damage, whereas the monolayer did show evidence of DNA damage along with apoptosis (Eguchi et al. 2010). Mitochondrial damage is thought to be the mediator of toxicity including gastrotoxicity and nephrotoxicity (Nuver et al., 2010).

With the use of the immortalized human dermal micro-vascular endothelial cell line (HMEC-1), Nuver et al (2010) were able to show that Cisplatin altered endothelial function, proliferation and inflammation. This was assessed by cytotoxicity and apoptosis assays (Nuver et al., 2010). It is hypothesised that patients treated with Cisplatin may be impacted by atherosclerosis, caused by endothelial dysfunction as a direct result of the treatment (Sekijima et al., 2011). Sekijima et al (2011) investigated the impact of Cisplatin on vascular endothelial dysfunction by measuring arterial stiffness on women treated with Cisplatin for ovarian cancer. Theyalso used HUVECs as an *in vitro* model for endothelial dysfunction. They found Cisplatin directly caused vascular endothelial dysfunction, and ultimately could lead to atherosclerosis (Sekijima et al., 2011).

Jiang et al (2014) found that cisplatin induced severe damage to blood vessel walls. They investigated the effect of Cisplatin on contractile function in thoracic aortic rings from Sprague-dawley rats. This was determined using 200µM of Cisplatin and electron microscopy analysis *in vivo (*Jiang *et al., 2014)*. It was also found that Cisplatin inhibited (ATP)-induced intracellular $Ca^{2+}$levels increase in HUVECs. Jiang et al then determined that Cisplatin does affect contractile function of thoracic aortas (Jiang et al., 2014).

A clinical study looking at patients with testicular cancer, treated with Cisplatin, have found that this treatment induces acute and transient endothelial dysfunction (Cameron et al., 2020). As well as nephrotoxicity in early treatment (Cameron et al., 2020).

As discussed, Sunitinib and Cisplatin are one of many chemotherapeutic compounds found to elicit such side effects. Another largely reported compound that has been implicated in such side effects is Doxorubicin.

#### 1.5.1.3. Anthracycline/Doxorubicin

Anthracyclines are a group of antibiotics that have been widely used to treat cancer patients since the 1960s (Mattioli et al., 2023). However, its link to cardiovascular toxicities has majorly restricted its use (Heger et al., 2013, Sawyer et al., 2010). Anthracycline induced cardiomyopathy is a well-known side effect, which has been reported in up to 48% of patients (Swain et al., 2003). This is reported to be initiated by endothelial cell damage, which has been previously discussed (Sonowal et al., 2018). Several ways to minimise this side effect have been investigated, including limiting its dose and encapsulating the drug in liposomes to limit myocardial uptake (Sawyer et al. 2010). Despite these efforts, the mortality and morbidity rates are high due to anthracycline-induced heart failures, partly because the mode of action is not fully understood (Sawyer et al. 2010).

Doxorubicin (figure 1.6) is an anthracycline anti-cancer drug is one of the oldest chemotherapeutic agents currently used (Chatterjee et al., 2010, McGowan et al., 2017, Corremans et al., 2019). It is the principal drug in a group discovered from streptomyces peuceticus (Chatterjee, 2010, McGowan et al, 2017, Corremans et al 2019). Doxorubicin is used to treat solid tumours and haematological malignancies, for example leukaemia, breast and lung (Volkova and Russell, 2011).

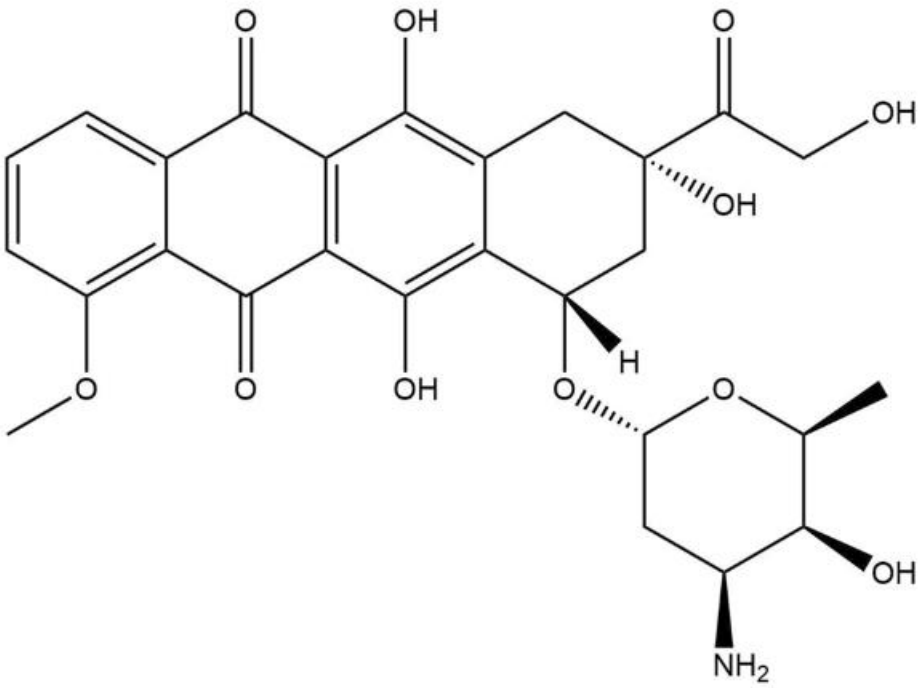


**Figure 1.6 Doxorubicin**

Chemical structure of Doxorubicin (Li et al., 2022b).

#### 1.5.1.3.1. Mechanism of Action of Doxorubicin

The cytotoxicity of Doxorubicin in cancer cells is mediated through several mechanisms, mainly by intercalating the DNA helix (Heger et al., 2013, Corremans et al., 2019). Firstly, by inhibiting DNA replication and RNA transcription (Thorn et al., 2011). Free radicals are generated that damage DNA or lipid peroxidation, direct membrane damage because of lipid oxidation and DNA cross linking and alkylation (Thorn et al., 2011). Anthracycline has also been shown to interfere with DNA unwinding, strand separation and the inhibition of topoisomerase II (TOP2) (Sawyer et al., 2010). These modes of actions have been shown to inhibit tumour growth (Sawyer et al., 2010, Corremans et al., 2019). Inhibiting TOP2 is known to result in oxidative damage of the DNA, which causes toxicity to endothelial cells and cardiomyocytes (Wolf and Baynes 2006).

Doxorubicin, known as a TOP2 poison which targets proliferative cancer cells (Nitiss, 2009, Corremans et al., 2019). Its role is to induce single and double strand breaks regulating topological changes that occur during DNA replication, transcription, recombination, and remodelling (McGowan et al., 2017). TOP2 is an adenosine triphosphate dependent enzyme, which can be expressed as two enzymes, TOP2α and TOP2β (Zhang et al., 2012a). Of which TOP2α is deemed to be the molecular basis of Doxorubicin anti-cancer mechanism (Zhang et al., 2012a).

Anthracyclines inhibit TOP2 preventing DNA repair, due to the formation of a ternary complex between DNA, TOP2 and anthracycline forming the TOP2-Doxorubicin-DNA cleavage complex (Heger et al., 2013, Corresman et al., 2019, Zhang et al., 2012a). This inhibits DNA resealing and results in DNA breaks, consequently preventing DNA replication and inducing apoptosis (Corresman et al., 2019). Doxorubicin prevents DNA resealing and stabilises the reaction when DNA strands are cut, where they covalently bond to the tyrosine residues of TOP2 (Heger et al., 2013). This results in damage to non-proliferating cells such as the heart muscle, which leads to heart muscle failure (This phenomenon will be covered in more detail in section 1.5.1.3.2) (Heger et al., 2013). This occurs when TOP2β is prevalent, in quiescent cells and cardiomyocytes, as TOP2α is more predominant in proliferating cells (McGowan et al, 2017, Corresman et al, 2019). However, expression of TOP2α in these cells varies during the cell cycle, as it is required for chromosomal segregation it is more prevalent (McGowan et al, 2017). Drugs that are known to target TOP2 generate enzyme mediated DNA damage (Nitiss, 2009). TOPα induced DNA damage is usually followed by an arrest in G1 and G2 in the cell cycle (Heger et al, 2013). On the contrary when Doxorubicin is bound to TOP2β it activates mitochondrial dysfunction by suppressing PPAR (peroxisome proliferator-activated receptor). This leads to a number of sequences such as the activation of the P53 tumour suppressor pathway, impaired calcium handling, mitochondrial dysfunction and increased apoptosis. However, without TOP2β Doxorubicin cannot bind to DNA, Zhang et al have shown the removal of TOP2β can protect against the cardiovascular toxicities of Doxorubicin (Zhang et al., 2012a).

In breast cancer specifically, a study has linked Doxorubicin treatment to cardiovascular toxicities in up to 48% of patients, whilst Lotrionte et al. (2013) have shown occurrence in 35% of breast cancer patients (Lotrionte et al., 2013, Swain et al., 2003).

#### 1.5.1.3.2. Cardiotoxic effect of Doxorubicin

The cardiotoxic effect of the drug is well established. In 1979 von Hoff et al. (1979) showed that 2.2% of 4000 patients treated with Doxorubicin developed clinical signs of heart failure (Von Hoff et al., 1979). Whereas a study demonstrated that 65% of patients, with childhood malignancy, show left ventricular contractile abnormalities linked to its use (Volkova and Russell 2011). A study in Spain found that 37.5% of patients experienced Doxorubicin induced cardiotoxicity, 2 years post treatment (López-Sendón et al., 2020). Cardiotoxic side effects diagnosed include arrhythmias, ventricular dysfunction, and congestive heart failure (Wojcik et al. 2015). It has been proposed that this damage affects the coronary endothelium (Wojcik et al. 2015).

At high doses Doxorubicin has been shown to cause apoptosis, and at low doses it induces telomere dysfunction, which results in stress-induced premature senescence (SIPS) (Spallarossa et al., 2010). Doxorubicin associated cardiomyopathy can be asymptomatic and occurs in 20% of cancer survivors, 5-20 years after treatment (Spallarossa et al., 2010). As a result of changes in the expression of proteins, required for cell cycle regulation, cytoskeletal and cellular architecture, this impaired function leads to apoptosis (Volkova and Russell, 2012). Clinical signs and symptoms of heart failure and a decrease in the left ventricular function, have been shown to be Doxorubicin induced (Volkova and Russell, 2012). Volkova and Russell have shown that if the cardiovascular toxicities remained moderate, asymptomatic LEVF formation would stabilise with the discontinuation of Doxorubicin (Volkova and Russell, 2011). The specific mechanism of action and the involved pathways that lead to cardiovascular toxicities are not currently fully understood (Chatterjee et al. 2010, Corremans et al. 2019, McGowan et al. 2017).

However proposed mechanisms include mitochondrial dysfunction, calcium dysregulation, inflammation and oxidative stress (Linders et al., 2024).

A mechanism of action of Doxorubicin linked to cardiovascular toxicities is oxidative stress. The quinone moiety of anthracyclines is known to induce the formation of ROS, it can also be generated by nitric oxide (NO) synthase (Förstermann et al., 2017, Shi et al., 2023)NO is also known to induce membrane damage of all tissue not just the heart redox cycling and ROS generation (Sawyer et al., 2010, Zhang et al., 2012a, Shi et al., 2023) . Oxidative stress may be caused by the release of free radicals from Doxorubicin, resulting in DNA damage and cell death (Kong et al., 2022). Doxorubicin is part of the quinone family, and this structure allows the molecule to act as electron acceptors in oxoreductive enzyme activate reactions (Vitale et al., 2024). Semiquinone radicals may facilitate free radical injury to DNA particularly if reacted with molecular oxygen generating superoxides (Cappetta et al., 2017).

Calcium overload has been described as a potential mechanism of toxicity (Shinlapawittayatorn et al., 2022). Wu et al. (2022a) found using Langendorff guinea pig hearts that Doxorubicin had differing effect on intracellular calcium. In hearts with a sinus rhythm, Doxorubicin resulted in calcium underload, which has been hypothesised as related to contractile dysfunction in cardiomyopathy (Wu et al., 2022a). However, it can lead to calcium overload in tachypaced hearts, which potentially causes calcium overload related toxicities (Wu et al., 2022a)

Anthracyclines exposure has been shown to result in myocyte death (Kong et al., 2022). The heart has a limited threshold for regeneration, once this threshold has been breached multiple forms of cardiac injury may occur via ventricle remodelling (Sawyer et al., 2010).. Biopsies have shown evidence of mitochondrial swelling and chromatin contractions markers of apoptosis (Sawyer et al., 2010). The measurement of cardiac sarcomeric troponins can be used for the detection of myocyte death further validates the theory (Sawyer et al., 2010).

The implications that the drug induces myocyte cell death has been shown in cells, animal models and humans (Kong et al., 2022). Experimentally it has been shown that the mechanism of cell death depends on the dose administered, with a low concentration of drug causing apoptosis and a high concentration necrosis (Vu et al., 2020). When investigating leukaemia, using SC, U-937 and MOLM-13 cells, Vu et al. (2020) found that high concentrations of Doxorubicin resulted in higher levels of necrosis compared to lower concentration (Vu et al., 2020).

As it has been said previously, anthracyclines produce cellular oxidative stress, which is thought to play a part in myocyte cell death (Narezkina et al., 2021). The presence of hydroxyl radicals in the heart increased with anthracycline use, however they can be inhibited by SOD (superoxide dismutase) (Sawyer et al., 2010). SODs such as catalase and dexrazoxane both suppress the anthracycline induced death (Sawyer et al., 2010). It has been shown in mouse models that over expression of SOD in myocytes increase metabolic vasodilation and mitochondrial function demonstrating a protection from mitochondrial damage (Yen et al., 1996, Kang et al., 2015).

The FDA (Food and Drug administrations) has approved Dexrazoxane as the only drug to prevent anthracycline-induced heart injury (Sawyer et al, 2010). Dexraoxane suppresses anthracycline-induced troponin elevation, a marker for myocyte cell death and cardiovascular toxicities (Sawyer et al, 2010). It has been demonstrated *in vitro* that oxidative stress induced myocyte apoptosis is closely related to anthracycline cardiovascular toxicities (Sawyer et al, 2010).

Doxorubicin cardiovascular toxicities has also been linked closely with endothelial cell damage, leading to conditions such as atherosclerosis (Bar-Joseph et al., 2011). Although the original damage is asymptomatic, the deteriorating condition of the endothelium leads to hyperlipidemia a condition closely linked to atherosclerosis (Luu et al., 2021). As previously discussed, an increase in ROS is linked with cardiotoxic effects of Doxorubicin. This mechanism increases the damage of the mitochondria which leads to endothelial cell loss via apoptosis (Monti et al., 2013).

Monti et al. (2013) found that an angiotensin-converting enzyme inhibitor was able to reduce endothelial cell apoptosis by inhibiting p53 and caspase-3 activation (Monti et al., 2013). Not only this Doxorubicin has also been linked with compromising tight junctions in the coronary microvasculature which leads to an increased permeable endothelium barrier (Monti et al., 2013). This increased permeability leads to infiltration of immune cells, as well as increased permeability of Doxorubicin itself (Wilkinson et al., 2018). Wilkinson et al. (2018) found that the preincubation of statins with human cardiac microvascular cells prevented Doxorubicin induced reduction of tight junction formation preventing the increase in permeability (Wilkinson et al., 2018). This increased permeability and increase in infiltration, as previously discussed, promote atherosclerosis (Davignon and Ganz, 2004).

Although there have been a number of investigations into the effect of Doxorubicin, it is still an effective anti-tumour compound used today. Many of these compounds can be utilised individually and in combination to increase anti-tumour effectiveness (Bayat Mokhtari et al., 2017).

#### 1.5.1.4. Radiotherapy

Radiotherapy has been a successful form of treatment for cancer patients, which can be given as a main treatment, prior to surgery to reduce tumour size and after to remove cancerous cells that may remain (Castaneda and Strasser, 2017). Its first use for cancer treatment was reported in the 1930s, in which radium needles and external beam with X-rays were utilised to treat breast cancer (Bradley and Mendenhall, 2018). In more recent times it can be delivered from an external beam which is known to damage normal tissue and can cause skin damage such as burns (Chan et al., 2014). Radiotherapy can also be administered as a drug, the radiolabelled drug is a radionucleotide attached to molecules that specifically bind to molecules expressed in malignant cells, where all toxicity has been shown to be reversible (Divgi, 2011, Stéen et al., 2018).

It causes DNA breaks and that leads to abnormal DNA base pairing, cellular damage and ultimately cell death (Borrego-Soto et al., 2015).

Within the vasculature, radiotherapy increases the generation of ROS that activates the pro-survival state causing impaired healing and endothelial dysfunction (Caron and Nohria, 2018). Radiotherapy damage can result in the inflammation of the arteries, leading to the development of neutrophilic infiltrate throughout the heart and fibrosis (Adams et al., 2003). Such effects in turn lead to the obstruction of the lumen and thrombi of platelets and fibrin to the capillary endothelial cells (Adams et al. 2003). Healthy endothelial cells then replicate but cannot generate enough unobstructed capillaries, leading to ischaemia and ultimately myocardial cell death (Adams et al. 2003).

It is also implicated with the bystander effect (see section 1.5.1.4.1), where the ionizing radiation triggers degradation of cell membranes (Boyd et al., 2006). Therefore, activating several signalling pathways because of the DNA damage of both targeted and the neighbouring cells (Boyd et al., 2006, Hara et al., 1998). The bystander effect is known to impact several generations of cells after initial treatment (Buonanno et al., 2011). This persistence can have detrimental long term health effects including second malignancies (Buonanno et al., 2011). They are also usually delayed, and in some cases are not noticed for many years after treatment. This has been seen *in vitro* and *in vivo*, however due to the nature of *in vitro* techniques it is difficult to study the effect of radiation on cells over the 10 plus years it can take for symptoms to be noticed clinically (Hargitai et al., 2021, Jabbari et al., 2019).

Modern radiotherapy techniques from 2000 onwards have reduced exposure to cardiovascular structures (Stewart et al., 2013). Abnormal narrowing of the entire vascular tract has been shown in cases of radiotherapy exceeding 40Gy (Adams et al., 2003). Whereas modern techniques of radiotherapy including IMRT (intensity-modulated radiotherapy) exposes the whole body to 2-3Gy, doses such as these have been shown to increase the risk of CVD (Stewart et al., 2013).

Patients who received treatment prior to these modern techniques have a higher risk of cardiac mortality over 10 years after treatment (Stewart et al., 2013).

#### 1.5.1.4.1. Bystander effect

Ionizing radiation triggers degradation of cell membranes and activates several signalling pathways due to the DNA damage, both the targeted cells and the neighbouring cells that were not irradiated, this is known as the bystander effect (Boyd et al., 2006, Hara et al., 1998). The bystander effect is hypothesised to be a result of intracellular communication mediated through intercellular gaps and ROS (Yin et al., 2015). This mechanism of using intercellular gaps is not universally accepted, however another hypothesis is that molecular factors are expressed into the extracellular medium and diffuse via concentration gradients (Peng et al., 2018). This is the result of low dosage radiation from external sources such as α, although it has also been seen in γ x-rays and low dose internal targeted nucleotides (Boyd et al., 2006, Konopacka et al., 2011). Once irradiated, DNA undergoes severe structural changes and double bond cleavage (Chen et al., 2018). The bystander effect is the result of molecular signals that are released by irradiated cells transmitted through intracellular communication (Konopacka et al., 2011). Studies have shown that media collected from radiated cells used with unirradiated cells have shown genetic changes in the non-irradiated cells (Konopacka et al., 2011). This effect can impact radio sensitivity and radioprotection (Chen et al., 2018).

The bystander effect is known to impact many generations after initial treatment (Buonanno et al., 2011). This persistence can have detrimental health effects in the long term which include second malignancies (Buonanno et al., 2011). It is believed that irradiated cells release signalling molecules such as ROS, cytokines, NO, and small molecules such as amino acids (Chen et al., 2018). These molecules released activate pathways such as the MAPK (JNK) and p53, they have also been seen to activate ATM (ataxia telangiectasia mutated protein) (Chen et al., 2018).

The different cascade reactions can impact healthy cells in a multiple of different ways, such as chromosomal damage, apoptosis, and cell cycle arrest (Chen et al., 2018). It is not yet understood if bystander effects from low linear energy transfer or high, that produce the same or different biological effects (Chen et al., 2018).

However, Chen et al. (2018) have shown that different forms of radiation induce different bystander effects. They found gamma radiation activated the ERK pathway, unlike the lithium heavy ion radiation treatment that only activates the p53 pathway (Peng et al., 2018). It has also been reported that the bystander effect influenced by dose, cell type, spatial and temporal modulation, and dose rate (Peng et al., 2018).

Bystander effects are usually delayed and in some cases are not noticed for many years after treatment (Peng et al., 2018). The delayed bystander effect has been shown *in vitro* and *in vivo*, however due to the nature of *in vitro* techniques it is hard to study the effect of radiation on cells over the 10 plus years it can take for symptoms to be noticed clinically (Peng et al., 2018). The main technique in studying the bystander effect is culture medium transfer, where cell to cell interactions can also be analysed (Chen et al., 2018). It is hypothesised that the radiation does not directly interact with DNA, but results in mutations, chromosomal aberrations, and long-term genetic instability (Boyd et al., 2005). This effect is not the result of proteins, as when Boyd et al. (2006) heated media from radiated cells to denature the proteins, the bystander effect was still shown in the next generation of cells (Boyd et al., 2006). Therefore, the implication of the effect on healthy cells and bystander mechanism requires further investigation with respect to cardiovascular toxicities.

#### 1.5.1.5. Combination Treatments

Combination treatments are a common use of available techniques and multiple chemotherapeutic agents (Najafi et al., 2021). This allows for multiple mechanisms of action to be utilized simultaneously. For most solid tumours surgery is always the method of choice for tumour removal (Najafi et al., 2021). Radiotherapy, neoadjuvant and adjuvant chemotherapy is given to shrink tumours and remove/kill any cells remaining before and after surgery (Zhang and Zhang, 2019, Vaidya, 2021). Chemoradiotherapy, the practice of concurrent chemotherapy and radiotherapy treatment has been shown to be effective.

Chemotherapy has been shown to induce the radio sensitivity of the cells, whilst radiotherapy induced damage can increase the incorporation of the drug into the cells (Eyck et al., 2018). Apoptotic cell death has also been seen in combination treatments due to the enhanced ROS, which reduced the mitochondrial membrane potential in Hela cells (Kang, 1994).

These drugs are an important anti-cancer agent and are effectively used in combination with monoclonal antibodies (Chatziathanasiadou et al., 2019). It inhibits many receptors associated kinases, such as VEGF PDGFR, which impairs angiogenesis tumour growth and metastasis formation (Chatziathanasiadou et al., 2019).

## 1.6. Cellular pathways mediating the effects of anti-cancer treatments

Given the damaging effects of chemotherapy and radiation on cells of the cardiovascular system, an important strategy is to identify the signalling pathways mediating these actions. And determine if any of these pathways can be therapeutically targeted to prevent the damage to the cells. This is underpinned by a clear understanding of pathways linked to cellular destruction and inflammation.

### 1.6.1. ATM

A key protein involved in the damaging effect of anti-cancer therapy is Ataxia telangiectasia mutated (ATM., First discovered in 1995 by Savitsky et al., whilst studying ataxia telangiectasia, an autosomal recessive disorder (Savitsky et al., 1995). ATM is a ser/thr protein kinase, a member of the phosphatidylinositol-3-OH-kinases (PI3K) family along with ATM-and-Rad3 related (ATR) kinases (Lavin, 2008, Kozlov et al., 2011). These proteins have domain motifs classically seen in the lipid kinase phosphatidylinositol 3-kinase (PIKKs) (Shiloh, 2003).

Their main function is to maintain genome stability, control cell cycle and cellular responses to DNA damage (Banin et al., 1998). There are 5 mammalian members of PI3K group ATM, ATR, mTor/FRAP, ATX/SMG-1 and DNA-PKcs (Mordes and Cortez, 2008). PI3Ks phosphorylates key proteins such as AKT, resulting in activating response pathways as a result to numerous stresses (Hemmings and Restuccia, 2012, Shiloh, 2003).

ATM is known to be the primary response to double strand breaks coordinating the DNA Damage Response by activating key molecules in numerous response pathways (Ahmed and Li, 2007). It is found in the nucleus of dividing cells, where it either activates or inhibits downstream processes (Shiloh 2003). A study found that in undamaged cells ATM lies as dimers, inactivated blocking the kinase domain with the FAT (FRAP-ATM-TRAPP) domain (García et al., 2022). After damage, ATM phosphorylates other ATM on serine residue 1981 in the FAT domain, phosphorylation releases 2 molecules forming fully activated monomers (Bakkenist and Kastan, 2003). This fast reaction can activate most ATM, and soon after the DSB ATM binds to the DSB site, where it divides between chromatin bound and free in the nucleus (García et al., 2022). After DSB ATM promotes a number of cellular mechanisms such as; apoptosis cell cycle arrest, senescence and metabolic reprogramming (García et al., 2022). This activation has been associated with

radiation and chemotherapy treatment. It has been shown in cell lines that ATM knockouts become more sensitive to radiation, therefore there has been research into the effect inhibiting ATM would have radiotherapy treatments (Jette et al., 2020).

However, ATM has also been implicated in cardiovascular toxicities. Using ATM knockout mice Zhan et al. (2016) have shown that fibroblasts mediate Doxorubicin induced cardiovascular toxicities through ATM (Zhan et al., 2016). A further study by Yoshida have also reported that Doxorubicin induced cardiovascular toxicities is mediated through ATM-p53-apoptosis pathway activated by oxidative DNA damage (Yoshida et al., 2009).

There have been a number of papers reporting a link between ATM and JNK activation related to autophagy and programmed cell death, therefore indicating JNK could be activated downstream due to ATM activation (Mavrogonatou et al., 2022, Wang et al., 2021). Further investigation into this link and cardiovascular toxicities could aid the findings of preventative measures.

### 1.6.2. NF-κB

The Nuclear factor-κB (NF-κB) pathway is renowned for its ability to regulate several genes involved in a number of biological responses including apoptosis, immune and inflammatory responses (Liu et al., 2017, Paul et al., 2018). The family comprises of 5 members p105/p50, p100/p52, p65 (RelA), RelB and c-Rel, which were initially discovered as inflammation activated factors (Picco and Pages, 2013). These are inducible transcription factors known to regulate genes involved in a number of mechanisms (Liu et al., 2017). The NF-κB members are held in the cytoplasm when inactive by inhibitory proteins, which includes IκB (Vallabhapurapu and Karin, 2009).

Activation of the pathway involves the canonical and the non-canonical pathway, however they both regulate inflammatory and immune responses (Liu et al., 2017).

The pathway is activated with the release of IκB molecules, due to the proteasomal degradation of the inhibitors (Hoesel and Schmid, 2013). The canonical pathway results in a fast transient transcription to regulate proinflammatory genes Yu et al., 2020). Whilst the non-canonical pathway occurs through tumour necrosis factor receptors. This means the resulting activation is slower but more persistent, to aid immune cell development and immune response (Yu et al., 2020).

When the canonical pathway is activated, it is well known that p65 and p50 are responsible for transcription of target genes Yu et al., 2020). They are sequestered in the cytoplasm by IκB proteins that consist of three groups IκBα, IκBβ and IκBε, p100 and p105 and other IκB proteins IκBζ, BCL-3 and IκBNS Yu et al., 2020).

The signal-induced phosphorylation of such IκB molecules by IKK activates the pathway. IKK has 2 catalytic subunits IKKα (non-canonical) and IKKβ (canonical) with IKKγ as a regulatory subunit (Yu et al., 2020). IKKβ activation leads to IκB protein phosphorylation causing the degradation of IκBs releasing NFκB dimers from the cytoplasm. Once released these dimers translocate to the nucleus to enable the transcription of target genes (Yu et al., 2020).

NF-kB, particularly the canonical pathway, has been implicated in chronic inflammatory diseases, for example asthma and rheumatoid arthritis (Lawrence, 2009). As this pathway is widely associated with inflammation it has been the primary focus of anti-inflammatory drugs (Lawrence, 2009). NF-kB has been shown to play a role in cardiovascular diseases such as myocarditis and heart failure (Matsumori, 2023). It has also been implicated with atherosclerosis where NF-kB has been detected in the nuclei of macrophages within the lesion (Brand et al., 1996, Matsumori, 2023).

### 1.6.2.1. Effect of Doxorubicin and Cisplatin on NF-κB

A limited number of studies have examined the effect Doxorubicin and Cisplatin have on the NF-kB pathway particularly with its roles in inflammation and cell survival. Doxorubicin has also been linked to heart disease and Doxorubicin induced cardiovascular toxicities. It has been reported that Doxorubicin activates the NF-kB pathway and studies have shown that by inhibiting NF-kB they have shown to protect from Doxorubicin induced cardiac damage (El-Agamy et al., 2019). Similarly, Nozaki et al. (2004) used mice models showing Toll like receptors (TLRs) that are known to activate the NF-kB contributed to Doxorubicin induced cardiovascular toxicities as a result of oxidative stress (Nozaki et al., 2004). Doxorubicin has also been shown to induce NF-kB activation in H9c2 embryonic rat cardiac cells; cells were treated for up to 90 minutes with 5μM of Doxorubicin to activate pp-65 (Guo et al., 2013). The study also linked the p38 and NF-kB pathways with the induction of Doxorubicin induced inflammatory response (Guo et al., 2013).

Ho et al. (2005) have shown however that in breast cancer cell lines MDA-MB-231, MDA-MB-435s and also HEK293 that IκBα is degraded with Doxorubicin whilst there is no p65 phosphorylation (Ho et al., 2005). Indicating that any NF-kB involvement is to reduce transcription (Ho et al., 2005). Another study has shown that NF-kB activation mediates Doxorubicin induced cell death in human neuroblastoma cell lines such as SH-EP1 (Bian et al., 2001). In accordance with Ho et al. (2005) it was found that IκBα was degraded and SH-SY5Y expressed a repressor form of I-κB resistant to Doxorubicin induced cell death.

Similarly, there have been studies looking into the effect of Cisplatin on the NF-kB. Cisplatin has been shown to activate NF-kB in the kidney, assessed using C57BL mice and a mice proximal tubular cell line (Ozkok et al., 2016). Kim et al. (2006) have shown in head and neck cancers NF-kB activation is important in Cisplatin induced apoptosis (Kim et al., 2006).

They showed that Cisplatin induced IκBα degradation and NF-κB transcriptional activation, following 4 hours of treatment with 40μM of Cisplatin and linked this to cell death in human head and neck squamous cell carcinoma cell lines which include HN3 and HN4 (Kim et al., 2006).

NF-kB has been implicated in Cisplatin resistance. As NF-kB is important in determining apoptotic insult, it is thought NF-kB will play an important role in Cisplatin resistance (Lagunas and Meléndez-Zajgla, 2008). It is believed that anti-cancer agents activate NF-kB after over an hour compared to TNF-α which takes a matter of minutes (Lagunas and Meléndez-Zajgla, 2008). It is believed that an increase in total NF-kB levels, nuclear and cytoplasmic translocation of IκBα and its degradation is involved in the resistance process (Chuang et al., 2002).

When looking into lung cancer Ryan et al have shown that NF-kB as an inflammatory mediator of Cisplatin resistance. They showed using a range of isogenic Cisplatin resistant cell lines (e.g A549, H460) have dysregulated NF-kB targets compared to wild type cells using proteomic analysis, identifying NF-kB as a target for Cisplatin resistance (Ryan et al., 2019).

NF-κB has also been linked with the ATM and JNK pathways. ATM has also been shown to directly activate IKKα and the NF-κB pathway by binding and phosphorylating Ser 85 of IKKγ (Fang et al., 2014). An ATM-IKKγ complex is then formed which in turn activates IKK and ultimately NF-κB (Fang et al., 2014). NF-kB and JNK have be shown to interact by a number of groups including Smeale et al. (2001) where they show that NF-κB down regulates the JNK pathway (De Smaele et al., 2001). Therefore, further investigation of this phenomenon could provide further insight into JNKs role in endothelial cell damage.

### 1.6.3. MAPK

The Mitogen-activated protein kinase family is a member of the largest superfamily of proteins – eukaryotic protein kinase family (Kultz, 1998). It was identified as an ultraviolet-responsive protein kinase and was first discovered in 1987 by Ray and Sturgill (Gu et al., 2018). They found that these kinases originally called microtubule associated protein kinases, regulate chemical and physical extracellular signals into intracellular responses (Brott et al., 1998). These protein kinases are found to be ubiquitous and regulate many important activities such as cell proliferation, differentiation, and apoptosis (D'Souza et al., 2008).

The MAPK family contains of a three-kinase cascade involving; MAPK, MAPK Kinase (MAPKK) and MAPK Kinase Kinase (MAPKKK) (Cargnello and Roux, 2011). These individual kinases both phosphorylate and activate downstream to establish a complex signalling cascade which is highly regulated. MAPKKK phosphorylates MAPKK which phosphorylates and activates the MAPK as illustrated in figure 1.7 (Cargnello and Roux, 2011). These Ser/Thr kinases themselves are frequently activated by phosphorylation or interaction with GTP-binding proteins such as Ras/Rho (Willoughby, 2003). MAPKKK activation initiated by external stimuli stimulates MAPKK activation which leads to the activation of MAPK due to the dual Thr/Tyr residue phosphorylation (Willoughby, 2003).

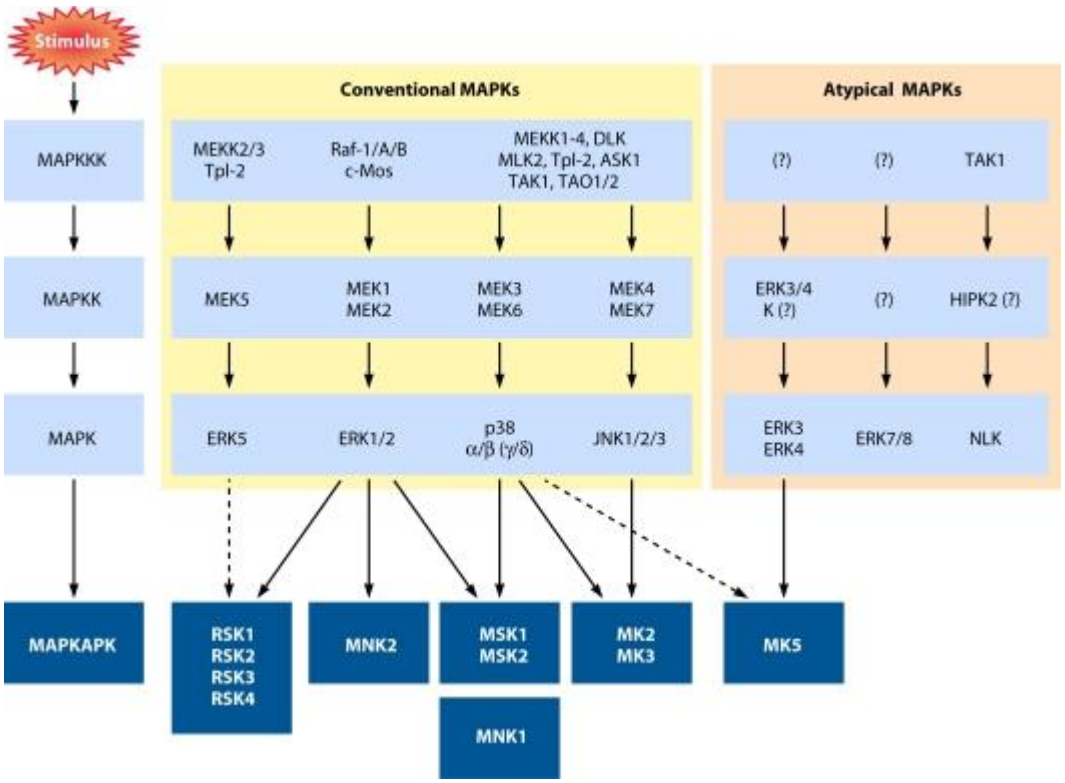


**Figure 1.7 Illustration of MAPK signalling cascade.**

Illustration of the MAPK signaling cascade following activation of extracellular stimuli. This cascade principle is utilised by all MAPK family members, where the activation of MAPKKK ultimately results in MAPK activation (Cargnello and Roux, 2012, Wang and Xia, 2012).

There are 14 members of the MAPK family in mammals, with distinct and overlapping functions. These functions include proliferation, differentiation and death (Wang and Xia, 2012). Members of the MAPK family include extracellular signal- regulated kinases (ERK), p38 and JNK (Cargnello and Roux, 2011). Each of these are activated by the dual phosphorylation of the Tyrosine and Threonine residues via the Threonine-X-Tyrosine motif (Thr-X-Tyr). The difference in the amino acid within the motif allows for the activation of specific substrates, for example p38s amino acid is glycine (Mittelstadt et al., 2009). The deregulation of this pathway leads to a number of diseases which include cancer, diabetes, inflammatory disorders and neurodegenerative diseases (for reviews see Bubici and Papa, 2014, Johnson and Nakamura, 2007, Kumar et al., 2015, Wu et al., 2019.).

### 1.6.4. JNK

c-Jun NH2-terminal kinase (JNK) is a member of the MAPK (mitogen activated protein kinase) family (Yan et al., 2024). JNK was discovered in the 1990s and is known as a stress activated protein kinase (SAPK) (Yan et al., 2024). It regulates a number of processes including cell death signalling, metabolism and immune responses (Yan et al., 2024).

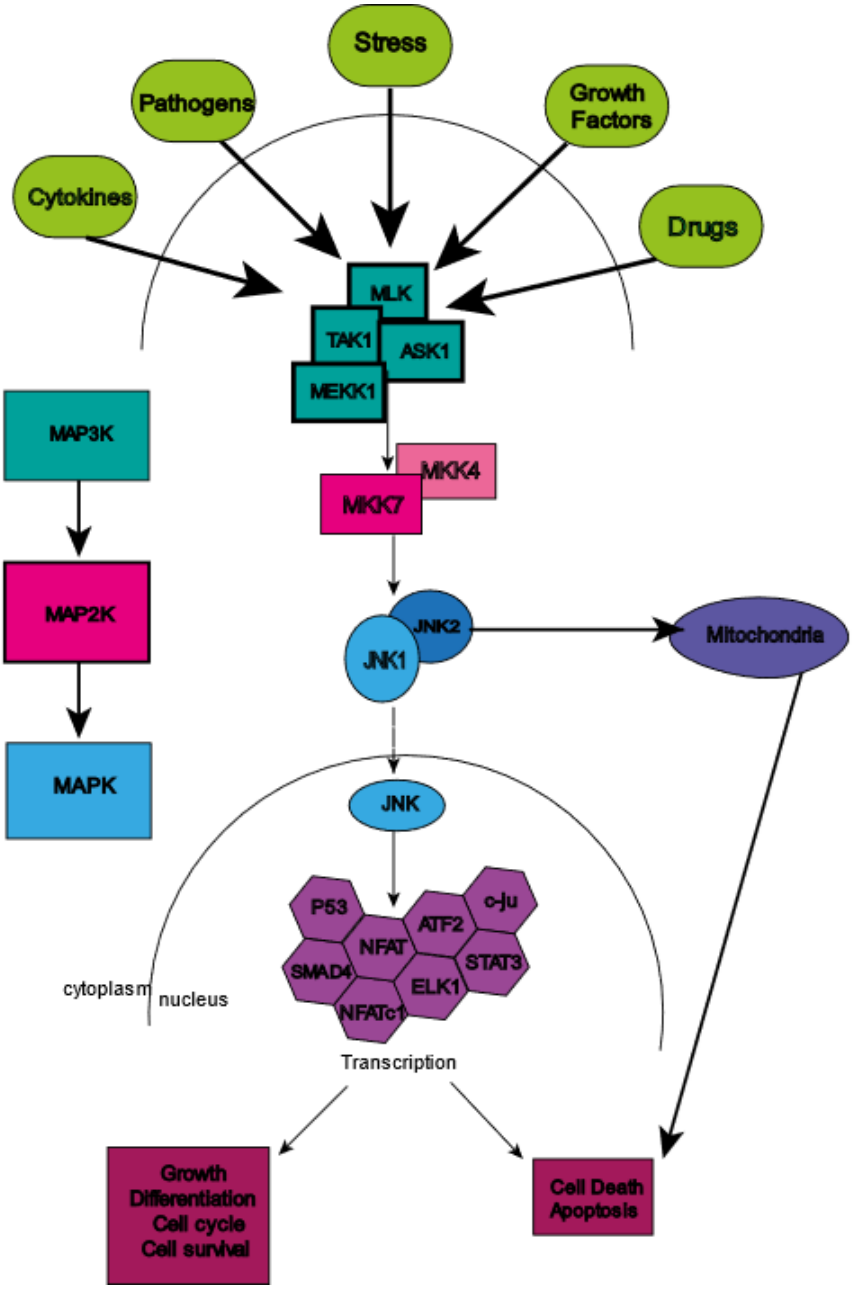


**Figure 1.8 Activation of the JNK pathway.**

Simplified model of JNK activation showing many different stimuli such as cytokines, and growth factors. These then activate MAPKKK such as ASK-1 to initiate the MAPK cascade where MAPKK (MKK4/7) is phosphorylated which then phosphorylates JNK.

Once activated JNK translocates into the nucleus to activate transcription factors. Simplified diagram signaling pathway of JNK modified from (Bubici and Papa, 2014).

JNK comprises three family members JNK1 (MAPK8), 2 (MAPK9) and 3 (MAPK10) of which there are 10 splice variants (Dreskin et al., 2001). JNK 3 is mainly found in the brain and testes, whereas JNK1 and 2 are ubiquitous. Recognised as a stress activated kinase, JNK can be stimulated by a number of signals both cellular and extracellular, including osmotic and heat shock, U.V radiation, ischaemic and hypoxic stress as well as cytokines, some growth factors and agonists at a number of GPCRs (Wang et al., 2012). These genes are also known to have distinct functions although some overlap, for example JNK1 has been shown to promote proliferation in MEFs and can activate c-Jun (Sabapathy et al., 2004, Wood et al., 2018). JNK2 however, has been shown to be a negative regulator by promoting c-Jun degradation and slows fibroblast proliferation (Sabapathy et al., 2004, Wood et al., 2018). As with all MAPKS, JNK is activated via a MAPK kinase complex.

JNK1, 2 and 3 have very similar structures with JNK1 and 3 having 75% identical amino acids, whilst JNK1 and 2 are 73% identical (Park et al., 2015). JNK1 (46kDa) and JNK2 (55kDa), are 83% similar in function, however their interaction with c-Jun is very different (Park et al., 2015). JNK2 is 25 times more efficient at binding to c-Jun than JNK1 (Kallunki et al., 1994). This difference has been deduced to be a small β strand near the catalytic pocket (Kallunki et al., 1994). The similarity in structure at the ATP binding site however is 98%, these high similarities is causing difficulties in producing specific drugs to affect JNK (Kallunki et al., 1994). This specificity is not only impaired between the 3 isoforms but also other MAPKs, as p38 at the ATP binding pocket has an 80% similarity to JNK (Park et al., 2015). The similarity of MAPKs can also be seen with the use of MKPs, these are enzymes that dephosphorylates MAPKS (Lawan et al., 2012). MAPKs including JNK, have a nuclear localization sequence (NLS) within the C-terminus, this allows MKPs to dephosphorylate the different MAPKS (Lawan et al., 2012).

These have a primary subcellular location of the nucleus, this dephosphorylation occurs by removing the phosphoryl moiety on both threonine and tyrosine residues on the activation loop (Cadalbert et al., 2010).

Specificity is defined by the Kinase interacting site (KIM) domain whilst the NLS or nuclear export sequence (NES) define the subcellular location (Lawan et al., 2012). There are 10 known homologues of this in mammals, each of which have different MAPK substrate specificities (Lawan et al., 2012). MKP-1 is located in the nucleus and active against ERK, JNK and p38. However, it has been shown to have a higher specification for p38 and JNK than ERK (Lawan et al., 2012). Similarly, MKP-2, also known as DUSP4, has been shown to be specific to ERK and JNK. It has been shown to be specific for JNK or ERK depending on the cell line (Lawan et al., 2012).

To activate the JNK pathway however, the MAPK cascade, illustrated in figure 1.8, is utilised. This tiered system allows for pathway crosstalk allowing multiple pathways to coordinate a response (Figure 1.8) (Liu et al., 2011). MKK7/4 (MAPKKs) are upstream isoforms of JNK and activate JNK by dual phosphorylation of the Thr and Tyr in response to several stimuli (Liu et al., 2011).

To facilitate the activation of MAPKKs by MAPKKKs scaffold proteins are utilised (Willoughby, 2003). Scaffold proteins help bind components of the pathway whilst regulating their location and activity (Willoughby, 2003, Stebbins et al., 2008). Several scaffold proteins can facilitate the activation of MAPKKs by MAPKKKs. An example of this is JIP-1 (JNK-interacting protein 1) scaffold protein binds to MKK7 and an MLK family member (Willoughby, 2003).

As figure 1.8 shows, MKK4 and MKK7 are MAPKKs, they are upstream of JNK and activate the pathway by dual phosphorylation (Gu et al., 2018). This activation leads to the phosphorylation of transcription factors and activating transcriptional regulation by forming other transcriptional factors, for example c-fos (Gu et al., 2018). Both MKK4 and 7 behave differently, with MKK4 has been shown to activate JNK and p38, which is primarily activated by environmental stimuli and preferably phosphorylates the tyrosine amino acid (Lin et al., 1995).

Whilst MKK7 has been shown to be specific to JNK, it is also activated by cytokines such as TNFα, and phosphorylates the Thr  (Lin et al., 1995).

#### 1.6.4.1. JNK activation and cell responses

The JNK pathway is activated in multiple situations dependent on the cell type and stimuli.  With respect to cell growth and proliferation, it has a number of diverging roles (Gutierrez et al., 2010).  For example, JNK is activated during G2 and the beginning of mitosis, it directly phosphorylates human Cdh1 preventing the activation of APC/C during G2. Gutierrez et al. (2010) have shown that APC/Ccdh1 regulates nuclear localized JNK during late-stage mitosis and G1 (Gutierrez et al., 2010).  By inhibiting JNK degradation during the cell cycle, abnormal spindle and chromosomal dynamics cause impaired entry to mitosis (Xu et al., 2015).

When activated, phosphorylated JNK translocates into the nucleus by binding to heterodimers of importin 3 with either importin 7 or 9 (Maik-Rachline et al., 2018).. This causes apoptosis by increasing gene expression of pro-apoptotic genes such as Bax (Bcl2-associted X protein) and PUMA (p53 up-regulated modulator of apoptosis) (Maik-Rachline et al., 2018). This is due to the activation of p73 a member of the p53 transcription factors family which also induces apoptosis (Dhanasekaran and Reddy, 2017, Jones et al., 2007) Once JNK has been phosphorylated, c-Jun helps to regulate gene expression in response to stimuli such as growth factors and cytokines (Cui et al., 2007). C-Jun is also an upstream activator of activator protein 1 (AP-1). AP-1 is a heterodimer made up of transcription factors such as c-Jun and c-fos to form an AP-1, this complex then effects apoptosis (Yang et al., 1997). AP-1 is regulated by JNK and once activated it can trans activate many mitogen and stress related genes (Chadee et al., 2002). This is through transactivation of transcription factors or through the modulation of mitochondrial proteins (Xu et al., 2015).

JNK can induce apoptosis via a mitochondria-dependent caspase activation (Tobiume et al., 2001). The MAPKKK, ASK-1 (Apoptosis signal-regulating kinase), is activated by TNFα, $H_2O_2$ and Fas which then activates MKK4 which can trigger continuous expression of ASK-1 which causes apoptosis through the mitochondrial-dependent cascade (Hatai, 2000, Tobiume et al., 2001).

The over expression of the ASK-1 can also inhibit TNFα and activate the Fas ligand to induce cell death (Sarker et al., 2003).

#### 1.6.4.2. JNK in Disease

##### 1.6.4.2.1. JNK in cancer

JNK activation has been implicated in several diseases including cancer and cardiovascular disease. The role of JNK isoforms within cancer is complex and renowned for their function as both oncoproteins and tumour suppressors. This role also differs depending on the cell type, as it can initiate cell proliferation and morphological changes (Wagner and Nebreda 2009). JNK has also been reported to be activated by key cancer treatments, such as radiation and chemotherapy (Stulpinas et al., 2024).

Cancer cells are known to use the JNK pathway to enable proliferation invasion and ultimately survival (Wagner and Nebreda, 2009). As AP-1 expression contributes to cell proliferation it is believed that the JNK pathway leads to an increase in cell proliferation, and when dysregulated can ultimately lead to cancer (Cellurale et al. 2011).

With respect to cancer, there have been several studies looking at the role of JNK using mouse models. Studies have found that JNK1 deficient mice display a decrease in carcinogen induced skin cancer whilst JNK2 deficient mice showed an increase (Cellurale et al., 2011).

In some cancer types, such as breast and pancreatic, MKK4 has been shown to be a tumour suppressor, as genetic inactivation of MKK4 on chromosome 17p (Wang et al., 2017a). When looking at breast cancer in particular, studies have shown that JNK pathway can suppress and drive tumour development (Cellurale et al., 2012, Chen et al., 2010). Cellurale et al. (2012), found that JNK deficiency led to an increased presence of breast cancer tumours in mammary glands in mice.

This suggested that JNK does play a role in the formation of mammary tumours. Whereas Chen et al. (2010) found that mice with JNK2 knockout express polyoma middle T antigen transgene, an oncogene that activates P13K and JNK, and have increased tumour with a reduced response to DNA damage (Chen et al., 2010). This all indicates that JNK does play an important role in cancer pathogenesis and the different isoforms have their own roles.

JNK has been implicated with both Doxorubicin and Cisplatin treatment of cancer (Brozovic et al., 2004, Kim and Freeman, 2003, Wu et al., 2019). Kim et al. (2003) have shown in breast cancer, using MCF-7 cells, that JNK plays an important role in Doxorubicin induced apoptosis and cell cycle withdrawal. By inhibiting JNK1 and c-Jun they were able to block differentiation and apoptosis therefore highlighting the role JNK can play in cancer treatments (Kim and Freeman, 2003). It is believed that Doxorubicin also initiates apoptosis by inducing AMP-activated protein kinase which activates p53 and JNK. Whilst p53 downregulates Bcl-2 and Bax proteins, JNK is believed to also mediate these proteins ultimately regulating apoptosis (Meredith and Dass, 2016). Bcl-2 is bound to the surface of mitochondria of which it has been linked to Doxorubicin JNK activation. Hoang et al. (2022) have suggested that mitochondrial ROS is the cause of Doxorubicin induced JNK activation. This was achieved through the blocking of JNK activation with an antioxidant that is selective for mitochondria in lung cancer cells (Hoang et al., 2022).

When looking into Cisplatin treatment of cancer, JNK is thought of as a double-edged sword, where it is responsible for cancer cell apoptosis but also resistance. As with Doxorubicin it has been documented that Cisplatin-mediated JNK activation is linked with p53 (Yan et al., 2016). Cisplatin treatment results in the increase of p53 which is activated by JNK resulting in cell cycle arrest and apoptosis. JNK is known to be activated by both the cis and transforms of Cisplatin which promotes the formation of complex between JNK and p73 leading to apoptosis (Jones et al., 2007). This has been reported in cases where tumours show inactive p53 resulting in an p73 mediated apoptotic response (Jones et al., 2007).

An example of this is a study by Jones et al. (2007) where H1299 cells a human lung cancer cell line, which lack p53, show that p73 is required for JNK-induced apoptosis (Jones et al., 2007). Also utilising wild type and JNK deficient MEFs (mouse embryonic fibroblasts) Jones et al. (2007) were used to illustrate that JNK is needed for p73 stabilisation and mediated apoptosis as a result of Cisplatin (Jones et al., 2007).

As previously mentioned, the accumulation of ROS activates p53 through JNK as shown in Doxorubicin. This activated p53 also increases ROS levels through pro-oxidant genes, further activating JNK thus resulting in apoptosis (Diao et al., 2010, Shi et al., 2014). Thus, sustained activation of JNK has been shown in ovarian carcinoma cells in response to Cisplatin where p53 is known to induce pro-apoptosis (Mansouri et al., 2003).

#### 1.6.4.2.2. JNK in other diseases

Aside from cancer, diabetes is known to induce oxidative stress leading to the activation of JNK, resulting in the suppression of insulin biosynthesis and the inability of insulin to function properly (Kaneto et al., 2005). JNK levels have also been found to be abnormally elevated in obesity and JNK1 has been shown to be involved with the development of type 2 diabetes (Jaeschke, 2004).

Obesity is known to cause JNK to phosphorylate adapter protein insulin receptor substrate, inhibiting the insulin receptor signals. JNK has therefore been implicated with the development of type 2 diabetes (Jaeschke, 2004). Jaeschke et al. (2004) have shown that the JNK interacting protein 1 scaffold is vital for JNK activation in the adipose tissue of obese mice. This link between JNK activation and diabetes could enable a target to prevent the development of diabetes. Similarly, Lanuza-Masdeu et al. (2013) were able to show that JNK activation could prevent insulin signalling in pancreatic β cells causing insulin resistance, without causing cell death (Lanuza-Masdeu et al., 2013). However, when JNK has been downregulated, insulin sensitivity is improved, indicating that JNK performs a crucial role in obesity and insulin resistance (Hirosumi et al., 2002).

Jaeschke et al. (2005) have also shown that JNK2 plays a role in type 1 diabetes, that is caused by autoimmune destruction of the β cells. They have shown that by disrupting the MAPK9 (the gene that encodes JNK2) there was an overall decrease in insulitis and reduced disease progression (Jaeschke et al., 2005).

#### 1.6.4.2.3. JNK in cardiovascular diseases

JNK has also been linked with heart disease, a major cause of mortality worldwide. It is believed that JNK is activated in ischaemic heart disease by oxidative stress caused by the generation of ROS, and in rat hearts JNK translocated into the nucleus during ischaemia and is phosphorylated during reperfusion (Clerk, 1998, Mizukami and Yoshida, 1997). Enhanced activation of JNK and p38 have also been observed in left ventricular tissue from patients with ischaemic heart disease, indicating it may play a role in the pathophysiology of the disease (Cook et al., 1999). Hypertrophic remodelling is a result of acute and chronic injury to the heart, of which signalling regulation is hypothesized to be the underlining cause. Cardiac hypertrophy is due to JNK activation inhibiting NFAT (nuclear factor of activated T- cell) (Liu et al., 2009). Maillet et al. (2009) have also shown that inhibiting the calcineurin NFAT activity reduced hypertrophy and can prevent heart failure (Maillet et al., 2009).

They achieved this by showing that cdc42 activated by JNK reduces calcineurin NFAT activity using mouse models with a cdc42 cardiomyocyte deletion (Maillet et al., 2009). Similarly, Kaiser et al. (2005) found that sustained JNK activation or inhibition both showed cellular protection, though they hypothesised that this was due to a different mechanism (Kaiser et al., 2005). Ischaemia/reperfusion injury is known to induce organ dysfunction in many disease states that include angina and myocardial infarction (Hreniuk et al., 2001). Hreniuk et al. (2001) found that the inhibition of JNK1 resulted in cardiac myocyte protection from ischaemia induced apoptosis, whereas JNK2 had no effect (Hreniuk et al., 2001).

The reperfusion injury has been linked to a number of mechanisms which include the generation of oxygen free radicals, postischaemis inflammation and calcium hemostasis (Ambrosio and Tritto, 1999, Hreniuk et al., 2001).

MKK7 has been shown to be vital in protecting cardiomyocytes against overload pressure (Liu et al., 2011). MKK7 knockout mouse models show increased ROS and in turn an increase in cardiomyocyte apoptosis (Liu et al., 2011). It is believed that JNK is activated in ischaemic heart disease by oxidative stress, caused by the generation of ROS (Clerk, 1998, Mizukami and Yoshida, 1997). It has been seen in rat hearts that JNK translocates to the nucleus during ischaemia and is phosphorylated during reperfusion (Clerk, 1998, Mizukami and Yoshida, 1997).

As already discussed, JNK plays a large role in cardiovascular disease, it has also been shown in endothelial damage and atherosclerosis (Amini et al., 2014). Li et al. (2021) investigated the link between endoplasmic reticulum/mitochondrial damage and endothelial dysfunction. They determined using HUVECs that endoplasmic reticulum markers such as CHOP and PERK were elevated in response to oxidised low-density lipoprotein. This also increased mitochondrial ROS levels and was found to activate the JNK pathway (Li et al., 2021). The levels of oxidised low-density lipoprotein were blocked by melatonin, and subsequently the activation of JNK protecting the endothelial cells from damage.

JNK has also been largely linked with atherosclerosis, where all cell types involved in atherosclerosis express JNK 1 and 2, endothelial, smooth muscles and T cells for example (Craige et al., 2019). Studies have shown JNK2 promoted atherosclerosis by increasing macrophage uptake of lipids, causing the formation of foam cells (Ricci et al., 2004). Whilst Liu et al. (2022) found that suppressing the ASK1-JNK signalling could reduce atherosclerosis. Using wild type and myeloid major vault protein knockout mice, they found that myeloid major vault protein prevented JNK signalling and alleviate unstable plaque formation (Liu et al., 2022).

JNK has been implicated in several diseases as already explored. For a number of these conditions the idea of inhibiting JNK has been studied from cardiovascular toxicities to neurological disorders. Studies have found that by inhibiting JNK signals it decreased apoptosis seen in both cardiomyocytes and endothelial cells (Bennett et al., 2001, Xu et al., 2015). Due to the implication of JNK in apoptosis inhibiting JNK could be an effective therapeutic tool (Nadel et al., 2023). As outlined in this section, JNK has been implicated with endothelial cell damage after cancer treatment. Therefore, it is important to investigate these effects in the aim to find a novel therapeutic target.

## 1.7. Aims

As discussed, cardiovascular toxicities are a significant side effect of anti-cancer treatment, which is a neglected health problem worldwide. Previous studies have shown that this damage is likely to manifest in the endothelium. Therefore, endothelial cells have been shown to be a useful target for this, however few studies have investigated the mechanisms behind this in detail. Therefore, the objective of this was to investigate the role of JNK in endothelial cell damage and cardiovascular toxicities caused by chemotherapeutic agents and radiation.

The purpose of this study was to investigate the effect chemotherapeutic agents have on an endothelial cell line (HUVEC) and the JNK pathway. We hypothesize that by inhibiting the JNK pathway, endothelial damage due to anti-cancer treatments would be significantly reduced.

The main aims of this project are outlined below:

- Characterise radiation and chemotherapeutic induced JNK signalling in endothelial cells.
- Inhibit the JNK pathway in endothelial cells.
- Determine if JNK has a role in the modulation of other pathways involved in endothelial cell damage.
- Investigate the effect JNK inhibition has on endothelial cells as a result of anti-cancer treatments.

# Chapter Two

**Materials and Methods**

# 2. Materials

## 2.1. General Materials

All materials and reagents used unless otherwise stated were obtained from Sigma Aldrich Chemical company Ltd (Pool, Dorset, UK).

### 2.1.1. Thermo Fisher Scientific UK Ltd (Leicestershire, UK)

Bovine Serum Albumin (BSA)

TrypLE™ Express

Fetal Bovine Serum (FBS)

Dithiothreitol (DTT)

4’6-diamidino-2-phenylindole (DAPI)

L-Glutamine

GibcoTM Penicillin-Streptomycin

GibcoTM Fetal Bovine Serum

Hypoxanthine, aminopterin and thymidine

Dulbeccos Modified Eagle Medium (DMEM)

Invitrogen™ CyQUANT™ LDH Cytotoxicity Assay

Cell culture plates and dishes

### 2.1.2. GE healthcare Ltd (Buckinghamshire, UK)

AmershamTMProtramTM – ECL nitrocellulose membrane

### 2.1.3. Lonza (Slough)

Endothelial Cell Basal Medium -2 (EMB-2)

Endothelial Growth Media (EGMTM-2) SingleQuots

### 2.1.4. Bio-Rad Laboratories (Hertfordshire, UK)

Bio-Rad AG® 1-X8 Resin, pre stained SDS-Page molecular markers

Precision Plus Protein Dual Colour Standard

Protein assay dye reagent concentrate

### 2.1.5. Promocell Gmbh (Heidleburg, Germany)

Endothelial Cell Basal Medium MV 2

Endothelial Cell Growth Medium MV 2 Supplemental Pack

Freezing Medium Cryo-SFM

### 2.1.6. Santa Cruz Biotechnology

Recombinant human TNF-α

### 2.1.7. Sarstedt AG & Co Ltd (Leicester, UK)

Serological pipette 5 ml

Serological pipette 10 ml

Serological pipette 25 ml

### 2.1.8. Corning B.V (Buckinghamshire, UK)

Tissue Culture flasks, 10cm dishes, graduated pipettes and falcon tubes

### 2.1.9. Insight Biotechnology Ltd (Middlesex, UK)

Recombinant human IL-1β

Recombinant human TNF-α

### 2.1.10. Whatmann (Kent, UK)

Nitrocellulose membrane, 3MM Blotting paper

### 2.1.11. CRISPR

#### 2.1.11.1. Sigma Aldrich

gRNA oligo

PEI linear polyethylenimine

Target sequences for CRISPR:

**Table 2.1 JNK1 and JNK2 targeting sequences**

Sequences selected using Synthego and ChopChop, online tools for genomic engineering.

| MAPK8 (JNK1) | Online tool | Sequences |
|---|---|---|
| JNK1,1 | Synthego | AGAAUCAGACUCAUGCCAAG |
| JNK1,2 | ChopChop | AACACCCGTACATCAATGTC |
| MAPK9 (JNK2) | | |
| JNK2,1 | Synthego | CUGCAUUUGAUACAGUUCUU |
| JNK2,2 | ChopChop | GAGAACGGTGAGTATAGCCG |

### 2.1.11.2. Addgene

Cas9 plasmid - pSpCas9-2A-Puro (1.24 µg/µl)

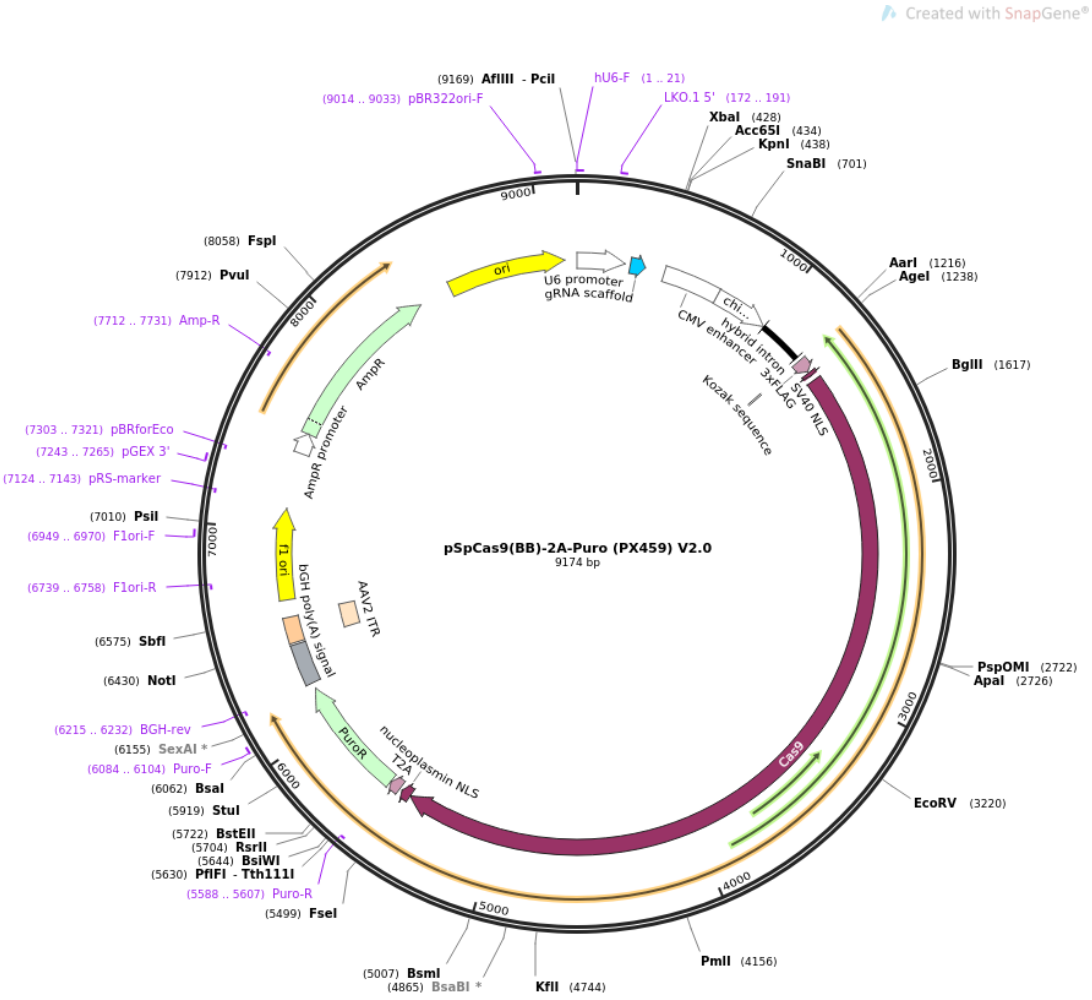


**Figure 2.1 Doxorubicin Cas9 plasmid**.

pSpCas9(BB)-2A-Puro (PX459) V2.0 was a gift from Feng Zhang (Addgene plasmid #62988; http://n2t.net/addgene:62988 ; RRID:Addgene_62988). Cas9 plasmid containing Puromycin resistant gene allowing for selection of cells containing desired knockout. Received as a glycerol stock

### 2.1.12. Qiagen

Qiagen Endofree Plasmid Maxi Kit

Qiagen Endofree Plasmid Midi Kit

### 2.1.13. Thermofisher

GeneJet PCR Purification kit

Parafilm

## 2.2. Methods

### 2.2.1. Cell Culture

All cell culture work was carried out under aseptic conditions in a class II culture hood (Haraeus instruments)

#### 2.2.1.1. EAhy926 Cells

EAhy926 (endothelial cells and lung adenocarcinoma hybrid) cells were cultured in 75cm$^3$ culture flasks with medium comprised of Dulbeccos Modified eagle Medium (DMEM) containing sodium pyruvate, pyridoxine hydrochloride and high glucose (Invitrogen, Paisley, UK), 10% Hi-FCS, 2mM L-glutamine, 100U/ml penicillin, 100µg/ml streptomycin and 10% HAT. Cells were cultured at 37°C in a humidified atmosphere of 5% $CO_2$. The medium was replaced every two to three days to maintain a healthy culture, and sub-cultured when 80% confluency was reached by trypsinization.

#### 2.2.1.2. Human Umbilical Vein Endothelial Cells (HUVECs)

HUVECs purchased from Lonza were Cryopreserved pooled HUVECs ≥ 500,000 cells/ml. They were cultured in endothelial basal medium containing EGM-2 SingleQuots Supplements (2% foetal bovine serum, hydrocortisone, hFGF-B, VEGF, R3-insulin like growth factor-1, ascorbic acid, hEGF, GA-1000 and heparin). Cells were seeded in T-75 flasks and incubated in 5% $CO_2$ at 37°C with media changed twice a week. Cells were passaged at 80% confluency using TrypLE™ Express until cells detach. Cells were washed down with media before centrifuging at 600 rpm for 5 minutes, the supernatant was aspirated, and the pellet was resuspension in 10 ml of fresh media. The cell suspension was diluted into T-75 flasks or seeded into appropriate plates using fresh media and used until passage 7.

### 2.2.2. Western Blots

#### 2.2.2.1. Preparation of whole cell extracts

HUVECs were grown in 12 wells plates till 80% confluency and stimulated with 10µl of the appropriate reagent at differing time points up to 24 hours and concentrations 0.1-100µM for Doxorubicin and Sunitinib and 0.1-300µM for Cisplatin. The plates were placed on ice, the monolayer was washed with 1ml ice cold PBS before 100µl of preheated Laemmlis sample buffer (LSB) (63mM Tris-HCL, (pH6.8), 2mM Na4P2O7, 5mM EDTA, 10% (v/v) glycerol, 2% (w/v) SDS, 50mM DTT, 0.007% (w/v) bromophenol blue) was added. Using the rubber end of a plunger, cells were scraped, and the DNA sheared by repeatedly passing the sample through a 23-gauge syringe. The samples were transferred into labelled 1.5ml Eppendorf with punctured lids and boiled for 5 minutes to denature the sample proteins and stored an -20$^{o}$C until required.

#### 2.2.2.2. SDS-Polyacrylamide gel electrophoresis (SDS-PAGE)/ western blotting

Two 1mm plates are sandwiched together and set in a Bio-Rad frame, these are then checked for leaks using $dH_2O$.10% resolving gels were prepared; (10% (w/v) acrylamide: [N, N' – methilenebis-acrylamide (30:0.8), 375mM Tris base (pH8.8), 0.1% (w/v) SDS and 10% (w/v) ammonium persulfate (APS), $H_2O$ and with N,N,N',N' – tetramethylethylenediamine (TEMED) added to initiate polymerization. The gel was added between the plates approximately 2/3 of the way up and 0.1%SDS was added. Once set the SDS was removed and the stacking gel comprised of $H_2O$, 125mM Tris base, 0.1% (W/V) SDS (pH6.8), acrylamide solution 10% APS and 0.05% (v/v) TEMED was prepared. This was added to the resolving gel and a 10 well comb promptly inserted between the plates. Once the stacking gel had set the plates were released from the frame and the comb removed, before being assembled in a Bio-Rad Mini-PROTEAN II™ electrophoresis tank. The tank was filled with running buffer ($H_2O$, 25mM Tris Base, 0.1% (w/v) and 192mM glycine). A 6µl of low molecular marker and 20µl of samples (10-15mg of protein routinely) were added to the wells of the gel using a Hamilton syringe. This was run at 130v for 1 hour and 45 minutes or until the blue of the sample buffer had ran off the gel.

#### 2.2.2.3. Electrophoretic transfer of proteins to nitrocellulose membrane

Following SDS-PAGE the proteins are then transferred onto a nitrocellulose membrane. 2 sheets of filter paper, 2 sponges and nitrocellulose blotting membrane, were all soaked in Running buffer (25mM Tris Base, 192mM glycine, 20% (v/v) Methanol and $H_2O$). The gel placed on the nitrocellulose membrane and sandwiched between the filter paper and sponges in a cassette. This cassette is then placed into a BIO-Rad Mini protean tank, with the addition of an ice pack. The tank was filled with running buffer and ran at 280mA for 110 minutes.

#### 2.2.2.4. Immunological detection of protein

Once the proteins have transferred onto the nitrocellulose membrane, any remaining protein was blocked by incubating the membrane at room temperature in 20ml of 30% Bovine Serum Albumin (BSA)(w/v), diluted in a 0.03% sodium Tris-Tween NATT buffer (150mM NaCl, 20mM Tris Base in $dH_2O$ pH7.4 (Hydrochloric acid was used for pH adjustment). This was incubated for 2 hours at 43rpm on a platform shaker. The BSA was removed, and the primary antibody (Table 2) was diluted in 0.3% BSA and added to the nitrocellulose membrane in a 50ml falcon tube and incubated in the cold room (2-4℃) overnight at 43rpm on a roller.

The following day the primary antibody was removed, and the membrane was washed using NATT for an hour and a half (exchanging the NATT every 20 minutes). The secondary antibody diluted in 0.3% BSA was added to the membrane and incubated at room temperature for 2 hours at 43rpm. The HRP (horseradish peroxidase) conjugated secondary antibody (table 2.2).

The secondary antibody was then removed, and the membrane was washed for a further hour and a half (with a NATT exchange every 20 minutes).

Once the final wash had been removed, the membrane was incubated in 4ml of enhanced chemiluminescence ECL1 and ECL2 respectively for 2 minutes. The membranes were then dried on paper towel and placed on an exposure cassette covered in clingfilm. The membranes were then exposed to Kodak X-OMAT Ls film for the required time and the JP-33 film processor was used to develop the film.

#### 2.2.2.5. Re-probing

The membranes were then stripped and re-probed for total protein. Membranes were stripped of the antibodies using Stripping buffer (2% SDS and 48mM of Tris-HCL) with 100mM beta-mercaptoethanol, for 50 minutes on a heated shaker at 60℃ at 43rpm. The nitrocellulose membranes were then washed with NATT 3 times changing the NATT every 5 minutes. The membranes were then left to incubate over night with the primary antibody diluted in 0.3% BSA Total P65 was incubated at room temperature in 15ml 0.3% BSA. The next day, day 2 of the western blot procedure was followed (as detailed in section 2.2.2.4).

### 2.2.2.6. Scanning and densitometry

The films were then scanned using the HP Deskjet 3520 scanner and saved as tiff files. The images were quantified using image J, where they were normalized against the total protein densitometry values. Statistical analysis and graphs were then produced using Graphpad prism 9.

**Table 2.2 Antibody Optimisation**

Information on antibodies used which includes the name and manufacturer.

| **Antibody** | **Dilution** | **Manufacturer** |
|---|---|---|
| Anti-P-SAPK/JNK | 1:1000 | Cell Signaling |
| JNK | 1:1000 | Cell Signaling |
| Phospho-NF-κB p65 (Ser536) | 1:3000 | Cell Signaling |
| NF-κB p65 (F-6) | 1:3000 | Santa Cruz |
| pATM | 1:1000 | Cell Signaling |
| ATM | 1:1000 | Cell Signaling |
| Caspase 3 | 1:1000 | Cell Signaling |
| yH2AX | 1:6000 | Cell Signaling |
| GSDME | 1:1000 | Cell Signaling |
| GAPDH | 1:150,000 | Cell Signaling |
| HRP-conjugated AffiniPure Goat Anti-rabbit IgG | 1:7500 | Jackson ImmunoResearch Laboratories |
| HRP-conjugated AffiniPure Donkey Anti-mouse IgG | 1:10,000 | Jackson ImmunoResearch Laboratories |

### 2.2.3. Clonogenics

350 HUVECs were seeded into 6cm dishes in triplicate and incubated at 37°C and 5% $CO_2$ overnight. After 24 hours the plates were x-irradiated at 2 and 5Gy. After 24 hours the media was then exchanged, and the cells were left for 10-15 days. The media was removed, and cells were washed with ice cold PBS then fixed with methanol for 10 minutes and stained with Giemsa for 20 minutes. The stain was removed, and the dishes rinsed with water. Colonies were counted by hand and the following equation was used to calculate the plating efficiency (PE) and survival fraction (SF):

$$PE = \frac{Average\ no.of\ control\ colonies}{no.of\ seeded\ cells}$$

$$SF = \frac{Average\ no.of\ colonies\ formed\ after\ treatment}{no.of\ seeded\ cells\ X\ PE}$$

### 2.2.4. MTT Assay

Using a 96 well plate HUVECs were seeded at $5x10^4$ cells/ml and incubated at 37°C 5% $CO_2$ overnight. They were then stimulated for a 24 and 48 hours respectively with Doxorubicin and Sunitinib (0.1-100µM) and Cisplatin (0.1-300µM). Once the stimulation has finished media was replaced by 100µl of fresh media and 10µl of MTT (3-(4,5-dimethylthiaxolyl-2)-2,5-diphenyltetrazolium bromide (10mg/ml) (Sigma Aldrich). The cells were then incubated for 2 hours at 37°C 5% CO2. The media was then replaced with 100µl of DMSO (Dimethylsulfoxide) (Sigma Aldrich) and the cells were incubated for a further 5 minutes at 37°C 5% $CO_2$. The plates were then quantified using POLARstar Omega plate reader at 570nm. Results were then shown as percentage of cell only control.

### 2.2.5. Adv.NLS-1 MKP-2 Transfections

Adenoviral vectors encoding MKP-2 (Adv.NLS-1 MKP-2) were created with the Adeno-X virus purification kit from Clontech Laboratories, Inc. (Mountain View, CA, USA) in-house. HUVECs, when approximately 50–60% confluent, were incubated with adenovirus up to 300pfu per cell for 40 hours in HUVEC growth media, with a media change after 16 hours. Cells were stimulated at 80% confluency with Doxorubicin (30 and 100µM) and Cisplatin (100 and 300µM) for the 24 hours in HUVEC growth medium.

### 2.2.6. Flow cytometry assay of apoptosis using fluorescence activating cell sorting (FACS)

HUVECs were grown in 12 wells plates till 80% confluency and stimulated with 10µl of the appropriate reagent at differing time points up to 24 hours and concentrations 0.1-100µM for Doxorubicin and Sunitinib and 0.1-300µM for Cisplatin. The media was collected from each well and placed into corresponding FACs tube. The cells were dissociated using Tryple E and added to the respective FACs tube. The cells were centrifuged for 5mins at 1000rpm, the supernatant was removed, and the cells were washed twice with PBS. 100µl of binding buffer (10mM HEPES/NaOH (pH7.4), 140nM NaCl and 2.5mM CaCl2) was added to each tube. 5µl of Annexin V was added to all sample tubes and appropriate controls, vortexed and incubated for 2 mins. The tubes were covered and incubated at room temp for 15 mins. 400µl of PI (Propridium Iodide and binding buffer) added to all tubes except control unstained and Apoptosis control and vortex. Samples were read using the Thermo Fisher Scientific 3 Laser (BVR) Attune NxT Flow Cytometer and analysed using Attune NxT Software. Cells were gated and analysed as a percentage of cells

counted as shown by figure 2.2

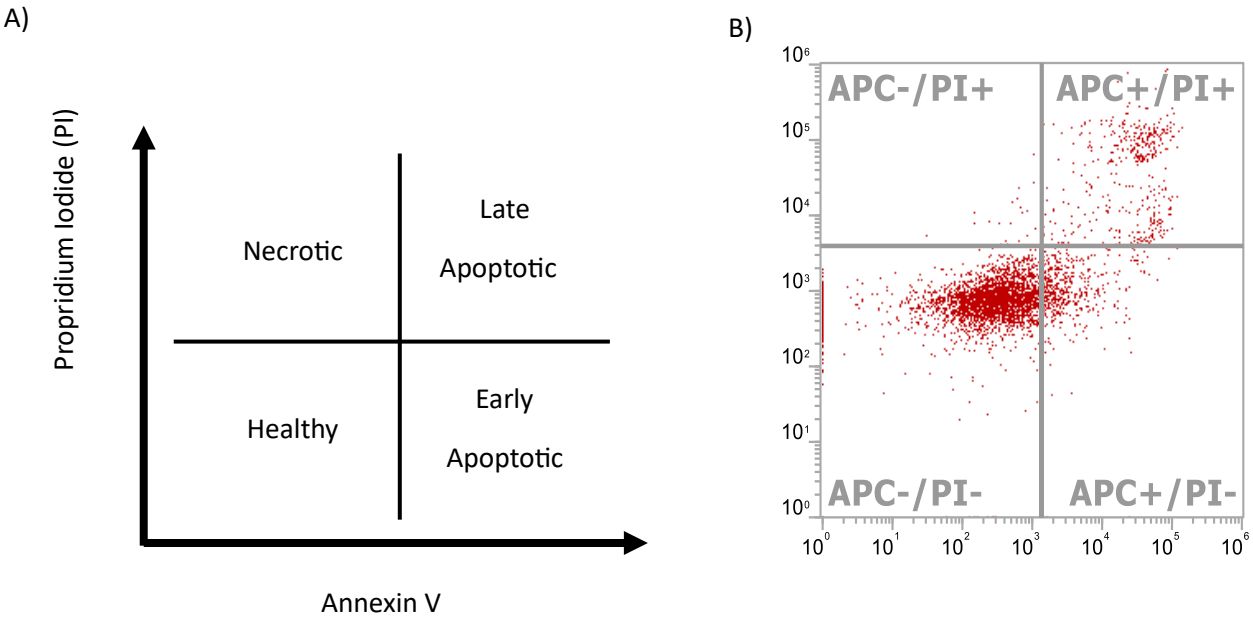


**Figure 2.2 Parameters used for FACs analysis**

A) Illustration of gating used for FACs analysis. B) representative example of untreated HUVECs stained with annexin V and PI

### 2.2.7. Irradiation exposure

The X-RAD 225 Biological Irradiator (225kV, 13mA) were used to irradiate HUVECs. Cells were seeded at 1 in 10 plated into 6cm dishes until 80% confluency and exposed to 5Gy. X-rays were at a fixed dose rate, of 2.3Gy/min at room temperature. For sham irradiation controls, cells were placed in the X-RAD for the same duration as the longest exposure, with x-rays not emitted. Cells were immediately returned to an incubator (37°C 5% $CO_2$) after irradiation. These cells were then prepared as stated in 2.2.2.1 for western blots.

### 2.2.8. Cytotoxicity Assay

Using the Invitrogen™ CyQUANT™ LDH Cytotoxicity Assay Quantity, a 12 well plate was seeded with HUVECs at a seeding density of 1 in 10 until 80% confluent. These cells were then treated with Doxorubicin (0.1-100µM) and Cisplatin (0.1-300µM) respectively with appropriate controls for 24 hours. 100µM of media was taken from 12 well plates in triplicate and transferred to a 96 well plate. 10µl of 10X lysis buffer in sterile water was added to the wells mixed by tapping gently and incubated at 37°C for 45minutes. 50µl of media from each well was then transferred into a flat bottomed 96 well plate in triplicate. 50µl of Reaction Mixture was then added to each well and mixed by gently tapping. The plate was then incubated at room temperature in the dark for 30 minutes. 50µl of stop solution was then added and mixed by gently tapping the plate. The absorbance was the read on a plate reader at 490nm and 680nm respectively. Cytotoxicity was then calculated by using the following equation:

$$\%\ Cytotoxicity = \frac{Compound\ treated\ LDH\ activity - spontaneous\ LDH\ activity}{Maximum\ LDH\ activity - Spontaneous\ LDH\ activity}\ x\ 100$$

### 2.2.9. Immunofluorescence

#### 2.2.9.1. Slide preparation.

HUVECs were seeded at 1 in 10 onto coverslips in 12-well plates and incubated at 5% $CO_2$, 37°C. At 60% confluency, cells were treated with Doxorubicin and Cisplatin respectively. Plates were then placed on ice, media aspirated and washed twice with 1 ml PBS. The coverslips were transferred to a new plate and incubated in 1 ml methanol for 10 minutes. Coverslips were then washed twice with 1 ml PBS then incubated in 1 ml Quench solution (50 mM ammonium chloride, 0.2% Triton-X-100) for 5 minutes. Quench solution was aspirated, and another the cells were incubated in 1 ml of Quench solution for a further 5 minutes. After the final quench incubation, the coverslips were washed twice with PBS before incubation with 1 ml blocking solution (1% BSA, 5% FBS, 0.2% Triton X-100, PBS) for 25 minutes. Primary antibodies were prepared using an antibody dilutant (1% BSA, 5% FBS, PBS) and 50µl of antibody was placed onto parafilm. Coverslips were then dipped in PBS and inverted cells down into the appropriate primary antibody and incubated in the dark for 30 minutes. FITC-conjugated secondary antibodies were prepared using the antibody dilutant and 50µl of antibody was again placed on fresh parafilm. Coverslips were dipped three times in PBS and inverted onto appropriate secondary antibody and incubated for 30 minutes in the dark. The DAPI counter stain was prepared by diluting 1:12,000 in PBS and 50µl was added to fresh parafilm. Coverslips dipped three more times in PBS, inverted onto DAPI and incubated in the dark for 12 minutes. Finally, the coverslips were washed again in PBS three times and inverted cells down onto a glass microscope slide. These slides were then stored at 2-8°C away from light for at least 24hours before imaging.

#### 2.2.9.2. Imaging

Slides were imaged using an Epifluorescent Upright Microscope with a Nikon Eclipse E600 camera attached using Metamorph software. ImageJ was used to merge images and add scale bars.

### 2.2.10. Brightfield Imaging

HUVECs were grown in 12 wells plates till 80% confluency and stimulated with 10µl of the appropriate reagent at differing time points up to 24 hours and concentrations 0.1-100µM for Doxorubicin and Sunitinib and 0.1-300µM for Cisplatin. These cells were stimulated as Cell morphology and growth imaged using Images were obtained using a Nikon Eclipse (TE300) inverted microscope, with a Leica EC3 digital camera affixed to a Leica DM IL LED inverted microscope. With images captured at x40 magnification. Image J was used to add scale bars.

### 2.2.11. Statistical Analysis

All statistics were calculated using GraphPad Prism version 9.3.1. Statistical significance of datasets was determined using a one-way ANOVA and Dunnet's multiple comparisons test or a paired non-parametric t test. P values $<0.05$ were considered significant and means ± standard error of the mean (SEM) was represented in all figures.

### 2.2.12. CRISPR

#### 2.2.12.1. gRNA design

As detailed in Chapter 4, two online tools were used to select target sites for JNK gRNAs. ChopChop and Synthego were used to find potential target sites for MAPK8 (JNK1) and MAPK9 (JNK2). 4 potential sequences were selected These sequences were then checked using the Santa Cruz Genome browser BLAT function to ensure that these sequences are accurate for their target site. The sequences where then ordered for both the 5' and reversed 5' sequences to total 8 sequences.

**Table 2.3 JNK gRNA sequences**

| | Sequences | 5' Forward | 5' Reversed | Source |
|---|---|---|---|---|
| MAPK8 (JNK1) | | | | |
| JNK 1,1 | AGAAUCAGACUC AUGCCAAG | CACC/AGAATCAGACT CATGCCAAG | AAAC/CCTTGGCATGA GTCTGATTCT | Synth ego |
| JNK 1,2 | AACACCCGTACAT CAATGTC | CACC/TCGCTACTACA GAGCACCCG | AAAC/CGGGTGCTCT GTAGTAGCGA | ChopC hop |
| MAPK9 (JNK2) | | | | |
| JNK 2,1 | CUGCAUUUGAUA CAGUUCUU | CACC/CTGCATTTGAT ACAGTTCTT | AAAC/AAGAACTGTAT CAAATGCAG | Synth ego |
| JNK 2,2 | GAGAACGGTGAG TATAGCCG | CACC/GAGAACGGTG AGTATAGCCG | AAAC/CGGCTATACTC ACCGTTCTC | ChopC hop |

Once the complementary strands were completed and reversed CACC was added to 5' forward and AAAC to the 5' reversed strand as indicated in table 2 To allow for complementary cut sites.

### 2.2.12.2. Cas9 purification

3 Agar plates were prepared containing 60µg/ml of Carboxacilin using aseptic conditions a sterile loop was used to retrieved plasmids from the original vial and spread over the agar plate. This was repeated three times. The plates were then incubated at 37°C overnight. The next day LB broth was prewarmed and 5mls added to 6 universal tubes. Using Aseptic techniques, a single colony was selected using a sterile pipette tip and added to the universal. This was repeated twice for each plate. The universals were then incubated at 37°C at 250rpm until turgid. Transfer 10mls of prewarmed LB broth to new universal tubes and add 500ul from the most turbid universal for each, return to the incubator and shake at 37°C. the next day 500ul of culture was added to 100mls of prewarmed LB Broth in a sterile conical flask and incubate shaking at 37°C. the next day the Endo-free maxi kit was used following manufacturer's instructions.

### 2.2.12.3. Restriction Digest

Restriction digest was set up with the plasmid vector, Buffer G, RNAse free water and Bbs1 enzyme that correlates to the Cas9. This mixture was incubated at 37°C at 5% CO2 for 2-3 hours. To allow for the plasmid to be cut into a linear strand removing the existing gRNA.

#### 2.2.12.4. Annealing Step

The 2 oligo strands (top and bottom strands) were combined with annealing buffer. Firstly, each oligo was reconstituted with TE buffer to a total concentration of 100µM (each oligo has a different stock concentration detailed on the information sheet provided from Sigma Aldrich) and vortexed thoroughly. The mixture was vortexed and briefly centrifuge. This mixture was placed in a tub of boiling water and sealed. This was left to gradually cool for around 3 hours and placed in the fridge overnight.

#### 2.2.12.5. Plasmid purification

Using the GeneJet PCR Purification kit. Restriction digest is removed from the incubator and made up to 100µl with TE buffer (80µl). an equal volume of binding buffer (provided in the kit) was added. The mixture was added to a purification column and vortexed. The flow through was then discarded and the column was washed as per the kits instructions. The column was then transferred to a new Eppendorf with prewarmed elution buffer added directly to the column. This was left to stand at room temperature for 1 minute and the elutant collected in the Eppendorf. This purified Cas9 was stored in the freezer until required.

#### 2.2.12.6. Ligation

Buffer, annealed Oligos, purified plasmid, RNAse free water and T4 DNA Ligase were vortexed then centrifuged and left at room temperature for 15minutes before being stored in the fridge overnight. For a negative control extra water was added to replace the oligos.

### 2.2.12.7. Purifying Oligos

Firstly, an agar plate was prepared for each ligation, positive and negative control, containing carbacillin (60µg/ml) and left to dry in a fume cupboard. The ligation tubes were removed from the fridge and 5µl added to a labelled Eppendorf tube stored on ice. Competent cells were then added to the ligation mix and gently mixed prior to a 30-minute incubation on ice. The cells were then heat shocked at 42˚C for exactly 30 seconds before being returned to ice. LB was then added to each tube without mixing and incubated in a shaking incubator at 250rpm 37℃ for 1 hour.

The contents of each tube were then poured on to the corresponding agar plate, and a spreader was used to ensure an even distribution on the agar plate. The plates were left in a fume cupboard to dry for around 30 minutes. After 30 minutes the plates are incubated overnight at 37˚C and returned to the fridge until required.

### 2.2.12.8. Selecting colonies

Ensuring the negative control is blank and the other plates contain colonies, universal tubes with 10mls of LB broth and 10µl of antibiotic was prepared for 2 colonies per agar plate. A single colony was selected with a pipette tip and added to the universal. This was then incubated at 220rpm 37℃ overnight.

### 2.2.12.9. Isolate II plasmid mini kit

Firstly, bacterial cells were harvested by each universal centrifuged at 3000rpm for 15 mins, the supernatant was removed, and tubes left to dry.

The cells were then lysed by adding resuspension buffer 1 and resuspending the pellet. Lysis buffer P2 was then added and inverted 8 times. This was then incubated at room temperature for 5 minutes. The neutralising buffer was added and inverted 8 times, the lysate was then spun for 5 minutes at 11000xg at room temperature.

To allow the DNA to bind a spin column was placed in a collection tube and sample was added to the column. This was then centrifuged at 11000xg for 1 minutes and the supernatant was discarded.

To wash the membrane, wash buffer PW1 was supplemented with ethanol and added to the pellet. This was then spun for 1 minute at 11000xg and supernatant was discarded.

To dry the membrane the tube was spun for a further 2minutes at 11000xg to remove the remaining ethanol and the column was placed in an Eppendorf tube.

Finally, to elute the DNA, elution buffer was added to the column and incubated at room temperature for 1 minute. Then centrifuged at 11000xg for a further minute. This was then added to the purified DNA and stored in the freezer until required.

A gel was then prepared for electrophoresis. 100mls of 1% agarose gel was prepared using Tris Borate Buffer (TBE) composed of Tris base, Boric acid and EDTA, this was poured into a gel cast and left to set for 30-60 minutes. The gel was then placed in the PCR tank with TBE, a 7µl ladder and 10µl of sample was added into the wells. The sample was prepared by mixing 1µl of 6x dye, 3µl of $dH_2O$ and 2µl of DNA. The gel was run for around 1 hour at 100 volts until samples are halfway down the gel. The gels were then scanned and saved.

A sample of each was also sent to SourceBioscience for genetic sequencing to confirm the correct sequence has been isolated.

#### 2.2.12.10. Kill curves

Using a 24 well plate, EAhy926 were seeded at 1 in 5 until 80% confluency and added to the plate with media containing the antibiotics. Concentrations of puromycin ranging from 0.1 to 3µl were added to the wells. The wells were checked every day to record cell death. The media containing antibiotics was replaced every 3 days for 14 days.

### 2.2.12.11. Transfections

EAhy926 cells were plated in 6 well plates to 60-70% confluent. PEI was defrosted and vortexed before being combined with DNA and media or media alone for controls. These were then left to incubate for 10-15minutes, when the cell plate was given fresh media. 200µlof the appropriate mixture was then added to the each well drop by drop. The plates were then returned to the incubator, with a media change the next morning. After 48 hours the cells were then treated with antibiotic media to ensure the survival of the successful transfection cells.

# Chapter Three

## Characterisation of Chemotherapeutic Agents on the JNK Pathway and Cell Viability

# 3. Characterisation of Chemotherapeutic Agents on the JNK Pathway and Cell Viability

## 3.1. Introduction

As previously discussed, the effect of cardiovascular toxicities as a result of cancer treatment is a major health concern. It has been reported that treatments such as Doxorubicin, Cisplatin and Radiotherapy are all responsible for such side effects. The use of Doxorubicin for example, has recorded a mortality rate that can be as great as 50% within 2 years (Sheibani et al., 2022). As mentioned in chapter 1, the results of cardiovascular toxicities can take over 10 years post treatment to present itself with damage incurred believed to begin with the endothelium (Clark et al., 2019, Steinherz, 1991).

The endothelium lines the vascular system and is therefore the first form of contact that chemotherapeutic compounds have with the body. The first form of damage, known as endothelial dysfunction, can present as foam cell formation, plaque formation and rupture (Gimbrone and García-Cardeña, 2016). As a result, such damage is known as the precursors of atherosclerosis, which can have fatal consequences (Chatterjee et al., 2009, Libby, 2012). Therefore, it is proposed that any change in the endothelium leading to cardiovascular toxicities caused by treatment including radiation would start with endothelial cells. Several studies looking into the damage to the endothelium have implicated the JNK pathway (Al-Mutairi et al., 2010, An et al., 2018, Feng et al., 2020).

The JNK pathway, as previously stated, is a stress activated member of the MAPK family. It regulates a number of roles including immune responses and cell death signalling (Mailloux et al., 2001). JNK has been shown to play a major role in endothelial damage and which is activated by several different stimuli (Wang et al., 2012). It has therefore been hypothesised that anti-cancer treatments play a major role in the activation of this stress activated MAPK pathway.

It is hoped that by knocking out or inhibiting the JNK pathway the resulting damage could be prevented. And provide novel models to enable more thorough investigations in the effects.

In this chapter the effect chemotherapeutic compounds and radiation have on the endothelium has been characterised using a human endothelial cell line, HUVECs (Human Umbilical Vein Endothelial Cells). Such analysis was carried out to investigate the effect the treatments have in relation to the JNK pathway. Fully understanding the effect of these treatments via the JNK pathway in HUVECs, could highlight the use of JNK as a novel therapeutic target.

## 3.2. Results

### 3.2.1. Doxorubicin induced JNK signalling in HUVECs

The preliminary experiments carried out were to determine if there is activation of the JNK pathway in HUVECs. As previously mentioned, it is important to understand if the damage caused by cardiovascular toxicities involve the JNK pathway. To do this the activation of the pathway was investigated initially using a known agonist, TNFα, in the endothelial cell line. Studies have shown TNFα can induce a JNK response after 15-minute incubation (Min et al., 2008) with this activation thought to be due to the signalling complex between the TNFα receptor and the adapter protein TRAF2 (Mong et al., 2008).

Figure 3.1 shows that TNFα activates the pathway in a time dependent manner. The optimum activation of pJNK, both 46 and 52 isoforms (JNKs 1 & 2) was shown to be significant at 15 minutes (stimulation: 35.23 ± 2.166, n=3, $P<0.05$). This activation was sustained over the 8-hour period, however, figure 3.1 shows this a biphasic response. There was a decline in activation of JNK until 1.5 hours (stimulation: 11.96 ± 6.280, n=3) in which there was a slight increase in activation until 8 hours (stimulation: 23.29 ± 6.208), however these are not significant. This figure demonstrated agonist-mediated activation of the JNK pathway via Western blotting prior to using chemotherapeutic compounds of interest. It was important to characterise the activation of the JNK pathway with a known agonist before any investigation with unknown compounds.

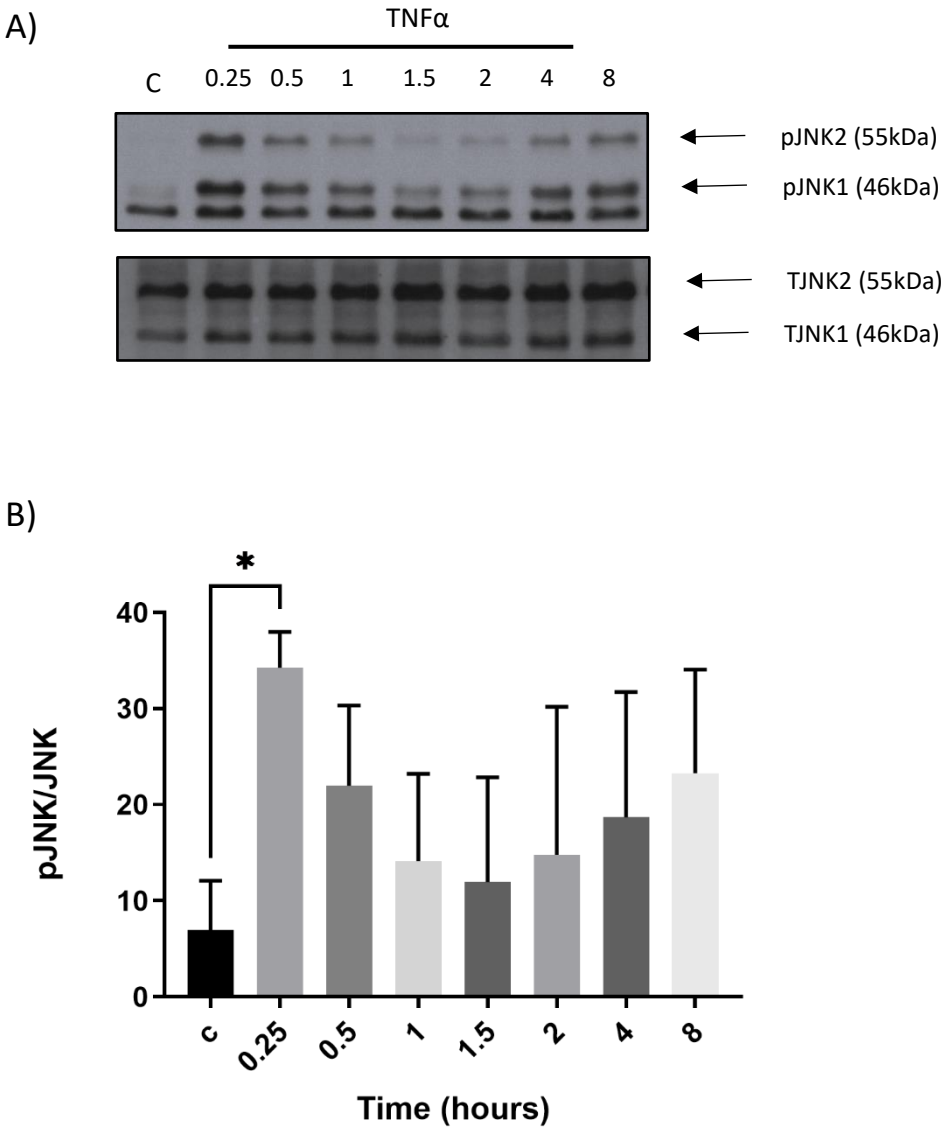


**Figure 3.1 TNFα mediated time-dependent activation of the JNK pathway in HUVECS.**

Confluent HUVECs were stimulated with TNFα (10ng/ml) for 15 minutes – 8 hours. Western blot analysis was performed for pJNK and Total JNK. Blots were semi-quantified as outlined in Methods section 2.2.2.6. A) Western blot representation. B) Semi-quantification for pJNK/TJNK ratio. Results represent mean ± S.E.M, n=3. *P<0.05, compared to control.

Once the activation of the pathway was demonstrated, an initial investigation into the effect of Doxorubicin on the JNK pathway was carried out. It has been reported by a number of studies, using cancer cell lines, that the JNK pathway becomes activated after being exposed to the chemotherapeutic agent Doxorubicin (Zhang et al. 2019b). As it is the effect of chemotherapeutic compounds on the JNK pathway that is important for this study, the next step was to characterise the effect of Doxorubicin on the JNK pathway, using HUVECs. For this, both the time course and concentration dependency were investigated to determine if the pathway is activated and the optimum conditions of activation.

HUVECs were therefore treated with Doxorubicin at 30μM for up to 24 hours. As figure 3.2 shows that after a significant delay relative to TNFα, activation of the pathway occurred at around 8 hours (stimulation: 85.92 ± 16.03, n=3, P< 0.01) and was sustained up to 24 hours. As the figure 3.2 A shows 24 hours (stimulation: 100.1 ± 13.47, n=3, P<0.01) also shows a significant activation of the JNK pathway. Therefore, it has been shown that Doxorubicin does activate the pathway in a time dependent manner.

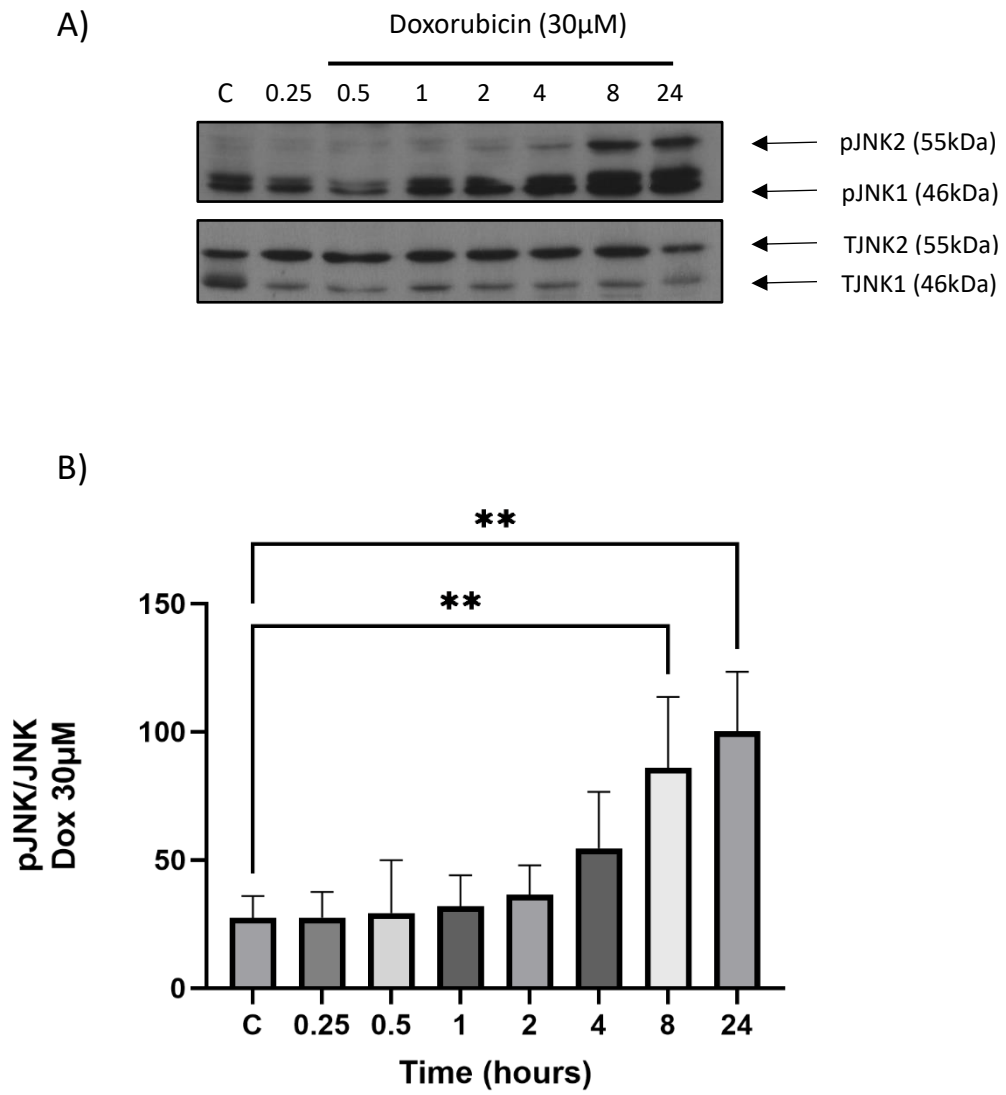


**Figure 3.2 Doxorubicin: Time-dependent activation of the JNK pathway in HUVECs.**

Confluent HUVECs were stimulated with Doxorubicin (30µM) for 24 hours. Western blot analysis was performed for p-JNK and total JNK. Blots were semi-quantified as outlined in Methods section 2.2.2.6. A) Western blot representation. B) Semi-quantification for p-JNK/TJNK ratio. Results represent mean ± S.E.M, n=3, **P<0.01, compared to control

To define the effect Doxorubicin has more accurately in relation to JNK activation, two concentrations of Doxorubicin were chosen to be further analysed over a longer time period. HUVECs were treated with 10µM and 30µM of Doxorubicin for extended time points 8-24 hours. Figures 3.3 and 3.4 show that between the time points of 8 and 24hours the JNK signal remains sustained with both 10µM and 30µM.

When focusing on 10µM, over 8-24 hours there was a clear pattern, the activation of both JNK isoforms increased from 8 hours relative to control (stimulation: 24.02±2.97, n=3, P<0.001), to 16 hours (stimulation: 46.66±7.09, n=3, p<0.001). After the significant peak at 16 hours, JNK activation gradually decreased at 20 and 24 hours (stimulation: 37.34±6.122, n=3, P<0.01), where this was also found to be significant. This decrease in activation was still higher than the activity observed at 8 hours which correlates to figure 3.2.

The same pattern of activation was found when exposing the HUVECs to 30µM over the extended timeframe, however the higher concentration gave a greater activation of the JNK pathway, particularly for the 54 kDa isoform. As figure 3.4 shows JNK activation increased until 16 hours (stimulation: 53.92±8.10, n=3, P<0.01), where it then decreased at 20 and 24 hours. Figure 3.4B also shows that this activation was significant at each time point. Both long course experiments (3.3 and 3.4) show the same pattern with JNK activation. As shown in both figures 3.2 and 3.3, JNK activation at 24 hours was higher than that observed at 8 hours regardless of concentration. Interestingly there is an increase in the phosphorylation of a lower molecular weight (M.W.) band. This is likely to be p44 MAP kinase, the antibody used is known to cross react with ERK. Total JNK levels where largely consistent although the cells were clearly compromised.

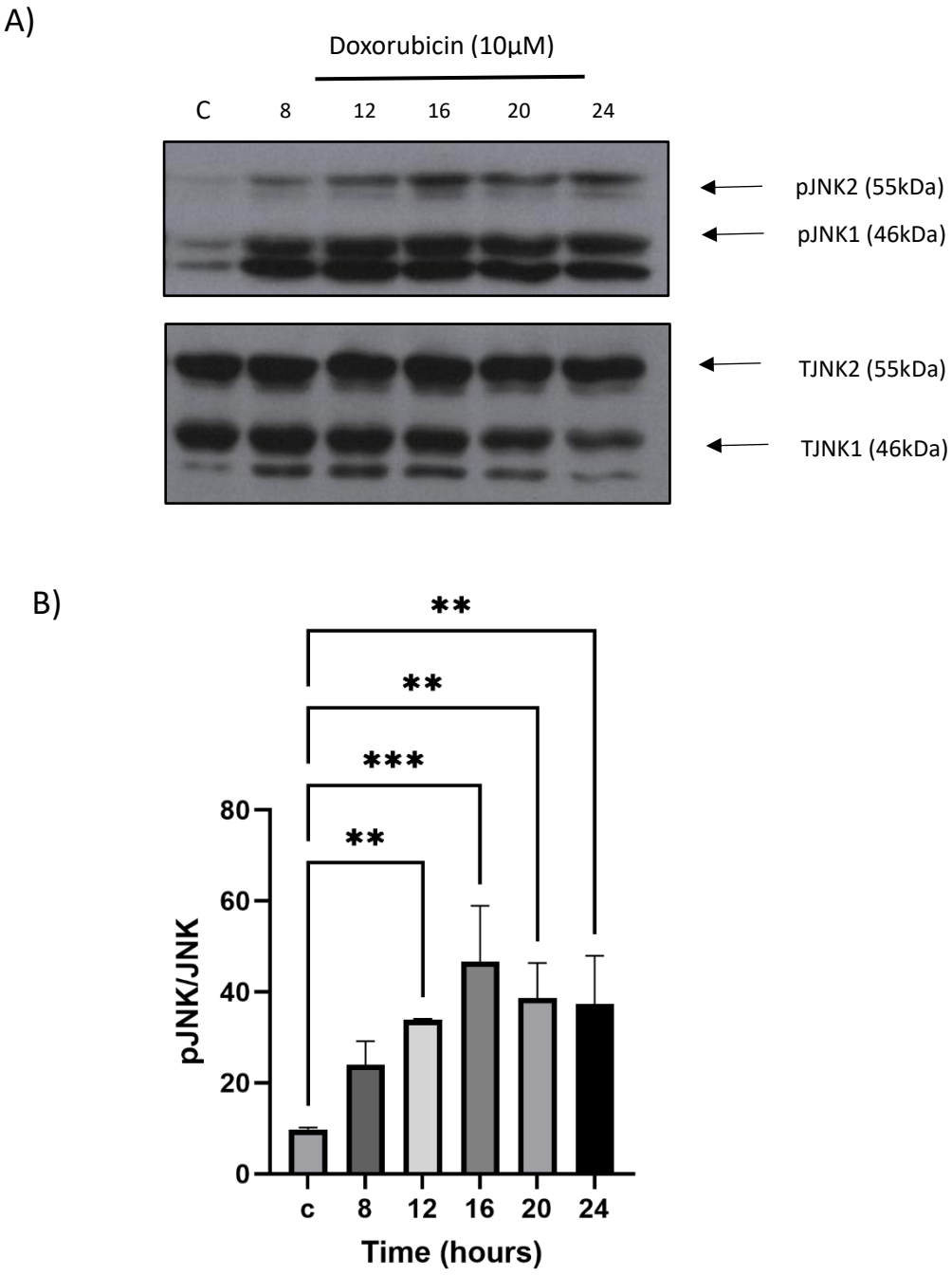


**Figure 3.3 Doxorubicin 10µM prolonged time-dependent activation of the JNK pathway in HUVECs.**

Confluent HUVECs were stimulated with Doxorubicin (10µM) for 8-24 hours. Western blot analysis was performed for pJNK and Total JNK. Blots were semi-quantified as outlined in Methods section 2.2.2.6. A) Western blot representation. B) Semi-quantification for pJNK/TJNK ratio. Results represent mean ± S.E.M, n=3, **P<0.01, ***P<0.001, compared to control

A)

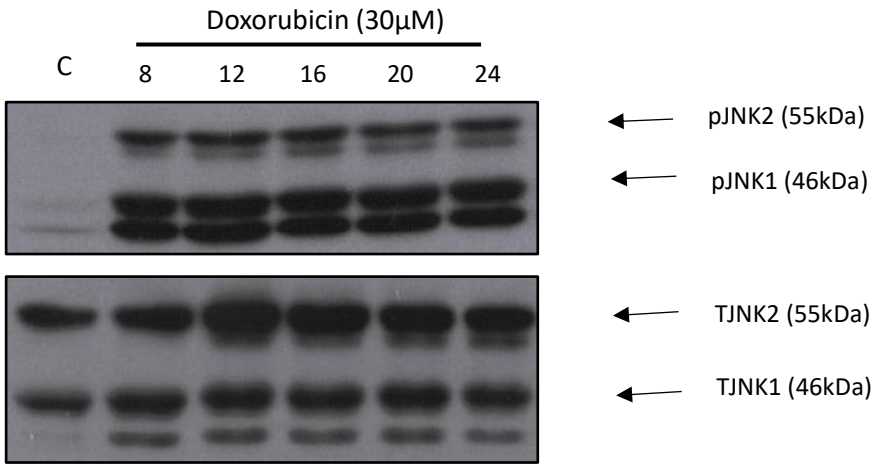


B)

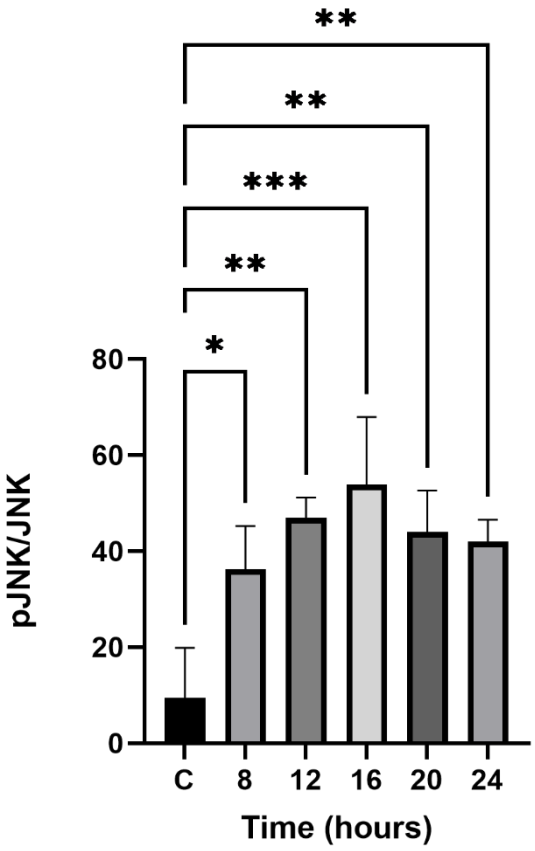


**Figure 3.4 Time-dependent activation of the JNK Pathway in HUVECs stimulated by Doxorubicin.**

Confluent HUVECs were stimulated with Doxorubicin (30µM) for up to 24 hours. Western blot analysis was performed for pJNK and Total JNK. Blots were semi-quantified as outlined in Methods section 2.2.2.6. A) Western blot representation. B) Semi-quantification for pJNK/TJNK ratio. Results represent mean ± S.E.M, n=3, *P<0.05, **P<0.01, ***P<0.001, compared to control.

After analysing the impact Doxorubicin had on HUVECS over a time course at 2 different concentrations, a concentration curve was then carried out. This was to more accurately determine the optimal stimulation conditions. Figure 3.5 shows that Doxorubicin caused a sustained activation of both p46 and p54 isoforms over the 24-hour time point, with an increase in concentration. Initial activation was shown to be at 1μM (stimulation: 23.55 ± 4.405, n=3) which gradually increased with increasing concentrations up 100μM (stimulation at 100μM: 51.28 ±23.25, n=3, $P<0.05$).

After looking at both the Western blot for time and concentration dependent activation (Fig 3.2 and 3.5), the 30μM concentration at a 24hour time point was used in subsequent experiments.

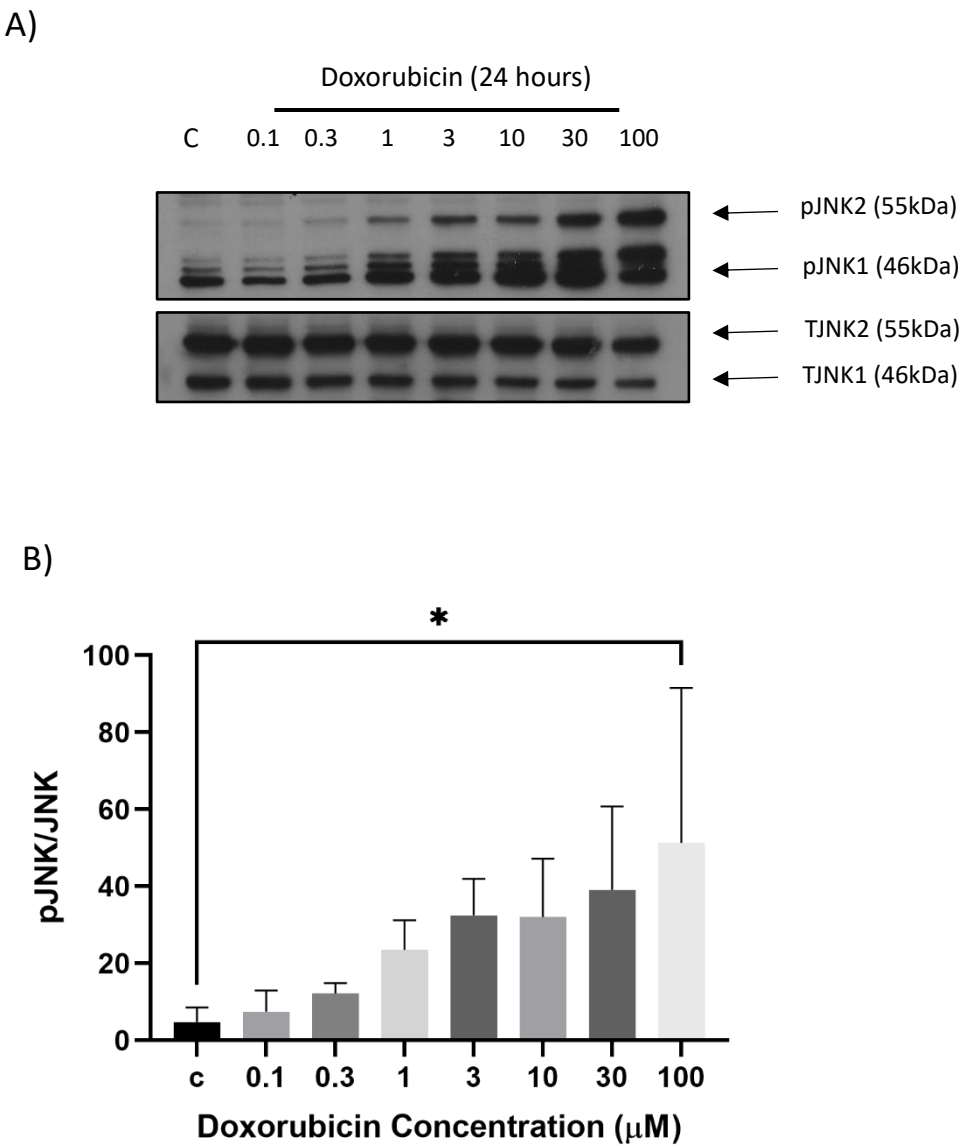


**Figure 3.5 Doxorubicin concentration dependent activation of the JNK pathway in HUVECs.**

Confluent HUVECs were stimulated with 0.1-100μM of Doxorubicin for 24 hours. Western blot analysis was performed for pJNK and Total JNK. Blots were semi-quantified as outlined in Methods section 2.2.2.6. A) Western blot representation. B) Semi-quantification for pJNK/TJNK Results represents mean ± S.E.M, n=3, *P<0.05, compared to control.

### 3.2.2. Activation of the canonical NF-κB pathway in response to Doxorubicin

It has been well established that the NF-κB pathway is involved in both cell survival (Luo, 2005), but also programmed cell death, where it has been shown to supress JNK activation (Bubici et al., 2004, Papa et al., 2006). Therefore, investigations were carried out to determine whether there is a link between the activation of JNK by Doxorubicin and the NF-κB pathway. The initial experiment looked at Doxorubicin and TNFα together in relation to p-p65 activation. As figure 3.2 shows that Doxorubicin induces a JNK response at 4 hours it was determined that any role the NF-κB pathway would play in the response would be prior to this time point. Therefore, it was determined that a time point of 15 minutes to 2 hours would be investigated for potential involvement of both the canonical and non-canonical NF-κB pathways.

Initially the canonical pathway was investigated by blotting for p65 activation via serine-536 phosphorylation. This isoform is one of the main heterodimers responsible for the induction of genes regulated by the canonical NF-κB pathway (Yu et al., 2020). Thus, by blotting for p65 it would show if the activation of the JNK pathway by Doxorubicin was induced through the canonical NF-κB pathway. It is well documented that TNFα can activate the p-65 pathway at 15 minutes, therefore TNFα was chosen as a positive control. As figure 3.6A shows TNFα activated p-p65 at 15 minutes (stimulation: 47.74±2.361, n=3). However, Doxorubicin did not induce an increase in p-p65 over a similar time period. Therefore, this result shows that the Doxorubicin induced activation of JNK is independent of the canonical NF-κB pathway.

The effect of Doxorubicin on the cellular IκBα levels was then investigated. IκBα is one of the most studied member of the IκB family, and its degradation confirms the canonical activation of NF-κB (Shin and Choi, 2019). Figures 3.7A and B show that TNFα stimulated a loss of IκBα between 15 (inhibition: 22.27±0.63, n=3) and 30

minutes returning to near basal values by 60-minutes (stimulation: 37.85±14.06, n=3). However, there was no degradation of IκBα following exposure to Doxorubicin as compared to TNFα.

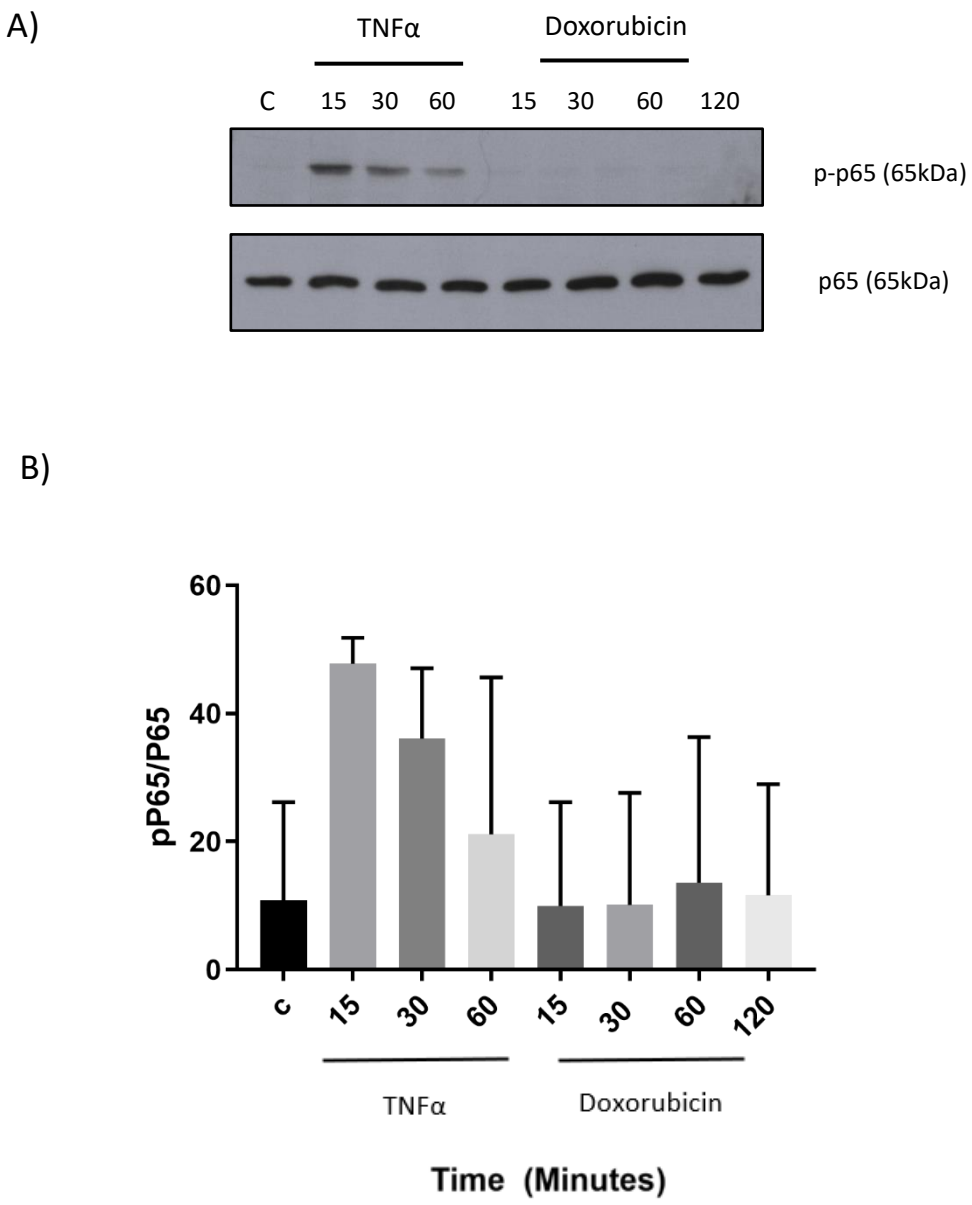


**Figure 3.1 : TNFα and Doxorubicin stimulated Time-dependent phosphorylation of pp65 in HUVECs.**

Confluent HUVECs were stimulated with TNFα (10ng/ml) and Doxorubicin (30μM) for 15-120 minutes. Western blot analysis was performed for pJNK and Total JNK. Blots were semi-quantified as outlined in Methods section 2.2.2.6. A) Western blot representation. B) Semi-quantification for pp65/p65 ratio. Results represent mean ± S.E.M, n=3, non-significant, compared to control.

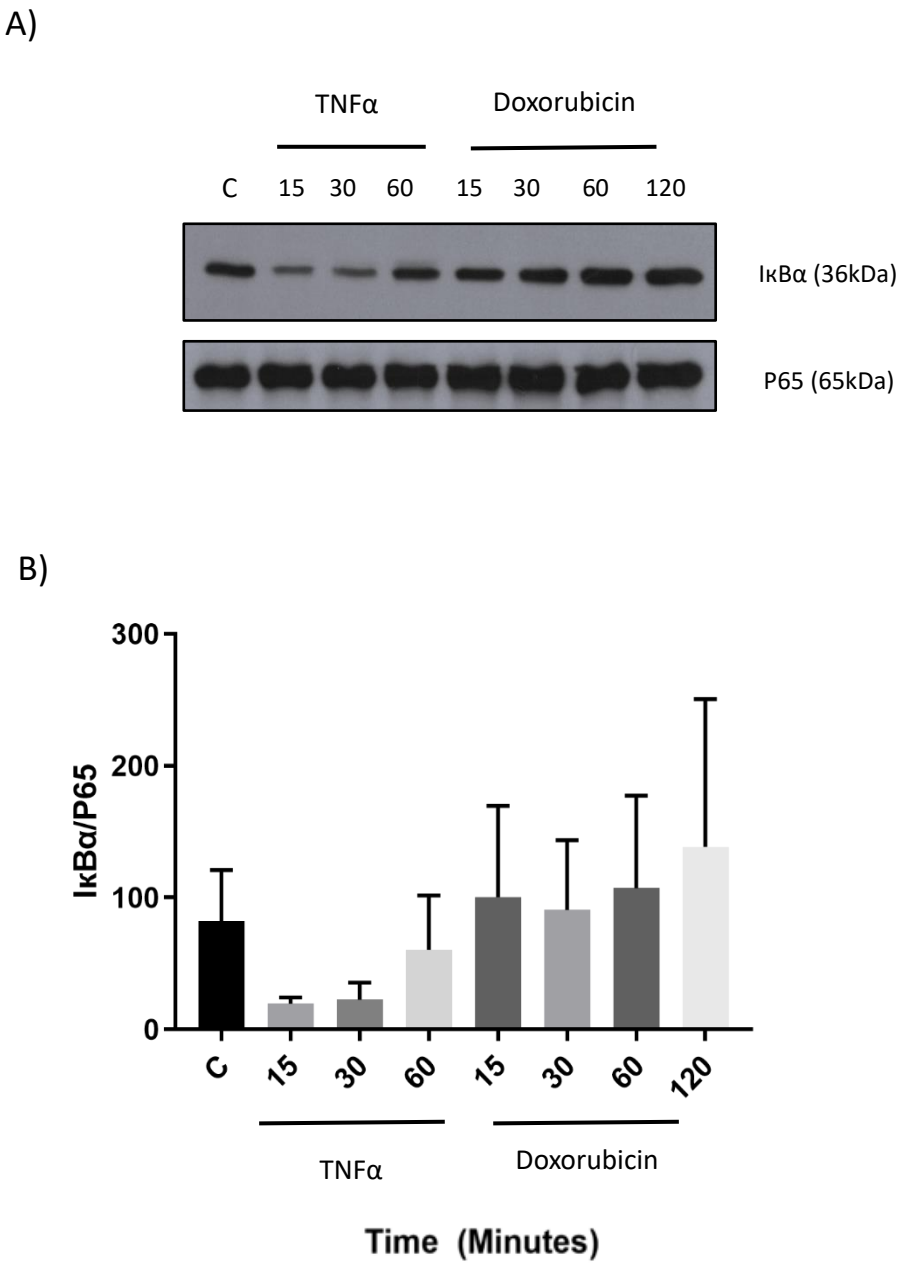


**Figure 3.2 TNFα and Doxorubicin Time dependent cellular degradation of IκBα pathway in HUVECs.**

Confluent HUVECs were stimulated with TNFα (10 ng/ml) and Doxorubicin (30μM) for 15-120 minutes. Western blot analysis was performed for IκBα and P65. Blots were semi-quantified as outlined in Methods section 2.2.2.6. A) Western blot representation. B) Semi-quantification for IκBα/p65 ratio. Results represent mean ± S.E.M, n=3, non-significant, compared to control.

### 3.2.3. Cisplatin Induced JNK signalling in HUVECs

As it has been shown that Doxorubicin activates the JNK pathway, similar experiments were carried out to investigate the effects of Cisplatin. Cisplatin is also a well-known anti-cancer agent which, as previously mentioned, has been linked with cardiovascular toxicities (Camacho et al., 2023). It was therefore important to determine whether this agonist activated the JNK pathway in the HUVECs and the optimum conditions. As with Doxorubicin, initial experiments examined the kinetics of Cisplatin stimulation over a 24-hour period.

Firstly, HUVECs were treated with 100µM of Cisplatin for up to 24 hours. As figure 3.8 shows, there was little JNK activation up to and including 8 hours with an increased in pJNK a the 24-hour time point (stimulation: 120.0±29.47 $p<0.0001$, $n=3$). At this higher concentration there is a slight reduction in total JNK as shown in Figure 3.8B, indicating potential loss in cellular protein. As with Doxorubicin, to further investigate the relationship between the concentration and time dependent responses, Cisplatin at 100µM and 30µM was examined in HUVECs for 8-24 hours. Figures 3.9 and 3.10 show the effect these concentrations have on the JNK pathway.

When exposed to 100µM of Cisplatin for a prolonged time course figure 3.9 shows a similar pattern to Doxorubicin with a peak at 16 hours (stimulation: 25.68±9.78, $n=3$) and a decrease to 24 hours (stimulation: 18.77±3.10, $n=3$). In comparison, 30µM Cisplatin promoted a slightly less pronounced increase in pJNK, particularly the p54 isoform up to 24 hours. Both 20 (stimulation 36.62±4.357, $n=3$, $P<0.01$), and 24hour time points (stimulation: 49.12±10.65, $n=3$, $P<0.001$), gave a significant increase in stimulation. For 100mM there was considerable loss in total JNK indicative of cellular compromise and protein loss.

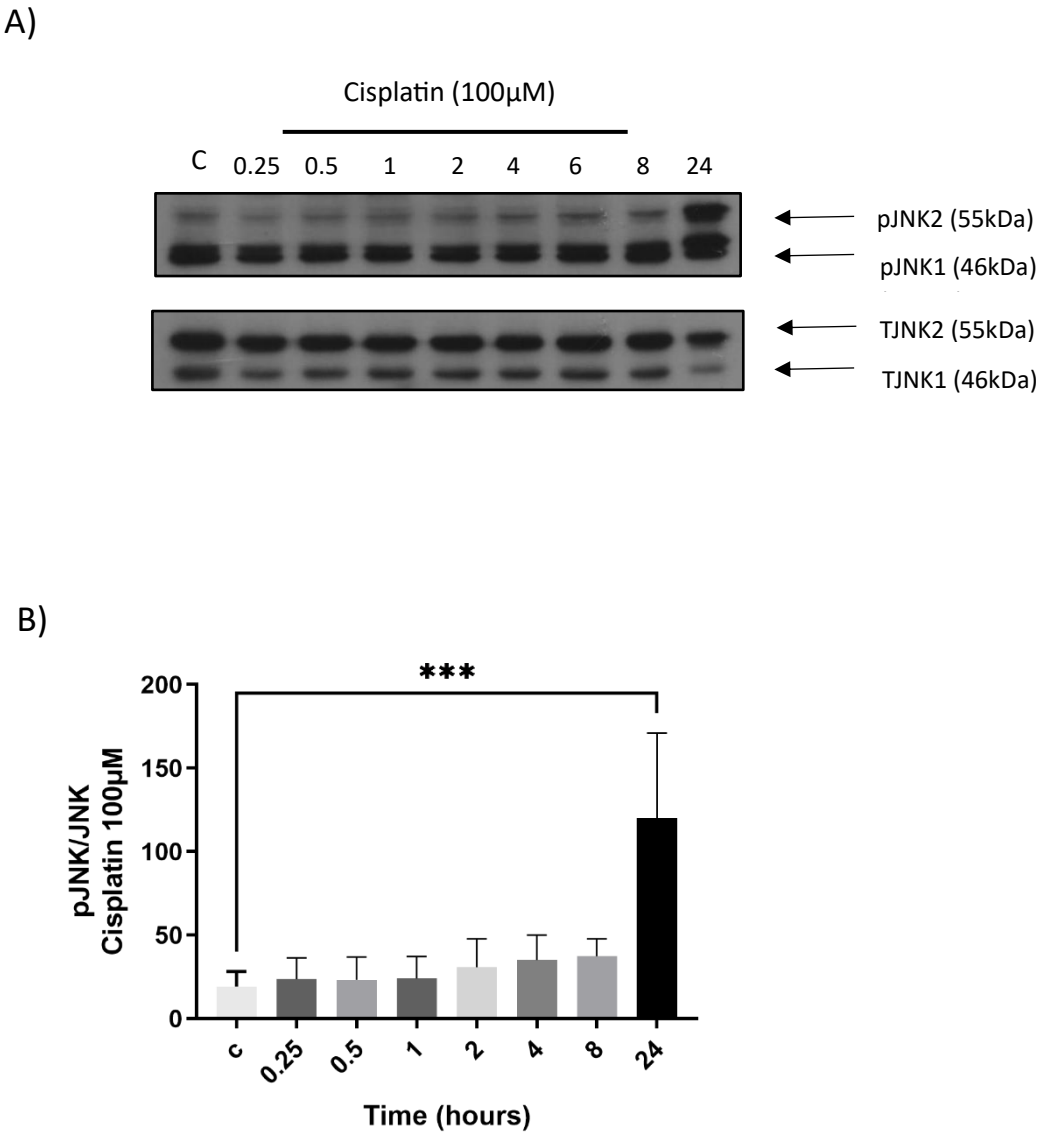


**Figure 3.3 Cisplatin mediated activation of the pJNK phosphorylation in HUVECs.**

Confluent HUVECs were stimulated with Cisplatin (100µM) over 24 hours. Western blot analysis was performed for pJNK and Total JNK. Blots were semi-quantified as outlined in Methods section 2.2.2.6. A) Western blot representation. B) Semi-quantification for pJNK/TJNK ratio. Results represent mean ± S.E.M, n=3, ***P<0.001 compared to control.

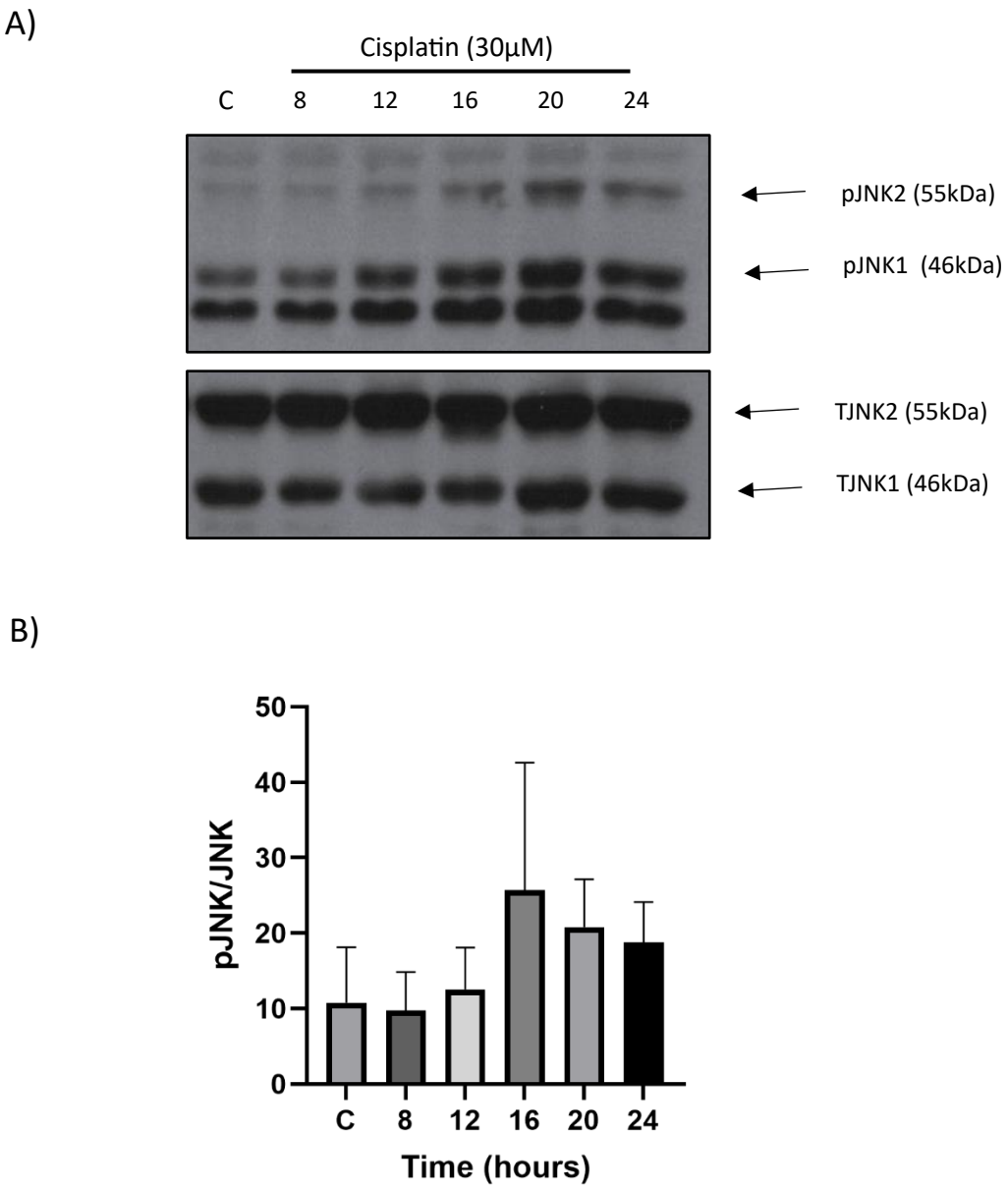


**Figure 3.4 Cisplatin (30µM) time mediated activation of the pJNK pathway in HUVECs.**

Confluent HUVECs were stimulated with Cisplatin (30µM) for up to 24 hours. Western blot analysis was performed for pJNK and Total JNK. Blots were semi-quantified as outlined in Methods section 2.2.2.6. A) Western blot representation. B) Semi-quantification for pJNK/TJNK ratio. Results represent mean ± S.E.M, n=3, non-significant, compared to control.

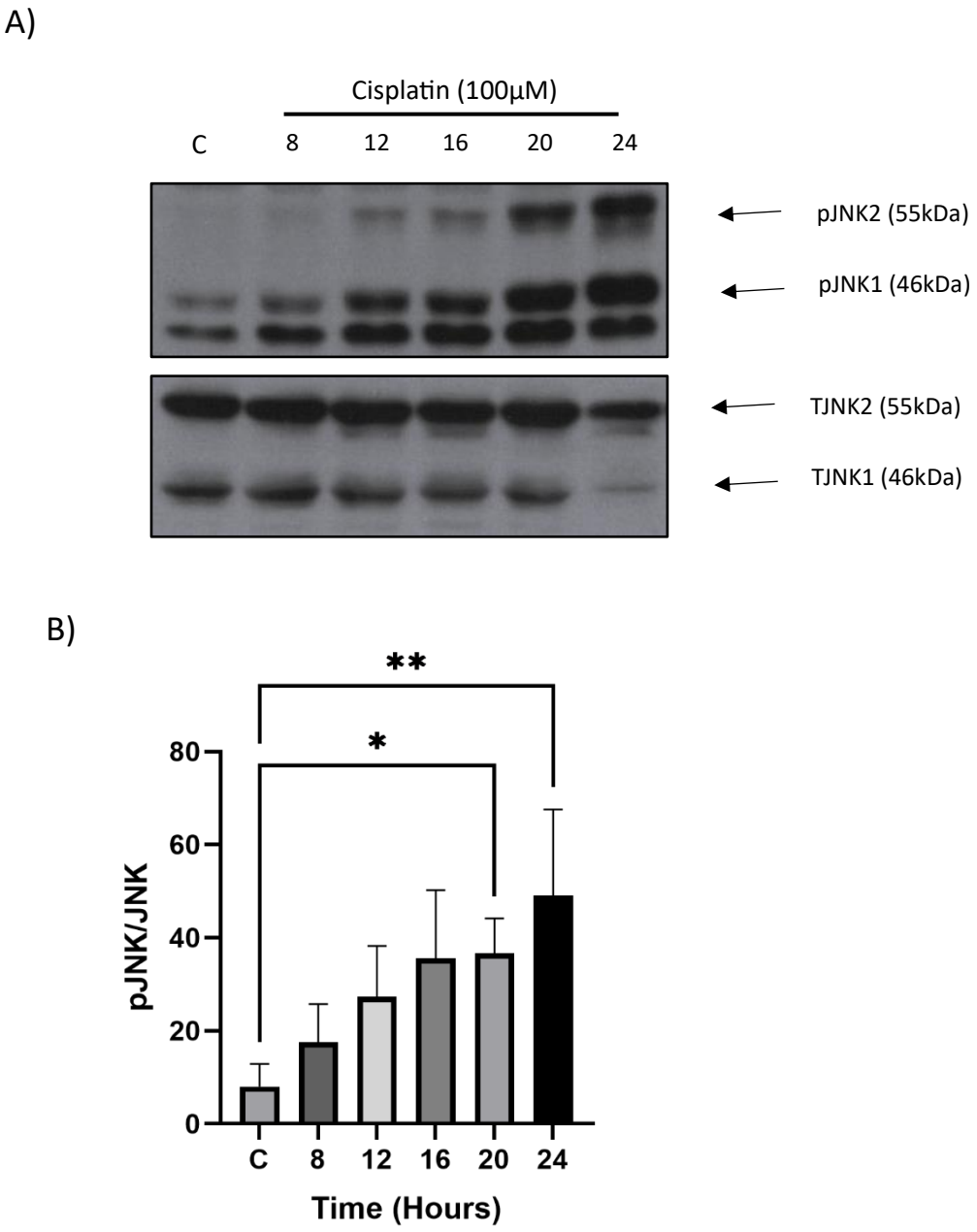


**Figure 3.5 100µM Cisplatin time dependent activation of the pJNK pathway in HUVECs.**

Confluent HUVECs were stimulated with Cisplatin (100µM) for up to 24 hours. Western blot analysis was performed for pJNK and Total JNK. Blots were semi-quantified as outlined in Methods section 2.2.2.6. A) Western blot representation. B) Semi-quantification for pJNK/TJNK ratio. Results represent mean ± S.E.M, n=3, *P<0.05, **P<0.01, compared to control.

As the different concentrations of Cisplatin resulted in different activation patterns, a full concentration curve was carried out. The Western blot in figure 3.11A shows that JNK is activated by Cisplatin at the 24-hour mark with a very low potency, with a slight increase at 30µM with a much higher level of stimulation at 100µM (100µM Cisplatin stimulation:135.9 ± 54.22, n=3) and 300µM respectively (300µM Cisplatin stimulation: 592.0 ± 254.0, $P<0.001$, n=3). There is also a clear loss in protein levels when looking at the total JNK blot (figure 3.11A), indicating that Cisplatin is causing substantial cell death at those concentrations. Both the concentration dependent experiments and the time courses in figures 3.8 and 3.10 show that even though there is a significant activation of the JNK pathway at 24 hours, there is also considerable protein loss. This may suggest that the activation of the JNK pathway by Cisplatin is linked to cell death.

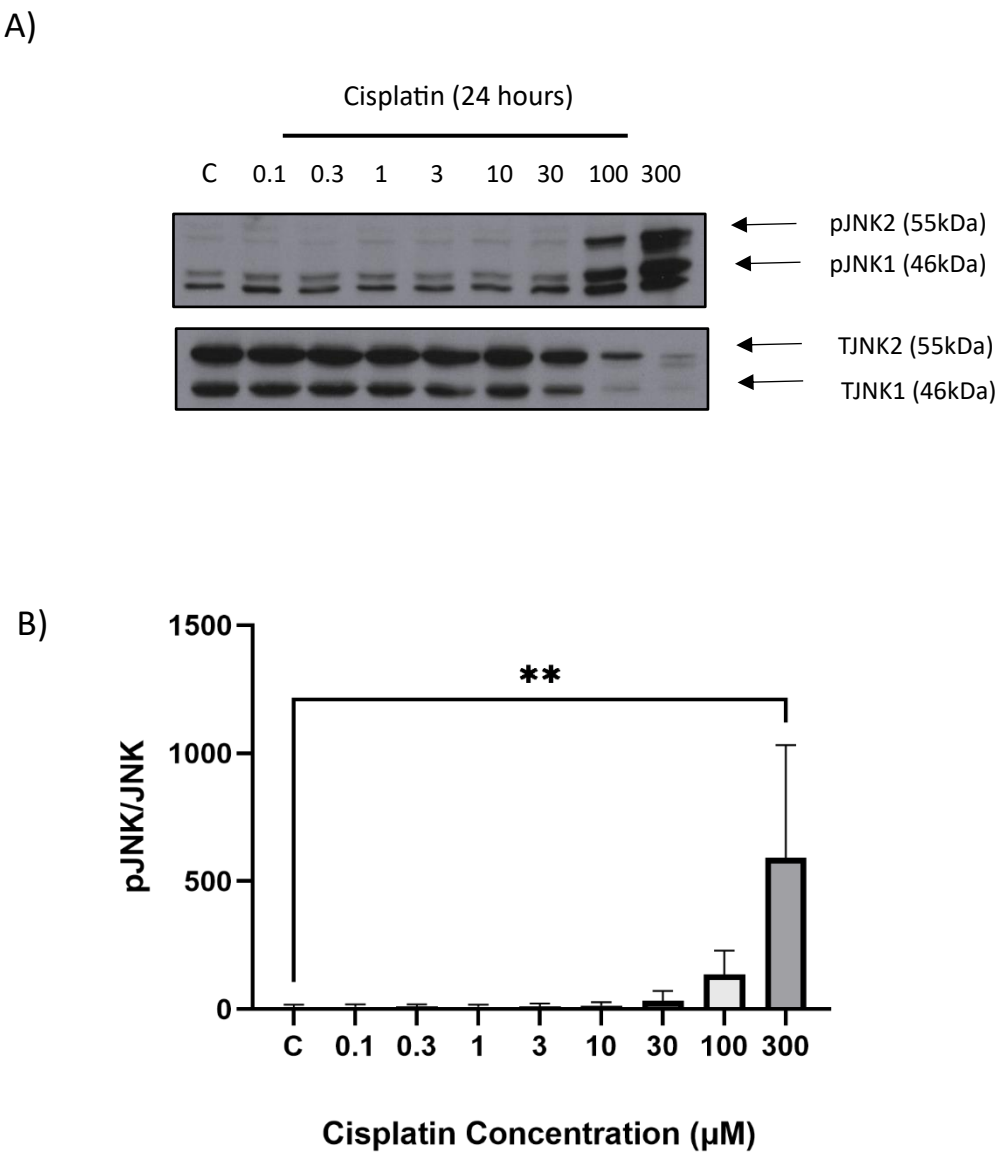


**Figure 3.6 Cisplatin mediated activation of the pJNK pathway in HUVECs.**

Confluent HUVECs were stimulated with Cisplatin (100μM) over 24 hours. Western blot analysis was performed for pJNK and Total JNK. Blots were semi-quantified as outlined in Methods section 2.2.2.6. A) Western blot representation. B) Semi-quantification for pJNK/TJNK ratio. Results represent mean ± S.E.M, n=3, **P<0.001 compared to control.

### 3.2.4. Sunitinib effect on JNK signalling in HUVECs

As with Doxorubicin and Cisplatin, Sunitinib is a renowned chemotherapeutic agent that has been known to induce cardiovascular toxicities as mentioned previously (Chu et al., 2007, Joensuu, 2007). It was therefore important to investigate the effect this compound has on HUVECs and specifically the JNK pathway. For this a concentration dependent investigation was carried out using increasing concentrations of Sunitinib ranging from 0.1µM to 100µM for 24 hours.

As figure 3.12 shows, Western blot analysis was used to visualise the effect Sunitinib has on the JNK pathway. Both figure 3.12A and B show that Sunitinib does not induce phosphorylation of the JNK pathway at any concentration at the 24-hour time point. This is evident when compared to the positive control (Cisplatin, 100µM). It is clear however, that Sunitinib does have an effect on HUVEC viability with there being a significant loss of total JNK protein visible at the 100µM. This loss is evident not only by the lack of total protein at 100µM but there is also a concentration dependent reduction in protein from 3µM. Figure 3.12A also shows a decrease in protein at 30µM with a considerable decrease in JNK 1 (46kDa). Therefore, in contrast to Cisplatin and DOX, there seems to be a clear distinction between cell death and JNK activation.

A)

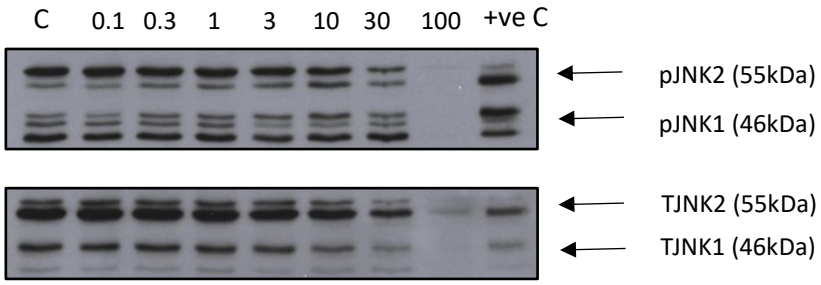


B)

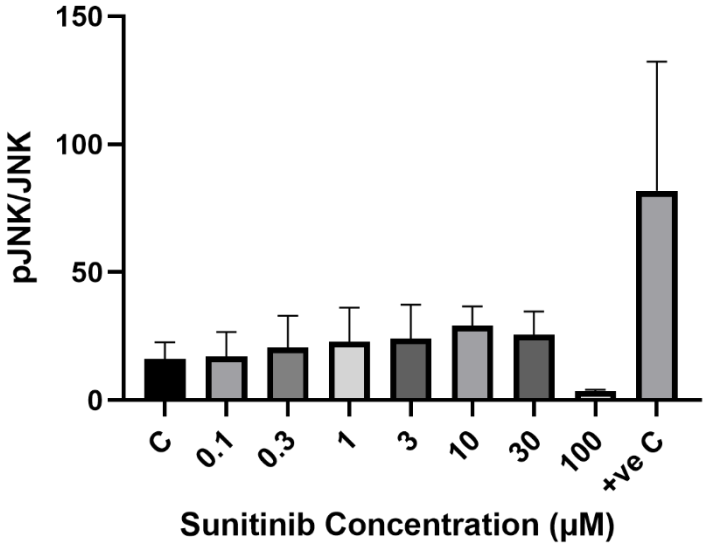


**Figure 3.7 Sunitinib Concentration dependent activation of the JNK pathway in HUVECs.**

Confluent HUVECs were stimulated with Sunitinib (0.1µM - 100µM) or 30µM Doxorubicin as +ve C (positive control) for up to 24 hours. Western blot analysis was performed for pJNK and Total JNK. Blots were semi-quantified as outlined in Methods section 2.2.2.6. A) Western blot representation. B) Semi-quantification for pJNK/TJNK ratio. Results represent mean ± S.E.M, n=3, non-significant, compared to control.

Due to the visible impact that Sunitinib had on the viability of the HUVECs, an MTT assay was carried out to investigate this phenomenon further. For this the same conditions were used as for the Western blot analysis, HUVECs were treated for 24 hours with concentrations of Sunitinib from 0.1 µM to 100 µM. Figure 3.13 shows that Sunitinib has a marked effect on the cell viability, with significant cell death noted at 10µM which decreased viability to 76%. Both concentrations higher than 30 µM (44.4% viability) and 100µM had a substantial effect on cell survival. 100µM of Sunitinib over the 24 hours caused over 90% cell death with only 8.9% viability, this correlated with the total loss of protein that was indicated by the Western blot analysis in figure 3.12. When examining both figures 3.12 and 3.13 it can be concluded that although Sunitinib is negatively affecting cell viability, this is independent of the JNK pathway.

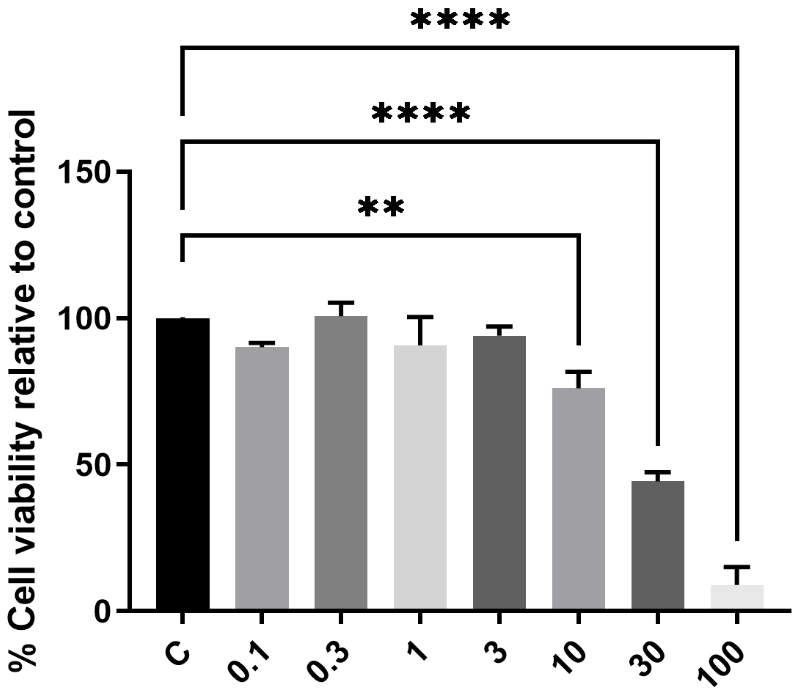


**Figure 3.8 Decrease in HUVEC viability by Sunitinib is concentration dependent.**

HUVEC cell viability was measured using an MTT assay, as outlined in section 2.2.4. Confluent HUVECs were treated with concentrations of Sunitinib ranging from 0.1µM to 100µM for 24 hours. Data represents mean ±S.E.M, n=3 **P<0.0015 ****P<0.0001 compared to control.

### 3.2.5. Effect of Doxorubicin on cell viability in HUVECs

Having identified that Doxorubicin and Cisplatin reduced cellular protein levels in the Western blotting experiments, overall cell viability was investigated. For the initial experiments MTT assays were carried out to determine the extent of cell death for both Doxorubicin and Cisplatin on the HUVECs. HUVECs were treated with both Doxorubicin and Cisplatin at increasing concentrations for 24 hours prior to the MTT assay.

Doxorubicin caused a clear concentration-dependent decrease in cell viability, from 0.1µM (83.3%) up to 100µM (32.3%), with a total reduction in cell viability of over 50% (Figure 3.14 A). This correlates with the JNK activation observed in fig 3.2, further indicating that cell death and JNK activation could be linked, and that the surrounding healthy endothelium is being affected by the cancer chemotherapeutic agents, as well as the tumours.

An MTT experiment was also carried out to investigate whether Doxorubicin over a longer time point, 48 hours, would cause a differing effect on HUVEC viability. Figure 3.14 B shows in a single preliminary experiment, there is a similar pattern shown in cell viability although unsurprisingly, is more potent over the longer period. Cell viability decreases as concentration increases with a visible decrease at 3µM of approximately 80%.

As MTT is a limited approach to assessing cell death, analysis of apoptosis was utilised to give a more detailed look at how Doxorubicin affects HUVEC cell viability and provide an insight into the mechanism of cell death.

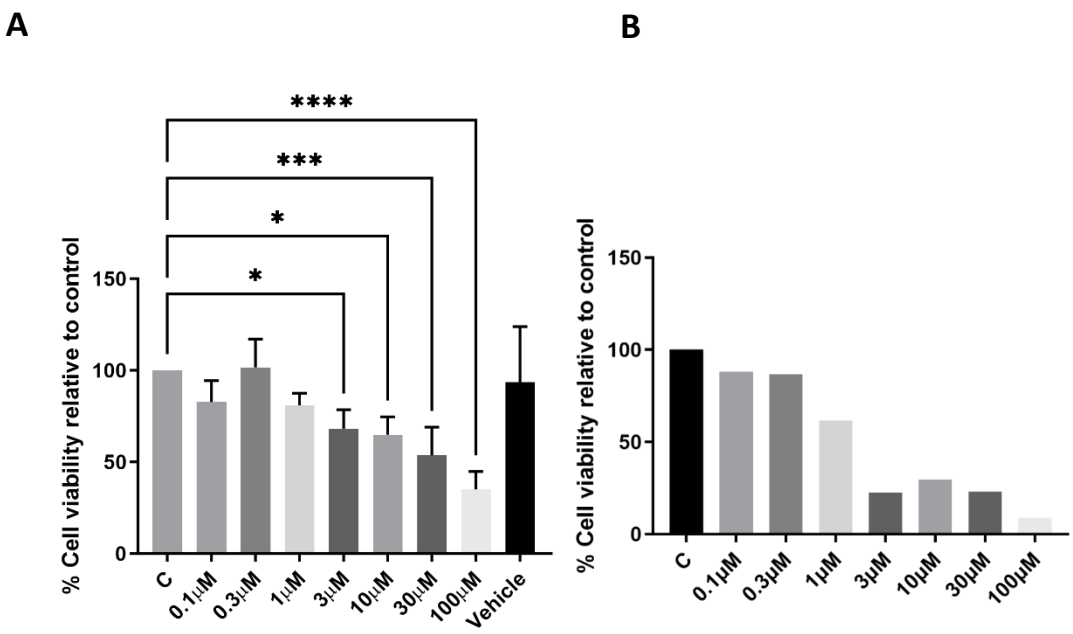


**Figure 3.14 Concentration Decrease in HUVEC viability mediated by Doxorubicin.**

HUVEC cell viability was measured using an MTT assay, as outlined in section 2.2.4. Confluent HUVECs were treated with concentrations of Doxorubicin ranging from 0.1µM to 100µM for A) 24 hours and B) 48 hours. A) Data represents mean ±S.E.M, n=3 *P<0.05 ***P<0.005 ****P<0.0001 compared to control. B) n=1

As with the initial MTT assay, FACS analysis was then carried out on the HUVECS that have been treated with concentrations of Doxorubicin from 0.1µM to 100µM for 24 hours as shown in Figure 3.15. Panel A represents the histoplot generated by FACS giving a visual of the impact the reagents are having on the cells. Cells in the bottom right represents the healthy cells, bottom left shows the cells in the early apoptotic stage, top right cells are those in late apoptosis whilst necrosis is shown in the top left-hand corner of the graph. Graphs were then calculated using these numbers to show an accurate representation of cell death in the HUVECs after treatment.

As figure 3.15 A and B shows even at low concentrations Doxorubicin induced apoptosis in the HUVECs, in particular late apoptosis. Figure 3.15B highlights the effect the drug had on the cell viability, by looking at the healthy cells; there was a significant ($p<0.0001$) drop in cell viability relative to the control with concentrations as low as 0.1µM causing approximately 50% cell loss. Concentrations higher than 0.1µM showed a significant decrease in viability in a downward trend, with 100µM reducing the % of healthy cells by over 99%.

Early apoptosis gave a similar pattern of cell viability to those with healthy cells. Compared to 10% of cells showing early apoptosis in the control, cells treated with 0.1µM Doxorubicin showed reduced early apoptosis at approximately 6%, compared to cells treated with 100µM which showed 0.03% of cells as early apoptotic (figure 3.15). These results do suggest Doxorubicin results in a decreased survival of healthy cells and a loss in early apoptosis at concentrations far below those required to initiate JNK signalling.

In contrast there was a significant increase in late apoptosis in response to Doxorubicin. Figure 3.15 B (III) shows that compared to a control value of 42% there was a significantly higher percentage of cells in late apoptosis at 10µM (59.26±3.346) and 30µM (59.29±3.015). This is consistent with effects observed for healthy cells and early apoptotic cells.

Concentrations higher than 1µM have shown that cell death seems to follow the same mechanism and results in around 60% cell death, across all Doxorubicin concentrations, which are characterised as late apoptotic. Although apoptosis has not been thought to have been the main mechanism of cell death for Doxorubicin, several studies have shown that Doxorubicin elicits cell death through apoptosis. One study has shown that Doxorubicin causes apoptosis in HUVECs after 24hour exposure and 8 days after initial treatment with Doxorubicin (Graziani et al., 2022).

However, all concentrations of Doxorubicin had a significant effect on necrotic cell death. As shown in figure 3.15B (IV), compared to a control value of 4.7% Doxorubicin causes marked necrosis peaks as low as 1µM where around 60% of cells show necrosis with a significance of $P<0.0001$. At higher Doxorubicin concentrations there is a relative decline in necrosis: at 100µM, 42.55% of cells were found to be necrotic. These findings along with the MTT data shows that Doxorubicin has a significant impact on cell viability.

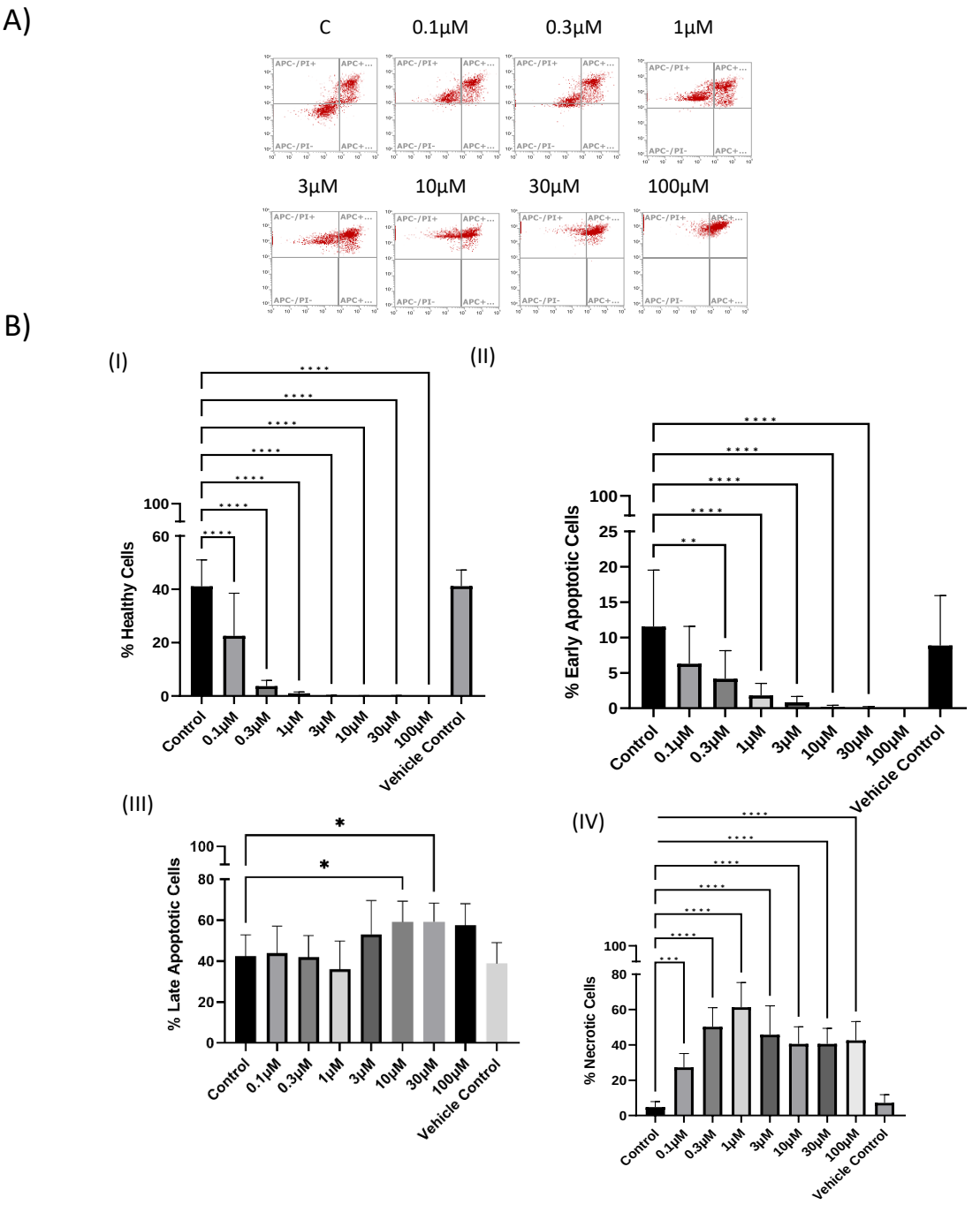


**Figure 3.15 The Effect of Doxorubicin on HUVEC cell death using FACS analysis.**

HUVEC cell viability was measured using Flow Cytometry. Confluent HUVECs were stimulated Doxorubicin (0.1µM-100µM) for 24 hours. Cell viability was determined by PI and Annexin V-APC staining as outlined in methods section 2.2.6. Where, healthy (non), Early apoptosis (Annexin V-APC) Late apoptosis (PI and Annexin V-APC) and Necrosis (PI) cells were detected. A) Representative dot plots with double staining of Annexin V-APC/PI staining of Doxorubicin treated cells. B) Histograms showing percentage of I) Healthy, II) early apoptotic, III) late apoptotic and IV) necrotic cells. Data represents mean ±S.E.M, n=3, *P<0.05, **P<0.005, ***P<0.001, ****P<0.0001 compared to control.

### 3.2.6. Effect of Cisplatin on cell viability in HUVECs

As with Doxorubicin, the effect of Cisplatin on endothelial cells was investigated to determine if it induces cell death and the possible mechanisms involved. First, an MTT was carried out to show if the chemotherapeutic agent influences cell viability over a 24-hour period. As figure 3.16A shows there is little significant impact on cell viability until 100 and 300µM. At 300µM however the impact on cell viability is significant with approximately 60% reduction (38.9% cell viability). Although 100µM also has an impact on cell viability with a 25.2% reduction in viability, this was not deemed significant. These findings correlate with figure 3.11 in which the JNK pathway is activated at the same time points indicating a potential correlation between JNK activation and cell death.

A single MTT experiment was also carried out over a longer time point as figure 3.16 B shows. In this case HUVECs were treated with the same concentrations of Cisplatin (0.1-300µM) but exposed for 48 hours. Figure 3.16B shows that over the longer time point all concentrations show an impact on cell viability however the pattern of cell viability mirrors the impact of 24hours, in which 0.1µM to 30µM shows a similar cell viability of around 75% whereas at higher concentrations that have shown to activate the JNK pathway 100 and 300µM respectively have a significant impact reducing viability to almost zero.

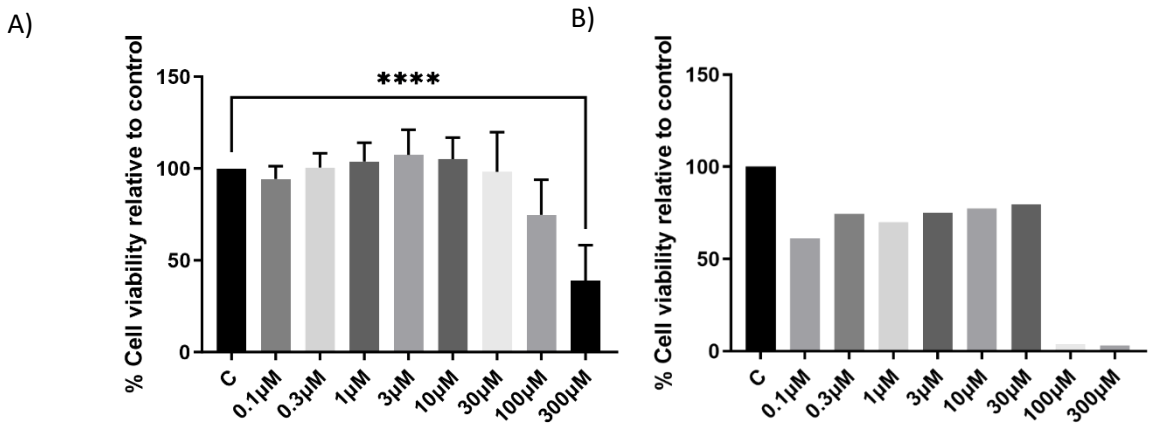


**Figure 3.16 ; The effect of Cisplatin concentration on endothelial cell Viability.**

HUVEC cell viability was measured using an MTT assay, as outlined in section 2.2.4. Confluent HUVECs were treated with concentrations of Cisplatin ranging from 0.1µM to 300µM for 24 hours (A) and 48hrs (B). Data represents mean ±S.E.M, n=3, ****P<0.0001 compared to control. N=1.

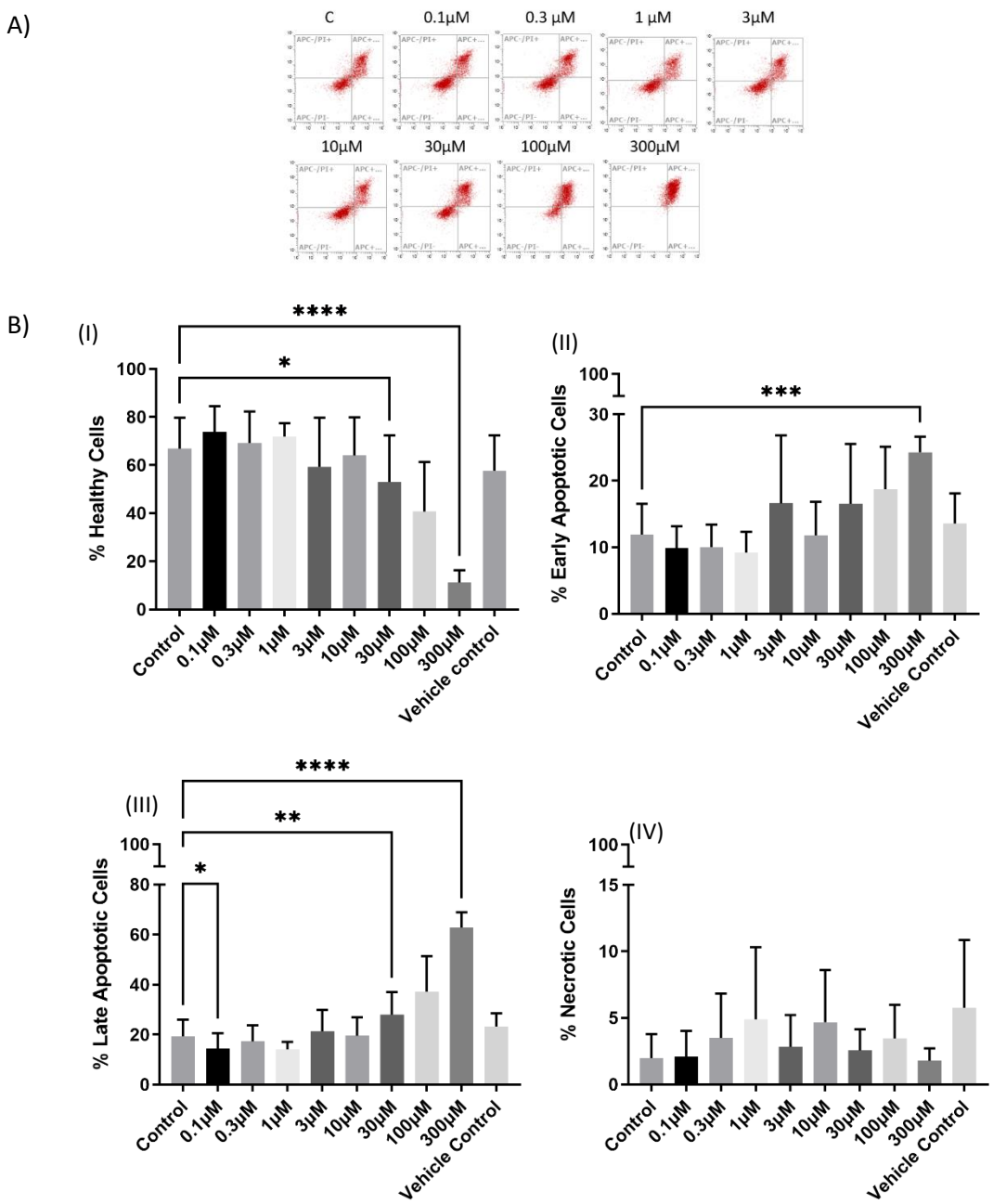


**Figure 3.17 The Effect of Cisplatin on HUVEC cell death using FACS analysis.**

HUVEC cell viability was measured using Flow Cytometry. Confluent HUVECs were stimulated with concentrations of Cisplatin (0.1µM-300µM) for 24 hours. Cell viability was determined by PI and Annexin V-APC staining as outlined in methods section 2.2.6 Where, healthy (non), Early apoptosis (Annexin V-APC) Late apoptosis (PI and Annexin V-APC) and Necrosis (PI) cells were detected. A) Representative dot plots with double staining of Annexin V-APC/PI staining of Cisplatin treated cells. B) Histograms showing percentage of I) Healthy, II) early apoptotic, III) late apoptotic and IV) necrotic cells. Data represents mean ±S.E.M, n=3, *P<0.05, **P<0.005, ***P<0.001, ****P<0.0001 compared to control.

To further investigate the mechanism of cell death further, Cisplatin was tested using FACS analysis and apoptosis/necrosis measured. As with the MTT analysis, HUVECs were treated for 24 hours with concentrations of Cisplatin ranging from 0.1µM to 300µM. Figure 3.17 shows the FACS dot plots (A) and the analysed data (B). FACs analysis show a significant impact upon cell viability occurred at concentrations higher than 30µM, figure 3.17 B (I) shows that at 300µM there was only around 10% of treated cells classified as healthy (8.56±1.854, *P<0.0001, N=3) as opposed to over 60% in the control (60.72±4.509, N=3). There is very little impact on cell viability below this concentration; this finding correlates with not only with the MTT assay (figure 3.16) but also figure 3.11 which showed total JNK expression. This is in sharp contrast to Doxorubicin where there was considerable cell death event at low concentrations.

Further analysis showed that in response to Cisplatin there was an increase in early apoptosis, from approximately 10% in the control (7.234±1.292, N=3) to over 25% at 300µM (18.30±3.176, N=3). Whilst early apoptosis tended to increase at 30 and 100µM this was not found to be significant for either concentration. However, again in contrast to Doxorubicin there was a significant increase in late apoptosis at both 100µM (42.43±4.472, **P<0.005, N=3) and 300µM (68.85±3.509, ****P<0.0001, N=3) compared to controls (26.19 ± 4.002, N=3) which accounts for 42% and 69% of cell death. Finally, it was found that Cisplatin did not stimulate a significant increase in necrotic cells with levels remaining between 5 and 10% even at higher concentrations (100µM: 5.055 ± 1.162, N=3) (300µM 4.654 ± 1.414, N=3). Which remained consistent with the control (3.685 ± 1.005, N=3) further indicating Cisplatin cell death is apoptotic.

### 3.2.7. Radiation induced JNK signalling

As radiation is a major aspect of cancer treatments and as discussed previously is a major factor in cardiovascular toxicities, HUVECs were treated with radiation and the effect was investigated. First of all, HUVECs were treated with a high level of radiation, 5Gy, and left at 37°C for 3,5 and 7 days. 5gy of radiation is a relatively high dose used on *in vitro* assays and concentrations below 2Gy are commonly used. Therefore, by using a higher concentration it should result in an activation of the pathway if the pathway is involved. These cells were then investigated using Western blot analysis to see if such treatment activated the JNK pathway. As figure 3.18 shows, there was no activation of the pathway at any of the chosen time points (Day 3 stimulation: 0.00±0.1813 and day 7 0.00±0.02461 respectively). These results alongside the literature would imply that the JNK pathway is not implicated in the cellular response to radiation.

As x-irradiation did not result in an activation of the JNK pathway it was then determined if radiation has an effect on HUVECs. Therefore, clonogenic assays were carried out using concentrations of both 2 and 5Gy radiation. This assay is commonly used to assess the effects of Gama radiation on cell survival. As figure 3.19 Shows radiation at both concentrations used had a significant effect on HUVEC viability. Figure 3.19 A shows the survival fraction is significantly reduced and, in a concentration dependent manner, with 5gy reducing the survival fraction to 0.05. Therefore, it has been shown that there is an irradiation induced effect on cell viability, however this is independent of the JNK pathway.

A)

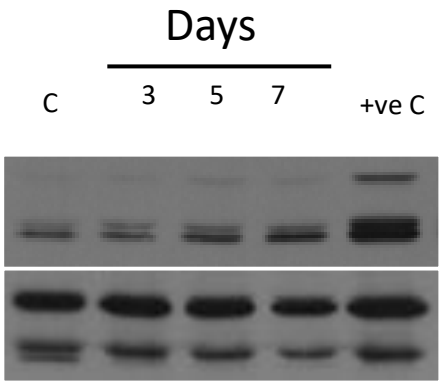


B)

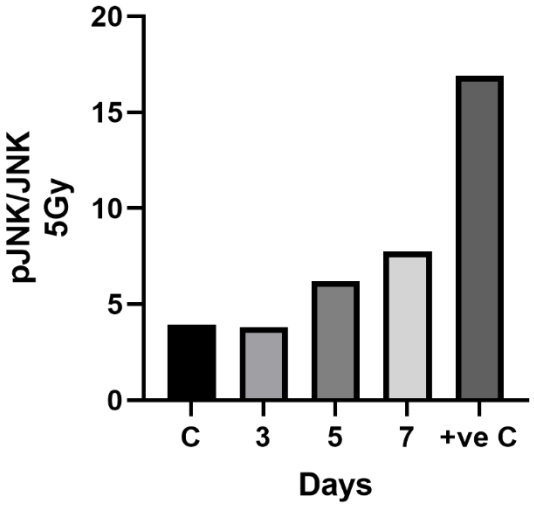


**Figure 3.18 X- irraadiation – mediated activation of the pJNK pathway in HUVECs.**

Confluent HUVECs were stimulated with 5Gy over 3, 5 and 7 days, or 30µM Doxorubicin for 24hours as +ve C (positive control). Western blot analysis was performed for pJNK and Total JNK. Blots were semi-quantified as outlined in Methods section 2.2.2.6. A) Western blot representation. B) Semi-quantification for pJNK n=1.

A)

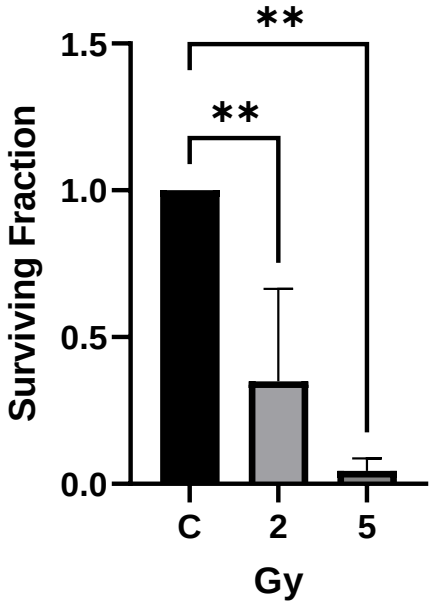


B)

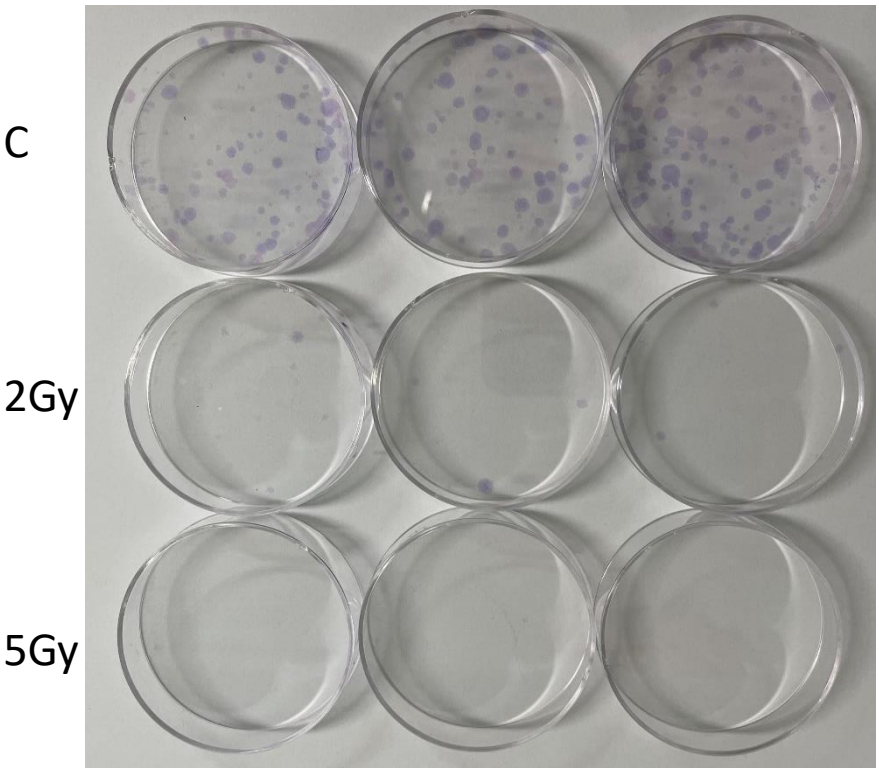


**Figure 3.19 The Effect of Irradiation on HUVEC cell death using Clonogenic assays.**

HUVEC cell viability was measured using clonogenic assay and calculating the surviving fraction, as outlined in section 2.2.3. A) 350 HUVECs were plated in each dish, they were irradiated 24 hours later with 2 and 5Gy. B) Cell viability was determined by calculating surviving fraction. Data represents mean ±S.E.M, n=3, **P<0.005 compared to control.

### 3.2.8. Doxorubicin induced ATM activation

After examining the impact of Doxorubicin on JNK activation and cell death, the pathway was investigated further by looking upstream at ATM activation and to establish whether there was a correlation between ATM activation and JNK signalling for the anti-cancer agents. As previously discussed, ATM is activated at the point of DNA damage and initiates the cells response to the damage. As figure 3.20 shows, ATM is phosphorylated with concentrations of Doxorubicin as low as 0.1µM. Phosphorylation then increases and reaches a maximum at 30µM doxorubicin (stimulation: 518.6±0, N=1). This shows that Doxorubicin is inducing DNA damage at concentrations far less than that observed for JNK activation.

Figure 3.21 shows the time dependent activation of ATM with 30µM of Doxorubicin. Activation of the pathway is observed as early as 15 minutes (stimulation: 36.89±0, N=1) and remains sustained for the 4 hours examined (stimulation: 63.74±0, N=1). Whilst it is possible that ATM may be upstream of the JNK pathway activated in response to doxorubicin, the significant differences in concentration dependency and onset of activation suggest the two events are not interlinked. Time constraints did not allow a similar assessment of Cisplatin or Sunitinib.

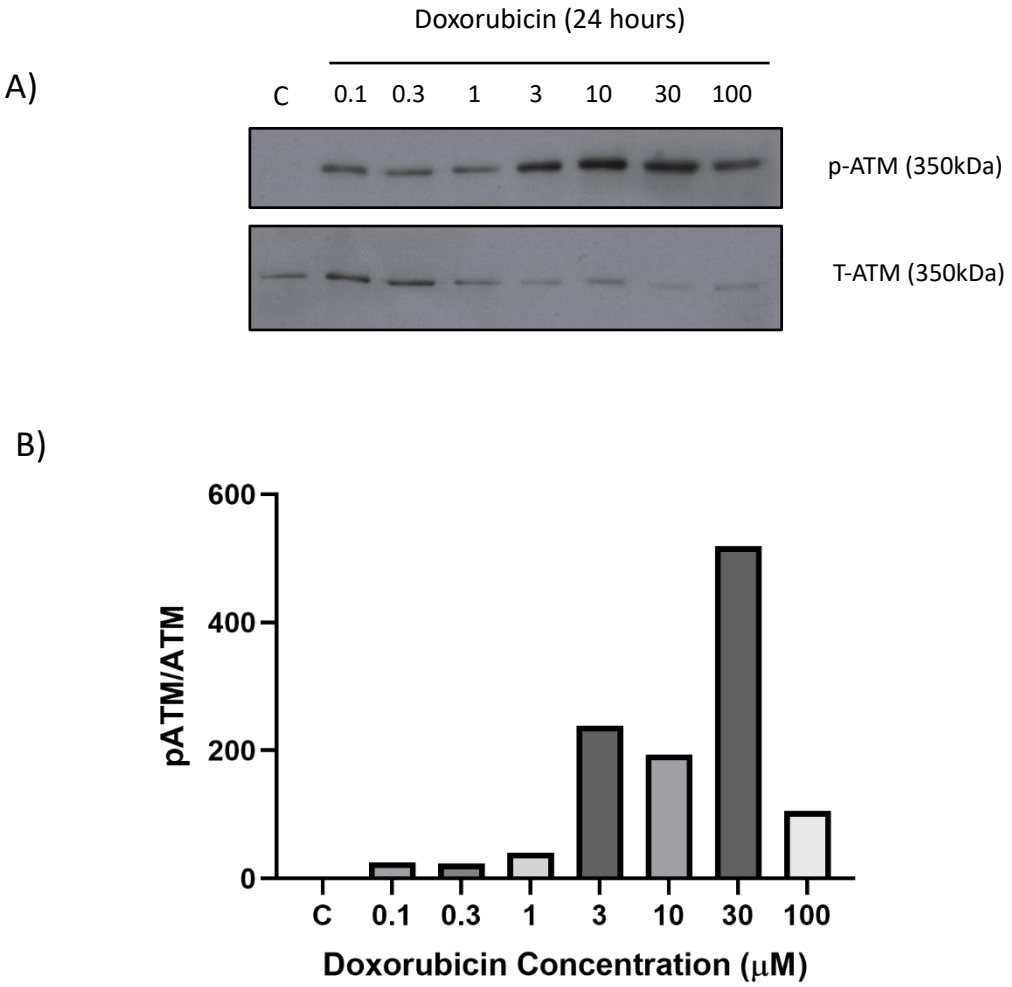


**Figure 3.20 : Doxorubicin dependent activation of ATM pathway in HUVECs.**

Confluent HUVECs were stimulated with Doxorubicin (0.1μM-100μM) for 24 hours. Western blot analysis was performed for pATM and Total ATM. Blots were semi-quantified as outlined in Methods section 2.2.2.6. A) Western blot representation. B) Semi-quantification for p-ATM, n=1.

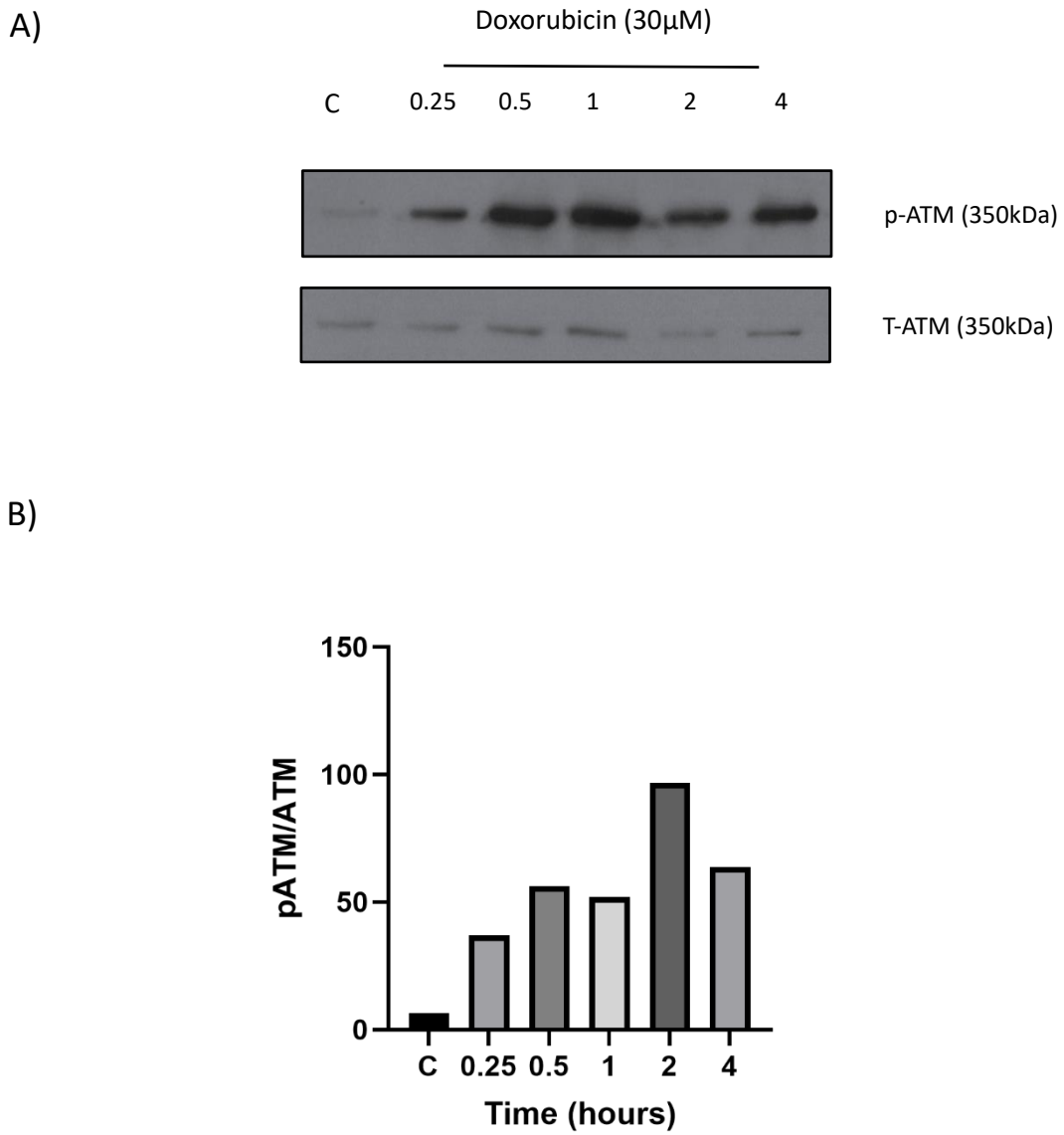


**Figure 3.21 Doxorubicin Time dependent activation of ATM pathway in HUVECs.**

Confluent HUVECs were stimulated with 30µM Doxorubicin for 0.25-4 hours. Western blot analysis was performed for pATM and Total ATM. Blots were semi-quantified as outlined in Methods section 2.2.2.6. A) Western blot representation. B) Semi-quantification for pATM, n=1.

## 3.3. Discussion

The objective of this chapter was to identify the effect that different cardiotoxic cancer treatments have on JNK signalling and correlate this with effects on cell survival. As previously mentioned, the JNK pathway is a stress activated pathway that has been linked to endothelial damage. Here it has been shown using HUVECs to investigate endothelial cell function that the JNK pathway is activated by Doxorubicin and Cisplatin, but not Sunitinib. Previous studies have also shown that JNK can be stimulated by both Doxorubicin and Cisplatin in other cell types (Helbig et al., 2011, Kim et al., 2010, Sánchez-Perez et al., 1998). Kim et al (2010) found that in liver and breast cancer cells 3.5µM of Doxorubicin induced JNK1 activation at 20 hours (Kim et al., 2010). They state that JNK enables the activation of Stat3 may induce the repair of DNA breakage (Kim et al., 2010). Whereas Helbig et al (2011) found that in human fibroblast cells concentrations above 50µM induced JNK activation from 6 hours, showing sustained activation until 24 hours of exposure. Both studies, using different cell lines have shown that JNK activation by such chemotherapeutic agents induce delayed and sustained JNK activation, which corresponds with the findings of this chapter. This delayed and sustained activation has been linked to cell death (Wong et al., 2010).

It has been shown in other studies that cardiovascular toxicities is initially believed to begin with the endothelium and this damage has been shown to lead to atherosclerosis (Bar-Joseph et al., 2011). The activation of the JNK pathway has been linked to endothelial dysfunction and was assessed with flow-mediated dilation (Bretón-Romero et al., 2016). Cytokines and ROS have both been implicated with the activation of the JNK pathway and ultimately endothelial dysfunction (Li et al., 2016b). A number of studies have shown that this damage is related to the activation of the JNK pathway (Hui, 2007, Ricci et al., 2004).

Ricci et al (2004) used an atherosclerosis mouse model with either a JNK1 knockout or a JNK2 deletion, this ultimately showed that JNK2 promoted the formation of atherosclerosis lesions.

This highlighted the importance of JNK2 phosphorylation for the development of foam cells, as it phosphorylates SR-A (scavenger receptor-A) which is needed for the lipid uptake of macrophages which leads to foam cell formation. Whereas another study has linked the JNK pathway with atherosclerosis. By knocking out JNK in a mouse model they were able to show the protection of macrophages from apoptosis which leads to the acceleration of atherosclerosis (Babaev et al., 2016). Therefore, further work will be carried out to understand if this activation is linked to endothelial dysfunction and possibly cardiovascular toxicities.

Not only has this study shown that these compounds activate the JNK pathway, it has also shown that this is a sustained activation of JNK which is linked to cell death (Dhanasekaran and Reddy, 2017). This sustained JNK activation correlates with the MTT and FACS analysis of cell death from both compounds. This phenomenon has been found by a number of studies (Brantley-Finley et al., 2003, Brozovic et al., 2004). Brantley-Finley et al (2003) found that Doxorubicin treated KB-3 cells activated JNK, which was sustained from 8 to 48 hours. The sustained activation was found to correlate with an increase in cell death. Doxorubicin has been well documented at causing cell death in a number of cell types. This delayed and sustained from of activation has been linked with cell death, which confirms the findings of this chapter. Shin et al (2015) found that Doxorubicin does this by increasing the cells in subG1 phase and preventing cell proliferation by arresting the cell cycle in G2/M phase to S phase (Shin et al., 2015). This pattern of apoptosis shown for Cisplatin is also consistent with previous results. It has been well documented that Cisplatin induces apoptosis and studies including Chen et al, 2022 have also documented that cell viability is affected above 20µM with significant cell death at 100µM.

It has been observed that Cisplatin activation of JNK resulted in a sustained activation of the pathway of over 72 hours, with the use of the JNK inhibitor II they were able to correlate the sustained activation of JNK with apoptosis (Brozovic et al., 2004). Cisplatin has also shown to delay and even arrest cells in the S and G2 phase (He et al., 2011, Shen et al., 2013). As Cisplatin has shown little concentration dependent effect, this indicates a different mechanism to Doxorubicin induced cell death. This could indicate that even though both agents cause sustained JNK activation and late apoptotic cell death, the mechanisms differ.

It is believed that there would be a possible link between the activation of the NF-κB pathway and the activation of the JNK pathway. This study has shown that there is little to no effect seen on either p-65 or IκBα, therefore confirming that this mechanism is independent of the NFκB pathway and not used in HUVECs. Other studies including Klim et al. 2010, has shown that Doxorubicin does not induce p65 over 2hrs in HUVECs. It is well established the NF-κB pathway plays a role in inflammation, cell survival (Papa et al. 2006). It has been shown that NF-κB plays a role in programmed cell death, where NFκB mediates the suppression of the JNK pathway and activity of ROS (Papa et al., 2006). By using knockout mouse models, it has also been shown that TNFα in a normal model would induce a pJNK response at 30-60 mins (Papa et al., 2006). However, by blocking the NF-κB pathway, it results in a prolonged activation of the JNK pathway, causing cell death. It was therefore investigated using the canonical NFκB pathway, to see if prior to the 4 hours taken to see JNK activation, Doxorubicin induced a pro-survival mechanism facilitated by the NF-κB pathway.

The other pathway investigated was ATM as the results show DNA damage and ATM activation begins at low concentrations within 15 minutes of treatment. Suggesting that ATM activation occurs prior to JNK and there would be a link between the ATM DNA damage response and JNK activation. To further validate these initial findings the ATM antibody should be optimised further, due to the size of the protein western blot protocol was amended.

Time restraints prevented further optimisation where tubulin would be used as a loading control, as total ATM is known to degrade and could not be used as a stable loading control. However, the ATM has been shown to be activated in other studies including Kurz et al, 2004 where they treated ATM proficient and deficient cell lines with concentrations as low as 1µM of Doxorubicin for 2 hours (Kurz et al., 2004).

It has also been shown by other studies that ATM is activated prior to JNK indicating further exploration of the pathway between ATM and JNK could be investigated. Other studies have linked ATM and JNK activation using other compounds, such as Wang et al. They have shown that ATM activation by HKH40A (RTA 502), a topoisomerase I inhibitor, activates ATM and JNK in liver cancer resulting in apoptosis (Wang et al., 2009).

ATM activation is known to be a result of ionising radiation, and a cancer treatment that has been linked with cardiovascular toxicities. Therefore, x-irradiation was investigated with HUVECs to look at the implication's radiotherapy may have on the JNK pathway. Radiotherapy is one of the major treatments for cancer, it can be used both on its own and in combination with chemotherapy. As well as chemotherapy radiotherapy has been linked with cardiovascular toxicities.

Currently within the UK both gamma radiation and x-irradiation are used for cancer treatment. In this study we have shown that x-irradiation such as given to cancer patients has a significant impact on cell viability and the health of endothelial cells, with the cell viability significantly affected after exposure to 2Gy of radiation. There have been several studies however that also show that radiation effects the vascular endothelial cells (Helm et al., 2016, Jabbari et al., 2019). Studies such as the one carried out by Rombout et al (2013) have shown that x-radiation does induce DNA damage and apoptosis in endothelial cells. This was shown in both HUVECs and the immortalised endothelial cell line EAhy.926 (Rombouts et al., 2013).

However, when investigating the effect on HUVECs it can be concluded that this damage is not through the JNK pathway. Experiments were carried out over a series of time points from 0.25 -24hrs up to 7 days post radiation all showing no increase in pJNK expression.

This demonstrates that JNK is not involved in any part x-irradiation damage from initial cell survival to cell death mechanisms. It is, however, well known that ultraviolet (UV) radiation activates the JNK pathway, where it was found to activate JNK by increasing the JIP3 MEKK1 interaction (Song and Lee, 2007). However, there is little evidence in the literature that shows this is also true of x-irradiation.

One theory for this could be that an increase in caspase 3 due to the radiation prevents the binding of the JNK complex, therefore preventing the activation of the pathway. This concept has been shown in a study by (Vaishnav et al., 2011). Caspase 3 is known to increase in the cellular cytoplasm as a result of radiation, therefore in a future study this mechanism could be further investigated to understand if as a result of x-irradiation the JNK pathway is prevented from activating and the effect this has. If this is the case further research will be needed to understand this mechanism and if this is to protect the cells or if this leads to a more direct form of cell death.

Caspase 3 plays a key role in pyroptosis, this is a form of cell death that differs to both apoptosis and necrosis (Jiang et al., 2020). This mechanism of programmed cell death was first discovered by Friedlander in 1986 when looking at the effect anthrax had on mouse macrophages (Friedlander, 1986). This newly discovered form of cell death is believed to be a defence mechanism from pathogens and is considered an inflammatory response (Loveless et al., 2021). Unlike apoptosis the cell membrane swells and leaks the contents rupturing the cell and releasing intracellular contents resulting in an immune response leading to the death of the cell (Lu et al., 2022).

This form of cell death is often difficult to distinguish between apoptosis and necrosis using Annexin V and PI as used in assays such as FACS therefore other techniques are required (Abe and Morrell, 2016, Vande Walle and Lamkanfi, 2016).

To further investigate this form of cell death and the link between cell death and JNK, various inhibition mechanisms have been investigated.

These were used to examine whether these previously used compounds induce pyroptosis programmed cell death via the JNK pathway. If so, by inhibiting JNK could this reduce the cell damage observed. Therefore, Doxorubicin and Cisplatin will be further investigated for its effect on HUVECs and the involvement of the JNK pathway.

# Chapter Four

## The Role of JNK in Doxorubicin and Cisplatin mediated endothelial cell death.

# 4. The Role of JNK in Doxorubicin and Cisplatin mediated endothelial cell death

## 4.1. Introduction

The experiments carried out in the previous chapter show that the chemotherapeutic agents that are known to cause cardiovascular toxicities affect endothelial cell lines and activate the JNK pathway. It has also been previously established that there is a link between the kinetics of JNK activation and cell death (Antlsperger et al., 2003). We have also shown that in HUVECs there is a sustained activation of JNK following treatment with Doxorubicin and Cisplatin. It is important to understand if inhibiting JNK could impact these responses. Therefore, the aim of this chapter is to knockout or inhibit JNK to analyse the impact this has on HUVEC cell viability. It is hypothesised that by inhibiting the JNK pathway it would protect the cells from damage by the chemotherapeutic reagents. For this a JNK CRISPR knockout cell line was designed and the use of the well-known JNK inhibitor SP600125, and virus.

Several different tools were utilised to investigate this. A pharmacological tool SP600125 and an adenovirus encoding a modified version of MKP-2, and the relatively new technique of CRISPR cas9. This would allow an assessment of how effective each approach is but also would allow a full analysis of how these chemotherapeutic agents affect the cells and the impact the JNK pathway has. With respect to pharmacological inhibition, SP600125 is a well-known JNK inhibitor which binds to the ATP binding site within JNK (Heo et al., 2004). This pharmacological tool has been used many times in literature to inhibit the JNK pathway for studies including cardiovascular toxicities, thyroid cancer and neurological diseases, although there are some limitations with respect to specificity (Grassi et al., 2015, Zheng et al., 2022, Zhou et al., 2015). The MKP-2 used virus was a modified version of adenoviral MAP kinase phosphatase -2 used previously in our group and elsewhere (Al-Mutairi et al., 2010, Lawan et al., 2012, Misra-Press et al., 1995).

MKP-2 dephosphorylates MAP kinases in the nucleus, namely ERK and JNK (Al-Mutairi et al. 2010). The modified Adv.NLS-1 MKP-2 lacked the ERK binding sequence (Misra-Press et al. 1995) which also encodes an NLS, but this construct retained nuclear location due to presence of an additional bipartite sequence (Sloss et al., 2005). This conferred some specificity towards nuclear JNK. Prior to this study there was very little in the literature regarding JNK CRISPR cas9, therefore all sequences were designed using the tools available. These will all be investigated on their effect with both the compounds and cell death.

There has been considerable expansion of the modes of cell death induced by anti-cancer agents. In addition to apoptosis there are a number of other routes including, necroptosis, ferroptosis and pyroptosis (Strasser and Vaux, 2020). Pyroptosis is a new form of cell death, that results in an inflammatory related programmed cell death (Wu et al., 2022b). Pyroptosis can be induced by the activation of both GSDME and GSDMD, which cleave the N-terminal. This N terminal then translocates the cell membrane, resulting in cell swelling and bursting (Shen et al., 2021). It has been shown that caspase 3 mediates the GSDME activation of pyroptosis which has also been linked to the JNK pathway in breast and colon cancer research (Jiang et al., 2020, Yu et al., 2019c, Zhang et al., 2021). As the previous chapter shows, Doxorubicin and Cisplatin cause significant cell death, however it has been reported that both these compounds also activate caspase-3 and GSDME therefore the cell death reported in chapter 3 could be pyroptosis. There are reports in the literature that the GSDME pathway for pyroptosis is linked to the JNK pathway (Yu et al. 2019b). Therefore, in this chapter the effect of the 3 JNK degradation techniques will be used to investigate how this affects endothelial cell viability with particular attention on pyroptosis.

## 4.2. Results

### 4.2.1. JNK inhibition using SP600125

First, a pharmacological inhibitor, SP600125, was used to analyse the effect JNK had on cell viability through inhibition of the pathway. SP600125 was the first commercial JNK inhibitor, developed in 2001 by Bennett et al. It is an ATP competitive inhibitor that is known to occupy the hydrophobic pocket in JNK at the ATP binding site with over 20-fold selectivity (Bennett et al., 2001, Bogoyevitch and Arthur, 2008, Heo et al., 2004, Wang et al., 2007). This gives a reversible and ATP competitive inhibition, which would be a more clinically relevant model (Bogoyevitch and Arthur 2008). For this, two concentrations of both Doxorubicin and Cisplatin were chosen. 10µM and 30µM respectively were used for Doxorubicin and 30µM and 100µM of Cisplatin. HUVECs were exposed to these concentrations after being pretreated with SP600125 at 10µM and 20µM respectively.

It was important to confirm whether the inhibitor effectively prevented phosphorylation of JNK pathway before moving forward. Other studies have shown successful inhibition JNK in HUVECs with 10µM and above of SP600125 (Li et al., 2016a, Miho et al., 2005, Zhang et al., 2016). Therefore 10 and 20µM of SP600125 were then chosen to go forward. HUVECs were pre-treated with the selected concentrations of inhibitor (10µM and 20µM) and stimulated with 30µM of Doxorubicin.

Therefore, HUVECs were pre-treated with 10µM and 20µM of SP600125 for 1 hour prior to treatment with 30µM of Doxorubicin for a further 24hours. As figure 4.1 shows, there is a slight inhibition of phosho-JNK levels. Although this has shown to be non-significant there is a decrease in JNK activity with the use of the inhibitor. Doxorubicin at 30µM stimulated an increase in pJNK at 24 hours (Stimulation: 71.02±6.738, N=3).

Pretreatment with SP600125 caused a concentration dependent decrease in JNK; 10µM reduced phosphorylation levels by approximately 20% (Stimulation: 52.52±8.062, N=3) and 20µM (Stimulation: 52.68±12.31, N=3) respectively. Figure 4.1 also indicates a reduction in JNK2 levels, this band shows visible reduction with the inhibitor compared to JNK1 which shows only a slight reduction in levels with 20µM of SP600125. This demonstrates that SP600125 has a slight effect when inhibiting JNK, which is in line with the literature where Zhang et al (2016) have also shown a reduction in JNK expression using HUVECs (Bennett et al., 2001, Wood et al., 2018). Zhang et al (2016) also used 10 µM of SP600125 in HUVECs, 1 hour prior to treatment. Although a reduction in JNK expression can be seen as with this study this is not complete inhibition (Zhang et al., 2016).

A)

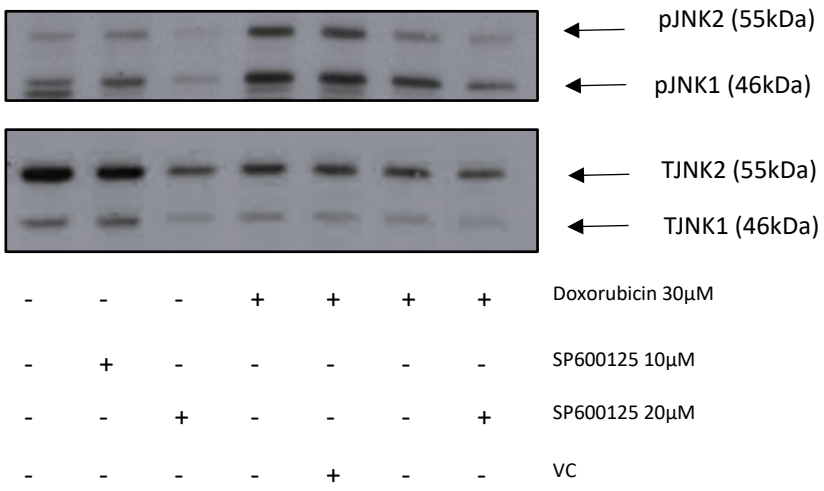


B)

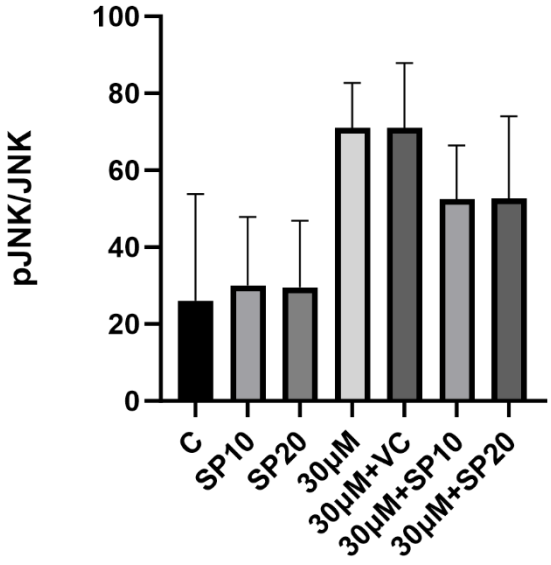


**Figure 4.1 Effect of SP600125 on Doxorubicin stimulated pJNK expression in HUVECs.**

Confluent HUVECs were pretreated with SP600125 (10 and 20µM) or DMSO as VC (vehicle control) for 1 hour prior to being stimulated with Doxorubicin (30µM) for 24 hours. Western blot analysis was performed for pJNK and Total JNK. Blots were semi-quantified as outlined in Methods section 2.2.2.6. A) Western blot representation. B) Semi-quantification for pJNK, Results represent mean ± S.E.M, n=3, Non-significant, compared to control.

This was then repeated with Cisplatin as the stimulation agent. It was found that the SP600125 inhibitor had a similar effect on Cisplatin as compared to Doxorubicin. Figure 4.2 A and B show that there is an increase in pJNK as expected and a decrease in activation with the introduction of the inhibitor, although this inhibition does not reach significance. The higher concentration of 20µM of SP600125 does show a greater reduction in phosphorylation (Stimulation: 15.41±9.838, N=3). The same protective phenomena can also be observed when looking at the total JNK blot where protein preservation may be indirectly indicated, this is particularly the case for JNK2; Cisplatin reduced JNK2 which is recovered by preincubation with the inhibitor. Further investigation is required to show whether there is a cellular protective element from SP600125. However, compared to figure 4.1 and the effect of Doxorubicin, there is a distinctive effect on the individual isoforms particularly JNK2. This could be due to the mechanism of action SP600125 has on the cells in combination with the different mechanisms of action of Cisplatin and Doxorubicin.

A)

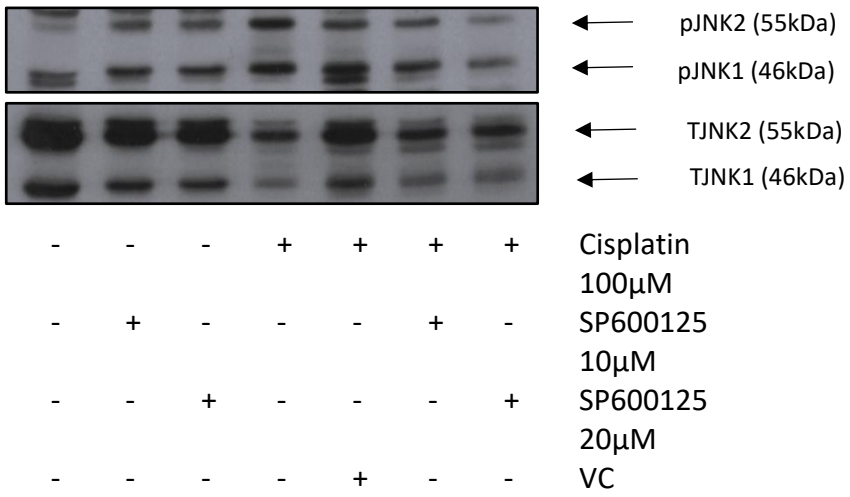


B)

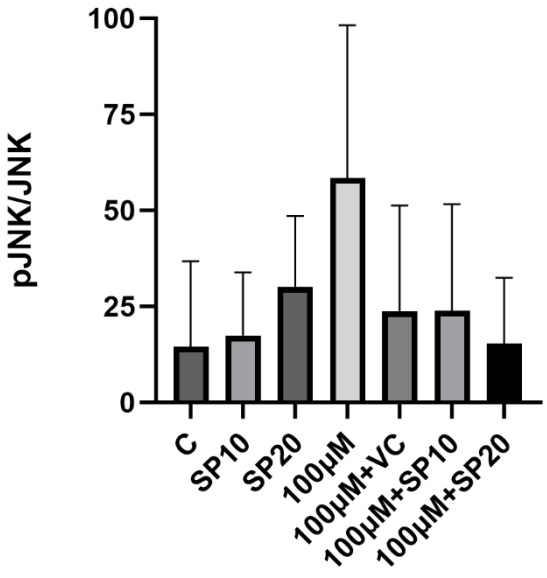


**Figure 4.2 Effect of SP600125 on Cisplatin-stimulated pJNK expression in HUVECs.**

Confluent HUVECs were pretreated with SP600125 (10 and 20µM) or DMSO for VC (vehicle control) for 1 hour prior to being stimulated with Cisplatin (100µM) for 24 hours. Western blot analysis was performed for pJNK and Total JNK. Blots were semi-quantified as outlined in Methods section 2.2.2.6. A) Western blot representation. B) Semi-quantification for pJNK Results represent mean ± S.E.M, n=3, Non-significant, compared to control.

To further investigate the impact SP600125 had on cell survival, DNA damage markers were utilized. These included γH2.AX, Caspase 3 and GSDME which not only further increased the understanding as to the nature of the damage these treatments caused but also to see if by pre-treating the HUVECs there is any protection.

First, the known DNA damage marker γH2.AX was investigated in respect to both Doxorubicin and Cisplatin stimulation at 30µM and at 100µM respectively (figures 4.3 and 4.4). γH2.AX is phosphorylated by ATM, which can also be an indicator of double strand breaks (Mah et al., 2010). When looking at the two western blots together it is clear that both drugs activate the phosphorylation of γH2.AX, indicating DNA damage, which has been previously shown in HUVECs (Ziegler et al., 2020). The stimulation for each agent is similar between Doxorubicin at 30µM (Stimulation: 49.45±17.04, N=2) and 100µM of Cisplatin at approximately 50-fold (Stimulation: 58.96±7.821, N=3). However, both figures 4.3 and 4.4 also show that SP600125 does not provide protection from DNA damage to the cells as measured by this marker. For Doxorubicin (figure 4.3) there is activation of the pathway with 30µM (Stimulation: 36.36±6.932, N=3), and there is a slight increase with the 10µM of inhibitor (Stimulation: 39.77±6.932) however with the higher concentration there is minimum difference between cells treated with the inhibitor and those without (Stimulation 36.06±7.338, N=3). These results indicate that the inhibitor does not protect from initial damage but may prevent further downstream pathways.

The reverse is apparent when looking specifically at Cisplatin stimulation. When stimulated with 100µM of Cisplatin alone there is an increase in pγH2A.X levels (Stimulation: 58.96±7.82, N=3) when compared to cell only (control stimulation: 26.79±12.20, N=3). There is a no difference however, following pretreatment with the lower concentration of inhibitor (SP600125 10mM stimulation: 58.26±15.35 N=3) compared to the cells treated with Cisplatin alone (Stimulation: 58.96±7.821, N=3). Unlike with Doxorubicin the higher concentration has been shown to further activate pγH2A.X (Stimulation: 62.16±7.934, N=3).

It should also be noted that in both experiments, the higher concentration of SP6000125 mediated an increase in resting pγH2A.X phosphorylation. This was consistent with the loss in protein recovery in the JNK blots suggesting some form of cellular damage. Here the effects on GAPDH were inconsistent but may suggest an off-target effect of SP600125 at this concentration.

A)

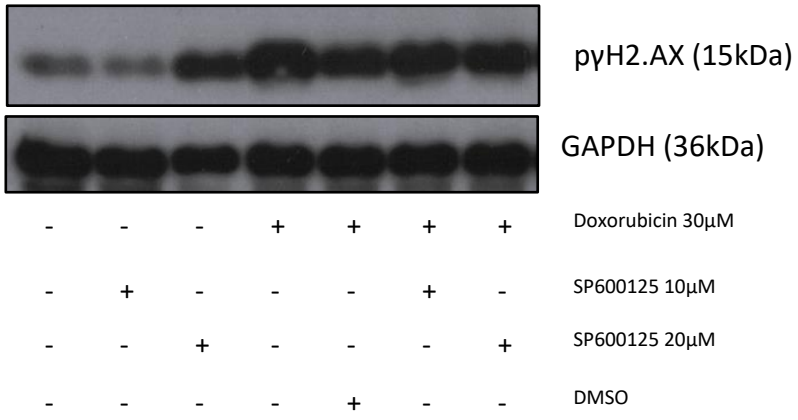


B)

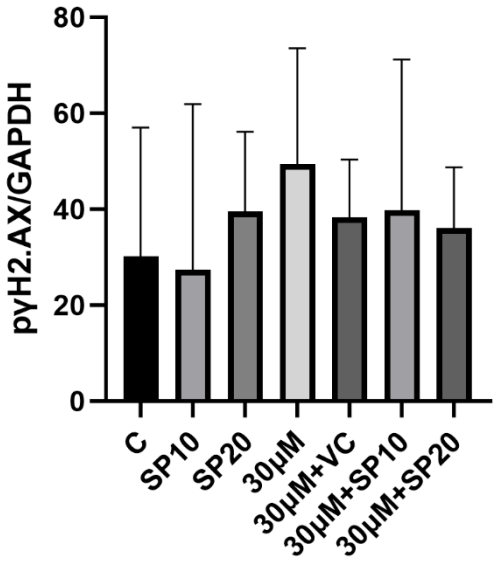


**Figure 4.3 Effect of SP600125 on Doxorubicin-stimulated pγH2.AX expression in HUVECs.**

Confluent HUVECs were pretreated with SP600125 (10 and 20µM) or DMSO as VC (vehicle control) for 1 hour prior to being stimulated with Doxorubicin (30µM) for 24 hours. Western blot analysis was performed for pγH2A.X and GAPDH. Blots were semi-quantified as outlined in Methods section 2.2.2.6. A) Western blot representation. B) Semi-quantification for pγH2.AX Results represent mean ± S.E.M, n=3, Non-significant, compared to control.

A)

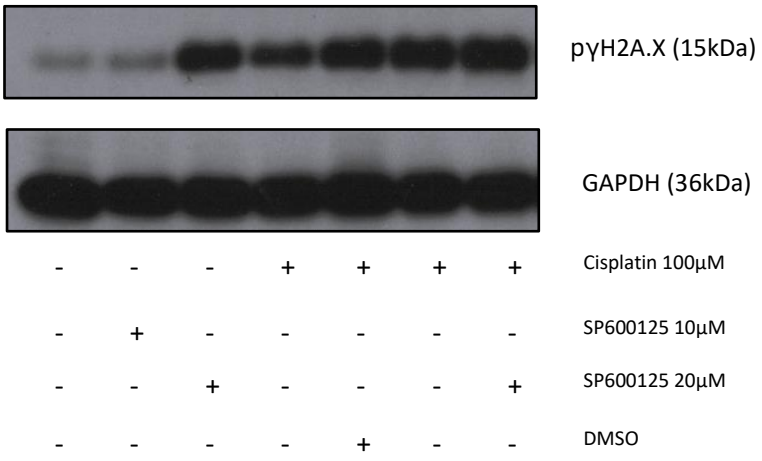


B)

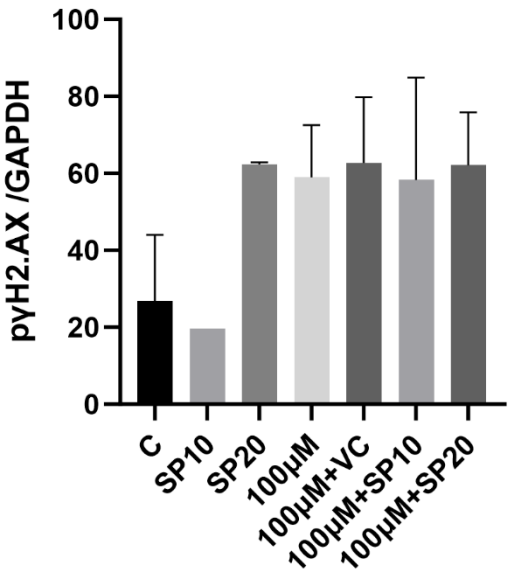


**Figure 4.4 Effect of SP600125 on Cisplatin-stimulated pγH2.AX expression in HUVECs.**

Confluent HUVECs were pretreated with SP600125 (10 and 20µM) or DMSO as VC (vehicle control) for 1 hour prior to being stimulated with Cisplatin (100µM) for 24hours. Western blot analysis was performed for pγH2A.X and GAPDH as loading control. Blots were semi-quantified as outlined in Methods section 2.2.2.6. A) Western blot representation. B) Semi-quantification for pγH2.AX. Results represent mean ± S.E.M, n=3, non-significant, compared to control.

### 4.2.2. Effect of SP600125 on Caspase-3 activation and GSDME in HUVECs

As previously stated, caspase 3 and GSDME have both been shown to be involved in the pyroptosis pathway (Jiang et al. 2020). Therefore, the effect of Cisplatin and Doxorubicin on theses markers of pyroptosis was assessed. Zhang et al (2019b) found that Doxorubicin elicits activation of both caspase 3 and GSDME in breast cancer cells (Zhang et al., 2019b). Cisplatin has also been shown to activate the pathways in lung cancer cell lines (Zhang et al., 2019a). Several articles have also shown the potential link between GSDME pyroptosis and the JNK pathway (Shen et al., 2021, Yu et al., 2019c, Zhang et al., 2021). Therefore, it was decided to investigate whether an inhibitor of the JNK pathway could have an effect on this mechanism of cell death in HUVECs. Initially, two concentrations of Doxorubicin were utilised, 30µM a concentration which was shown in the previous chapter to induce cell death and JNK activity, but also a lower concentration to determine if the pathways can be dissociated with JNK.

Initially for Doxorubicin, addition to the cells at the lower concentration of 10µM (Stimulation:23.98±1.50 N=2) resulted in a slight increase in cleaved caspase 3 levels when compared to the control (Stimulation:14.57±11.20 N=2). However, expression was increased slightly following pretreatment with SP600125 at either 10µM (Stimulation:36.48±14.73, N=2) or 20µM (Stimulation: 38.25±4.04, N=2). Using Doxorubicin at 30µM resulted in a strong activation of cleaved caspase 3 formation (Stimulation: 71.42±24.94, N=2). Pretreatment with the inhibitor at the higher concentration did not have an impact on the caspase 3 levels with a very slight decrease observed at 20µM (Stimulation: 64.56±43.86, N=2). This possibly indicates that the damage caused by the higher concentration of Doxorubicin cannot be reversed by the addition of SP600125.

However, using Cisplatin does reveal a differing profile of effect by SP600125. As figure 4.6 shows there was strong stimulation of caspase 3 cleavage with Cisplatin at 100µM (Stimulation:114.6±9.43, N=2). However, there was a visible reduction in cleaved caspase 3 levels following preincubation with either 10µM (Stimulation: 94.76±8.69, N=2) or 20µM (Stimulation 72.26±6.67, N=2) of inhibitor respectively. This can also be observed in caspase 3 levels as expression is reduced with 100µM Cisplatin, and increases with the addition of inhibitor, as seen in figure 4.6A.

As with γH2A.X, the higher concentration of SP6000125 mediated an increase in resting caspase 3 cleavage. Also, there was a loss in protein recovery in the GAPDH blots suggesting some cellular damage. Here the effects on GAPDH were inconsistent but generally SP600125 treatment resulted in increased protein recovery following Cisplatin treatment. This may suggest both an effect on the JNK pathway which reverses Cisplatin induced cell damage but also an off-target effect of SP600125 at these concentrations.

A)

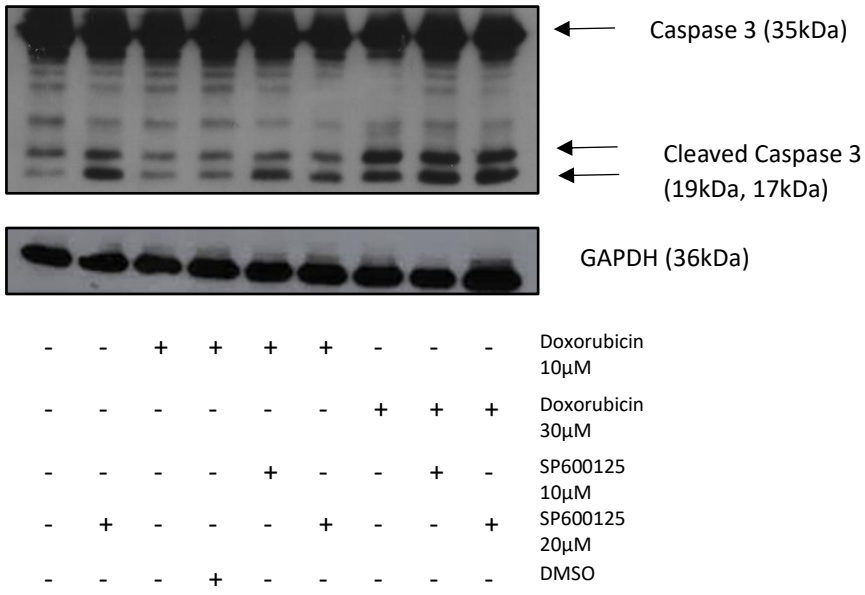


B)

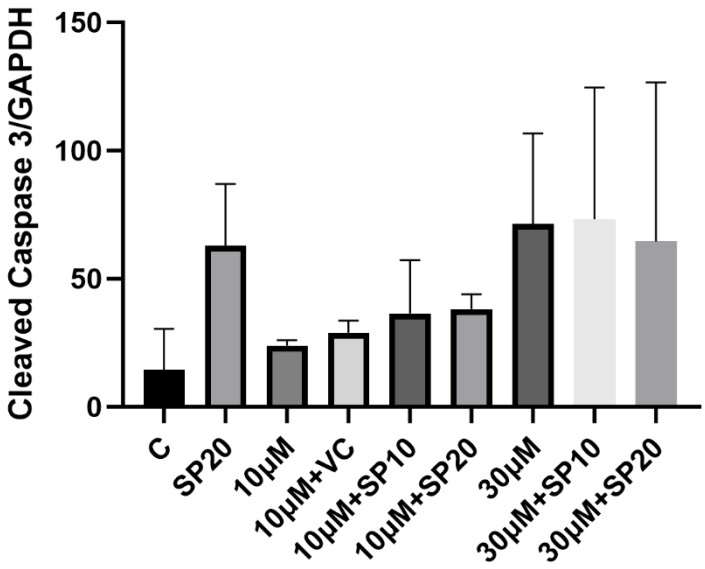


**Figure 4.5 Effect of SP600125 on Doxorubicin-stimulated caspase 3 cleavage in HUVECs.**

Confluent HUVECs were pretreated with SP600125 (10 and 20µM) or DMSO as VC (vehicle control) for 1 hour prior to being stimulated with Doxorubicin (10µM and 30µM) for 24 hours. Western blot analysis was performed for cleaved Caspase 3 and GAPDH. Blots were semi-quantified as outlined in Methods section 2.2.2.6. A) Western blot representation. B) Semi-quantification for cleaved Caspase 3, N=2.

A)

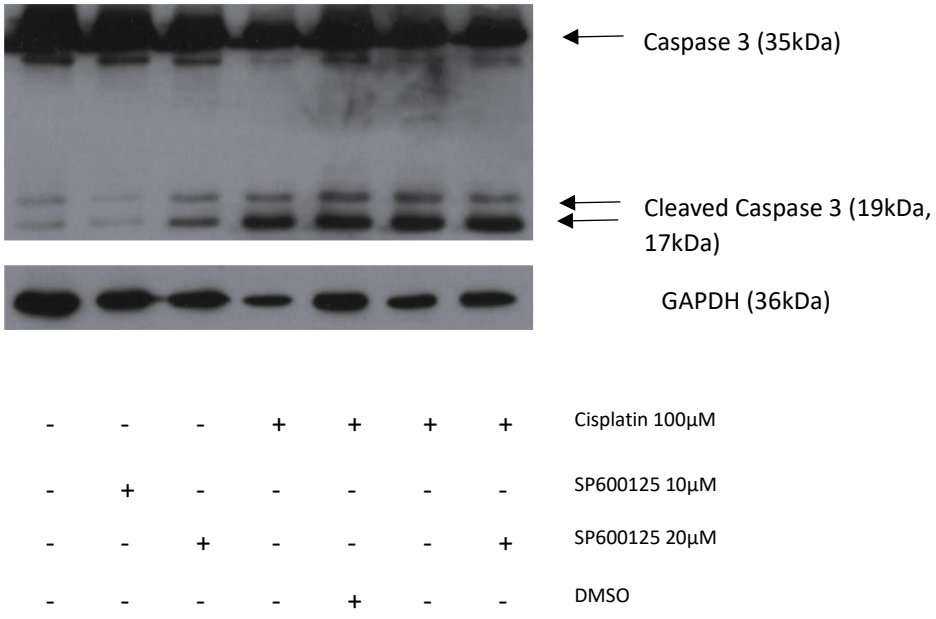


B)

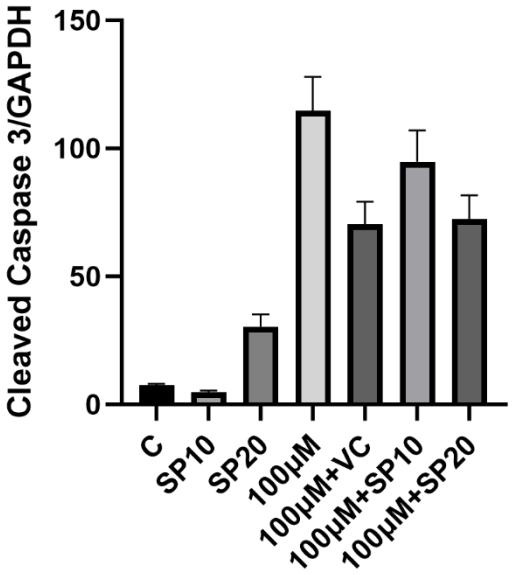


**Figure 4.6 Effect of SP600125 on Cisplatin-stimulated caspase 3 cleavage in HUVECs.**

Confluent HUVECs were pretreated with SP600125 (10 and 20µM) or DMSO for VC (vehicle control) for 1 hour prior to being stimulated with Cisplatin (100µM) for 24 hours. Western blot analysis was performed for cleaved Caspase 3 and GAPDH as loading control. Blots were semi-quantified as outlined in Methods section 2.2.2.6. A) Western blot representation. B) Semi-quantification for cleaved Caspase 3, N=2.

The next set of experiments examined the effect of JNK inhibition on Doxorubicin and Cisplatin-mediated GSMDE cleavage as this is a more definitive marker of the pyroptosis pathway. As Doxorubicin at a concentration of 30µM, gave a clearer stimulation of caspase 3 cleavage, this was used for the assay of GSDME cleavage. Figure 4.7 shows that Doxorubicin stimulated a marked increase in the formation of cleaved GSMDE, GSMDE-N which is the active form (Stimulation:66.09±11.69, N=3), suggesting that the pyroptosis pathway is being stimulated in these the cells. However, there was little impact on GSDME levels following pretreatment with SP600125 at either 10µM (Stimulation: 69.00±4.625, N=3) or 20µM (Simulation: 67.52±1.480, N=3) compared to the vehicle control. Inhibition of JNK by pretreatment with SP600125 may not be enough to protect the cells from the damage induced by Doxorubicin. As GSDME-N is the active form of GSDME the consistent levels of GSDME observed in figure 4.7 A also confirm the little impact on GSDME levels following SP600125 (Li et al., 2022a).

The effect of SP600125 on Cisplatin stimulation of GSDME cleavage is observed in figure 4.8 (figure 4.8). The blots and the quantified data show that 100µM Cisplatin stimulated an increase in GSDME-N formation (Stimulation: 102.2±14.75, N=3) suggesting that cell death for this drug could be via pyroptosis. This increase in GSDME-N expression is mirrored by the decrease of GSDME levels. This level of GSDME-N expression was slightly but not significantly reduced following pretreatment with the inhibitor at 20µM (85.51±8.429, N=3), when compared with the drug vehicle control. This shows that both Doxorubicin and Cisplatin stimulate intracellular mechanisms which result in the activation of pyroptosis. However, the concentration of Doxorubicin required to increase JNK levels does not result in increased levels of GSDME suggesting that JNK and pyroptosis are not interlinked. Similarly, whilst Cisplatin at 100µM increases phosphorylation of JNK and GSDME-N formation the lack of effect of SP600125 again suggests that there is no causal effect between these pathways.

A)

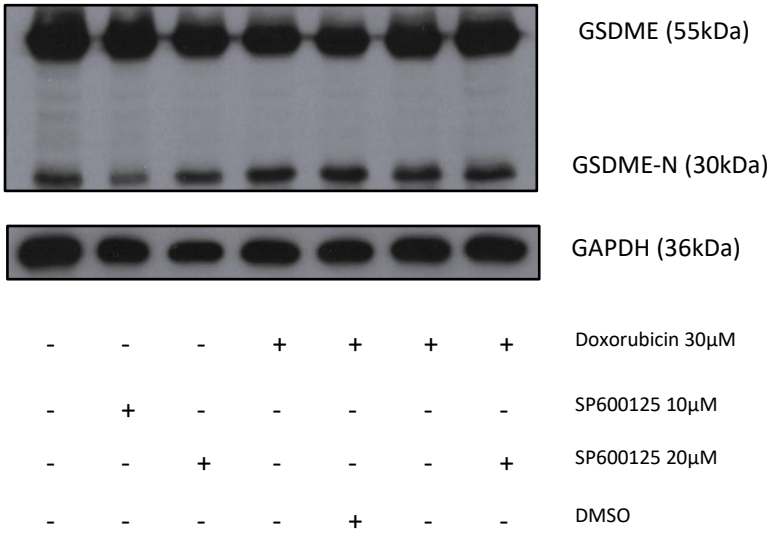


B)

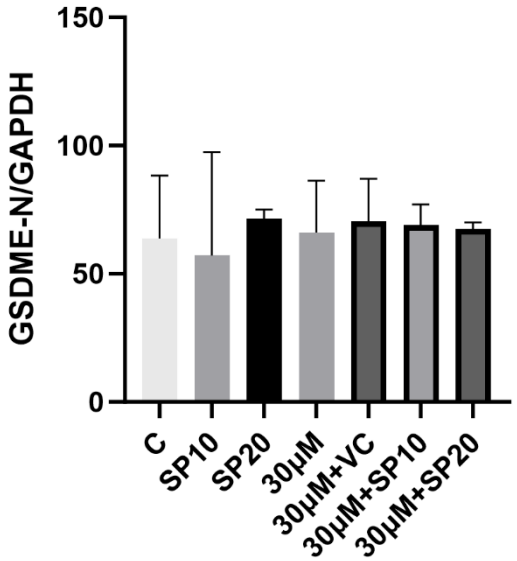


**Figure 4.7 Effect of SP600125 on GSDME-N expression stimulated by Doxorubicin in HUVECs**

Confluent HUVECs were pretreated with SP600125 (10 and 20µM) for 1 hour prior to being stimulated with Doxorubicin (30µM) or DMSO for VC (vehicle control) for 24 hours. Western blot analysis was performed for GSDME-N and GAPDH as a loading control. Blots were semi-quantified as outlined in Methods section 2.2.2.6. A) Western blot representation. B) Semi-quantification for GSDME-N. Results represent mean ± S.E.M, n=3, non-significant, compared to control.

A)

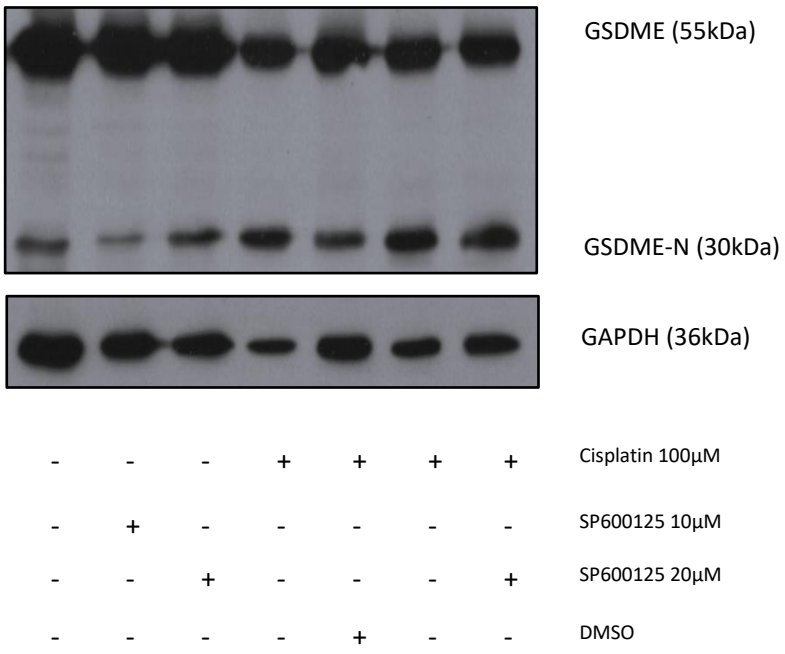


B)

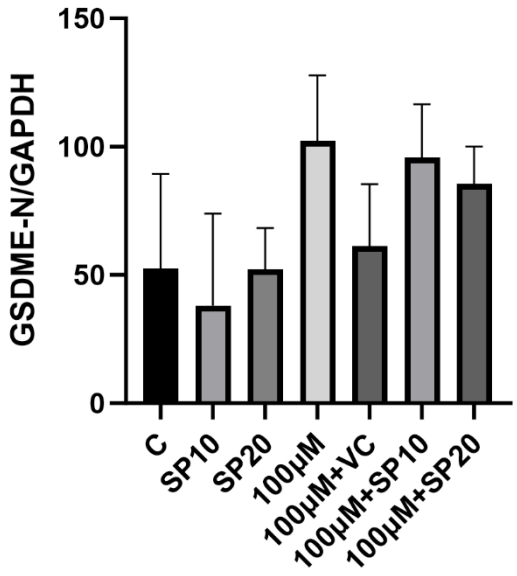


**Figure 4.8 Effect of SP600125 on GSDME-N expression in Cisplatin stimulated HUVECs.**

Confluent HUVECs were pretreated with SP600125 (10 and 20µM) or VC (vehicle control) for 1 hour prior to being stimulated with Cisplatin (100µM) for 24 hours. Western blot analysis was performed for GSDME-N and GAPDH used as a loading control. Blots were semi-quantified as outlined in Methods section 2.2.2.6. A) Western blot representation. B) Semi-quantification for GSDME-N. Results represent mean ± S.E.M, n=3, non-significant, compared to control.

### 4.2.3. FACS Analysis of the effect of SP600125 on Doxorubicin and Cisplatin Stimulated Cell death

To further investigate the potential protective impact the inhibitor may have on cell death, FACS analysis was employed using PI staining to identify necrotic cells and Annexin V-APC to identify apoptotic cells. Analysis was carried out for both Doxorubicin and Cisplatin alone or following pretreatment with the SP600125 inhibitor. For this analysis, two concentrations of each drug were chosen to see if the inhibitor would be more effective with a lower concentration of drug.

For Doxorubicin 10µM and 30µM were chosen respectively, as it has already been shown that over the 24-hour time point both concentrations elicit a JNK response. As figure 4.9 panel B shows Doxorubicin at both concentrations had a significant negative effect on the percentage of healthy cells. Even the lower concentration of Doxorubicin reduced the overall percentage of healthy cells from around 60% to near zero. Pretreatment of the cells with SP600125 at either 10 or 20µM had no effect on the effect of Doxorubicin. Furthermore, it was found that treatment with SP600125 reduced the percentage of healthy cells in a concentration dependent manner and at 20µM levels were reduced to approximately 20%

The same pattern can be observed when investigating early apoptosis (II), all cells treated with Doxorubicin reduced control levels of early apoptosis to near zero. Pretreatment of cells with SP600125 had no significant reversal effect. Once again, the inhibitor alone was found to stimulate early apoptosis in a concentration-dependent manner.

When assessing late apoptosis (III) and necrosis (IV) there is very little difference between not only the effects of the different concentrations of Doxorubicin but also the effect of the inhibitor, as figure 4.9 B shows. Doxorubicin at both concentrations stimulated a significant increase in the percentage of cells in late apoptosis (10µM 66%±2.11 and 30µM 71%±1.83 respectively).

Once again pretreatment with SP600125 did not reverse the effect of Doxorubicin, levels remained at stimulated values. Again, figure 4.9 shows that alone SP600125 caused an increase in late apoptosis, but interestingly this was not additive with Doxorubicin suggesting the levels of late apoptosis has reached a maximum level. Similar to late apoptosis, Doxorubicin at both concentrations stimulated a clear increase in necrosis increasing from resting levels of 3.1% to over 31.82% at 10µM and 28.03% at 30µM respectively (figure 4.9). Again, SP600125 alone was without effect but stimulated significant necrosis at the higher concentration. Taken together these results suggest that Doxorubicin activation of apoptotic cell death is not viva activation of the JNK pathway.

A)

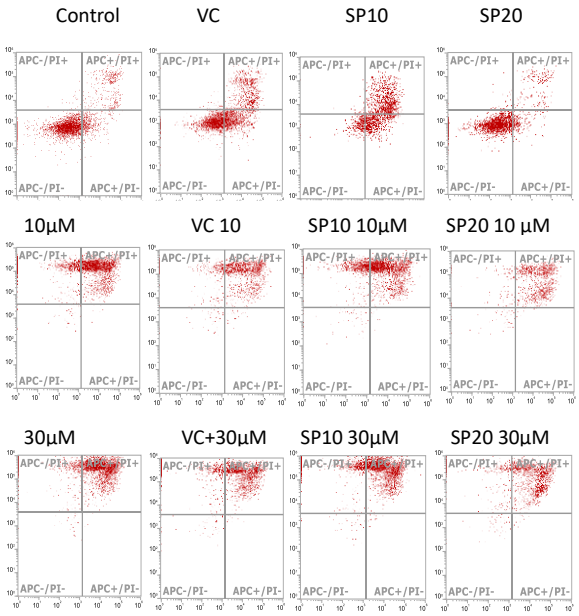
Control
VC
SP10
SP20
10µM
VC 10
SP10 10µM
SP20 10 µM
30µM
VC+30µM
SP10 30µM
SP20 30µM
APC-/PI+
APC+/PI+
APC-/PI-
APC+/PI-

B)

I)

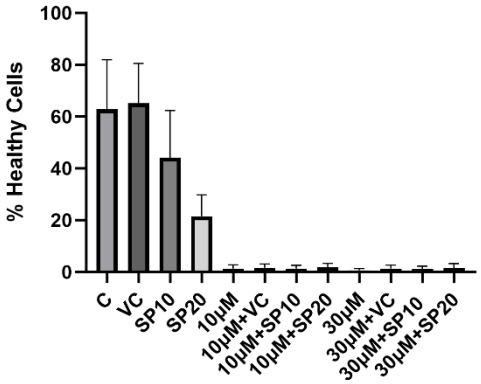
% Healthy Cells
100
80
60
40
20
0
C
VC
SP10
SP20
10µM
10µM+VC
10µM+SP10
10µM+SP20
30µM
30µM+VC
30µM+SP10
30µM+SP20

II)

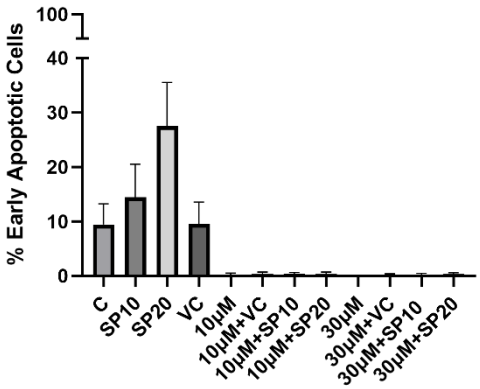
% Early Apoptotic Cells
100
40
30
20
10
0
C
SP10
SP20
VC
10µM
10µM+VC
10µM+SP10
10µM+SP20
30µM
30µM+VC
30µM+SP10
30µM+SP20

III)

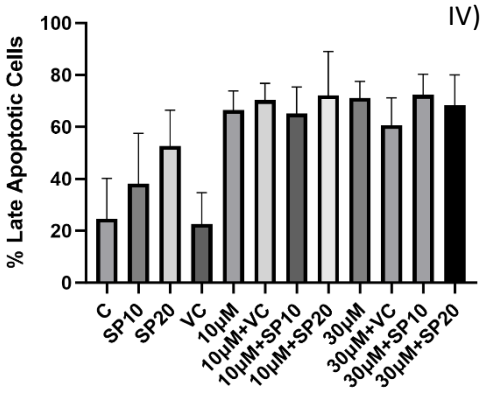
% Late Apoptotic Cells
100
80
60
40
20
0
C
SP10
SP20
VC
10µM
10µM+VC
10µM+SP10
10µM+SP20
30µM
30µM+VC
30µM+SP10
30µM+SP20

IV)

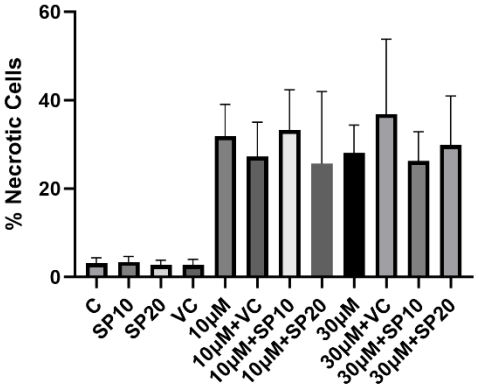
% Necrotic Cells
60
40
20
0
C
SP10
SP20
VC
10µM
10µM+VC
10µM+SP10
10µM+SP20
30µM
30µM+VC
30µM+SP10
30µM+SP20

**Figure 4.9 The effect of SP600125 on Doxorubicin stimulated HUVEC cell death using FACS analysis.**

HUVEC cell viability was measured using Flow Cytometry, as outlined in methods section 2.2.6. Confluent HUVECs were pretreated with 10 and 20µM of SP600125 or vehicle control (VC) DMSO for 1 hour prior to being stimulated with Doxorubicin (10µM and 30µM) for 24 hours. Cell viability was determined by PI and Annexin V-APC staining. Where, healthy (non), Early apoptosis (Annexin V-APC) Late apoptosis (PI and Annexin V-APC) and Necrosis (PI) were detected. A) Representative dot plots with double staining of Annexin V-APC/PI staining of Doxorubicin treated cells. B) Histograms showing percentage of I) Healthy, II) early apoptotic, III) late apoptotic and IV) necrotic cells. Results represent mean ± S.E.M, n=3, Non-significant, compared to Drug only control.

The next set of experiments examined the effect of Cisplatin on cell viability and the effect of SP600125 treatment (figure 4.10). Similar to Doxorubicin, Cisplatin stimulated a significant decrease in the percentage of healthy cells, with a concentration dependent effect apparent for 30µM and 100µM Cisplatin. However, the decrease in viability was not as pronounced as for Doxorubicin with 10% of healthy cells remaining at 100µM. The figure also shows that whilst SP600125 had no significant effect on the Cisplatin response however, SP600125 alone reduced cell via ability by up to 40% (both SP10 (%:44.10±5.26, N=3) and SP20 (%:21.50±2.38, N=3)) (figure 4.10 B).

When also looking at early apoptosis (Figure 4.10 B (II)) there is a significant increase in early apoptotic cells compared to control (9.44%) with Cisplatin alone at 100µM (24.35%) and 30µM (14.74%). However, when the cells were pretreated with SP600125 the levels of early apoptosis are shown to increase in the lower concentration. Figure 4.10B shows that 10 µM inhibitor (%:22.37±1.76, **P<0.005, N=3) and 20µM of inhibitor (%:21.08±1.20, **P<0.005, N=3) increase early apoptosis. However, when compared to the inhibitors effect with 30µM there is little change in early apoptotic levels with 10µM of inhibitor 24.24% and compared with 20µM at 20.34%. This indicates that the mechanism of action of the inhibitor may increase apoptosis and therefore the cellular damage caused by Cisplatin treatment. When looking in detail at the late apoptosis 10µM of inhibitor alone (14.42%) there is an increase in levels of early apoptosis which is much more evident with 20µM of the inhibitor alone (23.06%). Further demonstrating that the inhibitor itself if impacting the cell survival.

Late apoptosis has the largest proportion of cells across all treatment types, as with Doxorubicin (figure 4.10 B (III)). However, as with the healthy and early apoptosis the effect of the lower Cisplatin concentration again differs from the higher concentration. Untreated cells show 24.59% late apoptosis which increases with Cisplatin at 30µM 46.02% and 53.70% with 100µM.

As with this treatment there is a higher percentage of late apoptotic cells found with the inhibitors effect, again showing the inhibitor is not protecting cellular damage. With 30µM Cisplatin the inhibitor increases late apoptosis by up to 20% (SP10 58.72% and SP20 56.23%). Whereas the inhibitor has no effect on the percentage of late apoptosis of 100µM, as there is no change in levels of late apoptosis (SP10 57.58% and SP20 61.02%). However again SP10 and SP20 have shown to increase late apoptosis independently as seen in early apoptosis with 38.09% and 52.73% respectively. Therefore, further indicating that SP600125 is having an adverse effect on cell viability independently.

However, when looking at the necrotic cells, this pattern has flipped, with necrosis seeming to stay constant across the lower concentrations rather than the higher. Cisplatin has shown to induce necrosis in HUVECs by 3% with 30µM (6.28%) compared to 3.74% with 100µM where levels stay the same. Again, highlighting concentration-based differences between the cell death pathways. When looking at the effect the inhibitor has on the cells it can been seen that this does not offer an effective protection against damage to the HUVECs when used with a number of concentrations. When looking at 100µM of Cisplatin necrosis can be seen to increase with inhibition (SP10, 4.92% compared to SP20, 6.36%). However, this pattern is not seen with 30µM of Cisplatin where the level of necrosis remains the same (SP10: 5.73%, SP20: 6.54%). Indicating the inhibitor effects the cells differently depending on the effect of the drug treatment. However, when looking at the inhibitor independently it can be seen that necrosis levels are not impacted by the inhibitor alone. Showing the increase in necrosis levels with 100µM Cisplatin is due to a synergistic effect.

As the results suggest SP600125 does not show protective properties to the HUVECs another method of inhibition should be explored. For this investigation an MKP-2 virus was then investigated to understand if a more specific target would enable the protection of the cells (see section 4.2.4).

A)

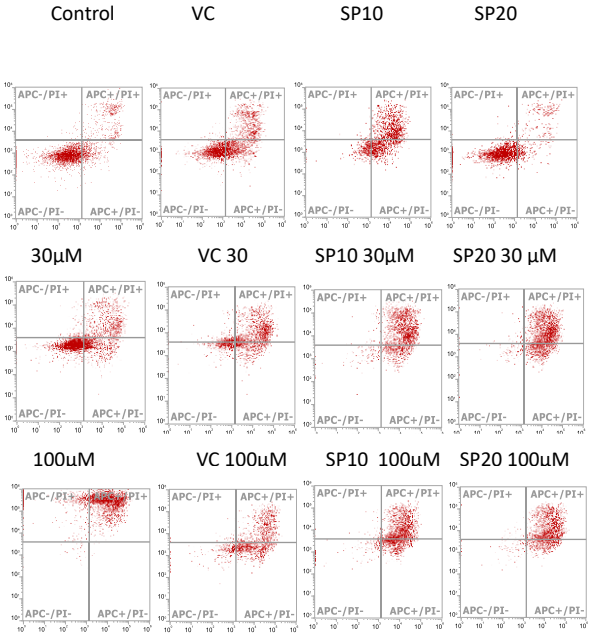
Control
VC
SP10
SP20
30µM
VC 30
SP10 30µM
SP20 30 µM
100uM
VC 100uM
SP10 100uM
SP20 100uM
APC-/PI+
APC+/PI+
APC-/PI-
APC+/PI-

B)

I)

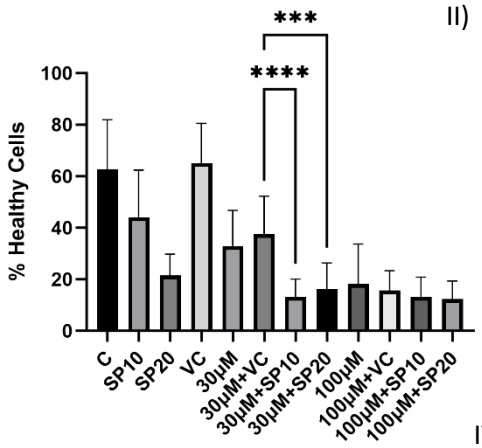
% Healthy Cells
***
****
C
SP10
SP20
VC
30µM
30µM+VC
30µM+SP10
30µM+SP20
100µM
100µM+VC
100µM+SP10
100µM+SP20

II)

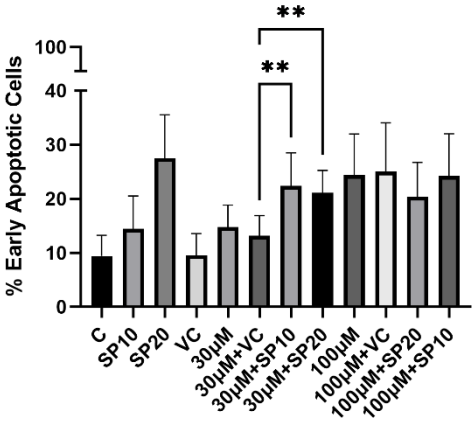
% Early Apoptotic Cells
**
**

III)

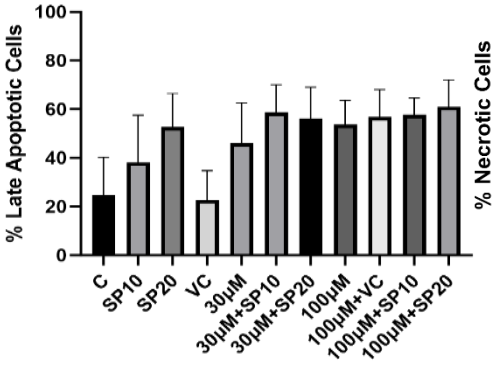
% Late Apoptotic Cells

IV)

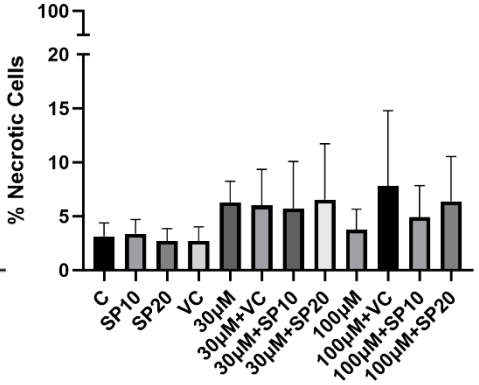
% Necrotic Cells

**Figure 4.10 The effect of SP600125 on Cisplatin stimulated HUVEC cell death using FACS analysis.**

HUVEC cell viability was measured using Flow Cytometry, as outlined in methods section 2.2.6. Confluent HUVECs were pretreated with 10 and 20µM of SP600125 for 1 hour prior to being stimulated with Cisplatin (30µM and 100µM), or vehicle control (VC) DMSO for 24 hours. Cell viability was determined by PI and Annexin V-APC staining. Where, healthy (non), Early apoptosis (Annexin V-APC) Late apoptosis (PI and Annexin V-APC) and Necrosis (PI) were detected. A) Representative dot plots with double staining of Annexin V-APC/PI staining of Doxorubicin treated cells. B) Histograms showing percentage of I) Healthy, II) early apoptotic, III) late apoptotic and IV) necrotic cells. Data represents mean ±S.E.M, n=3. **P<0.05, ***P<0.0005, ****P<0.0001 Compared to Drug Control

### 4.2.4. MKP-2 Mediated inhibition of the Doxorubicin and Cisplatin mediated JNK activation and cell death

The second approach utilised for the inhibition of JNK activity was using an MKP-2 adenovirus. As previously mentioned Adv.NLS-1 MKP-2 is a dual specificity phosphatase, it is able to deactivate MAP kinases by removing phosphate groups from the threonine tyrosine residues (Theodosiou and Ashworth, 2002). This phosphatase was therefore utilised to investigate whether overexpression of MKP-2 could deactivate JNK in HUVECs and prevent Cisplatin or Doxorubicin-induced cell death. For this approach HUVECs were infected with an Adv.NLS-1 MKP-2 virus lacking NLS1 to give relative selectivity for JNK over ERK (Sloss et al., 2005).

Firstly, to confirm Adv.NLS-1 MKP-2 infection was successful immunofluorescence microscopy was used to visualise the Adv.NLS-1 MKP-2 expression in the cell as can be seen in figure 4.11. HUVECs were infected with 100, 200 and 300pfu of Adv.NLS-1 MKP-2 virus for 40 hours, they were then stained with DAPI and MKP-2 as outlined in methods section 2.2.5. Figure 4.12 shows the infection of Adv.NLS-1 MKP-2, and the clear concentration dependent increase of expression confirming the successful infection. Furthermore, despite lacking NLS-1 the MKP-2 protein still was retained mostly within the nucleus, however at higher concentrations, there was some staining in the cytosol indicating some leakage. Infection with beta-gal virus showed no staining, nor did control-generally endogenous MKP-2 virus levels were negligible.

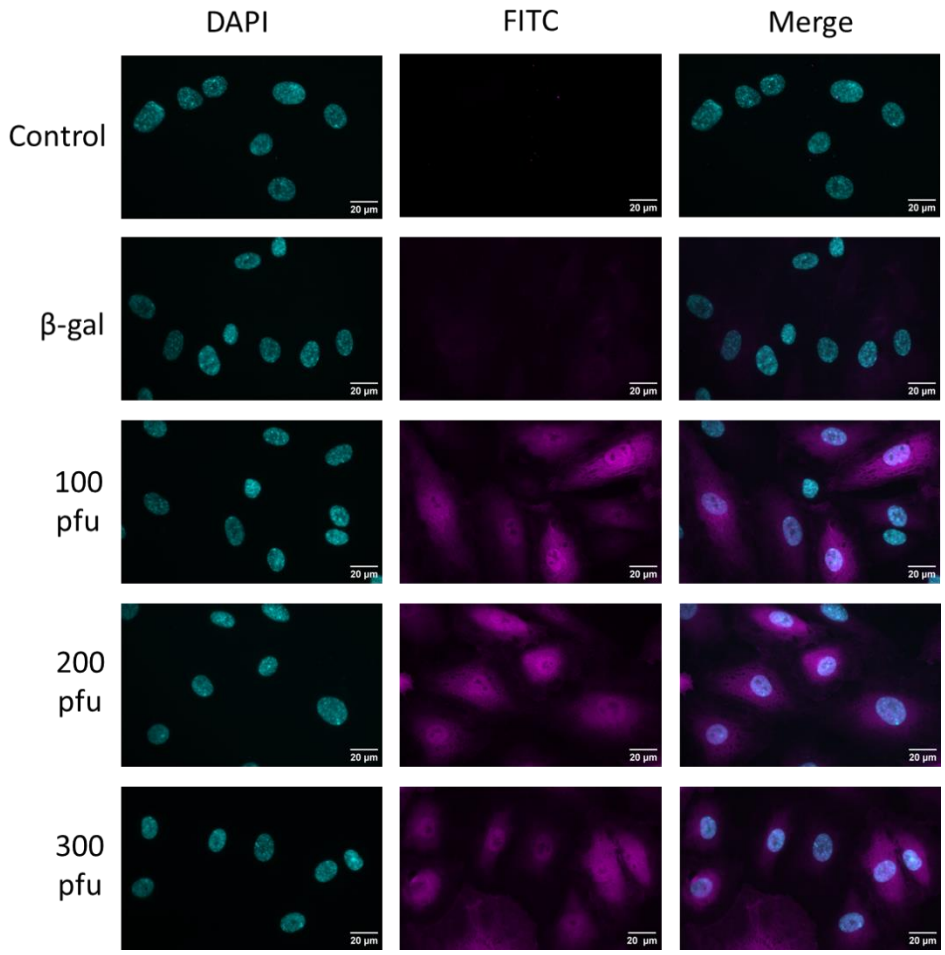


**Figure 4.11 Representation of MKP-2 expression in HUVECs transfected with Adv.NLS-1 MKP-2 virus by direct immunofluorescence.**

HUVECs were plated on coverslips for 24 hours and treated or untreated with Adv.NLS-1 MKP-2 at varying plaque forming units (pfu). Untreated cells and cells treated with βGal (300 pfu) were applied as controls. Cells were then fixed with 3% paraformaldehyde and stained with MKP-2 antibody and Dapi as outlined in Methods section 2.2.9. Images were captured on a Nikon Eclipse E600 Epifluorescent Upright Microscope at 60X magnification. N=2

Once expression of Adv MKP-2 had been visualised using immunofluorescence, cultures were infected with Adv.NLS-1 MKP-2 to optimise the effective concentration of Adv.NLS-1 MKP-2 to promote JNK dephosphorylation. HUVECs were infected with Adv.NLS-1 MKP-2 -NLS1 for 40 hours with 100-300pfu and stimulated with Doxorubicin at 10µM and 30µM. Figure 4.12 shows that there was an increase in MKP-2 expression in whole cell lysates with maximal expression of the protein at 100 pfu. Furthermore, Figure 4.12 also shows JNK phosphorylation levels decrease with the increased Adv.NLS-1 MKP-2 concentrations. As the results show both 10µM and 30µM Doxorubicin stimulated an increase JNK phosphorylation after 24 hours (10µM stimulation: 39.87±4.34, and 30µM stimulation: 62.98±4.43, N=2). Whilst infection with βGal was without large effect, Adv.NLS-1 MKP-2 infection had a marked inhibitory effect on the phosphorylation of both isoforms of JNK at all concentrations tested. Virtually full inhibition of JNK was achieved at the lowest concentration of Adv.NLS-1 MKP-2 (100pfu 10µM stimulation; 10.90±0.61, N=2). Total JNK was not affected by Adv.NLS-1 MKP-2 infection confirming that MKP-2 prevents phosphorylation of JNK with no effect on the JNK protein expression over the infection period.

A similar effect of Adv.NLS-1 MKP-2 was observed following Cisplatin stimulation of HUVECs. As shown in figure 4.13, Cisplatin caused a strong significant increase in JNK phosphorylation at 24 hours (stimulation: 90.98±25.43, **P<0.005, N=3). Whilst β-gal (300pfu) infection did not affect stimulated values, overexpression of MKP-2 strongly inhibited Cisplatin-induced JNK phosphorylation levels with the lowest concentration of 100pfu reducing the response to near control levels (stimulation: 6.04±1.06, **P<0.005, N=3). Whilst Adv.NLS-1 MKP-2 infection did not affect total JNK levels *per se,* it was noted that infection was able to reverse the loss in total JNK expression in response to Cisplatin, again suggesting that NLS-MKP-2 may be effective with respect to preventing cell death mediated by Cisplatin.

Figures 4.12 and 4.13 show that Adv.NLS-1 MKP-2 was effective in cells treated with both Doxorubicin and Cisplatin in decreasing JNK phosphorylation levels. Although both drugs have differing mechanisms of action it can be determined that their activation of the JNK pathway was inhibited with the Adv.NLS-1 MKP-2.

A)

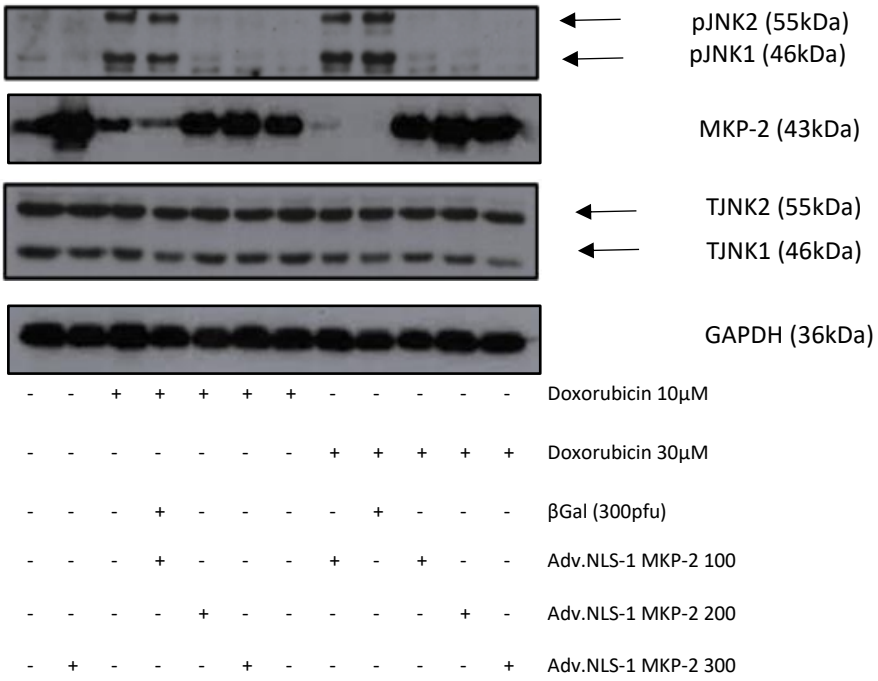


B)

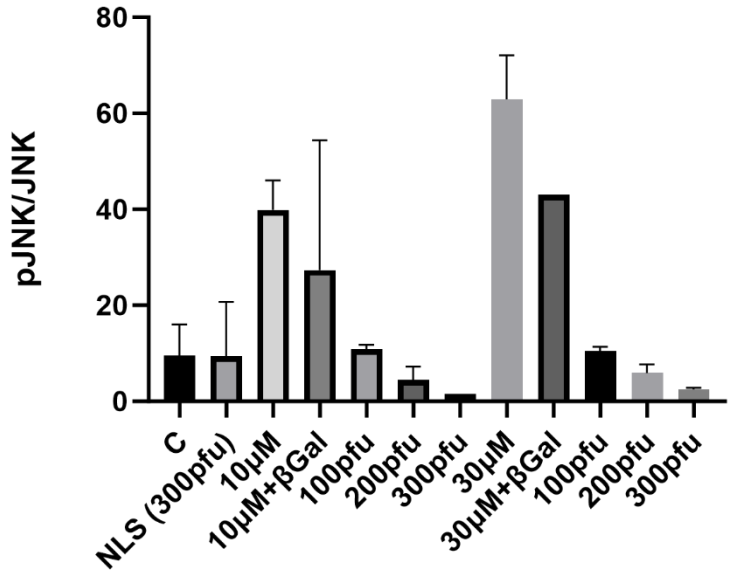


**Figure 4.12 Infection with Adv.NLS-1 MKP-2 prevents Doxorubicin-mediated activation of JNK phosphorylation in HUVECs.**

Sub-confluent HUVECs were infected with Adv.NLS-1 MKP-2 NLS (100-300pfu), and βGal (300pfu) for 40 hours and when confluent stimulated with Doxorubicin (10 and 30µM) for 24 hours. Western blot analysis was performed for pJNK, Total JNK, MKP-2 and GAPDH. Blots were semi-quantified as outlined in Methods section 2.2.2.6. A) Western blot representation. B) Semi-quantification for pJNK/TJNK Ratio. Results represent mean ± S.E.M, n=2.

A)

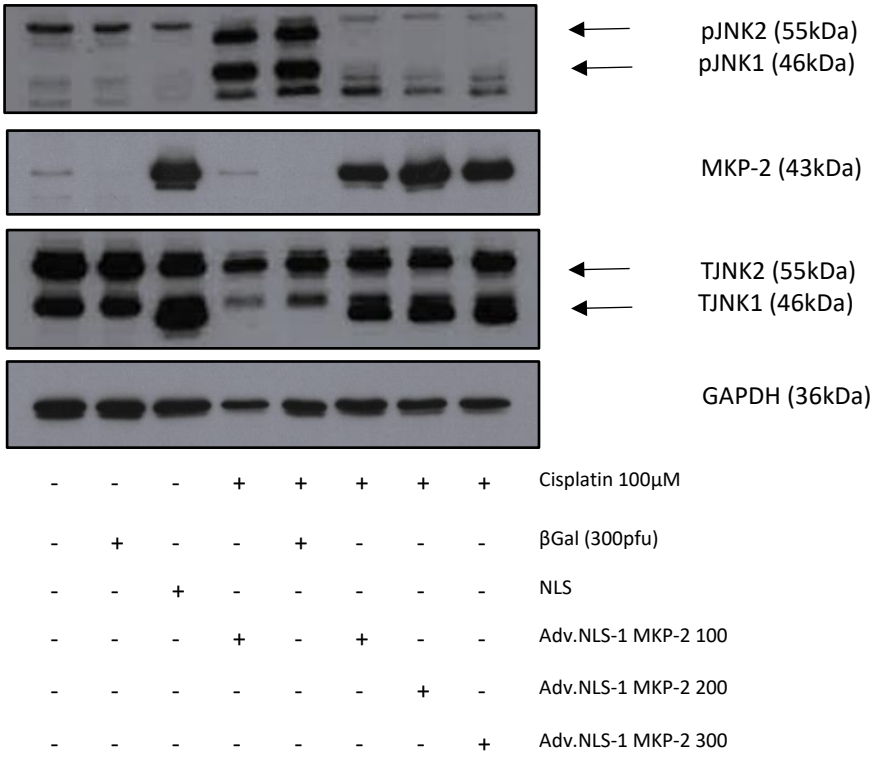


B)

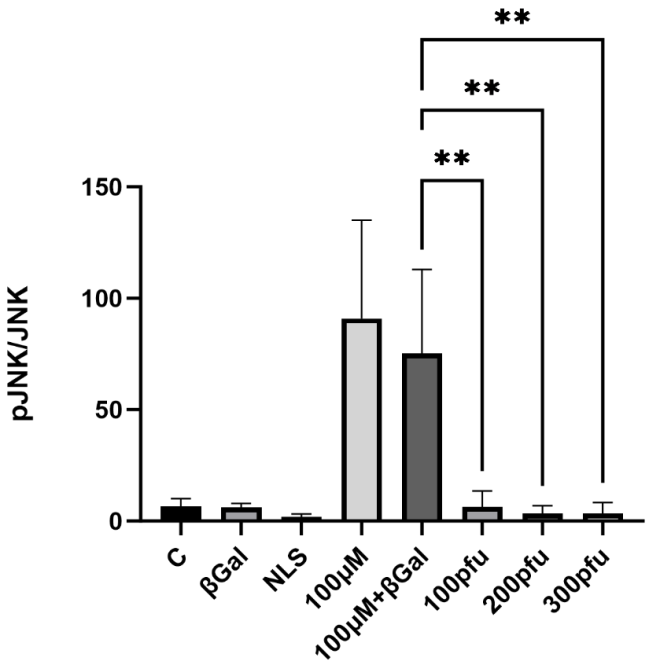


**Figure 4.13 Adv.NLS-1 MKP-2 prevents Cisplatin-mediated activation of JNK phosphorylation in HUVECs.**

Sub-confluent HUVECs were infected with Adv.NLS-1 MKP-2 virus (100-300pfu), and βGal (300pfu) for 40 hours and when confluent stimulated with Cisplatin (100µM) for 24 hours. Western blot analysis was performed for pJNK, Total JNK, MKP-2 and GAPDH. Blots were semi-quantified as outlined in Methods section 2.2.2.6. A) Western blot representation. B) Semi-quantification for pJNK/TJNK Ratio. Results represent mean ± S.E.M, n=3, **P<0.005, compared to drug and vehicle control.

Once it had been determined that Adv.NLS-1 MKP-2 is an effective tool for JNK dephosphorylation, Adv.NLS-1 MKP-2 was used to further examine the effect JNK activation has on cell viability. Firstly, the effect of DNA damage on the levels of, pγH2A.X and caspase 3, markers of DNA damage were investigated. To aid the understanding whether the deactivation of the JNK pathway would have further upstream consequences and prevent DNA damage. γH2A.X is produced after DNA damage by ATM, to allow DNA repair proteins to the site of damage (Lopez and Bouchier-Hayes, 2022).

Therefore, as an initial part of the DNA pathway this histone protein was examined first, as shown in figure 4.14. The western blot shows that Doxorubicin does not elicit pγH2A.X phosphorylation in HUVECs over a significant resting level of phosphorylation. Irrespective of a lack of stimulation, following Adv.NLS-1 MKP-2 infection, there is a minor, non-significant reduction in pγH2A.X levels in HUVECs as shown in figure 4.14. This decrease although not significant, was shown to be concentration dependent. Adv.NLS-1 MKP-2 at 300pfu gave a reduction in pγH2A.X levels (stimulation: 43.52±11.22, N=3) when compared to 100pfu (stimulation: 58.08±18.03, N=3). This reduction and dephosphorylation of JNK, as observed in figure 4.14, and infers that JNK deactivation reduces the damage Doxorubicin elicits on endothelial cells, although the effects are marginal.

This phenomenon was mirrored with DNA damage caused by Cisplatin (figure 4.15). The Adv.NLS-1 MKP-2 infected HUVECs were treated with 100µM of Cisplatin as shown in figure 4.15. As with Doxorubicin there is no change in pγH2A.X levels with Cisplatin at 100µM. As with the previous experiment, infection of Adv.NLS-1 MKP-2, 100pfu shows a moderate reduction in pγH2A.X levels (stimulation 104.1±17.19, N=3) which is further reduced at 300pfu (stimulation: 87.16±7.801, N=3). Interestingly it can be observed that Adv.NLS-1 MKP-2 shows a restoration of total JNK levels compared to Cisplatin only levels. Thus, even though significant changes in pγH2A.X levels were not demonstrated, there was restoration in cellular protein levels and as such may represent a stimulation.

As both Cisplatin and Doxorubicin do not significantly activate pγH2A.X, Caspase-3 was used to further investigate the DNA damage response.

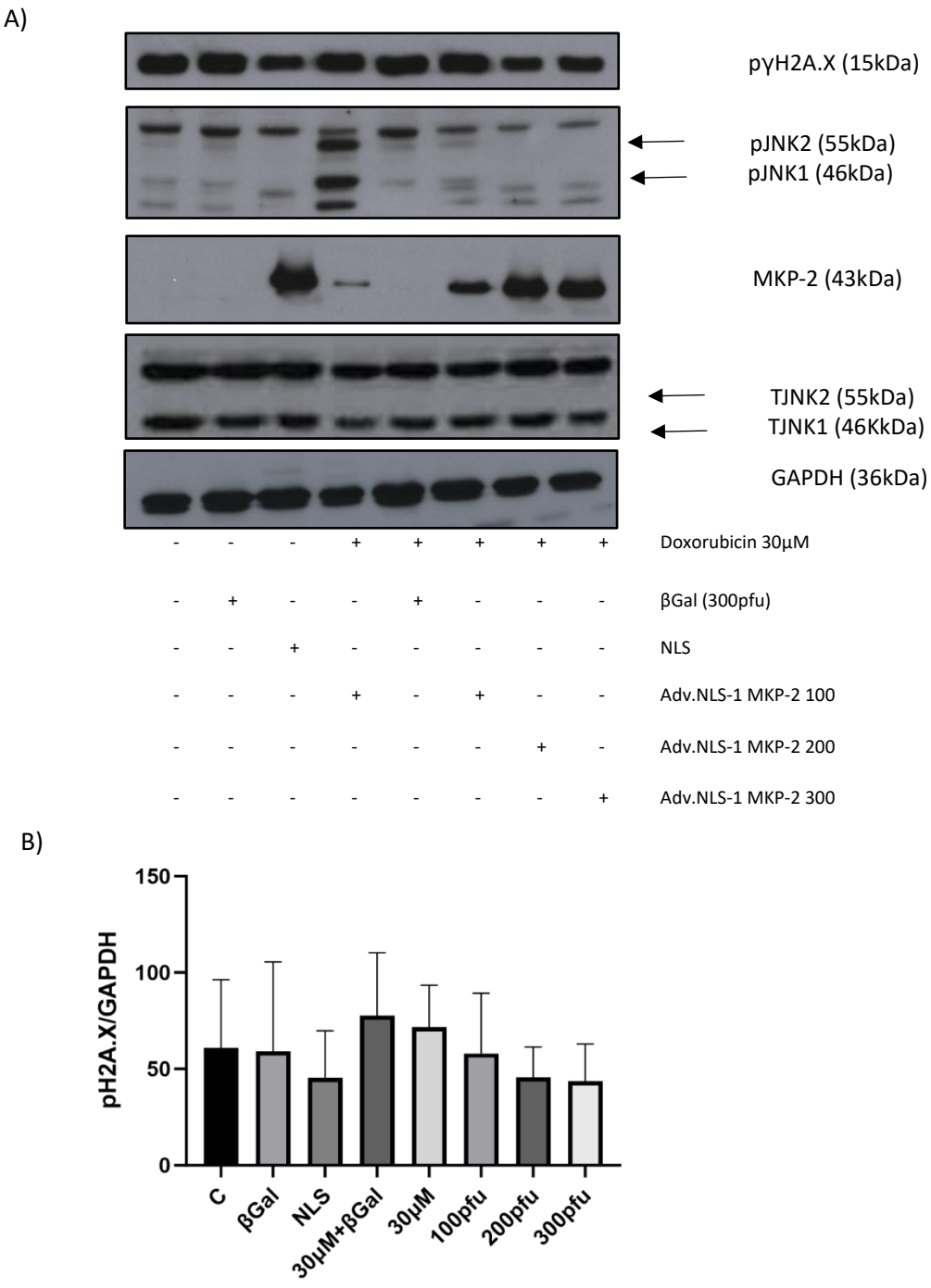


**Figure 4.14 Effect of Adv.NLS-1 MKP-2 on Doxorubicin-mediated activation of pγH2A.X in HUVECs.**

Sub-confluent HUVECs were infected with Adv.NLS-1 MKP-2 virus (100-300pfu), and βGal (300pfu) for 40 hours and when confluent stimulated with Doxorubicin (30μM) for 24 hours. Western blot analysis was performed for pγH2A.X, pJNK, Total JNK, MKP-2 and GAPDH. Blots were semi-quantified as outlined in Methods section 2.2.2.6. A) Western blot representation. B) Semi-quantification for pγH2A.X/GAPDH ratio. Results represent mean ± S.E.M, n=3, non-significant, compared to drug and vehicle control.

A)

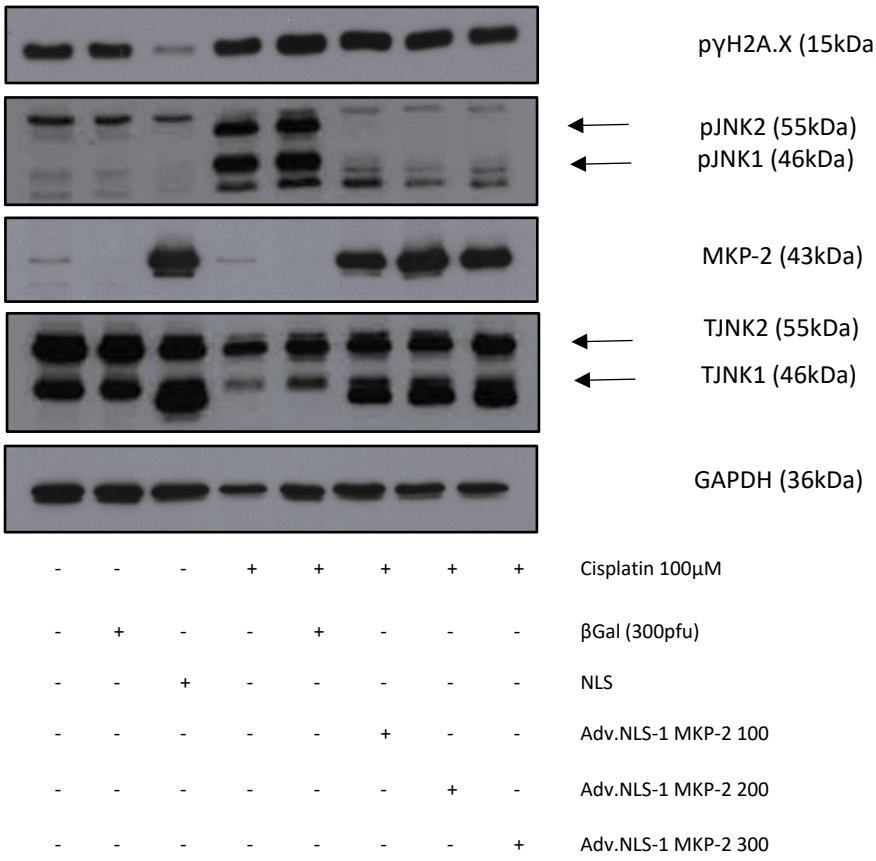


B)

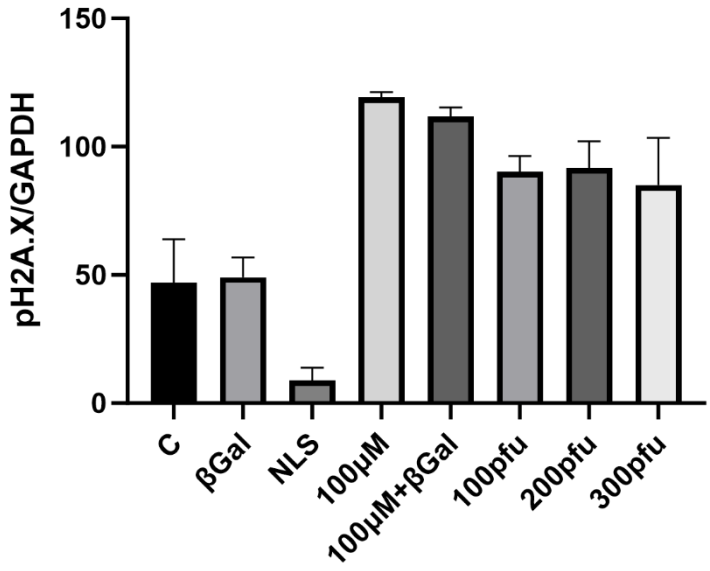


**Figure 4.15 Effect of Adv.NLS-1 MKP-2 on Cisplatin-mediated activation of pγH2A.X in HUVECs**

Sub-confluent HUVECs were infected with Adv.NLS-1 MKP-2 virus (100-300pfu), and βGal (300pfu) for 40 hours and when confluent stimulated with Cisplatin (100μM) for 24 hours. Western blot analysis was performed for pγH2A.X, pJNK, Total JNK, MKP-2 and GAPDH. Blots were semi-quantified as outlined in Methods section 2.2.2.6. A) Western blot representation. B) Semi-quantification for pγH2A.X/GAPDH ratio. Results represent mean ± S.E.M, n=3, non-significant, compared to drug and vehicle control.

Caspase 3 is an executioner caspase, part of the caspase family which are cysteine aspartate proteases, renowned for playing a vital role in cell death (Boice and Bouchier-Hayes, 2020, Lopez and Bouchier-Hayes, 2022). As an executioner, caspase-3 plays a vital role in apoptosis and pyroptosis, two forms of programmed cell death (Eskandari and Eaves, 2022, Wang et al., 2017b). Previous studies have shown that Doxorubicin and Cisplatin activate caspase 3 in a number of cell lines including HUVECs (Bruynzeel et al., 2007, Singh et al., 2013, Chen et al., 2022). Due to its implication in both DNA damage and cell death mechanisms cleaved caspase -3 levels were analysed when HUVECs were infected with increasing concentrations of Adv.NLS-1 MKP-2.

Stimulation of HUVECs with Doxorubicin caused a significant cleavage of caspase 3 and formation of cleaved caspase 3 which can be seen at a lower size (17 and 19kDa) (stimulation: 46.79±7.91, **P<0.005, N=3) (figure 4.16). Infection with Adv.NLS-1 MKP-2 was found to significantly decrease cleaved caspase-3 levels in a concentration-dependent manner, exemplified for values at 100pfu (stimulation: 21.89±6.624, * P<0.05, N=3) and 300pfu (stimulation 9.171±0.6362***P<0.005, N=3). Results demonstrated a 50% reduction in cleaved caspase 3 with 100pfu alone, and levels for 200pfu (stimulation:11.28±5.538, ***P<0.005, N=3) and 300pfu respectively are which are all levels below unstimulated cells. These data suggest that by deactivating JNK with Adv.NLS-1 MKP-2 in Doxorubicin treated HUVECs DNA damage markers are reduced.

Further experiments repeated the effect of Adv.NLS-1 MKP-2 using 100µM of Cisplatin as the stimulant and the same pattern of inhibition was observed (figure 4.17). Cisplatin stimulated a more noticeable increase in cleaved caspase formation relative to Doxorubicin giving an increase of 129.6±45.62 compared to 46.79±7.911 for Doxorubicin. However, following infection with Adv.NLS-1, MKP-2 Cisplatin-stimulated, cleaved caspase-3 levels were greatly reduced with levels over 75% lower for 300pfu (stimulation:25.95±10.63, N=3).

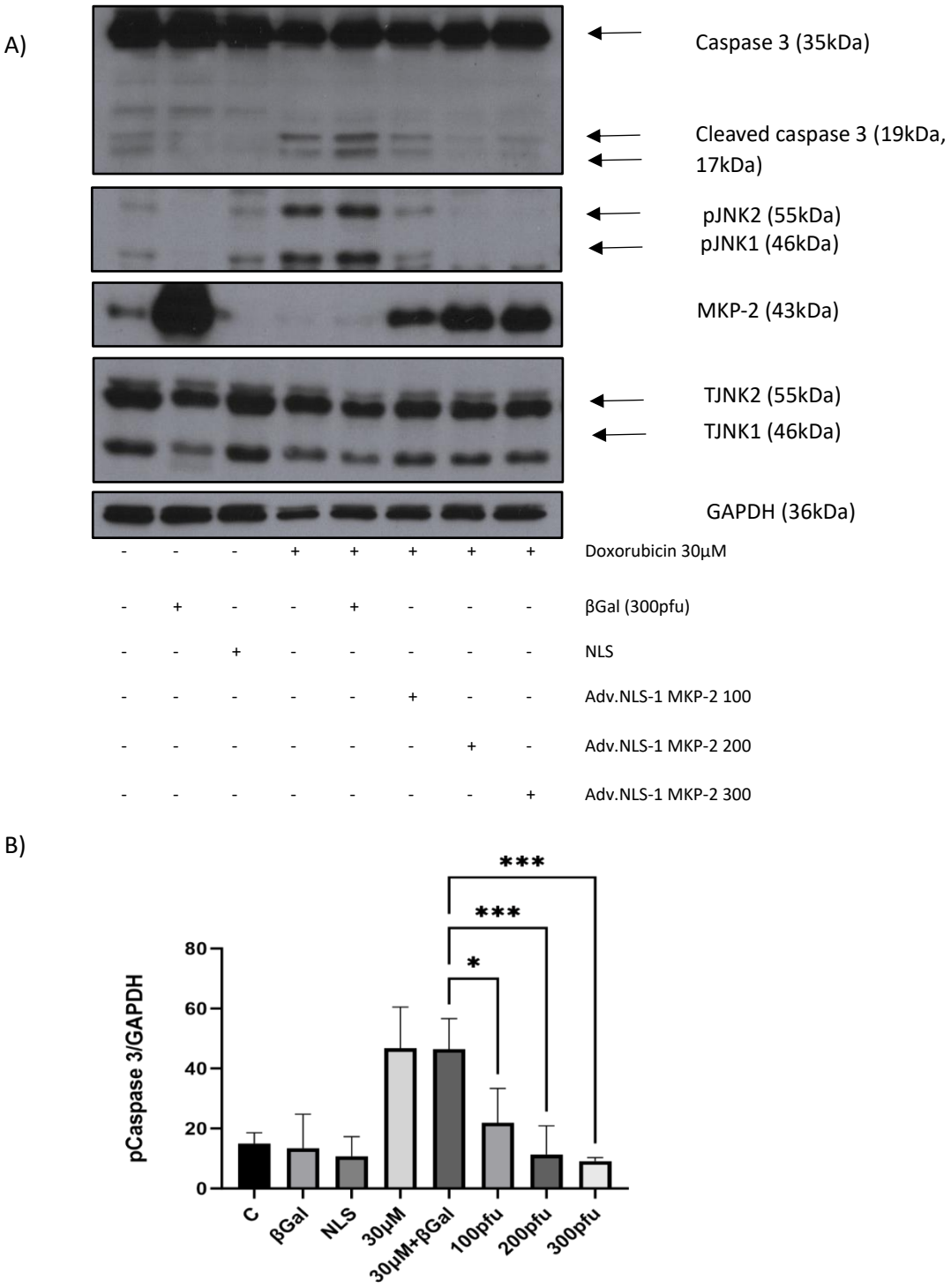


**Figure 4.16 Effect of Adv.NLS-1 MKP-2 on Doxorubicin-mediated activation of Caspase 3 cleavage in HUVECs.**

Sub-confluent HUVECs were infected with Adv.NLS-1 MKP-2 virus (100-200pfu), and βGal (300pfu) for 40 hours and when confluent stimulated with Doxorubicin (30µM) for 24 hours. Western blot analysis was performed for Cleaved Caspase 3, pJNK, Total JNK, MKP-2 and GAPDH. Blots were semi-quantified as outlined in Methods section 2.2.2.6. A) Western blot representation. B) Semi-quantification for Caspase 3/GAPDH ratio. Results represent mean ± S.E.M, n=3, *P<0.05, ***P<0.005, compared to drug and vehicle control.

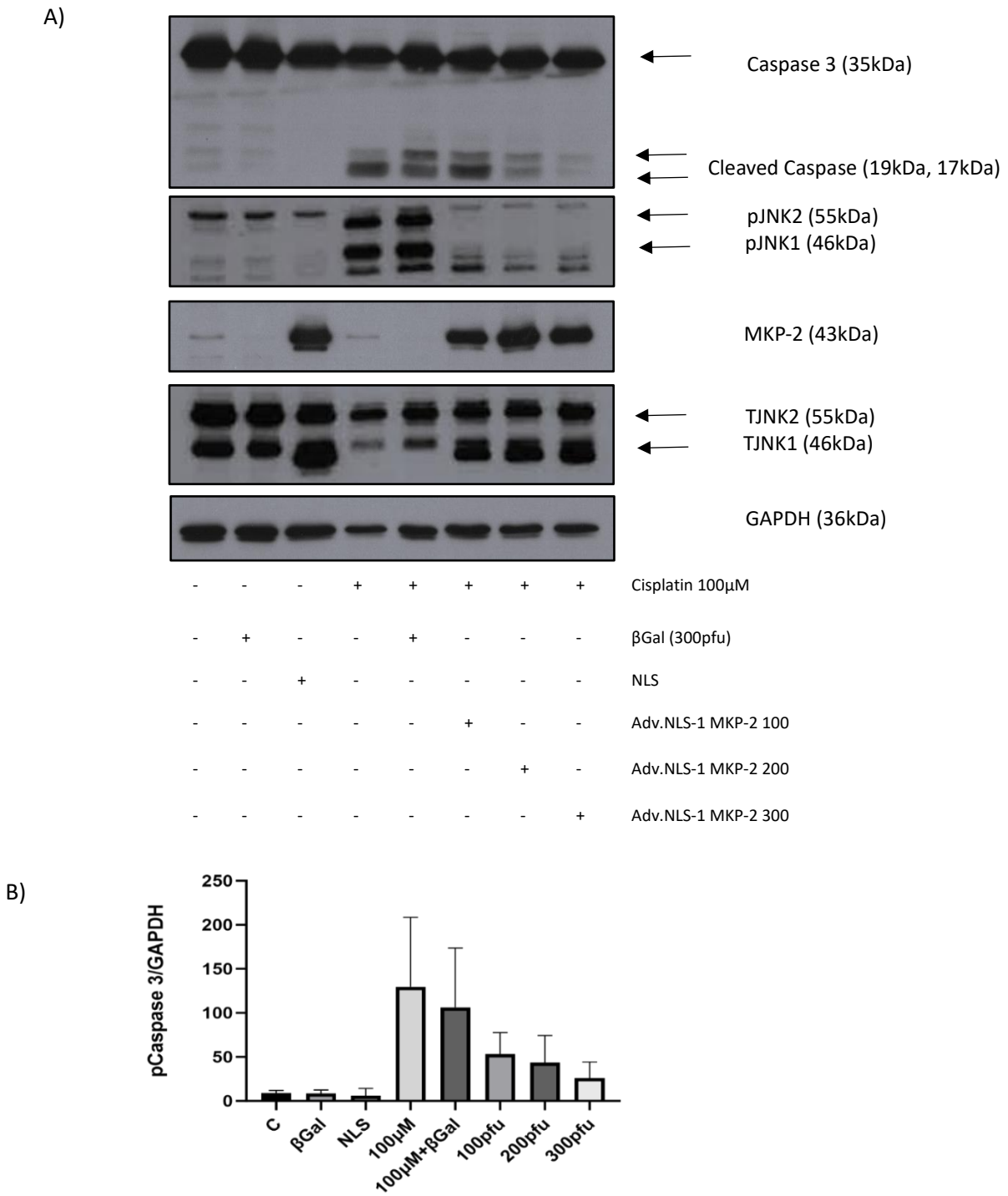


**Figure 4.17 : Inhibitory effect of Adv.NLS-1 MKP-2 on Cisplatin-mediated activation of Caspase 3 cleavage in HUVECs.**

Sub-confluent HUVECs were infected with Adv.NLS-1 MKP-2 virus (100-300pfu), and βGal (300pfu) for 40 hours and when confluent stimulated with Cisplatin (100µM) for 24 hours. Western blot analysis was performed for cleaved Caspase 3, pJNK, Total JNK, MKP-2 and GAPDH. Blots were semi-quantified as outlined in Methods section 2.2.2.6. A) Western blot representation. B) Semi-quantification for Caspase 3/GAPDH ratio. Results represent mean ± S.E.M, n=3, non-significant, compared to drug and vehicle control.

In stimulated cells, caspase-3 is responsible for the cleavage of GSDME, resulting in the active form of GSDME-N, which causes pyroptosis (Shen et al., 2021, Jiang et al., 2020). Thus, it was therefore important to investigate GSDME-N levels in HUVECS and to determine if treatment of chemotherapeutic agents result in pyroptosis in HUVECs. Also, to examine if Adv.NLS-1 MKP-2 infection could reduce or prevent this form of programmed cell death and protect the cells.

Figure 4.18 shows that Doxorubicin caused a significant increase in GSDME-N levels at both 10µM (stimulation: 38.36±7.77, N=3) and 30µM (stimulation: 57.46±12.82, N=3). This suggests that at both Doxorubicin concentrations cellular damage has occurred and indicates activation of pyroptosis. Interestingly, stimulated levels of GSDME-N fell with the increase in concentration of Adv.NLS-1 MKP-2 expression, as shown in figure 4.18, which correlated with a strong inhibition of pJNK. Intriguingly, the differing concentrations gave different results. HUVECs treated with 10µM Doxorubicin showed a slight reduction in GSDME-N levels (left hand part of the blot and data), there is little difference in GSDME-N levels at 10µM of Doxorubicin across the 3 concentrations of Adv.NLS-1 MKP-2. However, with 30µM Doxorubicin, GSDME-N were more notably reduced following infection with Adv.NLS-1 MKP-2. At a concentration of 300pfu, Adv.NLS-1 MKP-2 caused a significant reduction in GSDME (stimulation: 14.31±3.488, *P<0.05, N=3), which is below levels of untreated cells. Taken together these results suggest that higher Doxorubicin concentrations caused a correspondingly higher level of cellular damage and increased GSDME-N levels, which have been shown to be reversed with Adv.NLS-1 MKP-2.

These experiments were then repeated with 100µM of Cisplatin. Figure 4.19 shows that Cisplatin stimulated GSDME-N levels indicating the activation of pyroptosis. Infection with Adv.NLS-1 MKP-2 alone however slightly reduced GSDME-N stimulation. Although not significant, figure 4.19 shows a minor reduction in GSDME levels in a concentration-dependent manner, as with pγH2A.X and caspase-3. Cisplatin increased GSDME-N levels (stimulation: 74.14, N=2), whereas Adv.NLS-1 MKP-2 infection at 100pfu reduced the response (stimulation: 51.58, N=2) which marginally increased with 300pfu (stimulation: 60.00, N=2).

This minimal reduction observed indicates that inhibition of JNK does not impact the levels of both cleaved caspase 3 and GSDME-N. indicating that caspase and GSDME-N maybe independent of the JNK pathway.

A)

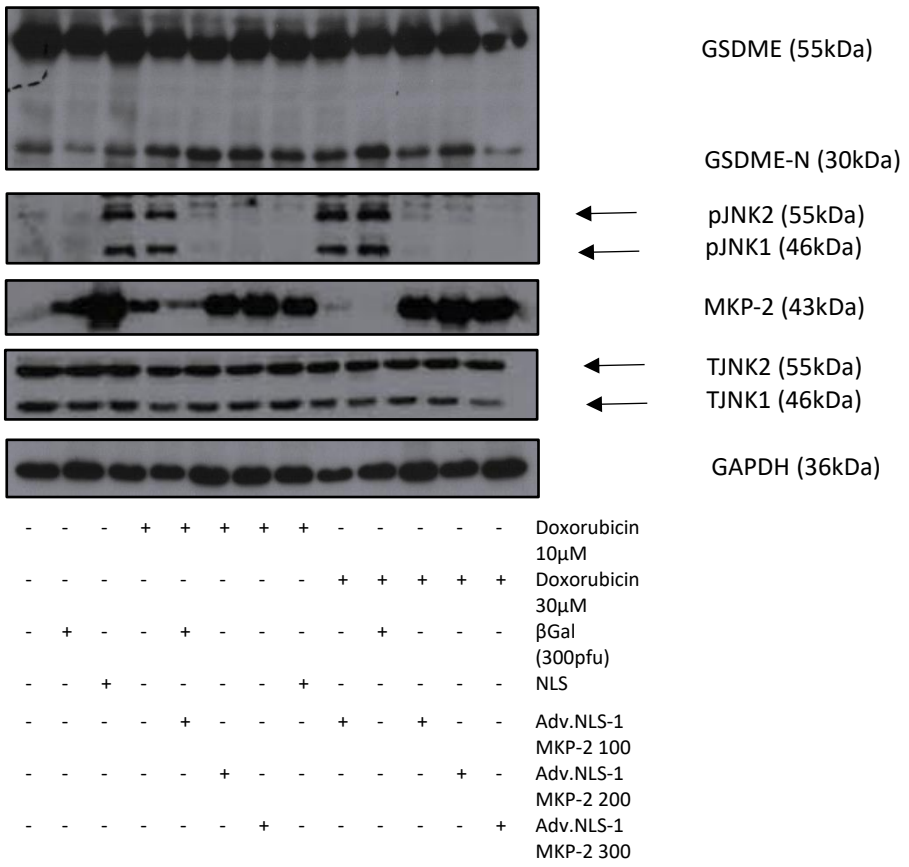


B)

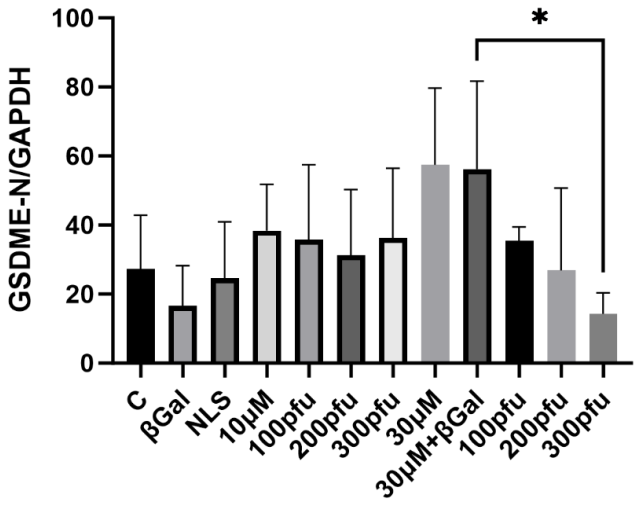


**Figure 4.18 : Inhibitory effect of Adv.NLS-1 MKP-2 on Doxorubicin-mediated activation of GSDME-N in HUVECs.**

Sub-confluent HUVECs were infected with Adv.NLS-1 MKP-2 virus (100-200pfu), and βGal (300pfu) for 40 hours and when confluent stimulated with Doxorubicin (10 and 30µM) for 24 hours. Western blot analysis was performed for GSDME-N, PP-JNK, Total JNK, MKP-2and GAPDH. Blots were semi-quantified as outlined in Methods section 2.2.2.6. A) Western blot representation. B) Semi-quantification for GSDME/GAPDH ratio. Results represent mean ± S.E.M, n=3, *P<0.05, compared to drug and vehicle control.

A)

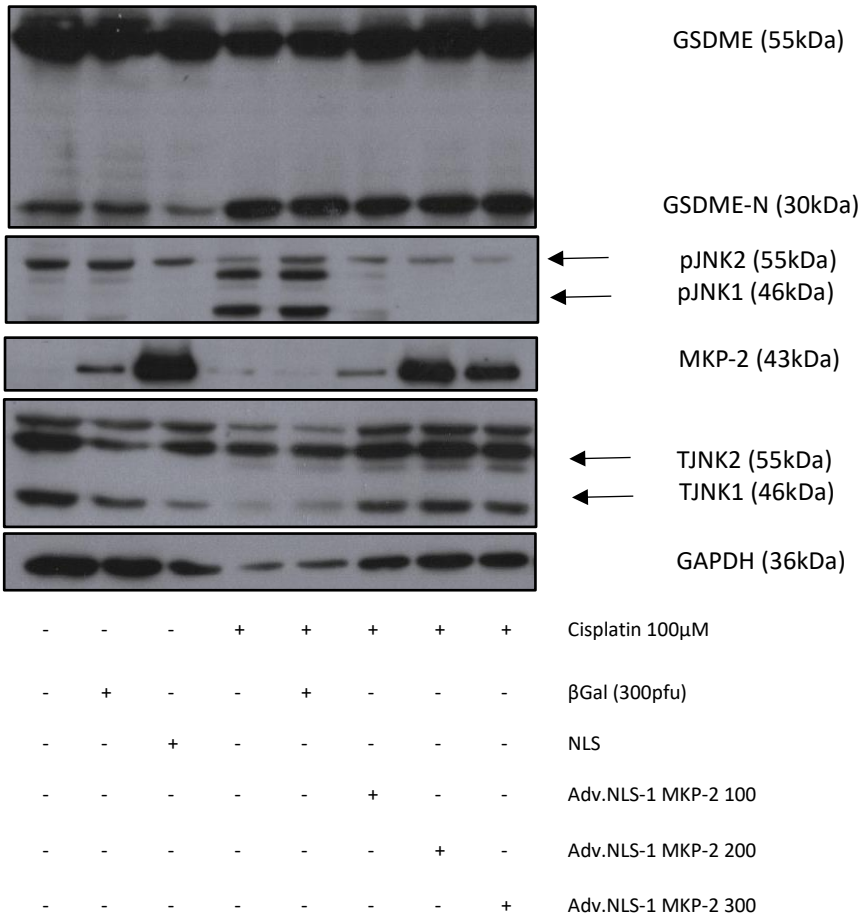


B)

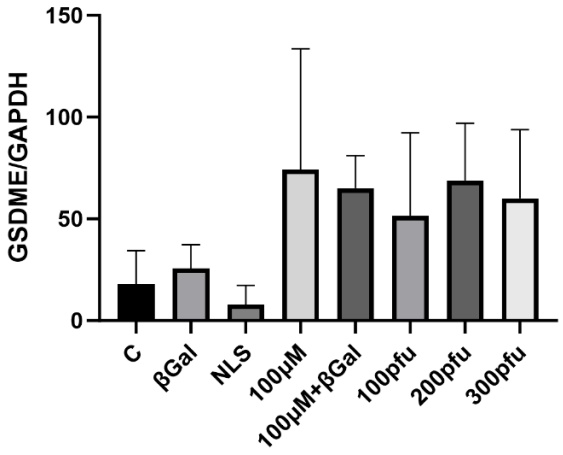


**Figure 4.19 : Inhibitory effect of Adv.NLS-1 MKP-2 on Cisplatin-mediated activation of GSDME-N in HUVECs**

Sub-confluent HUVECs were infected with Adv.NLS-1 MKP-2 virus (100-300pfu), and βGal (300pfu) for 40 hours and when confluent stimulated with Cisplatin (100µM) for 24 hours. Western blot analysis was performed for GSDME-N, pJNK, Total JNK, MKP-2 and GAPDH. Blots were semi-quantified as outlined in Methods section 2.2.2.6. A) Western blot representation. B) Semi-quantification for GSDME/GAPDH ratio. Results represent mean ± S.E.M, N=2.

### 4.2.6. Doxorubicin and Cisplatin induced pyroptosis mediated cell death

Another indicator of Pyroptosis alongside caspase-3 and GSDME levels is the release of cellular LDH (Lactate Dehydrogenase). It is known that when GSDME is cleaved by Caspase-3 into GSDME-N this results in the formation of membrane pores. The cell then swells and the membrane ruptures, releasing the cells contents which includes LDH (Rayamajhi et al., 2013, Wang et al., 2017b). Therefore, measuring the levels of LDH could give a good indication of pyroptosis. Using an Invitrogen™ CyQUANT™ LDH Cytotoxicity Assay both Doxorubicin and Cisplatin were examined to confirm if the compounds induce pyroptosis. As per the kits instructions % cytotoxicity was calculated using the equation in Methods section 2.2.8. HUVECs were also investigated further to understand if cells infected with Adv.NLS-1 MKP-2 can be protected from pyroptosis.

As 30µM Doxorubicin has been shown to cause significant cellular damage and increase levels of pyroptotic markers, as assessed by GSDME, this concentration was chosen for further analysis. Figure 4.20 shows that compared to the control, which was essentially zero, Doxorubicin caused a marked increase in LDH release reaching approximately 15% (16.49±1.65%, ****P<0.0001, N=3) cytotoxicity. This confirms that in response to Doxorubicin there is pyroptosis detected, which has been demonstrated in in other recent studies (Hwang et al., 2022, Meng et al., 2019). Infection with Adv.NLS-1 MKP-2 had a significant concentration dependent effect, stimulated LDH levels dropped by approximately 80% with the inactivation of JNK. As with previous experiments, the level of protection is concentration dependent with 200 and 300pfu reducing cytotoxicity of 30µM by approximately 12% (200pfu: 2.06±0.93%, ****P<0.0001, N=3 and 300pfu: 1.45±0.70%, ****P<0.0001, N=3). Although the levels of cytotoxicity are relatively low, with only 16% induced by Doxorubicin, Adv.NLS-1 MKP-2 is able to reverse this to almost zero. This data again supports the idea that by hypothesis that JNK mediates pyroptosis in HUVECs and inhibition causes some form of protection.

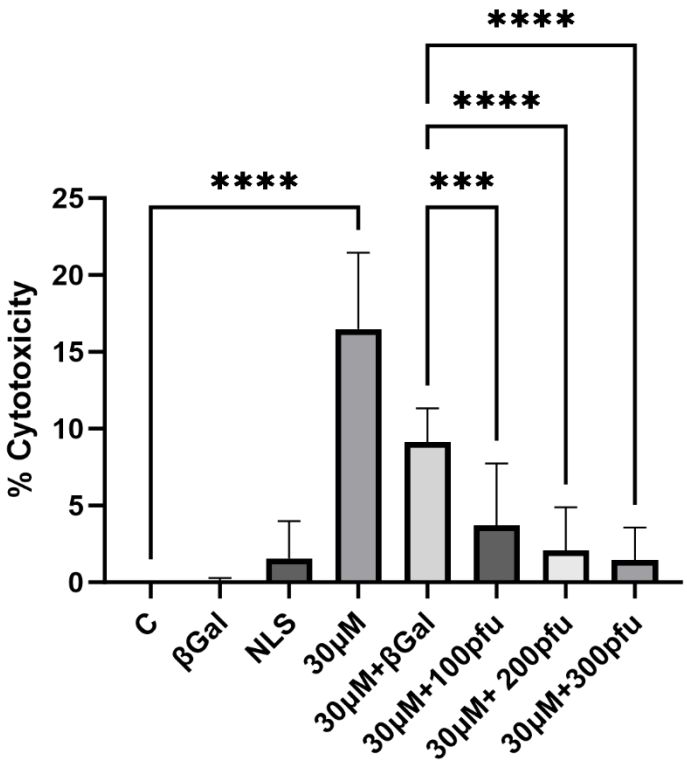


**Figure 4.20 Protective effect of Adv.NLS-1 MKP2 infection on Doxorubicin-mediated LDH cytotoxicity in HUVECs**

Sub-confluent HUVEC were infected with Adv.NLS-1 MKP-2 virus (100-300pfu), and βGal (300pfu) for 40 hours and when confluent stimulated with Doxorubicin (10μM and 30μM) for 24 hours. The Invitrogen™ CyQUANT™ LDH Cytotoxicity Assay Quantity was carried out as per manufacturer's instructions outlined in Methods section 2.2.8 Results represent mean ± S.E.M N=3, ***<P0.001, ****<P0.0001 compared to control

For further analysis the experiment was also repeated with Cisplatin at 100µM. Cisplatin was found to cause a significant increase in LDH release in HUVECs from near 0% to 21% cytotoxicity (21.74±2.75%, ****P<0.0001, N=3). However as with Doxorubicin, infection with Adv.NLS-1 MKP-2 at all concentrations tested caused a significant reduction in Cisplatin-stimulated LDH release, reducing levels from over 15% to 5% or less (figure 4.21) (300pfu: 5.45±1.93%, ****P<0.0001, N=3). Overall, Adv.NLS-1 MKP-2 significantly reduced cytotoxicity levels in response to Cisplatin, further indicating the link between JNK activation and pyroptosis.

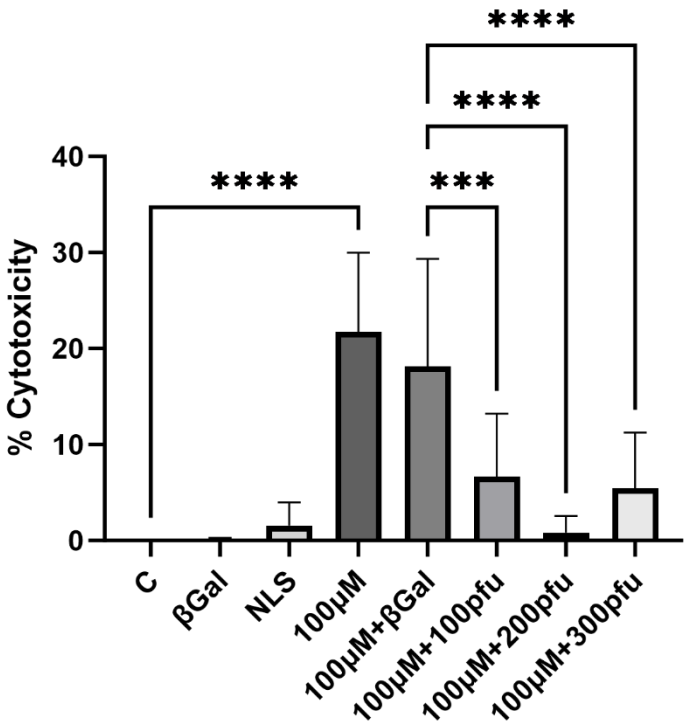


**Figure 4.21 Protective effect of Adv.NLS-1 MKP-2 on Cisplatin-mediated LDH cytotoxicity in HUVECs.**

Sub-confluent HUVECs were infected with Adv.NLS-1 MKP-2 virus (100-300pfu), and βGal (300pfu) for 40 hours and when confluent stimulated with Cisplatin (30μM and 100μM) for 24 hours. The Invitrogen™ CyQUANT™ LDH Cytotoxicity Assay Quantity was carried out as manufacturer's instructions outlined in methods section 2.2.8. Results represent mean ± S.E.M N=3. ***<P0.001, ****<P0.0001 compared to control

### 4.2.7. Protective effect of Adv.NLS-1 MKP-2 on Doxorubicin and Cisplatin induced pyroptosis cell morphology observations.

Previous studies have shown that pyroptosis causes cells to swell and release their contents, as shown by Zheng et al, in Doxorubicin treated cardiomyocytes (Zheng et al., 2020). Therefore, brightfield images were taken of HUVECs to further investigate whether the addition of Doxorubicin (figure 4.22) and Cisplatin (figure 4.23) have caused the atypical morphological changes expected with pyroptosis, namely swelling and signs of blebbing and bubbles.

Figure 4.22 shows the morphology of the cells in equivalent conditions to the LHD assay when treated with Doxorubicin. In control, 300pfu Adv.NLS-1 MKP-2 and βGal (300pfu) infected cells there is very little visible damage to the cell membrane and the absence of blebbing and bubbles. However, when HUVECs were treated with Doxorubicin alone (figure 4.22 B), the HUVEC morphology changed compared to the control (figure 4.21 A). The treated cells were visibly larger, swollen and rounded -all physiological features of pyroptosis. Examination of the cells following infection with Adv.NLS-1 MKP-2 prior to drug treatment, as shown in panels 4.22 C, D and E, indicated that the morphology still differed from the control, non-stimulated cells. The cells looked swollen and large, however there is visibly less blebbing and bubbles, than Doxorubicin alone treated cells. This supports the finding, using the LDH assays, that Doxorubicin stimulated pyroptosis may be reduced with the over expression of Adv.NLS-1 MKP-2. This also shows to be as a result of Doxorubicin treatment and the effect of the Adv.NLS-1 MKP-2 on those treated cells. The controls βGal (300pfu) and Adv.NLS-1 MKP-2 alone do not cause such morphological changes in the HUVECs.

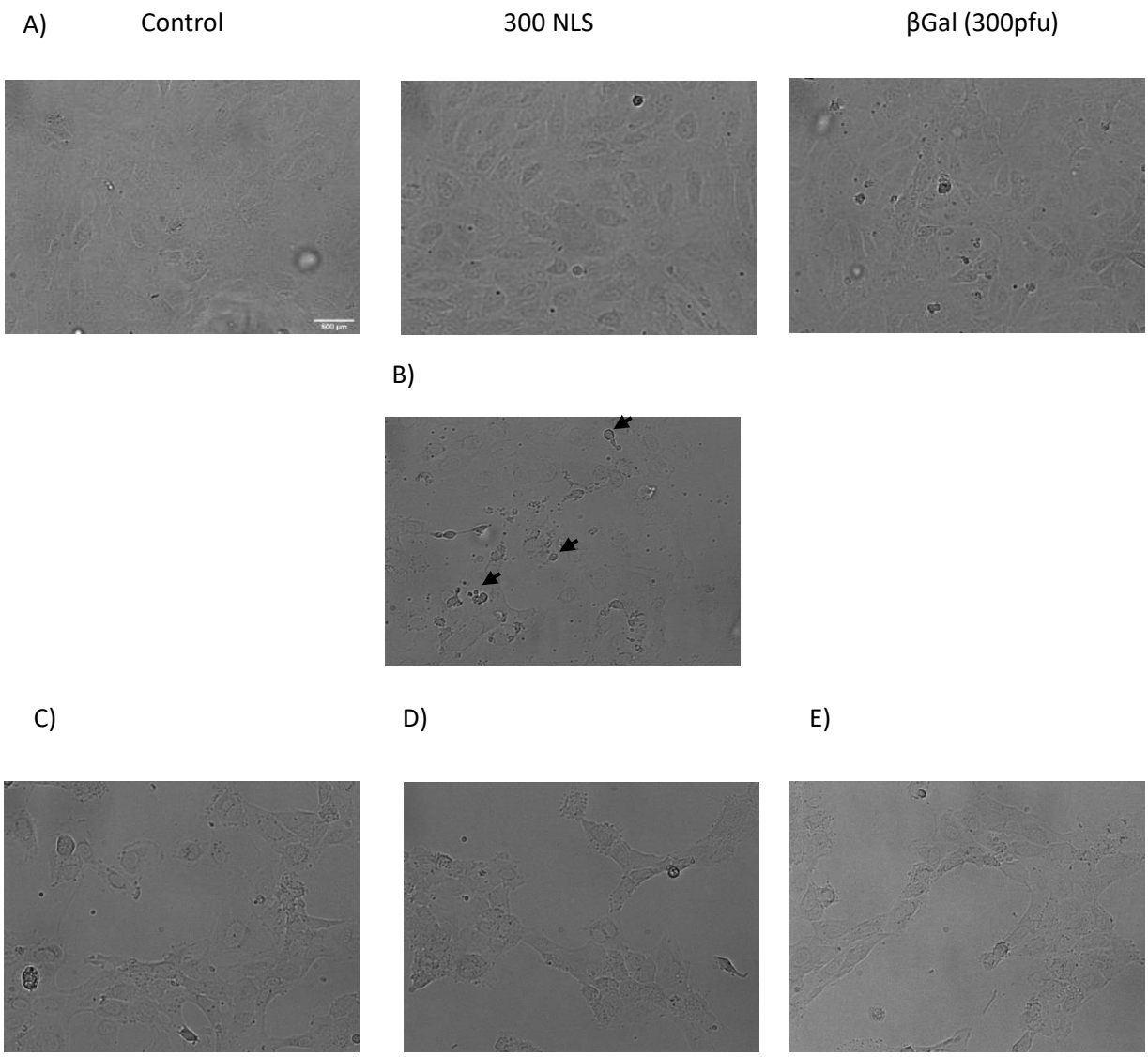


**Figure 4.22 Brightfield images of Adv.NLS-1 MKP-2 inhibition of Doxorubicin-induced membrane damage in HUVECs.**

Sub-confluent HUVECs were infected with Adv.NLS-1 MKP-2 virus (100-300pfu), and βGal (300pfu) for 40 hours and when confluent stimulated with Doxorubicin (30µM) for 24 hours as outlined in methods section 2.2.10. A) Control, βGal (300pfu) and Adv.NLS-1 MKP-2 alone controls, B) HUVECs treated with 30µM Doxorubicin arrows indicating cellular release, C-E) HUVECs transfected with 100-300pfu respectively treated with 30µM Doxorubicin. Images were obtained using the Nikon Eclipse (TE300) Inverted microscope (x40 magnification). N=2

Figure 4.23 shows the effect 100µM of Cisplatin has on the morphology of the HUVECs, as shown with Doxorubicin, Cisplatin 100µM elicits similar morphological effects. The treated cells have swollen and rounded compared to the control (A) with noticeable blebbing and bubbles. This would be expected when investigating pyroptosis and mirrors the findings of the LDH cytotoxicity assay. The introduction of Adv.NLS-1 MKP-2 (figure 4.23 C, D and E) also shows a reduction in blebbing, and bubbles seen although the HUVECs still look enlarged and swollen compared to the control. These data suggest that Adv.NLS-1 MKP-2 is having a protective effect on the cells. As the Adv.NLS-1 MKP-2 and βGal (300pfu) control show a slight increase in cell size, however there is no substantial morphological change in the cells.

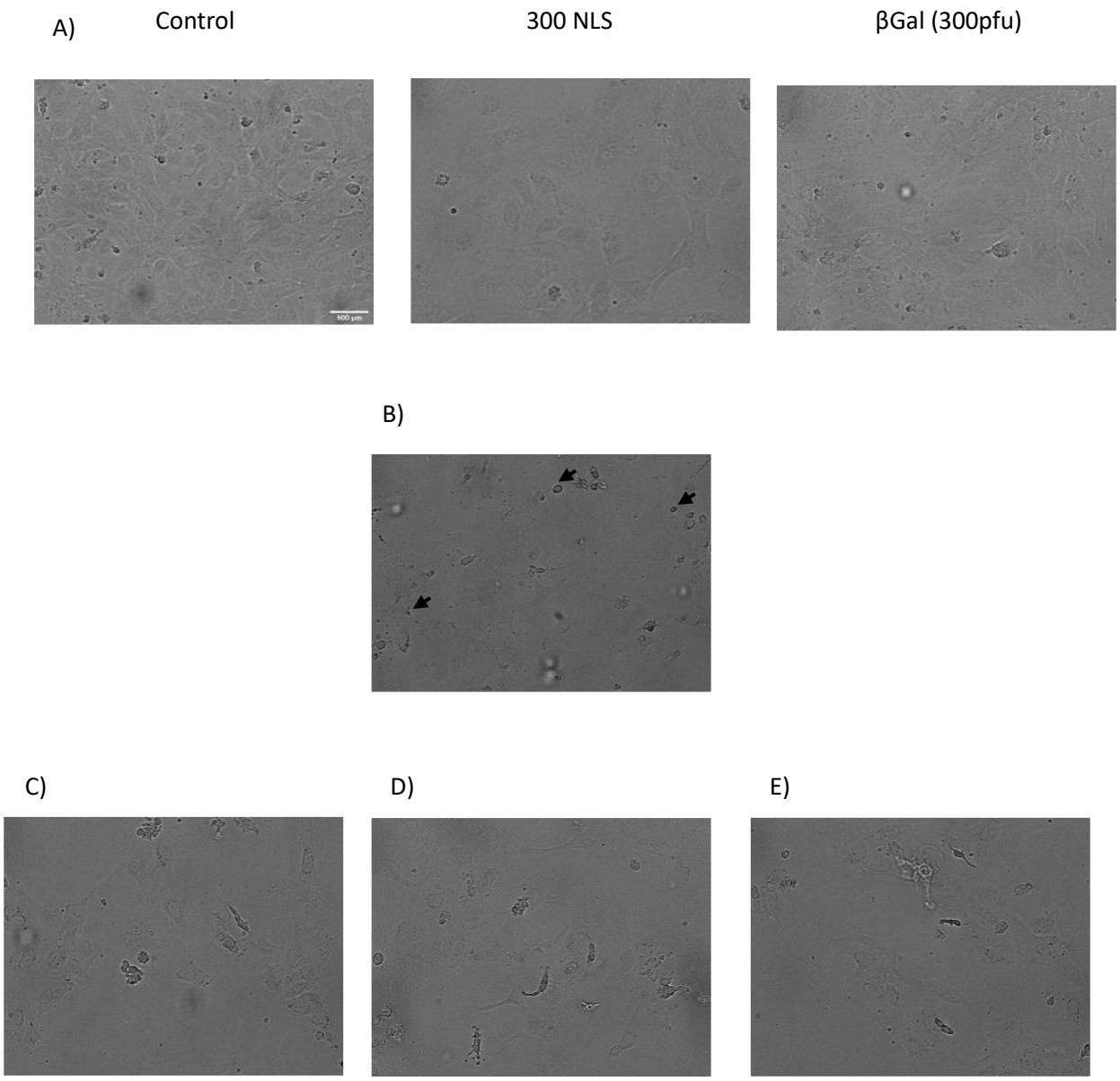


**Figure 4.23 Brightfield images of Adv.NLS-1 MKP-2 inhibition of Cisplatin -induced membrane damage in HUVECs.**

Sub-confluent HUVECs were infected with Adv.NLS-1 MKP-2 NLS virus (100-300pfu), and βGal (300pfu) for 40 hours and when confluent stimulated with Cisplatin (100µM) for 24 hours as outlined in methods section 2.2.10. A) Control, βGal (300pfu) and Adv.NLS-1 MKP-2 alone controls, B) HUVECs treated with 100µM Cisplatin arrows indicating cellular release, C-E) HUVECs transfected with 100-300pfu respectively treated with 100µM Cisplatin. Images were obtained using the Nikon Eclipse (TE300) Inverted microscope (x40 magnification). N=2

After using multiple approaches to identify pyroptosis in chemotherapy-treated cells, FACS analysis was used to determine if infection with Adv.NLS-1 MKP-2 protected the cells from all forms of cellular damage, including apoptosis or necrosis. Figure 4.24 represents the FACS analysis of cell populations where the HUVECs were infected with Adv.NLS-1 MKP-2 and treated with Doxorubicin. For these experiments, infection of Adv.NLS-1 MKP-2 virus alone showed a comparable percentage of healthy cells to the level of control cells showing that the virus did not cause cellular damage. However, Doxorubicin at both concentrations, caused a dramatic decrease in cell viability. Figure 4.24 shows that with the addition of Doxorubicin at both 10µM and 30µM respectively, there was a drop in healthy cells from 65% (% cells: 65.24±3.69, N=3) to essentially zero (10µM % cells: 0.58±0.08, N=3, and 30µM 0.36±0.07, N=3). Infection of HUVECs with Adv.NLS-1 MKP-2 had no visible effect on the effect of Doxorubicin at either concentration.

A similar trend can be seen with early apoptotic cells, both concentrations of Doxorubicin reduced the level of early apoptotic cells from 5% to 0.1% with 10µM and 0.02% with 30µM respectively, highlighting the damage Doxorubicin causes to HUVECs. 10µM has shown 0.17% early apoptosis (% cells:0.17±0.05, N=3), which increased to 3% (% cells: 0.29±0.16, N=3) with 300pfu. When treated with Doxorubicin there are minimal cells in this group, indicating that cells treated with either concentration of Doxorubicin, even with Adv.NLS-1 MKP-2 infection, are mainly late apoptotic and necrotic.

Doxorubicin stimulated a significant increase in cells in late apoptosis (figure4.24 B III) from a control level of around 20% (% cells: 23.07±2.28, N=3) to over 50% (10µM% cells:53.13±3.12 and 30µM% cells: 53.75±2.84, N=3) at both 10 and 30µM respectively. When looking at the effect Adv.NLS-1 MKP-2 infected cells with the same drug treatment however, although not statistically significant, there is a decrease in late apoptotic cells. This was found to be significant at 200pfu (% cells: 36.18±1.987, N=3) and 300pfu (% cells: 40.88±2.229, N=3).

This inhibitory effect of Adv.NLS-1 MKP-2 was also found in cells treated with 30µM Doxorubicin, all concentrations were found to be inhibitory with a reduction to 39% with 300pfu (% cells:38.90±1.65, N=3).

However, this pattern may not be solely down to the effect of Adv.NLS-1 MKP-2 as cells infected with βgal at 300pfu show the same pattern of response (% cells:43.55±3.08, N=3). Indicating this could also be an effect of viral infection on the HUVECs. Lower concentrations of control virus would have to be examined for this possibility.

Doxorubicin does not seem to affect necrotic cell death over a 24hour period. When looking at necrosis (figure4.24 B IV) the results show similar levels of necrosis across the cell only control (% cells:9.60±2.71, N=3) and both 10µM (% cells: 7.73±1.47, N=3) and 30µM (% cells: 4.56±1.09, N=3). However, figure 4.24 shows that βgal (300pfu) and the Adv.NLS-1 MKP-2 only controls show an increase in necrosis (βgal (300pfu) % cells: 46.12±3.13, N=3 and Adv.NLS-1 MKP-2 % cells: 50.21±3.36, N=3). This shows that Doxorubicin does not cause necrosis in HUVECs. This indicates the infection with virus alone is impacting the cell viability. However, the infection of the Adv.NLS-1 MKP-2 virus independently has shown a significant increase in the percentage of necrotic cells detected, up to 63%. There is however slight concentration dependent decrease in necrotic cells with Adv.NLS-1 MKP-2 however, with cells treated with 10µM Doxorubicin and infected with 300pfu the highest concentration used resulting in 45% (% cells:45.86±2.81, N=3) of HUVECs found to be necrotic compared to 63% with 100pfu (% cells: 63.35±1.40, N=3). This is a significant increase when compared to HUVECs treated with 10µM drug control which shows 7.73% necrosis (% cells:7.73±1.47, N=3). This pattern is mimicked by cells treated with 30µM (% cells:4.56±1.09, N=3), where there is a slight Adv.NLS-1 MKP-2 concentration dependent decrease in necrotic cells however 300pfu with 30µM results in 58% (% cells:58.06±2.29, N=3) of cells being found to be necrotic.

Conversely, βGal (300pfu) was used as a control for the Adv.NLS-1 MKP-2 infection and in previous experiments has shown that it has not affected the JNK expression, however, the results have shown similar levels of necrosis as shown in Adv.NLS-1 MKP-2 infected cells. Indicating that the infection of the virus could be impacting the levels of necrosis in the cells not via the deactivation of JNK caused by MKP-2. For this further work is required to investigate the viral impact on HUVECs.

A)

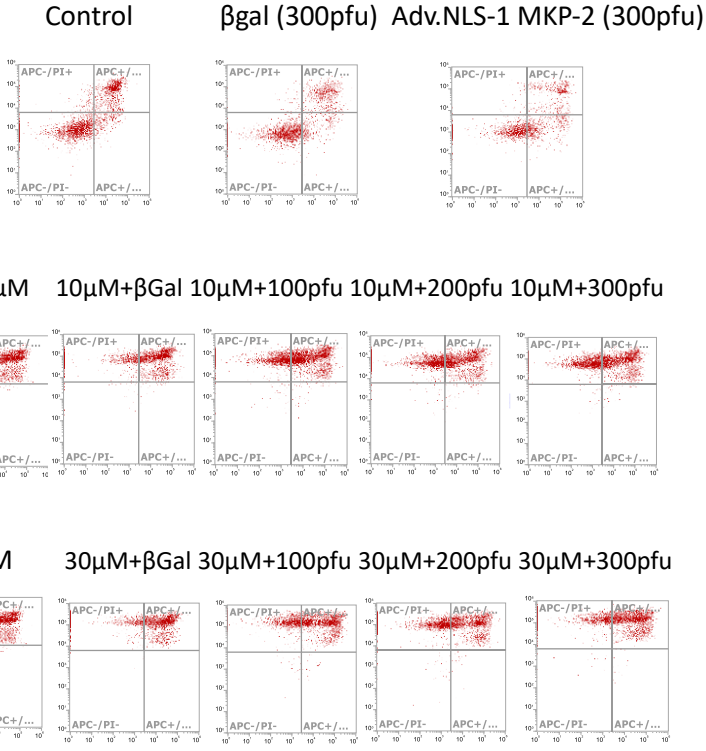
Control
βgal (300pfu)
Adv.NLS-1 MKP-2 (300pfu)
10μM
10μM+βGal
10μM+100pfu
10μM+200pfu
10μM+300pfu
30μM
30μM+βGal
30μM+100pfu
30μM+200pfu
30μM+300pfu
APC-/PI+
APC+/...
APC-/PI-
APC+/...

B)

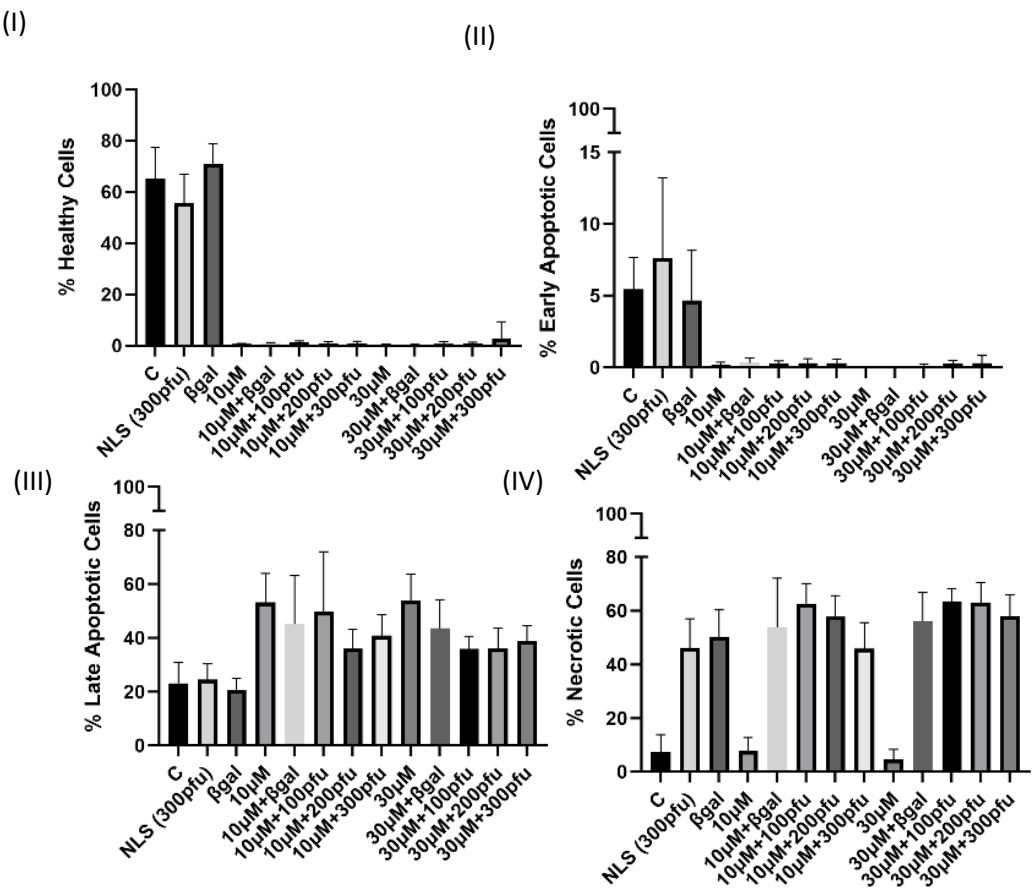
(I)
% Healthy Cells
(II)
% Early Apoptotic Cells
(III)
% Late Apoptotic Cells
(IV)
% Necrotic Cells
C
NLS (300pfu)
βgal
10μM
10μM+βgal
10μM+100pfu
10μM+200pfu
10μM+300pfu
30μM
30μM+βgal
30μM+100pfu
30μM+200pfu
30μM+300pfu

**Figure 4.24 The effect of Adv.NLS-1 MKP-2 on Doxorubicin-mediated HUVEC cell death using FACS analysis.**

HUVEC viability was measured using Flow Cytometry. Sub-confluent HUVECs were infected with Adv.NLS-1 MKP-2 Virus (100-300pfu) and βgal (300pfu) for 40 hours and when confluent stimulated with Doxorubicin (10μM and 30μM) for 24 hours. Cell viability was determined by PI and Annexin V-APC straining as outlined in methods section 2.2.6. Where, Early apoptosis (Annexin V-APC) Late apoptosis (PI and Annexin V-APC) and Necrosis (PI). A) Representative dot plots with double staining of Annexin V-APC/PI staining of Doxorubicin treated cells. B) Histograms showing percentage of I) Healthy, II) early apoptotic, III) late apoptotic and IV) necrotic cells. Results represent mean ± S.E.M, n=3, non-significant, compared to Drug and vehicle control.

After investigating the impact on cell viability with Doxorubicin, HUVECs were treated with Cisplatin. To fully investigate if cell viability and infection differs on the mechanism of action of the different compounds 30µM and 100µM were examined. Figure 4.25 shows that cell viability is different with Cisplatin treatment compared to Doxorubicin.

Cisplatin at 30µM had little effect on the percentage of healthy cells which was comparable to the untreated control (% cells: control 65.24±3.69, % cells: 30µM 57.76±2.85). Whilst the infection with βGal was without effect, Adv.NLS-1 MKP-2, at all concentrations tested, significantly decreased the percentage of healthy cells (% cells:100pfu 25.72±2.61, ****P<0.0001, n=3, 300 pfu 29.24±2.74, ****P<0.0001, N=3). However, at a higher concentration of Cisplatin (100µM), there was a significant decrease in the percentage of healthy cells (% cells: 25.88±3.45, N=3). However, there was no corresponding significant effect of Adv.NLS-1 MKP-2 on the Cisplatin response although there was a minor 5% increase in healthy cells at 300pfu (300pfu % cells: 31.61±2.37, N=3).

It has been observed that early apoptosis is similar in the untreated cells alongside those treated with Cisplatin at both concentrations, at around 5% early apoptosis. However, these levels are significantly increased with the infection of Adv.NLS-1 MKP-2, indicating that Adv.NLS-1 MKP-2 increases the percentage of early apoptosis in Cisplatin treated cells. The percentage of early apoptosis increased from 5% to 23% with 30µM Cisplatin 300pfu (% cells: 15.81±0.68, ****P<0.0001, N=3), whereas for 100µM early apoptosis is increased from 7% to 25% (% cells: 23.35±1.65, ***P<0.001, N=3). This shows that Adv.NLS-1 MKP-2 has significantly increased the percentage of early apoptotic cells by around 20% which has shown not to be concentration dependent. When looking at 100µM overall there is an increase in early apoptosis, however this does not show to be as concentration dependent as 30µM. Combining 100µM with 200pfu increases early apoptosis by 13% (% cells:22.69±1.91, ****P<0.0001, N=3).

Whereas both 100 and 300pfu increase levels by 16% respectively, (100pfu % cells: 26.41±2.87, ****P<0.0001N=3 and 300pfu % cells: 25.21±1.94, ****P<0.0001, N=3). This indicates that the mechanism of action of Adv.NLS-1 MKP-2 in combination with Cisplatin is similar at any concentration.

This similarity in pattern however differs when looking at late apoptosis. Adv.NLS-1 MKP-2 has differing effects on the two Cisplatin concentrations. When looking at 30µM of Cisplatin there is a significant increase of late apoptosis which was found to be significant when comparing cells with and without Adv.NLS-1 MKP-2, as 300pfu shows an increase of 20% (% cells: 42.02±2.283, *P<0.05, N=3). Yet, when used with 100µM there is a significant decrease in late apoptosis from 50% (% cells: 50.86±2.66, N=3) to 34% with 100pfu (% cells: 34.84±3.26, N=3) and 37% with 300pfu (% cells: 37.89±2.10, N=3). This indicates the concentration of Adv.NLS-1 MKP-2 does not have a significant impact on late apoptosis level, with 100 and 300pfu levels being comparable. However, this does seem to suggest a small level of cellular protection with the damage 100µM Cisplatin causes. Particularly when compared to the levels of necrosis.

Overall, the level of necrosis shows to slightly reduce with the effect of Adv.NLS-1 MKP-2 on Cisplatin treatment when comparing the untreated (% cells: 6.12±1.93, N=3) and drug only controls, as all show levels of around 7% necrosis (30µM % cells: 7.20±1.34, N=3, and 100µM % cells: 6.18±1.22, N=3). With Adv.NLS-1 MKP-2 infection there is a slight decrease by around 2% of necrosis with 30µM (300pfu % cells: 5.39±1.04, N=3), which is mimicked when looking at 100µM of Cisplatin where drug controls show 6.18% (% cells: 6.18±1.22, N=3) necrosis compared to 5.29% with 300pfu Adv.NLS-1 MKP-2 (% cells: 5.29±0.96, N=3). Interestingly both Cisplatin concentrations show more of a decrease in necrosis with 200pfu (% cells: 2.94±0.59, N=3). To further understand this phenomenon further analysis is required. when combined it can be deduced that Adv.NLS-1 MKP-2 does show a form of cellular protection from Cisplatin induced cell death.

This difference in how Adv.NLS-1 MKP-2 impacts cell survival is indicative of the mechanisms of action of the compounds examined. To fully understand the synergistic effect of the Adv.NLS-1 MKP-2 and differing chemotherapeutics mechanism of action, further investigation is required.

A)

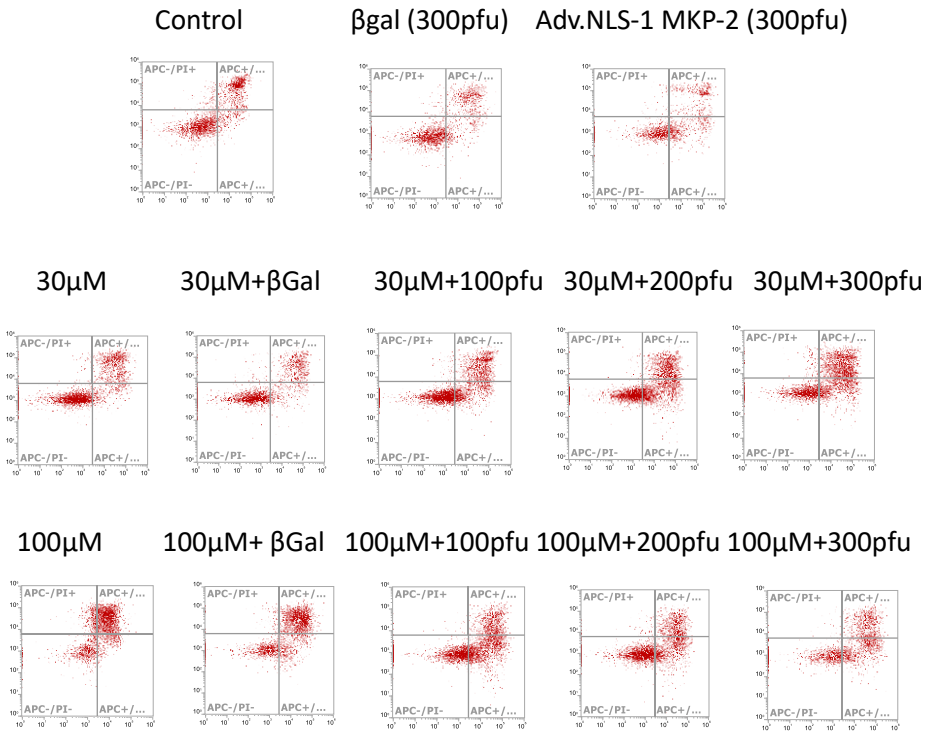
Control
βgal (300pfu)
Adv.NLS-1 MKP-2 (300pfu)
30μM
30μM+βGal
30μM+100pfu
30μM+200pfu
30μM+300pfu
100μM
100μM+ βGal
100μM+100pfu
100μM+200pfu
100μM+300pfu
APC-/PI+
APC+/...
APC-/PI-
APC+/...

B)

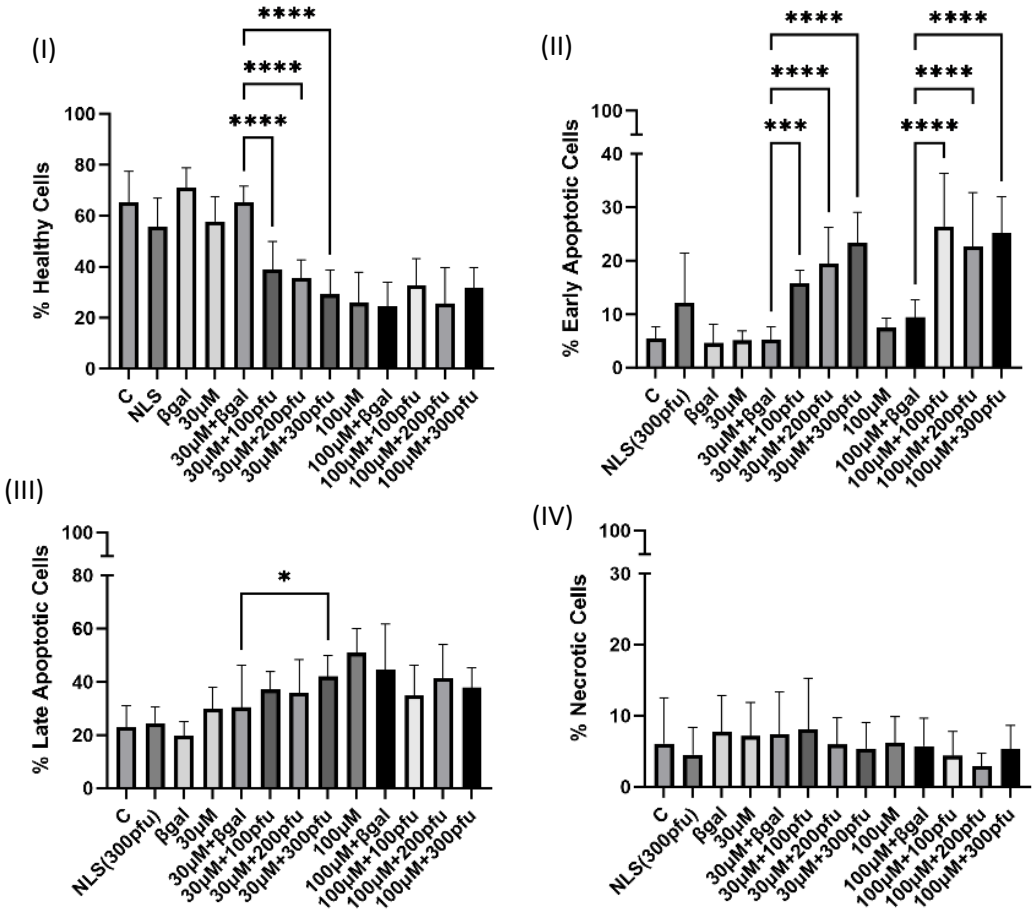
(I)
% Healthy Cells
(II)
% Early Apoptotic Cells
(III)
% Late Apoptotic Cells
(IV)
% Necrotic Cells
C
NLS
NLS(300pfu)
βgal
30μM
30μM+βgal
30μM+100pfu
30μM+200pfu
30μM+300pfu
100μM
100μM+βgal
100μM+100pfu
100μM+200pfu
100μM+300pfu

**Figure 4.25 The effect of Adv.NLS-1 MKP-2 on Cisplatin-mediated HUVEC death using FACS analysis.**

HUVEC cell viability was measured using Flow Cytometry. Sub-confluent HUVECs were infected with Adv.NLS-1 MKP-2 Virus (100-300pfu) and βgal (300pfu) for 40 hours and when confluent stimulated with Cisplatin (30μM and 100μM) for 24 hours. Cell viability was determined by PI and Annexin V-APC straining as outlined in methods section 2.2.6. Where, healthy (non), Early apoptosis (Annexin V-APC) Late apoptosis (PI and Annexin V-APC) and Necrosis (PI) were detected. A) Representative dot plots with double staining of Annexin V-APC/PI staining of Doxorubicin treated cells. B) Histograms showing percentage of I) Healthy, II) early apoptotic, III) late apoptotic and IV) necrotic cells. Data represents mean ±S.E.M, n=3, *P<0.05, ***P<0.001 ****P<0.0001 compared to drug and vehicle control.

### 4.2.9. Generation of JNK1 ad 2 CRISPR knockout cell with CRISPR

#### 4.2.9.1. Design and characterisation of gRNA

After investigating both a pharmacological tool and an adenovirus as approaches to inhibit JNK activation, a CRISPR knockout system was generated. As the first two methods did not fully inhibit JNK and have known off targets, CRISPR was chosen to enable JNK specific knockout models and investigate the differing effects of the different isoforms, namely JNK1 and JNK2.

Clustered Regularly Interspaced Short Palindromic Repeat (CRISPR) Cas 9 is fast becoming one of the most influential techniques of the 21st century. This relatively new technique allows for the alteration of the genome in a simple and inexpensive manner. Opening up the technique to all labs globally pathing the way for life altering treatments to some of the most life altering diseases (Ferreira and Choupina, 2022).

This phenomenon was first identified as a natural phenomenon in *Escherichia coli* by the Nakatas group in 1987. It was noted, while trying to identify the gene responsible for isozyme conversion, that the same sequence was found in different clones (Ishino et al., 1987). However, it was not until the 2000's that the link between spacer regions of the CRISPR and those sequences of the prokaryotic genomes was made by Mojica et al, (2005), paving the way for its use in research by 3 main groups Mojica , Pourcel and Bolotin (Mojica et al., 2005).

Therefore, establishing an endothelial JNK knockout cell line was important when investigating the effect JNK and its isoforms have on cardiovascular toxicities. EA.hy926 cells were chosen as an immortalized cell line for this technique. These cells were used when establishing CRSIPR knockouts of JNK1, JNK2 and JNK1 and 2.

#### 4.2.9.1.1. gRNA Design

To enable the investigation of the effect knocking out JNK would have on the endothelial cells, first a JNK Cas9 plasmid needed to be designed. An initial literature review failed to show any previous use of CRISPR to knock out JNK therefore new potential guide RNA (gRNA) would have to be designed. To do this, two online tools were utilised to highlight potential target sites, ChopChop and Synthego. These tools were used to find potential target sites for MAPK8 (JNK1) and MAPK9 (JNK2) in Homo sapiens for CRISPR/Cas9. Both sites gave a number of potential sequences, of which 4 potential sequences were selected based on a number of qualities: a low number of mismatches, a high GC content and a high efficiency. As shown in table 1, 2 target sites were selected for each family member, to increase the probability of success. These sequences were then checked using the Santa Cruz Genome browser BLAT function to ensure that these sequences are accurate for their target site. Multiple target sequences were then selected for a higher rate of success, with both target sites being in different exons to further increase the probability of an effective knockout of the gene. However, sites that target JNK can only be found on 1 exon, therefore both target sites selected are located at different sections of the same exon. For JNK1, this is encoded on exon 2 and JNK2 is coded on exon 3. Figure 1 shows the location and sequence shown on Synthego of JNK1,1 that was selected for use. The sequences were then ordered for both the 5' and reversed 5' sequences to total 8 sequences as shown in table 1.

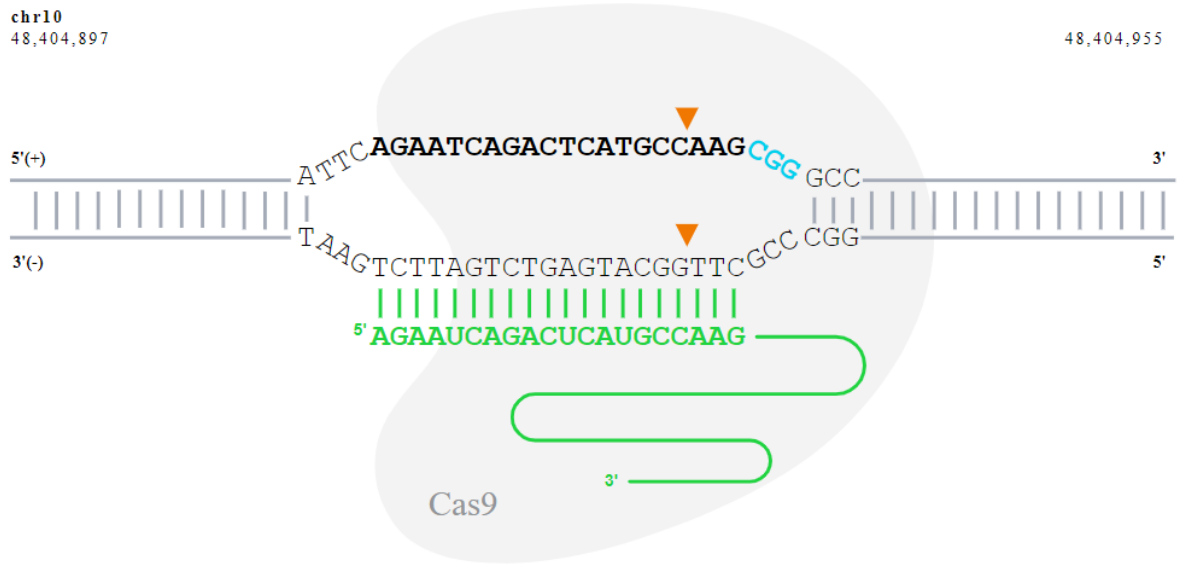


**Figure 4.26 Target location on the genome (Taken from synthego, 2019).**

The sequence in bold and black is the target sequence for JNK1,1 from Synthego. The red arrow shows the cut site which is directly before the PAM (protospacer adjacent motif) site (Blue). As shown in the diagram the cas9 binds to the complementary strand – guide strand in the 5' – 3' direction (as seen in green).

**Table 4.1 Selected JNK sequences**

Sequences were selected using CHOPCHOP and Synethgo. Sequences used in both 5' and 5' reversed ordered from Sigma Aldrich

| | Sequences | 5' Forward | 5' Reversed |
|---|---|---|---|
| MAPK8 (JNK1) | | | |
| JNK1,1 | AGAAUCAGACUCAUGCCAAG | CACC/TCTTAGTCTGAGTACGGTTC | CTTGGCATGAGTCTGATTCT |
| JNK1,2 | AACACCCGTACATCAATGTC | CACC/TTGTGGGCATGTAGTTACAG | GACATTGATGTACGGGTGTT |
| MAPK9 (JNK2) | | | |
| JNK2,1 | CUGCAUUUGAUACAGUUCUU | CACC/GACGTAAACTATGTCAAGAA | AAGAACTGTATCAAATGCAG |
| JNK2,2 | GAGAACGGTGAGTATAGCCG | CACC/CTCTTGCCACTCATATCGGC | CGGCTATACTCACCGTTCTC |

Once the sequences were selected, CACC was added to 5’ forward and AAAC to the 5’ reversed strand of the complementary and reverse strands as indicated in table 1. The AAAC and CACC are non-specified bases that will provide overhangs based on the BBs1 overhang site used in the Cas9 plasmid. The Cas9 plasmid was then linearized, the sequence of choice was then inserted to recreate a circular plasmid containing our sequence of choice. To confirm the success of the ligation, the plasmids were plated onto agar plates containing carboxacilin and incubated at 37°C overnight. I It was then determined that JNK1,1, JNK1,2 and JNK2,1 ligation was successful as colonies had formed on the agar plate.  As there were no colonies on the agar plate for JNK2,2 and due to time restraints, this sequence was then discarded from future stages.

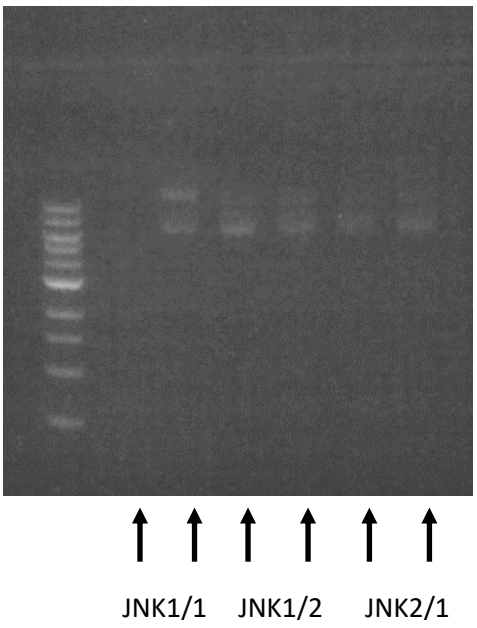


**Figure 4.27 Electrophoresis Gel confirming Insertion of JNK sequence into the plasmid.**

Electrophoresis was used to ensure that all insertion of sequences was effective. A gel was prepared and placed in the PCR tank with the prepared samples of JNK1,1, JNK1,2 and JNK2,1. Each sample was added in duplicate as the first was prepared using a low yield kit and the second using a high yield Isolate II Plasmid Mini Kit. The gel was run for around 1 hour at 100 volts. N=1

Next the plasmids of the successful sequences were ran using agarose electrophoresis., to confirm the plasmid was the correct size and circular. This should be confirmation the DNA had been inserted into the vector prior to any further analysis. The bands shown in figure 4.27, for JNK1,1, JNK1,2 and JNK2,1 confirm this. As these plasmids were deemed successful, they were sent for sequencing to SourceBioscience, to further confirm that the sequence was successfully inserted into the cas9 plasmid.

A)

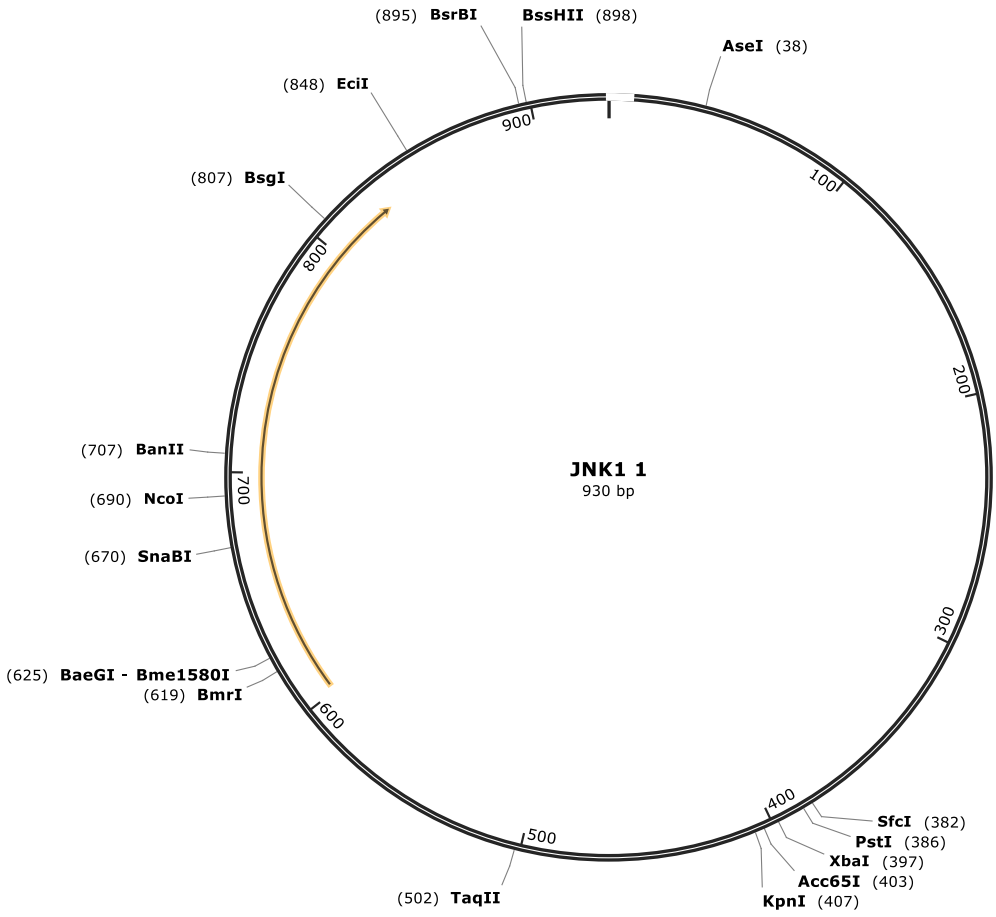
(895) BsrBI
BssHII (898)
AseI (38)
(848) EciI
(807) BsgI
(707) BanII
(690) NcoI
(670) SnaBI
(625) BaeGI - Bme1580I
(619) BmrI
(502) TaqII
SfcI (382)
PstI (386)
XbaI (397)
Acc65I (403)
KpnI (407)
JNK1 1
930 bp
100
200
300
400
500
600
700
800
900

D)

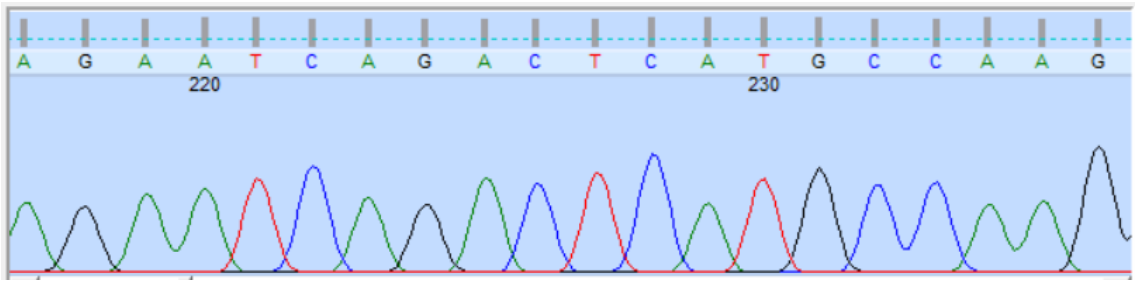
A G A A T C A G A C T C A T G C C A A G
220
230

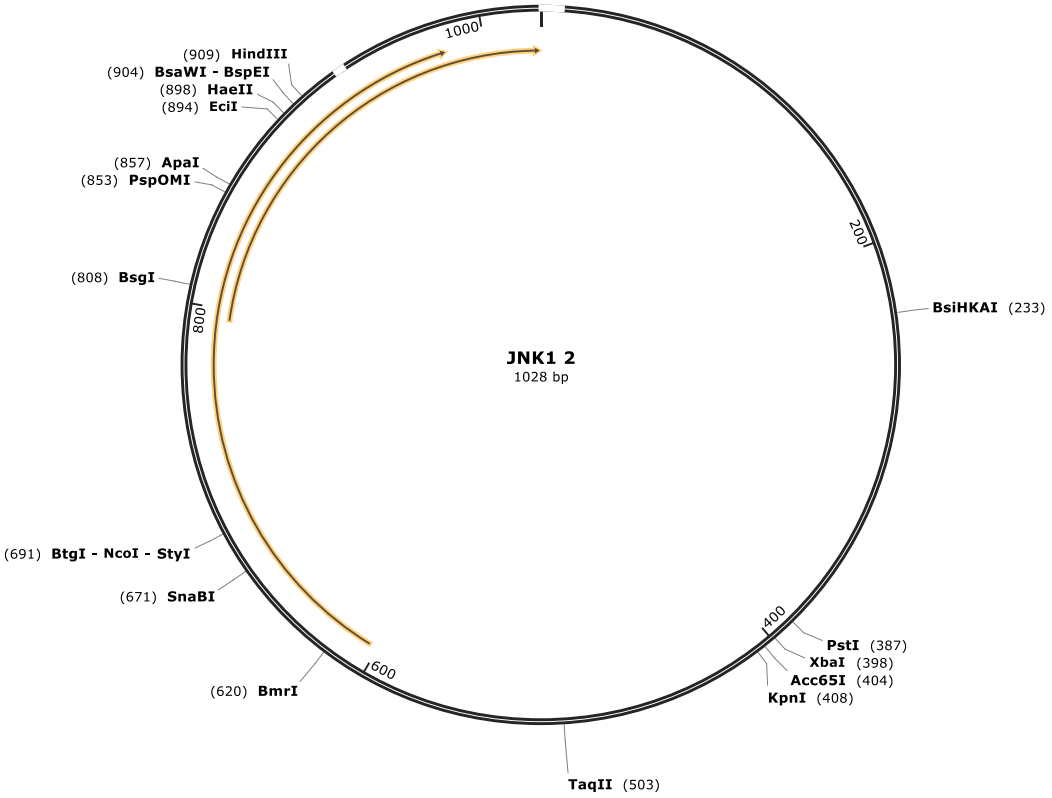
JNK1 2
1028 bp
1000
200
400
600
800
(909) HindIII
(904) BsaWI - BspEI
(898) HaeII
(894) EciI
(857) ApaI
(853) PspOMI
(808) BsgI
(691) BtgI - NcoI - StyI
(671) SnaBI
(620) BmrI
TaqII (503)
PstI (387)
XbaI (398)
Acc65I (404)
KpnI (408)
BsiHKAI (233)

B)

E)

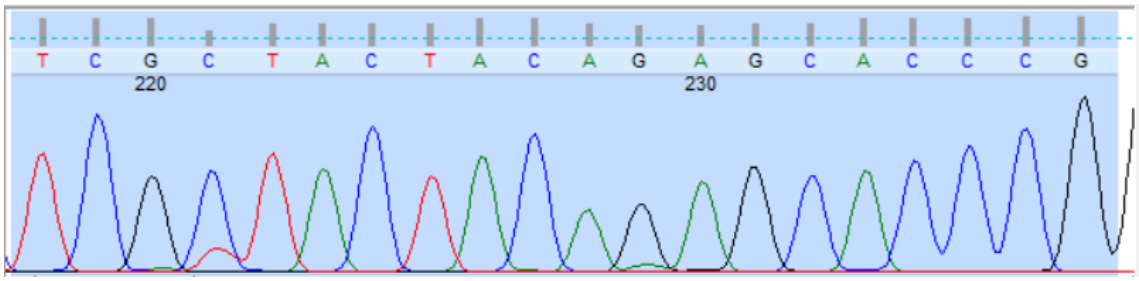
T C G C T A C T A C A G A G C A C C C G
220
230

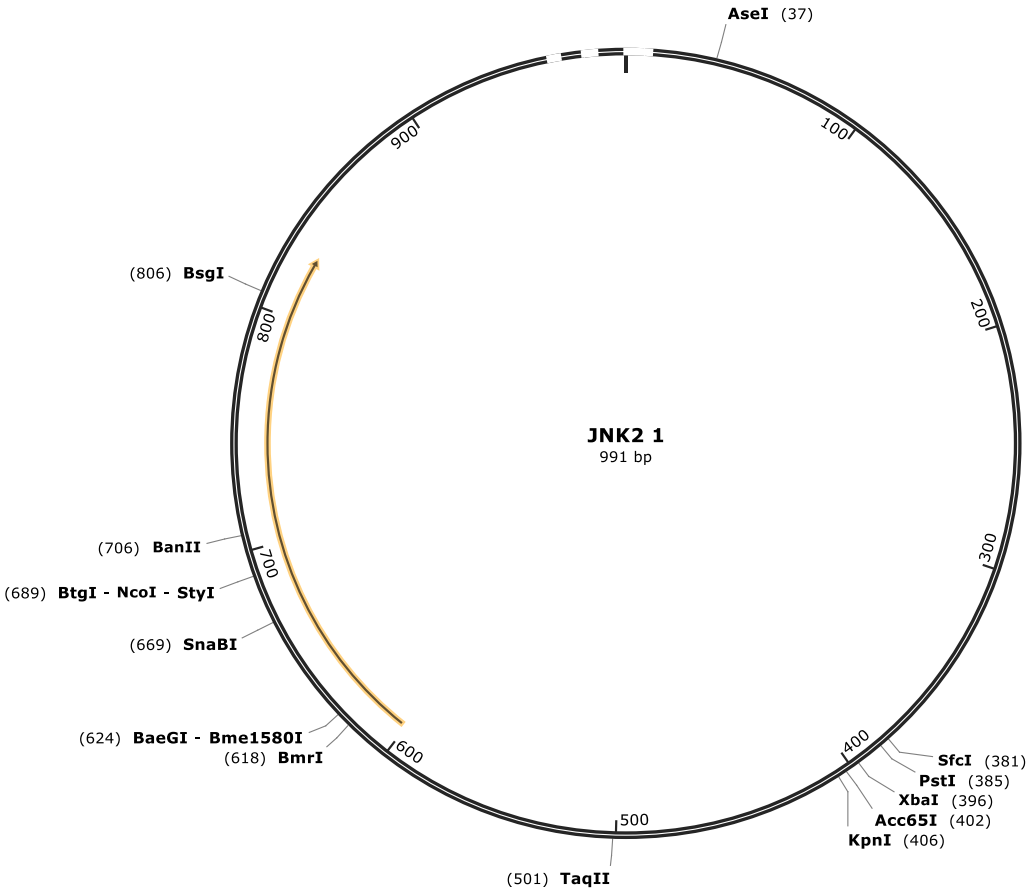


C)

F)

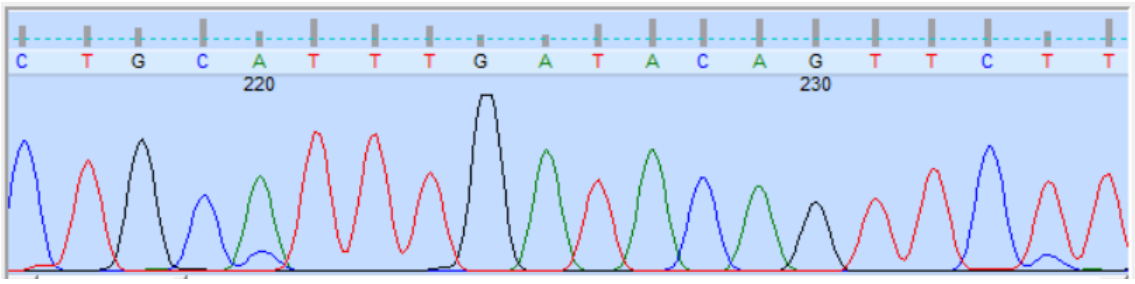


**Figure 4.28 Cas9 plasmid for JNK1 and JNK2 sequences confirmation from SourceBioscience.**

A-C) cas9 plasmids shown to contain the sequence for JNK1,1 JNK1,2 and JNK2,1 respectively. D-F) Finch TV results for the sequences inserted into each plasmid. Confirming that the cas9 plasmids contain the appropriate sequence chosen. N=1

Figure 4.28 A-C shows a circular representation of each plasmid, and the successful sequence has been highlighted by the orange arrow respectively. This is to infer that the insertion has been successful. For further confirmation, Finch TV, a chromatogram viewer, was utilised. With the use of this technology, the sequence of interest could be identified in the sequence, as shown in figure 4.28 (D-F). Each nucleotide was assigned their own unique colour - T=Red, A= Green C= Blue and G= Black. If the insertion had not been successful, the software would not clearly decipher between the colours, and more than one coloured line would overlap. Also, in the sequence above a letter, N would replace the T, A, C, G above the graph as it was unable to decipher the nucleotide.

As figure 4.28 D-F shows, each of the sequences match their chosen sequence as seen in table 1. This confirms that the chosen gRNAs have been successfully inserted into the cas9 Plasmid. Allowing for the plasmids to be transfected into cell lines.

#### 4.2.9.1.2. CRISPR knockout in endothelial cells

The plasmids were then purified and linearised to enable them to be transfected into the endothelial cells, for this an immortalized cell line EA.hy926 was used. This was to give more stability to the transfection. The HUVEC cell line is a primary cell line and therefore can only be used for 7 passages. This could reduce the possibility of transfection by limiting the time required for effective replication.

Once gRNAs were designed and characterised this enabled them to be used for transfections. Plasmids were transfected into 50% confluent EA.hy926 cells using polyethylenimine (PEI). Once transfected, an individual cell was selected and grown in a 96 well plate. Once there was enough of each clone, they were individually assessed for JNK knockout using western blot analysis. Each clone was then stimulated with 30µM of Doxorubicin for 8 hours and western blot analysis was utilised to assess knockout of JNK. It was during this screening that it was noted that there had not been a successful knockout. As figure 4.29 shows, when looking at JNK1 only, there is knockdown when stimulated with Doxorubicin compared to the EA.hy926 control. However, JNK1 bands can be seen in the total JNK blot indicating that this knockout was not as successful as the pJNK blot shows. To confirm protein levels GAPDH was ran, as figure 4.29 shows there is significant effect on the protein level compared to the EA.hy926 control. Therefore, the lack of expression visible on the blot could be due to the loss of protein in these cells. However, when looking at the JNK knockout, it can be seen in the pJNK blot that expression can still be detected after treatment with Doxorubicin. Indicating that there was little impact made by the CRISPR cas9. This can be confirmed by both the levels of total JNK in comparison to the EA.hy926 control and the knockout cells. As there was not sufficient evidence CRSIPR cas9 clones had been successful no further experiments were carried out.

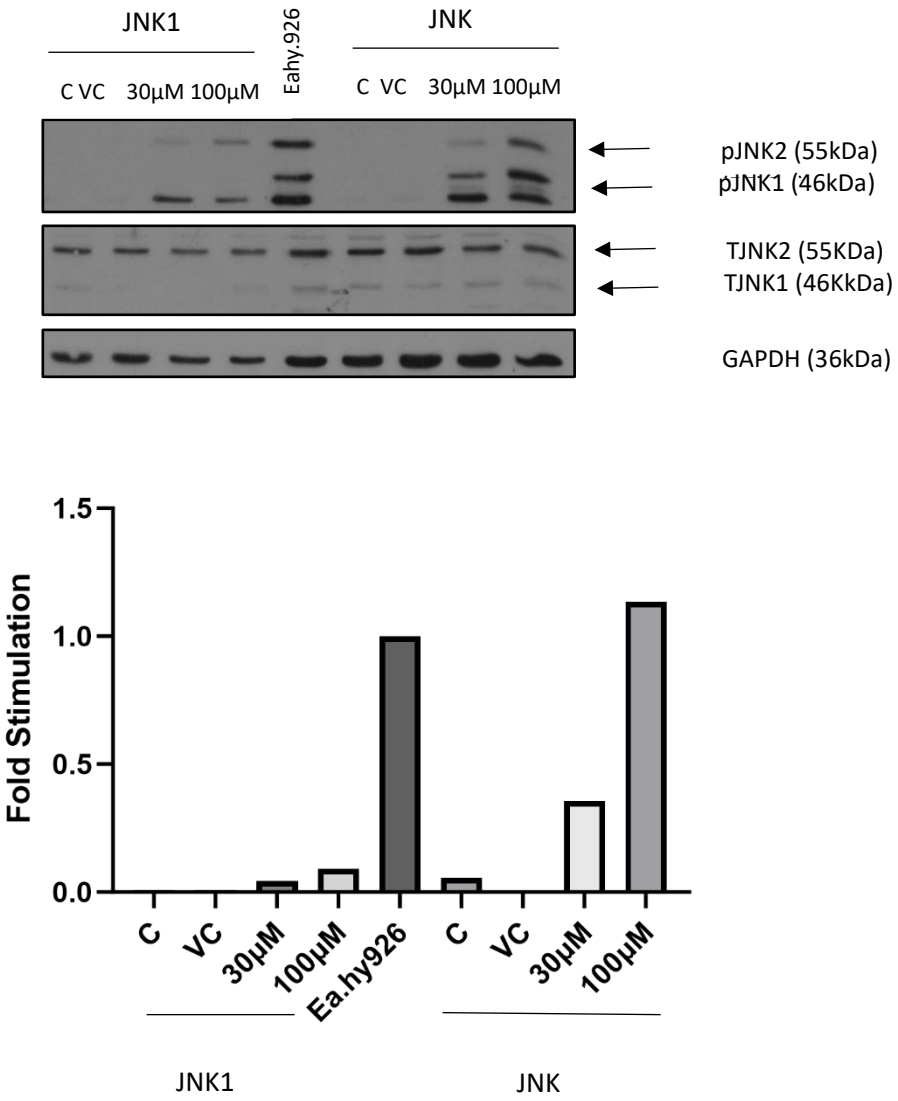


**Figure 4.29 Generation of EA.hy926 cell lines with JNK1 and JNK**

EA.hy926 cell lines were generated as stated in methods section 2.2.12.11. Using JNK1 and JNK targeting CRISPR cas9 plasmids. Results show western blot of JNK expression in the 2 cell lines plus EA.hy926 control with Total JNK and GAPDH as loading control. Blots were semi quantified as outlined in methods 2.2.2.6. A) western blot representation. B) Graphical representation of change in protein expression. Results represent N=1

The MAPK kinase family member JNK has been associated with cardiovascular toxicities and has been shown to play a vital role in atherosclerosis and endothelial dysfunction. Therefore, it is important to understand the pathway and investigate approaches which can protect endothelial cells from cardiovascular toxicities. In this study, three methods of inhibiting JNK activation have been investigated to determine the impact this has on cell viability. To do this, a pharmacological tool, virus and novel CRSIPR cas9 have been used to prevent JNK activation and examine the effect this has on HUVEC viability.

A widely studied pharmacological inhibitor used to inhibit JNK activation is SP600125. This anthrapyrazolone inhibitor, was designed by Bennett et al (2001) to specifically inhibit JNK activation (Bennett et al., 2001). It does this by functioning as an ATP competitive inhibitor, by binding at the hydrophobic pocket of the ATP-binding site though found to be selective to JNK it was also shown to be reversible (Wang et al., 2007). This compound inhibits all isoforms of JNK similarly (Bennett et al., 2001). Therefore, it was utilised as a reversible specific inhibitor of JNK. As a reversible pharmacological tool would be most advantageous in a clinical setting. If found to be effective, by only inhibiting JNK during treatment, this could effectively protect from long-term damage.

This compound has been used in several studies since its discovery in 2001, including cancer and inflammatory disease. It has been shown in this investigation that SP600125 inhibits JNK by holding it in an inactive conformation, therefore preventing phosphorylation of JNK in HUVECs (Lombard et al., 2018). However, this is a reversible reaction and following treatment with Cisplatin, p-JNK could be detected. This thesis also observed that there was little change shown in the DNA damage markers such as γH2.AX and caspase 3. As γH2.AX has been reported to be phosphorylated by JNK, some reduction in expression was expected. However, it has been observed in studies by Damrot and Deng. Doxorubicin has been shown to activate the γH2A.X in endothelial and cancer cells (Damrot et al., 2006).

Deng et al (2018) have shown that 50nm Doxorubicin activates γH2A.X in MDA-MB-231 and MCF-7 breast cancer cells. Showing that Doxorubicin causes DNA damage at very low concentrations (Deng et al., 2018).

This JNK/γH2.AX complex has been shown to be linked with caspase 3 leading to apoptosis (Lu et al., 2006). Therefore, by thoroughly investigating the relationships between these pathways, could ultimately protect endothelial cells from chemotherapeutic damage. This study found that by using SP600125 there was no change in γH2.AX, caspase 3 or GSDME levels. This could be a result of several reasons including incomplete inhibition of the pathway or off target effects of SP600125.

It is well documented that SP600125 is not specific to the JNK inhibition as there are a number of off target effects (Bain et al., 2003). Bain et al (2003) found when screening 28 protein kinases, 13 were inhibited by SP600125 some with greater potency than JNK. Among the other protein kinases found to be inhibited is SGK, CDK2 and S6K1. These proteins all relate to key processes within the cell which could relate to the effects of anti-cancer agents. By inhibiting these and JNK, the cellular effects shown in this chapter cannot answer if JNK inhibition affects the cells. The inhibition of these other protein kinases could explain why SP600125 was found not to reduce the percentage cell death in the FACS analysis. It was instead found to reduce healthy cells and increase apoptosis. Other studies such as Yu et al, found that inhibiting JNK with SP600125 triggered apoptosis in bladder cancer cells (Yu et al., 2019a) which could explain why apoptosis was increased in our study which was particularly apparent with Cisplatin treatment. As a result of these findings, examining another JNK inhibitor could allow more insight into the connections, which could pave the way for novel treatments to prevent cardiovascular toxicities by modulating these pathways.

Overall, this study shows that there is a need for more specific inhibitors. There have been a number of different inhibitors for JNK that have been widely used aside from SP600125. As JNK is implicated in a number of diseases there have been a number of inhibitors developed. Currently there are few JNK inhibitors aside from SP600125 in use, these inhibitors include AS601245 and JNK-IN-8 (Wu et al., 2020).

Another ATP binding site inhibitor, AS601245 ([1,3-Benzothiazol-2-yl-(2-{[2-(3-pyridinyl)ethyl]amino}b.-4-pyrimidinyl) acetonitrile)is extensively used in research, (Ferrandi et al., 2004). This inhibitor is also non-selective and inhibits all isoforms of JNK, which has also been shown to influence other MAPK such as ERK (Ferrandi et al., 2004, Carboni et al., 2004). Carboni et al (2004) have used AS601245 for *in vivo* neuroprotective studies where they have shown that the inhibitor protects against ischaemic insults in gerbils and mice models. However, it has been reported that only the phosphorylation of c-Jun is inhibited at high concentrations due to limited cell penetration and ATP concentration (Zhang et al., 2012b).

Another example is JNK-IN-8 which targets JNK to sensitize triple- negative breast cancer to lapatinib (Wu et al., 2020). This is irreversible inhibitor was found to be more selective than SP600125, however, it has low selectivity as it inhibits all 3 isoforms (Ebelt et al., 2017). This limits its use in any study which seeks to delineate isoform specific mechanisms. It binds to the Cys116 in the catalytic binding sites inhibiting c-Jun and ser63 phosphorylation (Zhang et al., 2012b). It was thought that cysteine-directed inhibitors would be more advantageous and would prolong pharmacodynamics (Zhang et al., 2012b). It has shown this by upregulating p65 and Nrf2 in triple negative breast cancer cells (Ebelt et al., 2017). In other breast cancer studies inhibitor IN-8 has shown to also inhibit p38 phosphorylation also indicating lack of specificity among MAPK pathway (Ozfiliz Kilbas et al., 2020).

Although other inhibitors have been developed and investigated on a number of cell lines, they still show similar problems to SP600125. Due to the differing roles of JNK and its isoforms it is difficult to formulate a specific inhibitor to target individual isoforms and also MAPKs. More research is required to fully understand JNK and the role its isoforms play to enable a specific and effective inhibitor of JNK to be used to protect the endothelium from damage.

An alternative strategy available in the laboratory was to utilize a MAP kinase phosphatase to inhibit JNK activation. MKP-2 (mitogen-activated protein kinase phosphatase) is a dual specific nuclear phosphatase that belongs to a family of DUSPs (dual-specificity phosphatases) of which there are 10 members which can be categorised by MAP kinase specificity, subcellular distribution, and regulation (Cadalbert et al., 2005, Chen et al., 2001, Lawan et al., 2012). They are found in a number of tissues and are known to dephosphorylate MAPKs (Sloss et al., 2005). Each MKP is specific for different MAPKs, MKP-1, located in the nucleus, dephosphorylates ERK, p38 and JNK, whilst the cytosolic MKP-3 is known to dephosphorylate ERK alone (Sloss et al., 2005, Cadalbert et al., 2010). Whereas MKP-2 dephosphorylates ERK and JNK, which has been shown to be nuclear located (Lawan et al., 2012, Cadalbert et al., 2010). Dephosphorylation occurs with the removal of the phosphoryl moiety on the threonine and tyrosine residues in the TXY motif (Cornell et al., 2012, Cadalbert et al., 2005, Cadalbert et al., 2010).

For class 1 MKPs, substrate specificity is due to the kinase interacting motif (KIM) which dictates ERK binding but not JNK (Seternes et al., 2019). Subcellular distribution is defined by targeting motifs; nuclear localisation sequences (NLS) or nuclear export sequences (NES). DUSP4/MKP-2 has a nuclear localization sequence in the C-terminus, allowing for localization into the nucleus which also encompasses the KIM domain (Lawan et al., 2012). A previous study from the Plevin group found that in addition to NLS-1, a second NLS, NLS2, also allows localisation of MKP-2 to the nucleus. Disruption of 2 localisation sequences is required for the full cytosolic retention and that either NLS alone is sufficient for nuclear targeting (Sloss et al., 2005).

The nuclear location was confirmed using immunofluorescence, however other studies have shown that this MKP-2 mutant could be cytoplasmic. Chen et al (2001) have shown that an MKP-2 R74A/R75A/R76A mutant at high concentrations could be found in the cytoplasm however at low concentrations it remained in the nucleus (Chen et al., 2001). Similar to these results, the current study demonstrated that Adv.NLS-MKP-2 whilst being predominantly in the nucleus did show some expression in the cytosol.

Adv.NLS-1 MKP-2 has been shown to dephosphorylate JNK as shown in the chapter, however the pJNK antibody has been known to cross react with pERK. The western blot has also shown a decrease in ERK levels with Adv.NLS-1 MKP-2, confirming that this mutant is not JNK specific despite not possessing the ERK binding motif. Whilst not the focus of this thesis, this observation suggests that other regions of MKP-2 in addition to the KIM domain function, bind MKP-2 to ERK. The continued use of Adv.NLS-1 MKP-2 and the pharmacological tools show that a more specific tool is required for JNK investigations. Although siRNA has been utlilised in a number of studies with promising results.

This study was, however, able to show that using the MKP-2 virus, JNK phosphorylation was effectively inhibited. Therefore, the impact of JNK deactivation could be further investigated. Currently there have been no studies on the effect MKP-2 may have on pyroptosis, therefore this study investigated the relationship between MKP-2 dephosphorylation and reduced cellular pyroptosis. Pyroptosis, first identified in 1992, it is another form of programmed cell death which is linked to inflammatory response (Zychlinsky et al., 1992, Zhaolin et al., 2019). This lytic form of cell death utilises the immune response to perform programmed cell death (Loveless et al., 2021).

There are two main mechanisms of pyroptosis both requiring members of the gasdermin protein family. There are 6 GSDM members all composed of an N-terminal and C-terminal. GSDMs are cleaved at the inter domain linker releasing the N domain which translocate to the cytoplasmic membrane resulting in osmotic swelling and lysis (Xu et al., 2022a). GSDMD is a well recognised mechanism of pyroptosis that is mainly linked to immunological stimulation, whilst GSDME is involved in drug-induced programmed cell death (Aki et al., 2022). In this study the focus remained with GSDME. GSDME is cleaved into the active form by caspase 3 and 7, once activated GSDME-N. The cell swells and due to N terminal binding to the membrane causing the formation of pores, cellular components leak launching an immune response (Li et al., 2023).

Pyroptosis has been linked to a number of conditions including cancer and cardiovascular disease. Since its discovery pyroptosis has been reported to play a role in various cardiovascular diseases and has been linked with endothelial cells (Zhaolin et al., 2019). In this study it was found that by deactivating JNK with MKP-2 there was a decrease in pyroptosis related genes, which was consistent with both chemotherapeutic agents. This decrease was observed to be concentration dependent but the levels of GSDME, caspase-3 and γH2.AX were all reduced to some extent. A study looking at atherosclerosis also implicated Pyroptosis and its link to endothelial dysfunction (Zhang et al., 2018). Zhang found using both mouse models that melatonin, an anti-inflammatory, reduced atherosclerotic plaques in the mice models. They also found a reduction in pyroptosis related genes in the aortic endothelium that was consistent with their observations in human aortic endothelial cells, highlighting the importance pyroptosis may play in preventing such conditions.

As a form of programmed cell death, Pyroptosis can be prevented by inhibiting cellular processes unlike necrosis (Jorgensen et al., 2017). This mechanism was investigated by FACS cell death analysis and a cytotoxicity assay, where it was hypothesised MKP-2 would reduce cell death.

The cytotoxicity assay for both Doxorubicin and Cisplatin showed that by preventing JNK activation, cytotoxicity was significantly reduced. With the use of brightfield images it was also able to show a reduction in cellular release with the use of MKP-2, indicating that pyroptosis can be reversed by inhibiting the JNK pathway. Zhang et al (2021) found that there was a link between JNK and pyroptosis through their breast cancer study. They were able to show that Doxorubicin induced pyroptosis in breast cancer cells. They showed the ROS accumulation due to Doxorubicin activated JNK and caspase-3, and it was this accumulation of caspase 3 that lead to GSDME initiated pyroptosis (Zhang et al., 2021).

Caspase-3 is a cysteine protease known for cleaving specific target proteins, in mammals there are 18 caspases where caspase-3 is known as a initiator caspase (Eskandari and Eaves, 2022). Activation of caspase-3 occurs in the cytoplasm and the cleaved caspase-3 can translocate into the nucleus via a nuclear export signal (Luo et al., 2010). Studies looking into colon cancer have found that Lobaplatin (a chemotherapeutic agent) activates caspase-3 which enhances pyroptosis. Which activates the ROS/JNK/Bax pathway resulting in mitochondrial apoptosis which releases cytochrome c. This mechanism has been found to be a positive feedback loop which increases the activation of caspase 3 (Yu et al., 2019b). Another study looking at head and neck cancers by Lan et al (2021) found in OEC-M1 cells (Human oral squamous carncinoma) that JNK was activated by paclitaxel which lead to caspase-3 activation resulting in apoptosis (Lan et al., 2021).

The reduction in JNK mediated by MKP-2 was also seen to reduce levels in apoptosis in Doxorubicin treated HUVECs. However, this was matched by increased necrosis. This phenomenon was not replicated in the Cisplatin treated cells, where early apoptosis was found to increase with other forms showing a reduction. It can be determined however that there was not an increase in healthy cells detected for either compound.

This could be due to the different mechanisms of action of the drugs, the viral vector or the specificity of MKP-2. MKP-2 has been reported in the literature to dephosphorylate both ERK and JNK *in vitro*, studies have shown this to be selective for JNK in cellular systems (Cadalbert et al., 2005, Al-Mutairi et al., 2010). To fully understand the effect of JNK more specific inhibitors should be utilised.

It is also well known that the different isoforms of JNK have different roles in cell function, therefore investigating the effect these individual isoforms have on pyroptosis levels could give more of an insight into how overall JNK is involved with pyroptosis.

Other studies have linked JNK and pyroptosis. Recently it was found by Chen et al (2023) whilst investigating SHP2 (Src homology 2-containing phosphatase 2) and triple negative breast cancer that inhibiting JNK phosphorylation resulted in a decrease in LDH levels using MDA-MB-231 cells and mouse models. They found SHP2 bound to JNK preventing phosphorylation of the protein which led to a reduction in LDH levels and ultimately preventing pyroptosis. They also found that SHP2 knockdown mediated pyroptosis was a result of JNK phosphorylation (Chen et al., 2023), also confirming our findings that a reduction in JNK leads to reduced LDH levels in the HUVECs. Another group investigated the effect the JNK/caspase 3 pathway had on stroke models. They found that an increase in ALDH2 (Aldehyde dehydrogenase 2) suppressed JNK activation, reduced caspase-3 levels and resulted in reduced apoptosis and reduced the LDH levels in cortical neurons and PC12 cells (Xia et al., 2020). Indicating that this phenomenon is found in a variety of cell types.

As previously stated Adv.NLS-1 MKP-2 is unable to discriminate between the different JNK isoforms, a more selective strategy was required. For this it was decided to use the novel technique CRSIPR cas9. CRSIPR cas9 is a now widely utilised technology, although relatively new, that allows for the permanent knock out or in of any gene (Yu et al., 2019d). It has been utilised in many animal, plant and cell-based studies, for a variety of different diseases and implications.

Before this investigation it was found that there currently was not an example of a JNK Crispr cas9 model. Therefore, it was decided to develop a JNK 1, JNK 2 and JNK 1/2 knock out cell lines. This novel strategy would allow the full investigation into the impact JNK has individually on HUVEC viability.

CRISPR cas9 was identified as a natural phenomenon in *Escherichia coli* by the Nakatas group in 1987. It was noted, while trying to identify the gene responsible for isozyme conversion, that the same sequence was found in different clone (Ishino et al., 1987). It was in 2005 when Mojica et al (2005) discovered that these repeated sequences, known as spacers, were found in a number of prokaryotic species (Mojica et al., 2005). Mojica was also one of the first to hypothesis this phenomenon was part of the bacterial immune system (Gostimskaya, 2022). Though it was in 2020 that Charpentier and Doudna were awarded the Nobel prize for this gene editing technology.

This technology utilises the ability of the bacteria to recognize and store small pieces of DNA from each infection. This results in future infections with the same pathogen being removed and destroyed. In the laboratory a guide RNA is generated using a PAM site and a 20bp nucleotide. A PAM (protospacer adjacent motif), is 2-5bp adjacent to the target sequence, this allows the cas9 to determine between self and non self (Gleditzsch et al., 2019). Cas9 detects this downstream of the sequence to know to bind and cut. Thus, forming double strand breaks at the PAM sites removing the sequence (Doudna and Charpentier, 2014).

This more selective method of JNK knockout would allow for the investigations of the individual isoforms of JNK. As it is known, JNK 1 and 2 specifically have different roles. Therefore, using online tools gRNA was generated and was ensured to be specific to human JNK genes. As HUVECs are a primary cell line it was decided that they would be unsuitable, as they are limited to 6 passages. Therefore the EA.hy926 cells were chosen as they are an endothelial cell hybrid that would enable more passages before transformation.

It was reported in this study that the sequences were specific to Human JNK and that also the sequences were successfully inserted into the cas9 plasmid.

It has been observed that when attempting to knockout JNK1, there was a large impact on the expression of JNK2. It was also noted that the protein levels for this cell line were significantly reduced. This lack of protein may be causing the reduced expression visualised by the western blot rather than the success of the plasmid and transfection. Therefore, it was decided not to continue the investigation as this could not be confirmed in the time scale. As this study has shown, further work is needed to invest in the generation of a successful CRISPR cell line. Due to time restraints this investigation was unable to establish successful knockout models. With more time and attention on transfection methods this could become successful.

When looking into the use of CRISPR knockout of JNK there are a number of publications. However, these publications have knocked out other proteins that are either upstream or downstream of JNK. An example of this is where Zhou et al (2022) used CRISPR to knockout MiRNA-363-3p in DLBCL cells, indirectly knocking out JNK activity (Zhou et al., 2022). The micro-RNA MiRNA-363-3p has been linked with resistance to chemotherapy in Diffuse large B-cell lymphoma. The miRNA-363-3p mechanism of resistance has been shown to be via DUSP10 and JNK. Zhou et al (2022) were therefore able to inhibit JNK activation and through the knockout of miRNA-363-3p (Zhou et al., 2022). Whereas Zeissig et al (2024) knocked out the chemokine receptor CCR1 in human myeloma cell line OPM2 (Zeissig et al., 2024). By inhibiting CCR1, this negatively regulated IRE1 expression which is upstream of JNK therefore resulting in the inhibition of JNK activation (Zeissig et al., 2024). This indicates how complex JNK knockouts are and explains why there has not yet been a successful JNK knockout in cells via CRISPR.

In conclusion, this chapter shows that both Cisplatin and Doxorubicin induce endothelial cell death, which can be identified as pyroptosis. The genes involved in pyroptosis have also been reported to be induced with both compounds.

Previous studies have shown that Adv.NLS-1 MKP-2 reduces JNK activity, pyroptotic genes and ultimately reduces cytotoxicity, suggesting a potentially protective mechanism that could alleviate anti-cancer treatment induced endothelial cell damage. However, the findings of this thesis refute this. Adv.NLS-1 MKP-2 did not reduce endothelial cell dysfunction, suggesting that further understanding of this toxic mechanism is required. It can also be determined as there was no reduction in the pyroptosis markers that SP600125 was not selective enough to inhibit pyroptosis which was seen with Adv.NLS-1 MKP-2. By further understanding the role of JNK with the use of CRISPR cas9 and the different isoforms a potential novel target could be utilised to protect from chemotherapeutic damage.

# Chapter Five

## General Discussion

# 5. General Discussion

## 5.1. General Discussion

For several years there has been great interest in the cardiotoxic side effects of cancer treatments and the need to protect against this side effect. This side effect impacts 20% of cancer survivors and has been known to develop up to 20 years post treatment (Clark et al., 2016, Mulrooney et al., 2009). Therefore, treatment options and preventative measures are vital to prevent such life altering damage. The aim of this study was to investigate the mechanism behind damage to endothelial cells through the JNK pathway. Therefore, it was hypothesised that radiation and chemotherapeutic agents would result in JNK activation.

As discussed previously cardiovascular toxicities have been shown to start with damage to the endothelium. Cancer treatments such as chemotherapy and radiation have been shown in other studies to induce endothelial dysfunction (Clayton et al., 2020b). Therefore, the emphasis of this study was to understand the damage such treatments cause to endothelial cells by using the primary cell line HUVEC.

Initially the focus was to characterize the effect of Doxorubicin, Cisplatin, Sunitinib and x irradiation on HUVECs and the JNK signalling pathway. It was shown in chapter 3 that Sunitinib and x-irradiation induced significant cell death in HUVECs. However, JNK signalling pathway was not activated at any time point or concentration tested. There is very little literature on JNK and x-irradiation, however, other studies have also shown Sunitinib does not activate the JNK pathway. Mahalingam et al. (2019) have shown that sunitinib does not activate the JNK pathway in colorectal cancer cell lines. They used 5µM for 24 hours which correlates with the concentration curve carried out in chapter 3. However, it is shown to activate JNK when in combination with another agent, tumour necrosis factor-related apoptosis-inducing ligand (Mahalingam et al., 2019).

Further indicating that Sunitinib used in combination may utilise the JNK pathway. Whereas Fenton et al. (2010) discuss that Sunitinib inhibits the JNK pathway when looking at thyroid cancer (Fenton et al., 2010). They show that the mechanism sunitinib uses to inhibit cell proliferation may be by blocking SAPK/JNK and MEK/ERK (Fenton et al., 2010). Therefore, this could be an aspect of JNK activation that should be explored, to understand if the lack of activity is because the treatments do not activate the JNK pathway or if the pathway is inhibited to enhance further mechanisms. The lack of JNK activity as a result of both Sunitinib and x-irradiation has been documented in the literature, and in multiple cell lines indicating that the mechanism of endothelial damage for these treatments may omit the pathway. Therefore, the focus remained on Doxorubicin and Cisplatin, where a delayed and sustained activation of JNK was shown. It was found that stimulating HUVECs with both Doxorubicin and Cisplatin resulted in JNK pathway activation. Ramer et al. (2018) found that low concentration of Cisplatin (0.01 and 1µM) did not elicit an effect on endothelial cells, which correlates with the findings of this study. However they used cultured media from treated cancer cells, which could be an area to be further explored. They show that the toxicities of Cisplatin on the endothelium maybe due to the cancer release of tissue inhibitor of matrix metalloproteinases-1 rather than the drug itself (Ramer et al., 2018). This is an area which should be further explored in relation to all treatment options explored in this study.

Lu et al. (2007) have shown that this delayed, sustained activation is a well characterised sign of apoptosis and cell death (Lu et al., 2007). Which has shown to be very different from growth factor activation of the pathway, which is shown to be much earlier and transient, for example TNFα (Wullaert et al., 2006). As has been shown in chapter 3 with TNFα activating JNK at 15 minutes until 60 minutes compared to Doxorubicin and Cisplatin activating JNK after 8 hours for over 24hours. This has also been shown in a number of studies and cell lines such as ovarian cancer, fibroblasts and cardiomyocytes (Helbig et al., 2011, Al-Mutairi and Habashy, 2022, Chang et al., 2011, Mansouri et al., 2003, Ramer et al., 2018).

The sustained activation has recently been shown as a result of JNK-mitochondrial SH3-domain binding protein5 (SH3BP5/SAB)-ROS activation loop (Win et al., 2018). This was discovered when investigating liver disease. It was first identified that a mitochondrial outer membrane protein (SH3BP5) was a target for pJNK binding (Wiltshire et al., 2002). This phenomenon has been further explored by a number of groups but was confirmed by Win et al. (2016). Using knock down models, they have shown that the binding and phosphorylation of Sab by JNK on the outer mitochondrial membrane results in SHP1 and DOK4 dependent inactivation of p-Src on the inner membrane. Inactivation of Src on the inner membrane inhibits electron transport, increasing ROS and sustaining JNK activation (Win et al., 2016). Although investigated in liver injury, this phenomenon could aid the implication and treatment of cardiovascular toxicities.

Alongside JNK, other pathways were also investigated to further understand the mechanism of endothelial cell dysfunction. The NFκB signalling pathway was investigated as it is known to play a role in cell survival and inflammation (Hoesel and Schmid, 2013). It was hypothesised that there would be link between the activation of the JNK pathway and the NFκB signalling pathway. However, it was found that there was no link between JNK and NFκB, as Doxorubicin and Cisplatin did not activate the NFκB pathway. NFκB has been shown to suppress JNK activation in previous studies confirming the findings of this study (Papa et al., 2006). Where this study has shown that there is no effect on either p65 or IκBα in HUVECs to show this is independent of the canonical pathway. However, Wang et al. (2002) found that NFκB is pro-apoptotic in both endothelial cells and cardiomyocytes, where they suggest this is due to $H_2O_2$. As the removal of $H_2O_2$ protected the cells from damage (Wang et al., 2002). Wang et al. (2002) however did not carry out western blot analysis, mainly DNA-binding activity assays. As western blots detect protein and DNA-binding assays measure transcription factors interaction with DNA, this difference in detection maybe result in the different findings.

ATM was investigated to understand the mechanism from DNA damage through to JNK activation. In the preliminary data this study has shown the Doxorubicin elicits ATM activation at 15minutes of exposure in HUVECs. This indicates that ATM would be one of the effector genes in the pathway of cell damage. ATM and JNK have been shown to be interlinked in other studies (Wang et al., 2009, Liu et al., 2024, Mavrogonatou et al., 2022, Wang et al., 2021). Where Wang et al. (2009) results suggest that ATM influences autophagy in lung cancer cells through JNK (Wang et al., 2021, Wang et al., 2009). Whilst Liu et al. (2024) found that ATM inhibits TNF-α by inactivating JNK in breast cancer cells, and that ATM negatively regulates PD-L1 by downregulating JNK which could be utilised to enhance cancer treatments (Liu et al., 2024). These results suggest that ATM may regulate the JNK pathway, and this link should be investigated further particularly in relation to cardiovascular toxicities. Due to time constraints, it was not possible to optimise the antibody and allow for a full investigation. As the antibody was found to be difficult to blot for due to its size (350kDa).

As chapter 3 has highlighted, JNK activation due to Doxorubicin and Cisplatin induced a delayed and sustained activation of the pathway, which has been heavily linked to cell death. Therefore, MTT and FACS were used to further investigate cell death for these compounds. MTT assays give a preliminary insight into the viability of the cells and were used to confirm cell death prior to FACS. FACS has shown that both Doxorubicin and Cisplatin elicit substantial damage to cell viability. It has been shown that this correlates with a significant increase in apoptosis and necrosis in HUVECs treated with these chemotherapeutic agents, which was hypothesized to be linked to the sustained activation of JNK. It was then decided to further investigate the mechanism of cell death, with the aim to find novel targets for future treatments. Such mechanism included pyroptosis a newly identified for of programmed cell death.

As discussed in chapter 4 pyroptosis is a relatively new form of cell death implicated with immune response (He et al., 2021). Pyroptosis has also been shown to be promoted by atherosclerosis related factors such as ROS, mitochondrial dysfunction and post translational modifications to name but a few (He et al., 2021). Therefore, as well as FACS, which explores both apoptosis and necrosis, further investigation was used to examine pyroptosis levels. As part of this, LDH levels and caspase-3 and GSDME were investigated.

As shown in chapter 4, protein levels of caspase-3 and GSDME levels were slightly reduced with Adv.NLS-1 MKP-2, indicating that this pathway may be linked with JNK. Other studies have also shown that JNK is implicated in this pyroptosis pathway (Bradfield et al., 2023). Bradfield et al. (2023) for example showed that biphasic activation of JNK resulted in the generation of mitochondrial ROS. This was found to support inflammasome formation and GSDMD activation resulting in pyroptosis in mice models and a human lymphoma cell line (Bradfield et al., 2023). In this study, by inhibiting JNK with MKP-2, it was shown that levels of LDH, linked to pyroptosis, were reduced. This reduction also correlated with decreased levels of caspase-3 and GSDME indicating that this mechanism of action could be involved in the endothelial cell damage. Another study has shown that Doxorubicin induced pyroptosis in breast cancer cells via GSDME (Zhang et al., 2021). Zhang et al. (2021) also determined that Doxorubicin induced pyroptosis may be as a result of caspase-3 dependent reaction through the JNK signalling pathway (Zhang et al., 2021). They conclude that Doxorubicin induced cardiovascular toxicities and pyroptosis can be minimised by reducing GSDME levels. However, for this study, further investigation is required to fully explore this target. As cell viability was not increased with the reversal of pyroptosis in the HUVECs.

## 5.2. Limitations

The main limitation to this study is the low N numbers, particularly in chapter 4. This limits the ability to determine if the findings are significant. By increasing the n numbers in the investigation and determining the significance would give weight to the findings. Another large limitation of this study was the inability to fully investigate the different isoforms of JNK. It is well documented that JNK1 and JNK2 have shared and different roles within the cell. Although not well characterized, JNK1 has been shown to be vital for c-Jun activation (Liu et al., 2004). Liu et al. (2004) demonstrated in JNK1 null and JNK2 null mice that c-Jun activation was diminished in JNK1null mice and increased in JNK2 null mice models. This was also confirmed by the findings of Sabapathy et al, where they have also shown that JNK1 is required for c-Jun activation in mouse fibroblasts (Sabapathy et al., 2004). Sabapathy et al. (2004) have also shown that c-Jun is bound to JNK2 in unstimulated cells, where it appears JNK2 is responsible for c-Jun degradation. As there are differing mechanisms for the different isoforms, it is vital to further validate this study in a cell model that has specific JNK knockout. A further study investigating the knockout of the individual isoforms would also be invaluable. Unfortunately, due to time constraints, convincing JNK CRISPR models were not achieved.

Therefore, it would be important in future studies to generate specific JNK knockout models to fully understand the role it plays in cellular damage, as the models utilised in this study are known to have off target effects, and effect more than one protein. The accurate knockout of individual isoforms would also allow further investigation into the mechanism and allow for development of novel treatments.

## 5.3. Future Work

As mentioned, this study was unable to activate JNK via x-irradiation. A potential explanation could be that x-irradiation caused an increase in caspase 3 in the cytoplasm (Feng et al., 2005). It was found by Vaishnav et al. (2011) that an increase in caspase 3 could prevent the binding of the scaffold protein JIP1 therefore preventing the activation of JNK (Vaishnav et al., 2011). Therefore, in future studies the link between JIP1 levels and caspase 3 would be investigated. This mechanism could help further understand JNK mechanisms which could be used for novel targets or radiosensitisers.

Alongside FACS cell death analysis, cell cycle investigations should be carried out. This would give further insight into not only the effect the compounds have on HUVECs but also the inhibitors used. This could allow more investigation into how MKP-2 inhibition reduces pyroptosis, which could determine the direction of future experiments.

Further in-depth investigation into the pyroptosis markers would also give a broader indication to the pathway mechanism. By investigating when caspase 3 and GSDME activation begins and ends in relation to JNK activation. Also, the optimisation of the ATM antibody would also allow the possible link between the DNA damage marker and JNK activation to be thoroughly investigated. As all these markers have been linked to JNK in the literature, it would improve the understanding of the pathway's mechanics in HUVECs to fully understand their role following cancer treatment. Combination treatments would also be an important aspect to analyse. As it is having been discussed cancer treatments often overlap and radiotherapy and chemotherapy can be given in combination. Future studies should investigate whether the combination of chemotherapy and even the combination of chemotherapy and radiation treatment could result in the activation of JNK. As studies have shown that sunitinib alone does not activate JNK but when combined with another agent greatly increases JNK activity (Mahalingam et al., 2019).

## 5.4. Conclusion

In conclusion, after analysing a number of different cancer treatments renowned for cardiovascular toxicities, only Doxorubicin and Cisplatin induce JNK activation. It has been shown that although irradiation and Sunitinib treatment of HUVECs did not activate the JNK signalling pathway, they did induce significant cell death. It was determined that both Doxorubicin and Cisplatin induced both a delayed and sustained activation of the pathway indicative of cell death.

It was investigated using multiple tools the impact silencing JNK would have on HUVEC cell viability. It was determined inhibiting JNK with the pharmacological tool SP600125 did not protect cells from cell death and other downstream effect of JNK activation such as GSDME, caspase 3 and γH2.AX were not changed. The use of the MKP-2 virus showed an effective JNK inhibitor, of which proteins such as GSDME, caspase 3 and γH2.AX were all reduced, indicating a reduction in Pyroptosis characteristics, however this did not protect cell viability. Therefore, further investigation into the pyroptosis JNK pathway is required.

This study confirms what has already been demonstrated that Doxorubicin and Cisplatin cause damage to endothelial cells. Although this study was unable to investigate the effect of the individual isoforms of JNK and their role in cell death. It has shown that there are major limitations in the available JNK inhibitors. This investigation was unable to identify JNK as a target for cardiovascular toxicities. However, it is still important to investigate the molecular effect these cancer treatments are having on the endothelium.

# Chapter Six

## References

# 6. References


ABDUL-RAHMAN, T., DUNHAM, A., HUANG, H., BUKHARI, S. M. A., MEHTA, A., AWUAH, W. A., EDE-IMAFIDON, D., CANTU-HERRERA, E., TALUKDER, S., JOSHI, A., SUNDLOF, D. W. & GUPTA, R. 2023. Chemotherapy Induced Cardiotoxicity: A State of the Art Review on General Mechanisms, Prevention, Treatment and Recent Advances in Novel Therapeutics. *Current Problems in Cardiology,* 48**,** 101591.

ABE, J.-I. & MORRELL, C. 2016. Pyroptosis as a Regulated Form of Necrosis. *Circulation Research,* 118**,** 1457-1460.

ADAMS, M., HARDENBERGH, P., CONSTINE, L. & LIPSHULTZ, S. 2003. Radiation-associated cardiovascular disease. *Critical Reviews in Oncology Hematology,* 45**,** 55-75.

AGGARWAL, S. K. 1998. Calcium Modulation of Toxicities Due to Cisplatin. *Metal-Based Drugs,* 5**,** 77-81.

AHMAD, A., ORMISTON-SMITH, N. & SASIENI, P. 2015. Trends in the lifetime risk of developing cancer in Great Britain: comparison of risk for those born from 1930 to 1960. *British Journal of Cancer,* 112**,** 943-947.

AHMED, K. M. & LI, J. J. 2007. ATM-NF-kappaB connection as a target for tumor radiosensitization. *Current cancer drug targets,* 7**,** 335-342.

AKI, T., FUNAKOSHI, T., UNUMA, K. & UEMURA, K. 2022. Inverse regulation of GSDMD and GSDME gene expression during LPS-induced pyroptosis in RAW264.7 macrophage cells. *Apoptosis,* 27**,** 14-21.

AL-MAJED, A., SAYED-AHMED, M., AL-YAHYA, A., ALEISA, A., AL-REJAIE, S. & AL-SHABANAH, O. 2006. Propionyl-L-carnitine prevents the progression of cisplatin-induced cardiomyopathy in a carnitine-depleted rat model. *Pharmacological Research,* 53**,** 278-286.

AL-MUTAIRI, M., AL-HARTHI, S., CADALBERT, L. & PLEVIN, R. 2010. Over-expression of mitogen-activated protein kinase phosphatase-2 enhances adhesion

molecule expression and protects against apoptosis in human endothelial cells. *British Journal of Pharmacology,* 161**,** 782-798.

AL-MUTAIRI, M. S. & HABASHY, H. O. 2022. DUSP4 Silencing Enhances the Sensitivity of Breast Cancer Cells to Doxorubicin through the Activation of the JNK/c-Jun Signalling Pathway. *Molecules,* 27.

ALEMAN, B. M. P., VAN DEN BELT-DUSEBOUT, A. W., DE BRUIN, M. L., VAN 'T VEER, M. B., BAAIJENS, M. H. A., BOER, J. P. D., HART, A. A. M., KLOKMAN, W. J., KUENEN, M. A., OUWENS, G. M., BARTELINK, H. & VAN LEEUWEN, F. E. 2007. Late cardiotoxicity after treatment for Hodgkin lymphoma. *Blood,* 109**,** 1878-1886.

ALTENA, R., HUMMEL, Y. M., NUVER, J., SMIT, A. J., LEFRANDT, J. D., DE BOER, R. A., VOORS, A. A., VAN DEN BERG, M. P., DE VRIES, E. G., BOEZEN, H. M. & GIETEMA, J. A. 2011. Longitudinal changes in cardiac function after cisplatin-based chemotherapy for testicular cancer. *Ann Oncol,* 22**,** 2286-93.

AMBROSIO, G. & TRITTO, I. 1999. Reperfusion injury: Experimental evidence and clinical implications. *American Heart Journal,* 138**,** S69-S75.

AMINI, N., BOYLE, J. J., MOERS, B., WARBOYS, C. M., MALIK, T. H., ZAKKAR, M., FRANCIS, S. E., MASON, J. C., HASKARD, D. O. & EVANS, P. C. 2014. Requirement of JNK1 for endothelial cell injury in atherogenesis. *Atherosclerosis,* 235**,** 613-8.

AN, D., HAO, F., HU, C., KONG, W., XU, X. & CUI, M.-Z. 2018. JNK1 mediates lipopolysaccharide-induced CD14 and SR-AI expression and macrophage foam cell formation. *FRONT PHYSIOL,* 8**,** 1075-1075.

ANAND, U., DEY, A., SINGH CHANDEL, A. K., SANYAL, R., MISHRA, A., PANDEY, D. K., DE FALCO, V., UPADHYAY, A., KANDIMALLA, R., CHAUDHARY, A., DHANJAL, J. K., DEWANJEE, S., VALLAMKONDU, J. & PÉREZ DE LA LASTRA, J. M. 2024. Corrigendum to 'Cancer chemotherapy and beyond: Current status, drug candidates, associated risks and progress in targeted therapeutics' [Genes & Diseases 10 (2023) 1367-1401]. *Genes Dis,* 11**,** 101211.

ANTLSPERGER, D. S. M., DIRSCH, V. M., FERREIRA, D., SU, J.-L., KUO, M.-L. & VOLLMAR, A. M. 2003. Ajoene-induced cell death in human promyeloleukemic cells does not require JNK but is amplified by the inhibition of ERK. *Oncogene,* 22**,** 582-589.

BABAEV, V. R., YEUNG, M., ERBAY, E., DING, L., ZHANG, Y., MAY, J. M., FAZIO, S., HOTAMISLIGIL, G. S. & LINTON, M. F. 2016. Jnk1 Deficiency in Hematopoietic Cells Suppresses Macrophage Apoptosis and Increases Atherosclerosis in Low-Density Lipoprotein Receptor Null Mice. *Arteriosclerosis, Thrombosis, and Vascular Biology,* 36**,** 1122-1131.

BAIN, J., MCLAUCHLAN, H., ELLIOTT, M. & COHEN, P. 2003. The specificities of protein kinase inhibitors: an update. *Biochemical Journal,* 371**,** 199-204.

BAKKENIST, C. J. & KASTAN, M. B. 2003. DNA damage activates ATM through intermolecular autophosphorylation and dimer dissociation. *Nature,* 421**,** 499-506.

BANIN, S., MOYAL, L., SHIEH, S.-Y., TAYA, Y., ANDERSON, C. W., CHESSA, L., SMORODINSKY, N. I., PRIVES, C., REISS, Y., SHILOH, Y. & ZIV, Y. 1998. Enhanced Phosphorylation of p53 by ATM in Response to DNA Damage. *Science,* 281**,** 1674-1677.

BANTSCHEFF, M., EBERHARD, D., ABRAHAM, Y., BASTUCK, S., BOESCHE, M., HOBSON, S., MATHIESON, T., PERRIN, J., RAIDA, M., RAU, C., READER, V., SWEETMAN, G., BAUER, A., BOUWMEESTER, T., HOPF, C., KRUSE, U., NEUBAUER, G., RAMSDEN, N., RICK, J., KUSTER, B. & DREWES, G. 2007. Quantitative chemical proteomics reveals mechanisms of action of clinical ABL kinase inhibitors. *Nature Biotechnology,* 25**,** 1035-1044.

BAR-JOSEPH, H., BEN-AHARON, I., TZABARI, M., TSARFATY, G., STEMMER, S. M. & SHALGI, R. 2011. In vivo Bioimaging as a Novel Strategy to Detect Doxorubicin-Induced Damage to Gonadal Blood Vessels. *PLoS ONE,* 6**,** e23492.

BAYAT MOKHTARI, R., HOMAYOUNI, T. S., BALUCH, N., MORGATSKAYA, E., KUMAR, S., DAS, B. & YEGER, H. 2017. Combination therapy in combating cancer. *Oncotarget,* 8**,** 38022-38043.

BAZARBASHI, S., ALZAHRANI, A., ALJUBRAN, A., ELSHENAWY, M., GAD, A. M., MARAIKI, F., ALZANNAN, N., ELHASSAN, T. & BADRAN, A. 2023. Combining Sunitinib and Bevacizumab for the Management of Advanced Renal Cell Carcinoma: A Phase I/II Trial. *The Oncologist,* 28**,** e254-e262.

BENNETT, B., SASAKI, D., MURRAY, B., O'LEARY, E., SAKATA, S., XU, W., LEISTEN, J., MOTIWALA, A., PIERCE, S., SATOH, Y., BHAGWAT, S., MANNING, A. & ANDERSON, D. 2001. SP600125, an anthrapyrazolone inhibitor of Jun N-terminal kinase. *Proceedings of the National Academy of Sciences of the United States of America,* 98**,** 13681-13686.

BIAN, X., MCALLISTER-LUCAS, L. M., SHAO, F., SCHUMACHER, K. R., FENG, Z., PORTER, A. G., CASTLE, V. P. & OPIPARI, A. W. 2001. NF-κB Activation Mediates Doxorubicin-induced Cell Death in N-type Neuroblastoma Cells. *Journal of Biological Chemistry,* 276**,** 48921-48929.

BOGOYEVITCH, M. A. & ARTHUR, P. G. 2008. Inhibitors of c-Jun N-terminal kinases: JuNK no more? *Biochim Biophys Acta,* 1784**,** 76-93.

BOICE, A. & BOUCHIER-HAYES, L. 2020. Targeting apoptotic caspases in cancer. *Biochim Biophys Acta Mol Cell Res,* 1867**,** 118688-118688.

BORREGO-SOTO, G., ORTIZ-LÓPEZ, R. & ROJAS-MARTÍNEZ, A. 2015. Ionizing radiation-induced DNA injury and damage detection in patients with breast cancer. *Genetics and Molecular Biology,* 38**,** 420-432.

BOUEIZ, A. & HASSOUN, P. M. 2009. Regulation of endothelial barrier function by reactive oxygen and nitrogen species. 77**,** 26-34.

BOYD, M., ROSS, S., DORRENS, J., FULLERTON, N., TAN, K., ZALUTSKY, M. & MAIRS, R. 2006. Radiation-induced biologic bystander effect elicited in vitro by targeted radiopharmaceuticals labeled with alpha-, beta-, and Auger electron-emitting radionuclides. *Journal of Nuclear Medicine,* 47**,** 1007-1015.

BRADFIELD, C. J., LIANG, J. J., ERNST, O., JOHN, S. P., SUN, J., GANESAN, S., DE JESUS, A. A., BRYANT, C. E., GOLDBACH-MANSKY, R. & FRASER, I. D. C. 2023. Biphasic JNK signaling reveals distinct MAP3K complexes licensing inflammasome formation and pyroptosis. *Cell Death & Differentiation,* 30**,** 589-604.

BRADLEY, J. A. & MENDENHALL, N. P. 2018. Novel Radiotherapy Techniques for Breast Cancer. *Annual Review of Medicine,* 69**,** 277-288.

BRAND, K., PAGE, S., ROGLER, G., BARTSCH, A., BRANDL, R., KNUECHEL, R., PAGE, M., KALTSCHMIDT, C., BAEUERLE, P. A. & NEUMEIER, D. 1996. Activated transcription factor nuclear factor-kappa B is present in the atherosclerotic lesion. *J Clin Invest,* 97**,** 1715-22.

BRANTLEY-FINLEY, C., LYLE, C. S., DU, L., GOODWIN, M. E., HALL, T., SZWEDO, D., KAUSHAL, G. P. & CHAMBERS, T. C. 2003. The JNK, ERK and p53 pathways play distinct roles in apoptosis mediated by the antitumor agents vinblastine, doxorubicin, and etoposide. *Biochem Pharmacol,* 66**,** 459-469.

BRAY, F., FERLAY, J., SOERJOMATARAM, I., SIEGEL, R., TORRE, L. & JEMAL, A. 2018. Global cancer statistics 2018: GLOBOCAN estimates of incidence and mortality worldwide for 36 cancers in 185 countries. *Ca-a Cancer Journal For Clinicians,* 68**,** 394-424.

BRETÓN-ROMERO, R., FENG, B., HOLBROOK, M., FARB, M. G., FETTERMAN, J. L., LINDER, E. A., BERK, B. D., MASAKI, N., WEISBROD, R. M., INAGAKI, E., GOKCE, N., FUSTER, J. J., WALSH, K. & HAMBURG, N. M. 2016. Endothelial Dysfunction in Human Diabetes Is Mediated by Wnt5a–JNK Signaling. *Arteriosclerosis, Thrombosis, and Vascular Biology,* 36**,** 561-569.

BROTT, B., PINSKY, B. & ERIKSON, R. 1998. Nlk is a murine protein kinase related to Erk/MAP kinases and localized in the nucleus. *Proceedings of the National Academy of Sciences of the United States of America,* 95**,** 963-968.

BROUNS, S. L. N., PROVENZALE, I., GEFFEN, J. P., MEIJDEN, P. E. J. & HEEMSKERK, J. W. M. 2020. Localized endothelial-based control of platelet aggregation and coagulation under flow: A proof-of-principle vessel-on-a-chip study. *Journal of Thrombosis and Haemostasis,* 18**,** 931-941.

BROZOVIC, A., FRITZ, G., CHRISTMANN, M., ZISOWSKY, J., JAEHDE, U., OSMAK, M. & KAINA, B. 2004. Long-term activation of SAPK/JNK, p38 kinase and fas-L expression by cisplatin is attenuated in human carcinoma cells that acquired drug resistance. *International Journal of Cancer,* 112**,** 974-985.

BRUYNZEEL, A. M. E., ABOU EL HASSAN, M. A., TORUN, E., BAST, A., VAN DER VIJGH, W. J. F. & KRUYT, F. A. E. 2007. Caspase-dependent and -independent suppression of apoptosis by monoHER in Doxorubicin treated cells. *British Journal of Cancer,* 96**,** 450-456.

BUBICI, C. & PAPA, S. 2014. JNK signalling in cancer: in need of new, smarter therapeutic targets. *British Journal of Pharmacology,* 171**,** 24-37.

BUBICI, C., PAPA, S., PHAM, C. G., ZAZZERONI, F. & FRANZOSO, G. 2004. NF-κB and JNK: An Intricate Affair. *Cell Cycle,* 3**,** 1524-1529.

BUONANNO, M., DE TOLEDO, S., PAIN, D. & AZZAM, E. 2011. Long-Term Consequences of Radiation-Induced Bystander Effects Depend on Radiation Quality and Dose and Correlate with Oxidative Stress. *Radiation Research,* 175**,** 405-415.

CADALBERT, L., SLOSS, C. M., CAMERON, P. & PLEVIN, R. 2005. Conditional expression of MAP kinase phosphatase-2 protects against genotoxic stress-induced apoptosis by binding and selective dephosphorylation of nuclear activated c-jun N-terminal kinase. *Cell Signal,* 17**,** 1254-1264.

CADALBERT, L. C., SLOSS, C. M., CUNNINGHAM, M. R., AL-MUTAIRI, M., MCINTIRE, A., SHIPLEY, J. & PLEVIN, R. 2010. Differential regulation of MAP kinase activation by a novel splice variant of human MAP kinase phosphatase-2. *Cell Signal,* 22**,** 357-65.

CAMACHO, C., MACIEL, D., TOMÁS, H. & RODRIGUES, J. 2023. Biological Effects in Cancer Cells of Mono- and Bidentate Conjugation of Cisplatin on PAMAM Dendrimers: A Comparative Study. *Pharmaceutics,* 15**,** 689.

CAMERON, A. C., MCMAHON, K., HALL, M., NEVES, K. B., RIOS, F. J., MONTEZANO, A. C., WELSH, P., WATERSTON, A., WHITE, J., MARK, P. B., TOUYZ, R. M. & LANG,

N. N. 2020. Comprehensive Characterization of the Vascular Effects of Cisplatin-Based Chemotherapy in Patients With Testicular Cancer.

CAPPETTA, D., DE ANGELIS, A., SAPIO, L., PREZIOSO, L., ILLIANO, M., QUAINI, F., ROSSI, F., BERRINO, L., NAVIGLIO, S. & URBANEK, K. 2017. Oxidative Stress and Cellular Response to Doxorubicin: A Common Factor in the Complex Milieu of Anthracycline Cardiotoxicity. *Oxid Med Cell Longev,* 2017**,** 1521020.

CARBONI, S., HIVER, A., SZYNDRALEWIEZ, C., GAILLARD, P., GOTTELAND, J.-P. & VITTE, P.-A. 2004. AS601245 (1,3-Benzothiazol-2-yl (2-{[2-(3-pyridinyl) ethyl] amino}-4 pyrimidinyl) Acetonitrile): A c-Jun NH<sub>2</sub>-Terminal Protein Kinase Inhibitor with Neuroprotective Properties. *Journal of Pharmacology and Experimental Therapeutics,* 310**,** 25-32.

CARDINALE, D., COLOMBO, A., LAMANTIA, G., COLOMBO, N., CIVELLI, M., DE GIACOMI, G., RUBINO, M., VEGLIA, F., FIORENTINI, C. & CIPOLLA, C. M. 2010. Anthracycline-induced cardiomyopathy: clinical relevance and response to pharmacologic therapy. *J Am Coll Cardiol,* 55**,** 213-20.

CARGNELLO, M. & ROUX, P. P. 2011. Activation and Function of the MAPKs and Their Substrates, the MAPK-Activated Protein Kinases. *Microbiology and Molecular Biology Reviews,* 75**,** 50-83.

CARGNELLO, M. & ROUX, P. P. 2012. Activation and Function of the MAPKs and Their Substrates, the MAPK-Activated Protein Kinases. *Microbiology and molecular biology reviews,* 76**,** 496-496.

CARON, J. & NOHRIA, A. 2018. Cardiac Toxicity from Breast Cancer Treatment: Can We Avoid This? *Current Oncology Reports,* 20**,** 8.

CASTANEDA, S. A. & STRASSER, J. 2017. Updates in the Treatment of Breast Cancer with Radiotherapy. *Surgical Oncology Clinics of North America,* 26**,** 371-+.

CELERMAJER, D. S., SORENSEN, K. E., GOOCH, V. M., SPIEGELHALTER, D. J., MILLER, O. I., SULLIVAN, I. D., LLOYD, J. K. & DEANFIELD, J. E. 1992. Non-invasive detection of endothelial dysfunction in children and adults at risk of atherosclerosis. *Lancet,* 340**,** 1111-1115.

CELLURALE, C., GIRNIUS, N., JIANG, F., CAVANAGH-KYROS, J., LU, S., GARLICK, D. S., MERCURIO, A. M. & DAVIS, R. J. 2012. Role of JNK in Mammary Gland Development and Breast Cancer. *Cancer Research,* 72**,** 472-481.

CELLURALE, C., SABIO, G., KENNEDY, N. J., DAS, M., BARLOW, M., SANDY, P., JACKS, T. & DAVIS, R. J. 2011. Requirement of c-Jun NH2-Terminal Kinase for Ras-Initiated Tumor Formation. *Molecular and Cellular Biology,* 31**,** 1565-1576.

CHADEE, D. N., YUASA, T. & KYRIAKIS, J. M. 2002. Direct Activation of Mitogen-Activated Protein Kinase Kinase Kinase MEKK1 by the Ste20p Homologue GCK and the Adapter Protein TRAF2. 22**,** 737-749.

CHAN, R., WEBSTER, J., CHUNG, B., MARQUART, L., AHMED, M. & GARANTZIOTIS, S. 2014. Prevention and treatment of acute radiation-induced skin reactions: a systematic review and meta-analysis of randomized controlled trials. 14**,** 53.

CHANG, W.-T., LI, J., HAUNG, H.-H., LIU, H., HAN, M., RAMACHANDRAN, S., LI, C.-Q., SHARP, W. W., HAMANN, K. J., YUAN, C.-S., VANDEN HOEK, T. L. & SHAO, Z.-H. 2011. Baicalein protects against doxorubicin-induced cardiotoxicity by attenuation of mitochondrial oxidant injury and JNK activation. *Journal of Cellular Biochemistry,* 112**,** 2873-2881.

CHATTERJEE, K., ZHANG, J., HONBO, N. & KARLINER, J. 2010. Doxorubicin Cardiomyopathy. *Cardiology,* 115**,** 155-162.

CHATTERJEE, T. K., STOLL, L. L., DENNING, G. M., HARRELSON, A., BLOMKALNS, A. L., IDELMAN, G., ROTHENBERG, F. G., NELTNER, B., ROMIG-MARTIN, S. A., DICKSON, E. W., RUDICH, S. & WEINTRAUB, N. L. 2009. Proinflammatory Phenotype of Perivascular Adipocytes. *Circulation Research,* 104**,** 541-549.

CHATZIATHANASIADOU, M., STYLOS, E., GIANNOPOULOU, E., SPYRIDAKI, M., BRIASOULIS, E., KALOFONOS, H., CROOK, T., SYED, N., SIVOLAPENKO, G. & TZAKOS, A. 2019. Development of a validated LC-MS/MS method for the in vitro and in vivo quantitation of sunitinib in glioblastoma cells and cancer patients. *Journal of Pharmaceutical and Biomedical Analysis,* 164**,** 690-697.

CHEN, B., ZHANG, P., SUNA, F., A, B. L., CHENA, Y., PEIA, S., ZHANGA, Z., MANZOORA, R., DENGA, Y., SUNA, C., SUIB, L., KONGB, F. & MAA, H. 2018. The mechanism

of bystander effect induced by different irradiation in human neuroblastoma cells. *Acta Astronautica*.

CHEN, C., CHENG, Y., LEI, H., FENG, X., ZHANG, H., QI, L., WAN, J., XU, H., ZHAO, X., ZHANG, Y. & YANG, B. 2023. SHP2 potentiates anti-PD-1 effectiveness through intervening cell pyroptosis resistance in triple-negative breast cancer. *Biomedicine & Pharmacotherapy,* 168**,** 115797.

CHEN, C. H., CHEN, M. C., HSU, Y. H. & CHOU, T. C. 2022. Far-infrared radiation alleviates cisplatin-induced vascular damage and impaired circulation via activation of HIF-1α. *Cancer Science*.

CHEN, P., HUTTER, D., YANG, X., GOROSPE, M., DAVIS, R. J. & LIU, Y. 2001. Discordance between the Binding Affinity of Mitogen-activated Protein Kinase Subfamily Members for MAP Kinase Phosphatase-2 and Their Ability to Activate the Phosphatase Catalytically*. *Journal of Biological Chemistry,* 276**,** 29440-29449.

CHEN, P., O'NEAL, J. F., EBELT, N. D., CANTRELL, M. A., MITRA, S., NASRAZADANI, A., VANDENBROEK, T. L., HEASLEY, L. E. & VAN DEN BERG, C. L. 2010. Jnk2 Effects on Tumor Development, Genetic Instability and Replicative Stress in an Oncogene-Driven Mouse Mammary Tumor Model. 5**,** e10443.

CHOW, E., CHEN, Y., HUDSON, M., FEIJEN, E., KREMER, L., BORDER, W., GREEN, D., MEACHAM, L., MULROONEY, D., NESS, K., OEFFINGER, K., RONCKERS, C., SKLAR, C., STOVALL, M., VAN DER PAL, H., VAN DIJK, I., VAN LEEUWEN, F., WEATHERS, R., ROBISON, L., ARMSTRONG, G. & YASUI, Y. 2018. Prediction of Ischemic Heart Disease and Stroke in Survivors of Childhood Cancer. *Journal of Clinical Oncology,* 36**,** 44-+.

CHU, T. F., RUPNICK, M. A., KERKELA, R., DALLABRIDA, S. M., ZURAKOWSKI, D., NGUYEN, L., WOULFE, K., PRAVDA, E., CASSIOLA, F., DESAI, J., GEORGE, S., HARRIS, D. M., ISMAIL, N. S., CHEN, J.-H., SCHOEN, F. J., VAN DEN ABBEELE, A. D., DEMETRI, G. D., FORCE, T., CHEN, M. H. & MORGAN, J. A. 2007. Cardiotoxicity associated with tyrosine kinase inhibitor sunitinib. *The Lancet,* 370**,** 2011-2019.

CHUANG, S.-E., YEH, P.-Y., LU, Y.-S., LAI, G.-M., LIAO, C.-M., GAO, M. & CHENG, A.-L. 2002. Basal levels and patterns of anticancer drug-induced activation of nuclear factor-κB (NF-κB), and its attenuation by tamoxifen, dexamethasone, and curcumin in carcinoma cells. *Biochemical Pharmacology,* 63**,** 1709-1716.

CLARK, R. A., BERRY, N. M., CHOWDHURY, M. H., MCCARTHY, A. L., ULLAH, S., VERSACE, V. L., ATHERTON, J. J., KOCZWARA, B. & RODER, D. 2016. Heart failure following cancer treatment: characteristics, survival and mortality of a linked health data analysis. *Internal Medicine Journal,* 46**,** 1297-1306.

CLARK, R. A., MARIN, T. S., MCCARTHY, A. L., BRADLEY, J., GROVER, S., PETERS, R., KARAPETIS, C. S., ATHERTON, J. J. & KOCZWARA, B. 2019. Cardiotoxicity after cancer treatment: a process map of the patient treatment journey. *Cardio-Oncology,* 5.

CLAYTON, Z. S., BRUNT, V. E., HUTTON, D. A., VANDONGEN, N. S., D'ALESSANDRO, A., REISZ, J. A., ZIEMBA, B. P. & SEALS, D. R. 2020a. Doxorubicin-Induced Oxidative Stress and Endothelial Dysfunction in Conduit Arteries Is Prevented by Mitochondrial-Specific Antioxidant Treatment. *JACC CardioOncol,* 2**,** 475-488.

CLAYTON, Z. S., BRUNT, V. E., HUTTON, D. A., VANDONGEN, N. S., D'ALESSANDRO, A., REISZ, J. A., ZIEMBA, B. P. & SEALS, D. R. 2020b. Doxorubicin-Induced Oxidative Stress and Endothelial Dysfunction in Conduit Arteries Is Prevented by Mitochondrial-Specific Antioxidant Treatment. *JACC CardioOncology.,* 2**,** 475-488.

CLERK, A. 1998. Stimulation of "Stress-regulated" Mitogen-activated Protein Kinases (Stress-activated Protein Kinases/c-Jun N-terminal Kinases and p38-Mitogen-activated Protein Kinases) in Perfused Rat Hearts by Oxidative and Other Stresses. 273**,** 7228-7234.

COOK, S. A., SUGDEN, P. H. & CLERK, A. 1999. Activation of c-Jun N-Terminal Kinases and p38-Mitogen-activated Protein Kinases in Human Heart Failure Secondary to Ischaemic Heart Disease. 31**,** 1429-1434.

COOPER, S., SANDHU, H., HUSSAIN, A., MEE, C. & MADDOCK, H. 2018. Involvement of mitogen activated kinase kinase 7 intracellular signalling pathway in Sunitinib-induced cardiotoxicity. *Toxicology,* 394**,** 72-83.

CORNELL, T. T., FLESZAR, A., MCHUGH, W., BLATT, N. B., LEVINE, A. M. & SHANLEY, T. P. 2012. Mitogen-activated protein kinase phosphatase 2, MKP-2, regulates early inflammation in acute lung injury. *Am J Physiol Lung Cell Mol Physiol,* 303**,** 251-258.

CORREMANS, R., ADÃO, R., DE KEULENAER, G. W., LEITE-MOREIRA, A. F. & BRÁS-SILVA, C. 2019. Update on pathophysiology and preventive strategies of anthracycline-induced cardiotoxicity. *Clin Exp Pharmacol Physiol,* 46**,** 204-215.

CRAIGE, S. M., CHEN, K., BLANTON, R. M., KEANEY, J. F., JR. & KANT, S. 2019. JNK and cardiometabolic dysfunction. *Biosci Rep,* 39.

CUI, J., ZHANG, M., ZHANG, Y. Q. & XU, Z. H. 2007. JNK pathway: diseases and therapeutic potential. *Acta Pharmacol Sin,* 28**,** 601-8.

D'SOUZA, W., CHANG, C., FISCHER, A., LI, M. & HEDRICK, S. 2008. The Erk2 MAPK Regulates CD8 T Cell Proliferation and Survival. *Journal of Immunology,* 181**,** 7617-7629.

DAMROT, J., NUBEL, T., EPE, B., ROOS, W., KAINA, B. & FRITZ, G. 2006. Lovastatin protects human endothelial cells from the genotoxic and cytotoxic effects of the anticancer drugs doxorubicin and etoposide. *British Journal of Pharmacology,* 149**,** 988-997.

DARBY, S., MCGALE, P., PETO, R., GRANATH, F., HALL, P. & EKBOM, A. 2003. Mortality from cardiovascular disease more than 10 years after radiotherapy for breast cancer: nationwide cohort study of 90 000 Swedish women. *British Medical Journal,* 326**,** 256-257.

DASARI, S. & BERNARD TCHOUNWOU, P. 2014. Cisplatin in cancer therapy: Molecular mechanisms of action. *European Journal of Pharmacology,* 740**,** 364-378.

DAVIGNON, J. & GANZ, P. 2004. Role of Endothelial Dysfunction in Atherosclerosis. *Circulation,* 109**,** III-27-III-32.

DE SMAELE, E., ZAZZERONI, F., PAPA, S., NGUYEN, D. U., JIN, R., JONES, J., CONG, R. & FRANZOSO, G. 2001. Induction of gadd45β by NF-κB downregulates pro-apoptotic JNK signalling. *Nature,* 414**,** 308-313.

DEBELA, D. T., MUZAZU, S. G. Y., HERARO, K. D., NDALAMA, M. T., MESELE, B. W., HAILE, D. C., KITUI, S. K. & MANYAZEWAL, T. 2021. New approaches and procedures for cancer treatment: Current perspectives. *SAGE open medicine.,* 9**,** 205031212110343.

DEMIRCI, S., NAM, J., HUBBS, J. L., NGUYEN, T. & MARKS, L. B. 2009. Radiation-induced cardiac toxicity after therapy for breast cancer: interaction between treatment era and follow-up duration. *Int J Radiat Oncol Biol Phys,* 73**,** 980-7.

DEMPKE, W. C. M., ZIELINSKI, R., WINKLER, C., SILBERMAN, S., REUTHER, S. & PRIEBE, W. 2023. Anthracycline-induced cardiotoxicity — are we about to clear this hurdle? *Eur J Cancer,* 185**,** 94-104.

DENG, Y., LI, F., HE, P., YANG, Y., YANG, J., ZHANG, Y., LIU, J., TONG, Y., LI, Q., MEI, X., SHU, Z. & ZHAO, Q. 2018. Triptolide sensitizes breast cancer cells to Doxorubicin through the DNA damage response inhibition. *Molecular Carcinogenesis,* 57**,** 807-814.

DHANASEKARAN, D. N. & REDDY, E. P. 2017. JNK-signaling: A multiplexing hub in programmed cell death. *Genes & Cancer,* 8**,** 682-694.

DIAO, Y., LIU, W., WONG, C. C., WANG, X., LEE, K., CHEUNG, P. Y., PAN, L., XU, T., HAN, J., YATES, J. R., 3RD, ZHANG, M. & WU, Z. 2010. Oxidation-induced intramolecular disulfide bond inactivates mitogen-activated protein kinase kinase 6 by inhibiting ATP binding. *Proc Natl Acad Sci U S A,* 107**,** 20974-9.

DIVGI, C. 2011. Targeted Systemic Radiotherapy of Pheochromocytoma and Medullary Thyroid Cancer. *Seminars in Nuclear Medicine,* 41**,** 369-373.

DOUDNA, J. A. & CHARPENTIER, E. 2014. The new frontier of genome engineering with CRISPR-Cas9. *Science (American Association for the Advancement of Science),* 346**,** 1077-1077.

DRESKIN, S., THOMAS, G., DALE, S. & HEASLEY, L. 2001. Isoforms of jun kinase are differentially expressed and activated in human monocyte/macrophage (THP-1) cells. *Journal of Immunology,* 166**,** 5646-5653.

DROŻDŻ, D., DROŻDŻ, M. & WÓJCIK, M. 2023. Endothelial dysfunction as a factor leading to arterial hypertension. *Pediatric Nephrology,* 38**,** 2973-2985.

DURSUN, B., HE, Z., SOMERSET, H., OH, D., FAUBEL, S. A. & EDELSTEIN, C. 2006. Caspases and calpain are independent mediators of cisplatin-induced endothelial cell necrosis. 291**,** F578-F587.

EBELT, N. D., KAOUD, T. S., EDUPUGANTI, R., VAN RAVENSTEIN, S., DALBY, K. N. & VAN DEN BERG, C. L. 2017. A c-Jun N-terminal kinase inhibitor, JNK-IN-8, sensitizes triple negative breast cancer cells to lapatinib. *Oncotarget,* 8**,** 104894-104912.

EBRAHIMI, N., FARDI, E., GHADERI, H., PALIZDAR, S., KHORRAM, R., VAFADAR, R., GHANAATIAN, M., REZAEI-TAZANGI, F., BAZIYAR, P., AHMADI, A., HAMBLIN, M. R. & AREF, A. R. 2023. Receptor tyrosine kinase inhibitors in cancer. *Cellular and Molecular Life Sciences,* 80**,** 104.

EGUCHI, R., FUJIMORI, Y., OHTA, T., KUNIMASA, K. & AND NAKAN , T. 2010. Calpain is involved in cisplatin-induced endothelial injury in an in vitro three-dimensional blood vessel model. *International Journal of Oncology,* 37.

EL-AWADY, E., MOUSTAFA, Y., ABO-ELMATTY, D. & RADWAN, A. 2011. Cisplatin-induced cardiotoxicity Mechanisms and cardioprotective strategies. *European Journal of Pharmacology,* 650**,** 335-341.

ESCALANTE, C. P., CHANG, Y. C., LIAO, K., ROULEAU, T., HALM, J., BOSSI, P., BHADRIRAJU, S., BRITO-DELLAN, N., SAHAI, S., YUSUF, S. W., ZALPOUR, A. & ELTING, L. S. 2016. Meta-analysis of cardiovascular toxicity risks in cancer patients on selected targeted agents. *Support Care Cancer,* 24**,** 4057-74.

ESKANDARI, E. & EAVES, C. J. 2022. Paradoxical roles of caspase-3 in regulating cell survival, proliferation, and tumorigenesis. *J Cell Biol,* 221**,** 1.

EYCK, B. M., VAN DER WILK, B. J., LAGARDE, S. M., WIJNHOVEN, B. P. L., VALKEMA, R., SPAANDER, M. C. W., NUYTTENS, J. J. M. E., VAN DER GAAST, A. & VAN

LANSCHOT, J. J. B. 2018. Neoadjuvant chemoradiotherapy for resectable oesophageal cancer. *Best Practice & Research Clinical Gastroenterology,* 36-37**,** 37-44.

FANG, L., CHOUDHARY, S., ZHAO, Y., EDEH, C. B., YANG, C., BOLDOGH, I. & BRASIER, A. R. 2014. ATM regulates NF-κB-dependent immediate-early genes via RelA Ser 276 phosphorylation coupled to CDK9 promoter recruitment. *Nucleic Acids Research,* 42**,** 8416-8432.

FENG, L., NING, R., LIU, J., LIANG, S., XU, Q., LIU, Y., LIU, W., DUAN, J. & SUN, Z. 2020. Silica nanoparticles induce JNK-mediated inflammation and myocardial contractile dysfunction. *J Hazard Mater,* 391**,** 122206.

FENG, Y., HU, J., XIE, D., QIN, J., ZHONG, Y., LI, X., XIAO, W., WU, J., TAO, D., ZHANG, M., ZHU, Y., SONG, Y., REED, E., LI, Q. Q. & GONG, J. 2005. Subcellular localization of caspase-3 activation correlates with changes in apoptotic morphology in MOLT-4 leukemia cells exposed to X-ray irradiation. *Int J Oncol,* 27**,** 699-704.

FENTON, M. S., MARION, K. M., SALEM, A. K., HOGEN, R., NAEIM, F. & HERSHMAN, J. M. 2010. Sunitinib inhibits MEK/ERK and SAPK/JNK pathways and increases sodium/iodide symporter expression in papillary thyroid cancer. *Thyroid,* 20**,** 965-974.

FERRANDI, C., BALLERIO, R., GAILLARD, P., GIACHETTI, C., CARBONI, S., VITTE, P. A., GOTTELAND, J. P. & CIRILLO, R. 2004. Inhibition of c-Jun N-terminal kinase decreases cardiomyocyte apoptosis and infarct size after myocardial ischemia and reperfusion in anaesthetized rats. *British Journal of Pharmacology,* 142**,** 953-960.

FERREIRA, P. & CHOUPINA, A. B. 2022. CRISPR/Cas9 a simple, inexpensive and effective technique for gene editing. *Mol Biol Rep,* 49**,** 7079-7086.

FLORESCU, M., CINTEZA, M. & VINEREANU, D. 2013. Chemotherapy-induced Cardiotoxicity. *Maedica (Bucur),* 8**,** 59-67.

FORSTERMANN, U. & SESSA, W. C. 2012. Nitric oxide synthases: regulation and function. *European Heart Journal,* 33**,** 829-837.

FÖRSTERMANN, U., XIA, N. & LI, H. 2017. Roles of Vascular Oxidative Stress and Nitric Oxide in the Pathogenesis of Atherosclerosis. *Circulation Research,* 120**,** 713-735.

FRIEDLANDER, A. M. 1986. Macrophages are sensitive to anthrax lethal toxin through an acid-dependent process. *J Biol Chem,* 261**,** 7123-7126.

FUERTES, M., ALONSO, C. & PEREZ, J. 2003. Biochemical modulation of cisplatin mechanisms of action: Enhancement of antitumor activity and circumvention of drug resistance. *Chemical Reviews,* 103**,** 645-662.

GANAI, S. A. 2017. Plant-derived flavone Apigenin: The small-molecule with promising activity against therapeutically resistant prostate cancer. *Biomedicine & Pharmacotherapy,* 85**,** 47-56.

GARCÍA, M. E. G., KIRSCH, D. G. & REITMAN, Z. J. 2022. Targeting the ATM Kinase to Enhance the Efficacy of Radiotherapy and Outcomes for Cancer Patients. *Seminars in radiation oncology.,* 32**,** 3-14.

GIMBRONE, M. A. & GARCÍA-CARDEÑA, G. 2016. Endothelial Cell Dysfunction and the Pathobiology of Atherosclerosis. *Circulation Research,* 118**,** 620-636.

GIROUD, C., MOREAU, M., MATTIOLI, T. A., BALLAND, V., BOUCHER, J.-L., XU-LI, Y., STUEHR, D. J. & SANTOLINI, J. 2010. Role of Arginine Guanidinium Moiety in Nitric-oxide Synthase Mechanism of Oxygen Activation. *Journal of Biological Chemistry,* 285**,** 7233-7245.

GLEDITZSCH, D., PAUSCH, P., MÜLLER-ESPARZA, H., ÖZCAN, A., GUO, X., BANGE, G. & RANDAU, L. 2019. PAM identification by CRISPR-Cas effector complexes: diversified mechanisms and structures. *RNA Biology,* 16**,** 504-517.

GOMEZ, J. A. 2022. Vascular endothelial growth factor-tyrosine kinase inhibitors: Novel mechanisms, predictors of hypertension and management strategies. *American Heart Journal Plus: Cardiology Research and Practice,* 17**,** 100144.

GOSTIMSKAYA, I. 2022. CRISPR–Cas9: A History of Its Discovery and Ethical Considerations of Its Use in Genome Editing. *Biochemistry (Moscow),* 87**,** 777-788.

GRANT, D. S., WILLIAMS, T. L., ZAHACZEWSKY, M. & DICKER, A. P. 2003. Comparison of antiangiogenic activities using paclitaxel (taxol) and docetaxel (taxotere). *International Journal of Cancer,* 104**,** 121-129.

GRASSI, E. S., VEZZOLI, V., NEGRI, I., LÁBADI, Á., FUGAZZOLA, L., VITALE, G. & PERSANI, L. 2015. SP600125 has a remarkable anticancer potential against undifferentiated thyroid cancer through selective action on ROCK and p53 pathways. *Oncotarget,* 6**,** 36383-99.

GRAZIANI, S., SCORRANO, L. & PONTARIN, G. 2022. Transient Exposure of Endothelial Cells to Doxorubicin Leads to Long-Lasting Vascular Endothelial Growth Factor Receptor 2 Downregulation. *CELLS-BASEL,* 11**,** 210.

GREUBER, E. K., SMITH-PEARSON, P., WANG, J. & PENDERGAST, A. M. 2013. Role of ABL family kinases in cancer: from leukaemia to solid tumours. *Nature Reviews Cancer,* 13**,** 559-571.

GU, H., DO, D., LIU, X., XU, L., SU, Y., NAH, J., WONG, Y., LI, Y., SHENG, N., TILAYE, G., YANG, H., GUO, H., YAN, J. & FU, X. 2018. The STAT3 Target Mettl8 Regulates Mouse ESC Differentiation via Inhibiting the JNK Pathway. *Stem Cell Reports,* 10**,** 1807-1820.

GUI, Y., ZHENG, H. & CAO, R. Y. 2022. Foam Cells in Atherosclerosis: Novel Insights Into Its Origins, Consequences, and Molecular Mechanisms. *Front Cardiovasc Med,* 9**,** 845942-845942.

GUO, R.-M., XU, W.-M., LIN, J.-C., MO, L.-Q., HUA, X.-X., CHEN, P.-X., WU, K., ZHENG, D.-D. & FENG, J.-Q. 2013. Activation of the p38 MAPK/NF-κB pathway contributes to doxorubicin-induced inflammation and cytotoxicity in H9c2 cardiac cells. *Molecular Medicine Reports,* 8**,** 603-608.

GUTIERREZ, G., TSUJI, T., CHEN, M., JIANG, W. & RONAI, Z. 2010. Interplay between Cdh1 and JNK activity during the cell cycle. *Nature Cell Biology,* 12**,** 686-U130.

HADI AR, H., CORNELIA, S. C. & JASSIM AL, S. 2005. Endothelial dysfunction: cardiovascular risk factors, therapy, and outcome. *Vascular Health and Risk Management,* 1**,** 183-198.

HANAHAN, D. & ROBERT 2011. Hallmarks of Cancer: The Next Generation. *Cell,* 144**,** 646-674.

HANAHAN, D. & WEINBERG, R. A. 2000. The Hallmarks of Cancer. *Cell,* 100**,** 57-70.

HARA, T., NAMBA, H., YANG, T.-T., NAGAYAMA, Y., FUKATA, S., KUMA, K., ISHIKAWA, N., ITO, K. & YAMASHITA, S. 1998. Ionizing Radiation Activates c-Jun NH2-Terminal Kinase (JNK/SAPK) via a PKC-Dependent Pathway in Human Thyroid Cells. *Biochemical and Biophysical Research Communications,* 244**,** 41-44.

HARGITAI, R., KIS, D., PERSA, E., SZATMÁRI, T., SÁFRÁNY, G. & LUMNICZKY, K. 2021. Oxidative Stress and Gene Expression Modifications Mediated by Extracellular Vesicles: An In Vivo Study of the Radiation-Induced Bystander Effect. *Antioxidants,* 10**,** 156.

HATAI, T. 2000. Execution of Apoptosis Signal-regulating Kinase 1 (ASK1)-induced Apoptosis by the Mitochondria-dependent Caspase Activation. 275**,** 26576-26581.

HE, G., KUANG, J., KHOKHAR, A. R. & SIDDIK, Z. H. 2011. The impact of S- and G2-checkpoint response on the fidelity of G1-arrest by cisplatin and its comparison to a non-cross-resistant platinum(IV) analog. *Gynecologic Oncology,* 122**,** 402-409.

HE, X., FAN, X., BAI, B., LU, N., ZHANG, S. & ZHANG, L. 2021. Pyroptosis is a critical immune-inflammatory response involved in atherosclerosis. *Pharmacol Res,* 165**,** 105447-105447.

HEGER, Z., CERNEI, N., KUDR, J., GUMULEC, J., BLAZKOVA, I., ZITKA, O., ECKSCHLAGER, T., STIBOROVA, M., ADAM, V. & KIZEK, R. 2013. A Novel Insight into the Cardiotoxicity of Antineoplastic Drug Doxorubicin. *International Journal of Molecular Sciences,* 14**,** 21629-21646.

HELBIG, L., DAMROT, J., HÜLSENBECK, J., KÖBERLE, B., BROZOVIC, A., OSMAK, M., FIKET, Z., KAINA, B. & FRITZ, G. 2011. Late Activation of Stress-activated Protein Kinases/c-Jun N-terminal Kinases Triggered by Cisplatin-induced DNA Damage in Repair-defective Cells. *Journal of Biological Chemistry,* 286**,** 12991-13001.

HELM, A., LEE, R., DURANTE, M. & RITTER, S. 2016. The Influence of C-Ions and X-rays on Human Umbilical Vein Endothelial Cells. *Frontiers in Oncology,* 6.

HEMMINGS, B. A. & RESTUCCIA, D. F. 2012. PI3K-PKB/Akt Pathway. *Cold Spring Harbor Perspectives in Biology,* 4**,** a011189-a011189.

HENNINGER, C. & FRITZ, G. 2017. Statins in anthracycline-induced cardiotoxicity: Rac and Rho, and the heartbreakers.

HEO, Y.-S., KIM, S.-K., SEO, C. I., KIM, Y. K., SUNG, B.-J., LEE, H. S., LEE, J. I., PARK, S.-Y., KIM, J. H., HWANG, K. Y., HYUN, Y.-L., JEON, Y. H., RO, S., CHO, J. M., LEE, T. G. & YANG, C.-H. 2004. Structural basis for the selective inhibition of JNK1 by the scaffolding protein JIP1 and SP600125. *The EMBO Journal,* 23**,** 2185-2195.

HICKLIN, D. J. & ELLIS, L. M. 2005. Role of the vascular endothelial growth factor pathway in tumor growth and angiogenesis. *J Clin Oncol,* 23**,** 1011-27.

HIROSUMI, J., TUNCMAN, G., CHANG, L., GORGUN, C., UYSAL, K., MAEDA, K., KARIN, M. & HOTAMISLIGIL, G. 2002. A central role for JNK in obesity and insulin resistance. *Nature,* 420**,** 333-336.

HO, W. C., DICKSON, K. M. & BARKER, P. A. 2005. Nuclear Factor-κB Induced by Doxorubicin Is Deficient in Phosphorylation and Acetylation and Represses Nuclear Factor-κB–Dependent Transcription in Cancer Cells. *Cancer Research,* 65**,** 4273-4281.

HOANG, D. H., SONG, M., KOVALE, L. M., TRAN, Q. H., CHOE, W., KANG, I., KIM, S. S. & HA, J. 2022. Beta-naphthoflavone and doxorubicin synergistically enhance apoptosis in human lung cancer cells by inducing doxorubicin accumulation, mitochondrial ROS generation, and JNK pathway signaling. *Biochemical and Biophysical Research Communications,* 635**,** 37-45.

HOESEL, B. & SCHMID, J. A. 2013. The complexity of NF-κB signaling in inflammation and cancer. *Molecular Cancer,* 12**,** 86.

HRENIUK, D., GARAY, M., GAARDE, W., MONIA, B. P., MCKAY, R. A. & CIOFFI, C. L. 2001. Inhibition of c-Jun N-terminal kinase 1, but not c-Jun N-terminal kinase

2, suppresses apoptosis induced by ischemia/reoxygenation in rat cardiac myocytes. *Molecular pharmacology,* 59**,** 867-874.

HSU, P.-Y., MAMMADOVA, A., BENKIRANE-JESSEL, N., DÉSAUBRY, L. & NEBIGIL, C. G. 2021. Updates on Anticancer Therapy-Mediated Vascular Toxicity and New Horizons in Therapeutic Strategies. *Frontiers in Cardiovascular Medicine,* 8.

HUANG, D., DING, Y., LI, Y., LUO, W., ZHANG, Z., SNIDER, J., VANDENBELDT, K., QIAN, C. & TEH, B. 2010. Sunitinib Acts Primarily on Tumor Endothelium rather than Tumor Cells to Inhibit the Growth of Renal Cell Carcinoma. *Cancer Research,* 70**,** 1053-1062.

HUI, D. Y. 2007. A No-No for NonO and JNK in Extracellular Matrix Homeostasis and Vascular Stability. *Arteriosclerosis, Thrombosis, and Vascular Biology,* 27**,** 1677-1678.

HUOT, J., HOULE, F., MARCEAU, F. & LANDRY, J. 1997. Oxidative stress-induced actin reorganization mediated by the p38 mitogen-activated protein kinase/heat shock protein 27 pathway in vascular endothelial cells. *Circulation Research,* 80**,** 383-392.

HWANG, S., KIM, S.-H., YOO, K. H., CHUNG, M.-H., LEE, J. W. & SON, K. H. 2022. Exogenous 8-hydroxydeoxyguanosine attenuates doxorubicin-induced cardiotoxicity by decreasing pyroptosis in H9c2 cardiomyocytes. *BMC Molecular and Cell Biology,* 23.

IQUBAL, A., SHARMA, S., ANSARI, M. A., NAJMI, A. K., SYED, M. A., ALI, J., ALAM, M. M., AHMAD, S. & HAQUE, S. E. 2019. Nerolidol attenuates cyclophosphamide-induced cardiac inflammation, apoptosis and fibrosis in Swiss Albino mice. *European Journal of Pharmacology,* 863**,** 172666.

ISHINO, Y., SHINAGAWA, H., MAKINO, K., AMEMURA, M. & NAKATA, A. 1987. Nucleotide sequence of the iap gene, responsible for alkaline phosphatase isozyme conversion in Escherichia coli, and identification of the gene product. *Journal of Bacteriology,* 169**,** 5429-5433.

IVESON, T., BOYD, K. A., KERR, R. S., ROBLES-ZURITA, J., SAUNDERS, M. P., BRIGGS, A. H., CASSIDY, J., HOLLANDER, N. H., TABERNERO, J., HAYDON, A., GLIMELIUS,

B., HARKIN, A., ALLAN, K., MCQUEEN, J., PEARSON, S., WATERSTON, A., MEDLEY, L., WILSON, C., ELLIS, R., ESSAPEN, S., DHADDA, A. S., HARRISON, M., FALK, S., RAOUF, S., REES, C., OLESEN, R. K., PROPPER, D., BRIDGEWATER, J., AZZABI, A., FARRUGIA, D., WEBB, A., CUNNINGHAM, D., HICKISH, T., WEAVER, A., GOLLINS, S., WASAN, H. & PAUL, J. 2019. 3-month versus 6-month adjuvant chemotherapy for patients with high-risk stage II and III colorectal cancer: 3-year follow-up of the SCOT non-inferiority RCT. *Health Technol Assess,* 23**,** 1-88.

JABBARI, N., NAWAZ, M. & REZAIE, J. 2019. Bystander effects of ionizing radiation: conditioned media from X-ray irradiated MCF-7 cells increases the angiogenic ability of endothelial cells. *Cell Communication and Signaling,* 17.

JAESCHKE, A. 2004. An essential role of the JIP1 scaffold protein for JNK activation in adipose tissue. *Genes & Development,* 18**,** 1976-1980.

JAESCHKE, A., RINCON, M., DORAN, B., REILLY, J., NEUBERG, D., GREINER, D., SHULTZ, L., ROSSINI, A., FLAVELL, R. & DAVIS, R. 2005. Disruption of the Jnk2 (Mapk9) gene reduces destructive insulitis and diabetes in a mouse model of type 1 diabetes. *Proceedings of the National Academy of Sciences of the United States of America,* 102**,** 6931-6935.

JETTE, N. R., KUMAR, M., RADHAMANI, S., ARTHUR, G., GOUTAM, S., YIP, S., KOLINSKY, M., WILLIAMS, G. J., BOSE, P. & LEES-MILLER, S. P. 2020. ATM-Deficient Cancers Provide New Opportunities for Precision Oncology. *Cancers,* 12**,** 687.

JIANG, M., QI, L., LI, L. & LI, Y. 2020. The caspase-3/GSDME signal pathway as a switch between apoptosis and pyroptosis in cancer. *Cell Death Discovery,* 6.

JIANG, Y., SHAN, S., GAN, T., ZHANG, X., LU, X., HU, H., WU, Y., SHENG, J. & YANG, J. 2014. Effects of cisplatin on the contractile function of thoracic aorta of Sprague-Dawley rats. *Biomedical Reports,* 2**,** 893-897.

JOENSUU, H. 2007. Cardiac toxicity of sunitinib. *Lancet,* 370**,** 1978-1980.

JOHN, C. M., KHADDAJ MALLAT, R., MISHRA, R. C., GEORGE, G., SINGH, V., TURNBULL, J. D., UMESHAPPA, C. S., KENDRICK, D. J., KIM, T., FAUZI, F. M.,

VISSER, F., FEDAK, P. W. M., WULFF, H. & BRAUN, A. P. 2020. SKA-31, an activator of Ca2+-activated K+ channels, improves cardiovascular function in aging. *Pharmacological Research,* 151.

JOHNSON, G. L. & NAKAMURA, K. 2007. The c-jun kinase/stress-activated pathway: Regulation, function and role in human disease. *Biochimica et Biophysica Acta (BBA) - Molecular Cell Research,* 1773**,** 1341-1348.

JONES, V., EMMA, DICKMAN, J., MARK & WHITMARSH, J., ALAN 2007. Regulation of p73-mediated apoptosis by c-Jun N-terminal kinase. *Biochemical Journal,* 405**,** 617-623.

JORGENSEN, I., RAYAMAJHI, M. & MIAO, E. A. 2017. Programmed cell death as a defence against infection. *Nature Reviews Immunology,* 17**,** 151-164.

KAISER, R. A., LIANG, Q., BUENO, O., HUANG, Y., LACKEY, T., KLEVITSKY, R., HEWETT, T. E. & MOLKENTIN, J. D. 2005. Genetic Inhibition or Activation of JNK1/2 Protects the Myocardium from Ischemia-Reperfusion-induced Cell Deathin Vivo. *Journal of Biological Chemistry,* 280**,** 32602-32608.

KALLUNKI, T., SU, B., TSIGELNY, I., SLUSS, H. K., DERIJARD, B., MOORE, G., DAVIS, R. & KARIN, M. 1994. JNK2 contains a specificity-determining region responsible for efficient c-Jun binding and phosphorylation. *Genes & Development,* 8**,** 2996-3007.

KANETO, H., MATSUOKA, T.-A., NAKATANI, Y., KAWAMORI, D., MIYATSUKA, T., MATSUHISA, M. & YAMASAKI, Y. 2005. Oxidative stress, ER stress, and the JNK pathway in type 2 diabetes.(endoplasmic reticulum, jun N-terminal kinase)(Author abstract). *Journal of Molecular Medicine,* 83**,** 429.

KANG 1994. Role of p38 MAPK and JNK in enhanced cervical cancer cell killing by the combination of arsenic trioxide and ionizing radiation. *Oncology Reports*.

KANG, P. T., CHEN, C.-L., OHANYAN, V., LUTHER, D. J., MESZAROS, J. G., CHILIAN, W. M. & CHEN, Y.-R. 2015. Overexpressing superoxide dismutase 2 induces a supernormal cardiac function by enhancing redox-dependent mitochondrial function and metabolic dilation. *Journal of Molecular and Cellular Cardiology,* 88**,** 14-28.

KARPURAPU, A., WILLIAMS, H. A., DEBENEDITTIS, P., BAKER, C. E., REN, S., THOMAS, M. C., BEARD, A. J., DEVLIN, G. W., HARRINGTON, J., PARKER, L. E., SMITH, A. K., MAINSAH, B., PLA, M. M., ASOKAN, A., BOWLES, D. E., IVERSEN, E., COLLINS, L. & KARRA, R. 2024. Deep Learning Resolves Myovascular Dynamics in the Failing Human Heart. *JACC Basic Transl Sci,* 9**,** 674-686.

KHATSENKO, O. G., GROSS, S. S., RIFKIND, A. B. & VANE, J. R. 1993. Nitric oxide is a mediator of the decrease in cytochrome P450-dependent metabolism caused by immunostimulants. 90**,** 11147-11151.

KIM, J.-H., LEE, S. C., RO, J., KANG, H. S., KIM, H. S. & YOON, S. 2010. Jnk signaling pathway-mediated regulation of Stat3 activation is linked to the development of doxorubicin resistance in cancer cell lines. *Biochem Pharmacol,* 79**,** 373-380.

KIM, J. & FREEMAN, M. R. 2003. JNK/SAPK Mediates Doxorubicin-Induced Differentiation and Apoptosis in MCF-7 Breast Cancer Cells. *Breast Cancer Research and Treatment,* 79**,** 321-328.

KIM, S. B., KIM, J. S., LEE, J. H., YOON, W. J., LEE, D. S., KO, M. S., KWON, B. S., CHOI, D. H., CHO, H. R., LEE, B. J., CHUNG, D. K., LEE, H. W. & PARK, J. W. 2006. NF-κB activation is required for cisplatin-induced apoptosis in head and neck squamous carcinoma cells. *FEBS Letters,* 580**,** 311-318.

KISHIMOTO, T., YOSHIKAWA, Y., YOSHIKAWA, K. & KOMEDA, S. 2019. Different Effects of Cisplatin and Transplatin on the Higher-Order Structure of DNA and Gene Expression. *International Journal of Molecular Sciences,* 21**,** 34.

KISS, R. C., XIA, F. & ACKLIN, S. 2021. Targeting DNA Damage Response and Repair to Enhance Therapeutic Index in Cisplatin-Based Cancer Treatment. *International Journal of Molecular Sciences,* 22**,** 8199.

KODERA, Y., KATANASAKA, Y., KITAMURA, Y., TSUDA, H., NISHIO, K., TAMURA, T. & KOIZUMI, F. 2011. Sunitinib inhibits lymphatic endothelial cell functions and lymph node metastasis in a breast cancer model through inhibition of vascular endothelial growth factor receptor 3. *Breast Cancer Research,* 13**,** R66.

KONG, C. Y., GUO, Z., SONG, P., ZHANG, X., YUAN, Y. P., TENG, T., YAN, L. & TANG, Q. Z. 2022. Underlying the Mechanisms of Doxorubicin-Induced Acute Cardiotoxicity: Oxidative Stress and Cell Death. *Int J Biol Sci,* 18**,** 760-770.

KONOPACKA, M., ROGOLINSKI, J. & SLOSAREK, K. 2011. Direct and bystander effects induced by scattered radiation generated during penetration of radiation inside a water-phantom. *Mutation Research-Genetic Toxicology and Environmental Mutagenesis,* 721**,** 6-14.

KOZLOV, S. V., GRAHAM, M. E., JAKOB, B., TOBIAS, F., KIJAS, A. W., TANUJI, M., CHEN, P., ROBINSON, P. J., TAUCHER-SCHOLZ, G., SUZUKI, K., SO, S., CHEN, D. & LAVIN, M. F. 2011. Autophosphorylation and ATM Activation. *Journal of Biological Chemistry,* 286**,** 9107-9119.

KUBES, P., SUZUKI, M. & GRANGER, D. N. 1991. Nitric oxide: an endogenous modulator of leukocyte adhesion. *Proceedings of the National Academy of Sciences,* 88**,** 4651-4655.

KULTZ, D. 1998. Phylogenetic and functional classification of mitogen- and stress-activated protein kinases. *Journal of Molecular Evolution,* 46**,** 571-588.

KUMAR, A., SINGH, U. K., KINI, S. G., GARG, V., AGRAWAL, S., TOMAR, P. K., PATHAK, P., CHAUDHARY, A., GUPTA, P. & MALIK, A. 2015. JNK pathway signaling: a novel and smarter therapeutic targets for various biological diseases. *Future Med Chem,* 7**,** 2065-86.

KURZ, E. U., DOUGLAS, P. & LEES-MILLER, S. P. 2004. Doxorubicin Activates ATM-dependent Phosphorylation of Multiple Downstream Targets in Part through the Generation of Reactive Oxygen Species. *Journal of Biological Chemistry,* 279**,** 53272-53281.

LAGUNAS, V. M. & MELÉNDEZ-ZAJGLA, J. 2008. Nuclear Factor-kappa B as a Resistance Factor to Platinum-Based Antineoplasic Drugs. *Metal-Based Drugs,* 2008**,** 1-6.

LAI, S., AMABILE, M. I., MAZZAFERRO, S., MITTERHOFER, A. P., MAZZARELLA, A., GALANI, A., IMBIMBO, G., CIANCI, R., PASQUALI, M. & MOLFINO, A. 2020. Effects of sunitinib on endothelial dysfunction, metabolic changes, and

cardiovascular risk indices in renal cell carcinoma. *Cancer Medicine,* 9**,** 3752-3757.

LAN, Y.-Y., CHEN, Y.-H., LIU, C., TUNG, K.-L., WU, Y.-T., LIN, S.-C., WU, C.-H., CHANG, H.-Y., CHEN, Y.-C. & HUANG, B.-M. 2021. Role of JNK activation in paclitaxel-induced apoptosis in human head and neck squamous cell carcinoma. *Oncology Letters,* 22.

LANTOINE, F., IOUZALEN, L., DEVYNCK, M.-A., BRUSSEL, E. M.-V. & DAVID-DUFILHO, M. 1998. Nitric oxide production in human endothelial cells stimulated by histamine requires Ca2+ influx. 330**,** 695-699.

LANUZA-MASDEU, J., AREVALO, M. I., VILA, C., BARBERA, A., GOMIS, R. & CAELLES, C. 2013. In Vivo JNK Activation in Pancreatic  -Cells Leads to Glucose Intolerance Caused by Insulin Resistance in Pancreas. *Diabetes,* 62**,** 2308-2317.

LAVIN, M. F. 2008. Ataxia-telangiectasia: from a rare disorder to a paradigm for cell signalling and cancer. *Nat Rev Mol Cell Biol,* 9**,** 759-769.

LAWAN, A., TORRANCE, E., AL-HARTHI, S., SHWEASH, M., ALNASSER, S., NEAMATALLAH, T., SCHROEDER, J. & PLEVIN, R. 2012. MKP-2: out of the DUSP-bin and back into the limelight. *Biochemical Society Transactions,* 40**,** 235-239.

LAWRENCE, T. 2009. The Nuclear Factor NF- B Pathway in Inflammation. *Cold Spring Harbor Perspectives in Biology,* 1**,** a001651-a001651.

LI, C., MA, D., CHEN, M., ZHANG, L., ZHANG, L., ZHANG, J., QU, X. & WANG, C. 2016a. Ulinastatin attenuates LPS-induced human endothelial cells oxidative damage through suppressing JNK/c-Jun signaling pathway. *Biochemical and Biophysical Research Communications,* 474**,** 572-578.

LI, C., REIF, M. M., CRAIGE, S. M., KANT, S. & KEANEY, J. F. 2016b. Endothelial AMPK activation induces mitochondrial biogenesis and stress adaptation via eNOS-dependent mTORC1 signaling. *Nitric Oxide,* 55-56**,** 45-53.

LI, D., SONG, C., SONG, C., TIAN, X., ZHANG, H., ZHANG, J. & ZHAO, X. 2024. Sunitinib induces cardiotoxicity through modulating oxidative stress and Nrf2-

dependent ferroptosis in vitro and in vivo. *Chemico-Biological Interactions,* 388**,** 110829.

LI, F., XIA, Q., REN, L., NIE, Y., REN, H., GUO, X., YU, J., XING, Y. & CHEN, Z. 2022a. GSDME Increases Chemotherapeutic Drug Sensitivity by Inducing Pyroptosis in Retinoblastoma Cells. *Oxidative Medicine and Cellular Longevity,* 2022**,** 1-29.

LI, M., KIM, J., RHA, H., SON, S., LEVINE, M. S., XU, Y., SESSLER, J. L. & KIM, J. S. 2023. Photon-Controlled Pyroptosis Activation (PhotoPyro): An Emerging Trigger for Antitumor Immune Response. *Journal of the American Chemical Society,* 145**,** 6007-6023.

LI, P., XIE, C., ZHONG, J., GUO, Z., GUO, K. & TU, Q. 2021. Melatonin Attenuates ox-LDL-Induced Endothelial Dysfunction by Reducing ER Stress and Inhibiting JNK/Mff Signaling. *Oxidative Medicine and Cellular Longevity,* 2021**,** 1-10.

LI, X.-R., CHENG, X.-H., ZHANG, G.-N., WANG, X.-X. & HUANG, J.-M. 2022b. Cardiac safety analysis of first-line chemotherapy drug pegylated liposomal doxorubicin in ovarian cancer. *Journal of Ovarian Research,* 15.

LIBBY, P. 2012. Inflammation in Atherosclerosis. *Arteriosclerosis, Thrombosis, and Vascular Biology,* 32**,** 2045-2051.

LIEBERTHAL, W., TRIACA, V. & LEVINE, J. 1996. Mechanisms of death induced by cisplatin in proximal tubular epithelial cells: Apoptosis vs. necrosis. *American Journal of Physiology-Renal Fluid and Electrolyte Physiology,* 270**,** F700-F708.

LIM, W., KIM, J. H., GOOK, E., KIM, J., KO, Y., KIM, I., KWON, H., LIM, H., JUNG, B., YANG, K., CHOI, N., KIM, M., KIM, S., CHOI, H. & KIM, O. 2009. Inhibition of mitochondria-dependent apoptosis by 635-nm irradiation in sodium nitroprusside-treated SH-SY5Y cells. *Free Radic Biol Med,* 47**,** 850-7.

LIN, A., MINDEN, A., MARTINETTO, H., CLARET, F., LANGE-CARTER, C., MERCURIO, F., JOHNSON, G. & KARIN, M. 1995. Identification of a dual specificity kinase that activates the Jun kinases and p38-Mpk2. *Science,* 268**,** 286-290.

LINDERS, A. N., DIAS, I. B., LÓPEZ FERNÁNDEZ, T., TOCCHETTI, C. G., BOMER, N. & VAN DER MEER, P. 2024. A review of the pathophysiological mechanisms of doxorubicin-induced cardiotoxicity and aging. *npj Aging,* 10**,** 9.

LIU, C., QIAN, X., YU, C., XIA, X., LI, J., LI, Y., XIE, Y., GAO, G., SONG, Y., ZHANG, M., XUE, H., WANG, X., SUN, H., LIU, J., DENG, W. & GUO, X. 2024. Inhibition of ATM promotes PD-L1 expression by activating JNK/c-Jun/TNF-α signaling axis in triple-negative breast cancer. *Cancer Letters,* 586**,** 216642.

LIU, J., MINEMOTO, Y. & LIN, A. 2004. c-Jun N-Terminal Protein Kinase 1 (JNK1), but Not JNK2, Is Essential for Tumor Necrosis Factor Alpha-Induced c-Jun Kinase Activation and Apoptosis. *Molecular and Cellular Biology,* 24**,** 10844-10856.

LIU, Q., PAN, J., BAO, L., XU, C., QI, Y., JIANG, B., WANG, D., ZHU, X., LI, X., ZHANG, H., BAI, H., YANG, Q., MA, J., WIEMER, E. A. C., BEN, J. & CHEN, Q. 2022. Major Vault Protein Prevents Atherosclerotic Plaque Destabilization by Suppressing Macrophage ASK1-JNK Signaling. *Arteriosclerosis, Thrombosis, and Vascular Biology,* 42**,** 580-596.

LIU, T., ZHANG, L., JOO, D. & SUN, S.-C. 2017. NF-κB signaling in inflammation. *Signal Transduction and Targeted Therapy,* 2**,** 17023.

LIU, W., ZI, M., CHI, H., JIN, J., PREHAR, S., NEYSES, L., CARTWRIGHT, E., FLAVELL, R., DAVIS, R. & WANG, X. 2011. Deprivation of MKK7 in cardiomyocytes provokes heart failure in mice when exposed to pressure overload. *Journal of Molecular and Cellular Cardiology,* 50**,** 702-711.

LIU, W., ZI, M., JIN, J., PREHAR, S., OCEANDY, D., KIMURA, T. E., LEI, M., NEYSES, L., WESTON, A. H., CARTWRIGHT, E. J. & WANG, X. 2009. Cardiac-Specific Deletion of Mkk4 Reveals Its Role in Pathological Hypertrophic Remodeling but Not in Physiological Cardiac Growth. *Circulation Research,* 104**,** 905-914.

LOMBARD, C. K., DAVIS, A. L., INUKAI, T. & MALY, D. J. 2018. Allosteric Modulation of JNK Docking Site Interactions with ATP-Competitive Inhibitors. *Biochemistry,* 57**,** 5897-5909.

LÓPEZ-SENDÓN, J., ÁLVAREZ-ORTEGA, C., ZAMORA AUÑON, P., BUÑO SOTO, A., LYON, A. R., FARMAKIS, D., CARDINALE, D., CANALES ALBENDEA, M., FELIU

BATLLE, J., RODRÍGUEZ RODRÍGUEZ, I., RODRÍGUEZ FRAGA, O., ALBALADEJO, A., MEDIAVILLA, G., GONZÁLEZ-JUANATEY, J. R., MARTÍNEZ MONZONIS, A., GÓMEZ PRIETO, P., GONZÁLEZ-COSTELLO, J., SERRANO ANTOLÍN, J. M., CADENAS CHAMORRO, R. & LÓPEZ FERNÁNDEZ, T. 2020. Classification, prevalence, and outcomes of anticancer therapy-induced cardiotoxicity: the CARDIOTOX registry. *Eur Heart J,* 41**,** 1720-1729.

LOPEZ, K. E. & BOUCHIER-HAYES, L. 2022. Lethal and Non-Lethal Functions of Caspases in the DNA Damage Response. *Cells (Basel, Switzerland),* 11**,** 1887.

LOTRIONTE, M., BIONDI-ZOCCAI, G., ABBATE, A., LANZETTA, G., D'ASCENZO, F., MALAVASI, V., PERUZZI, M., FRATI, G. & PALAZZONI, G. 2013. Review and meta-analysis of incidence and clinical predictors of anthracycline cardiotoxicity. *Am J Cardiol,* 112**,** 1980-4.

LOVELESS, R., BLOOMQUIST, R. & TENG, Y. 2021. Pyroptosis at the forefront of anticancer immunity. *Journal of Experimental & Clinical Cancer Research,* 40.

LU, C., ZHU, F., CHO, Y.-Y., TANG, F., ZYKOVA, T., MA, W.-Y., BODE, A. M. & DONG, Z. 2006. Cell Apoptosis: Requirement of H2AX in DNA Ladder Formation, but Not for the Activation of Caspase-3. *Molecular Cell,* 23**,** 121-132.

LU, G. D., SHEN, H. M., CHUNG, M. C. & ONG, C. N. 2007. Critical role of oxidative stress and sustained JNK activation in aloe-emodin-mediated apoptotic cell death in human hepatoma cells. *Carcinogenesis.,* 28**,** 1937-1945.

LU, L., ZHANG, Y., TAN, X., MERKHER, Y., LEONOV, S., ZHU, L., DENG, Y., ZHANG, H., ZHU, D., TAN, Y., FU, Y., LIU, T. & CHEN, Y. 2022. Emerging mechanisms of pyroptosis and its therapeutic strategy in cancer. *Cell Death Discovery,* 8.

LUBBERTS, S., GROOT, H. J., DE WIT, R., MULDER, S., WITJES, J. A., KERST, J. M., GROENEWEGEN, G., LEFRANDT, J. D., VAN LEEUWEN, F. E., NUVER, J., SCHAAPVELD, M. & GIETEMA, J. A. 2023. Cardiovascular Disease in Testicular Cancer Survivors: Identification of Risk Factors and Impact on Quality of Life. *J Clin Oncol,* 41**,** 3512-3522.

LUM, H. & ROEBUCK, K. A. 2001. Oxidant stress and endothelial cell dysfunction. *American Journal of Physiology-Cell Physiology,* 280**,** C719-C741.

LUO, J. L. 2005. IKK/NF- B signaling: balancing life and death - a new approach to cancer therapy. *Journal of Clinical Investigation,* 115**,** 2625-2632.

LUO, M., LU, Z., SUN, H., YUAN, K., ZHANG, Q., MENG, S., WANG, F., GUO, H., JU, X., LIU, Y., YE, T., LU, Z. & ZHAI, Z. 2010. Nuclear entry of active caspase-3 is facilitated by its p3-recognition-based specific cleavage activity. *Cell Research,* 20**,** 211-222.

LÜSCHER, T. F., BOULANGER, C. M., DOHI, Y. & YANG, Z. H. 1992. Endothelium-derived contracting factors. *Hypertension,* 19**,** 117-130.

LUU, A. Z., LUU, V. Z., CHOWDHURY, B., KOSMOPOULOS, A., PAN, Y., AL-OMRAN, M., QUAN, A., TEOH, H., HESS, D. A. & VERMA, S. 2021. Loss of endothelial cell-specific autophagy-related protein 7 exacerbates doxorubicin-induced cardiotoxicity. *Biochemistry and Biophysics Reports,* 25**,** 100926.

MADDAMS, J., UTLEY, M. & MØLLER, H. 2012. Projections of cancer prevalence in the United Kingdom, 2010–2040. *British Journal of Cancer,* 107**,** 1195-1202.

MAH, L. J., EL-OSTA, A. & KARAGIANNIS, T. C. 2010. γH2AX: a sensitive molecular marker of DNA damage and repair. *Leukemia,* 24**,** 679-686.

MAHALINGAM, D., CAREW, J. S., ESPITIA, C. M., COOL, R. H., GILES, F. J., DE JONG, S. & NAWROCKI, S. T. 2019. Heightened JNK Activation and Reduced XIAP Levels Promote TRAIL and Sunitinib-Mediated Apoptosis in Colon Cancer Models. *Cancers,* 11**,** 895.

MAIK-RACHLINE, G., ZEHORAI, E., HANOCH, T., BLENIS, J. & SEGER, R. 2018. The nuclear translocation of the kinases p38 and JNK promotes inflammation-induced cancer. *Sci Signal,* 11.

MAILLET, M., LYNCH, J. M., SANNA, B., YORK, A. J., ZHENG, Y. & MOLKENTIN, J. D. 2009. Cdc42 is an antihypertrophic molecular switch in the mouse heart.(Research article)(Report). *Journal of Clinical Investigation,* 119**,** 3079.

MAILLOUX, A., GRENET, K., BRUNEEL, A., BENETEAU-BURNAT, B., VAUBOURDOLLE, M. & BAUDIN, B. 2001. Anticancer drugs induce necrosis of human

endothelial cells involving both oncosis and apoptosis. *European Journal of Cell Biology,* 80**,** 442-449.

MANSOURI, A., RIDGWAY, L. D., KORAPATI, A. L., ZHANG, Q., TIAN, L., WANG, Y., SIDDIK, Z. H., MILLS, G. B. & CLARET, F. X. 2003. Sustained Activation of JNK/p38 MAPK Pathways in Response to Cisplatin Leads to Fas Ligand Induction and Cell Death in Ovarian Carcinoma Cells*. *Journal of Biological Chemistry,* 278**,** 19245-19256.

MATSUMORI, A. 2023. Nuclear Factor-κB is a Prime Candidate for the Diagnosis and Control of Inflammatory Cardiovascular Disease. *Eur Cardiol,* 18**,** e40.

MATTIOLI, R., ILARI, A., COLOTTI, B., MOSCA, L., FAZI, F. & COLOTTI, G. 2023. Doxorubicin and other anthracyclines in cancers: Activity, chemoresistance and its overcoming. *Molecular Aspects of Medicine,* 93**,** 101205.

MAVROGONATOU, E., ANGELOPOULOU, M., RIZOU, S. V., PRATSINIS, H., GORGOULIS, V. G. & KLETSAS, D. 2022. Activation of the JNKs/ATM-p53 axis is indispensable for the cytoprotection of dermal fibroblasts exposed to UVB radiation. *Cell Death & Disease,* 13**,** 647.

MCGOWAN, J., CHUNG, R., MAULIK, A., PIOTROWSKA, I., WALKER, J. & YELLON, D. 2017. Anthracycline Chemotherapy and Cardiotoxicity. *Cardiovascular Drugs and Therapy,* 31**,** 63-75.

MCLEAN, B. A., PATEL, V. B., ZHABYEYEV, P., CHEN, X., BASU, R., WANG, F., SHAH, S., VANHAESEBROECK, B. & OUDIT, G. Y. 2019. PI3Kα Pathway Inhibition With Doxorubicin Treatment Results in Distinct Biventricular Atrophy and Remodeling With Right Ventricular Dysfunction. *Journal of the American Heart Association*.

MCMULLEN, C. J., CHALMERS, S., WOOD, R., CUNNINGHAM, M. R. & CURRIE, S. 2021. Sunitinib and Imatinib Display Differential Cardiotoxicity in Adult Rat Cardiac Fibroblasts That Involves a Role for Calcium/Calmodulin Dependent Protein Kinase II. *Frontiers in Cardiovascular Medicine,* 7.

MENA, A. C., PULIDO, E. G. & GUILLÉN-PONCE, C. 2010. Understanding the molecular-based mechanism of action of the tyrosine kinase inhibitor: sunitinib. *Anticancer Drugs,* 21 Suppl 1**,** S3-11.

MENG, L., LIN, H., ZHANG, J., LIN, N., SUN, Z., GAO, F., LUO, H., NI, T., LUO, W., CHI, J. & GUO, H. 2019. Doxorubicin induces cardiomyocyte pyroptosis via the TINCR-mediated posttranscriptional stabilization of NLR family pyrin domain containing 3. *J Mol Cell Cardiol,* 136**,** 15-26.

MEREDITH, A.-M. & DASS, C. R. 2016. Increasing role of the cancer chemotherapeutic doxorubicin in cellular metabolism. *Journal of Pharmacy and Pharmacology,* 68**,** 729-741.

MIHO, N., ISHIDA, T., KUWABA, N., ISHIDA, M., SHIMOTE-ABE, K., TABUCHI, K., OSHIMA, T., YOSHIZUMI, M. & CHAYAMA, K. 2005. Role of the JNK pathway in thrombin-induced ICAM-1 expression in endothelial cells. *Cardiovasc Res,* 68**,** 289-298.

MIN, W., LIN, Y., TANG, S., YU, L., ZHANG, H., WAN, T., LUHN, T., FU, H. & CHEN, H. 2008. AIP1 Recruits Phosphatase PP2A to ASK1 in Tumor Necrosis Factor–Induced ASK1-JNK Activation. *Circulation Research,* 102**,** 840-848.

MIR, H., RAJAWAT, J., VOHRA, I., VAISHNAV, J., KADAM, A. & BEGUM, R. 2020. Signaling interplay between PARP1 and ROS regulates stress-induced cell death and developmental changes in Dictyostelium discoideum. *Experimental Cell Research,* 397**,** 112364.

MISRA-PRESS, A., RIM, C. S., YAO, H., ROBERSON, M. S. & STORK, P. J. S. 1995. A Novel Mitogen-activated Protein Kinase Phosphatase. STRUCTURE, EXPRESSION, AND REGULATION. *J Biol Chem,* 270**,** 14587-14596.

MITTELSTADT, P. R., YAMAGUCHI, H., APPELLA, E. & ASHWELL, J. D. 2009. T Cell Receptor-mediated Activation of p38α by Mono-phosphorylation of the Activation Loop Results in Altered Substrate Specificity. *Journal of Biological Chemistry,* 284**,** 15469-15474.

MIZUKAMI, Y. & YOSHIDA, K.-I. 1997. Mitogen-activated protein kinase translocates to the nucleus during ischaemia and is activated during reperfusion. 323**,** 785-790.

MOJICA, F. J. M., D**?**EZ-VILLASE**?**OR, C. S., GARC**?**A-MART**?**NEZ, J. S. & SORIA, E. 2005. Intervening Sequences of Regularly Spaced Prokaryotic Repeats Derive from Foreign Genetic Elements. *Journal of Molecular Evolution,* 60**,** 174-182.

MONG, P., PETRULIO, C., KAUFMAN, H. & WANG, Q. 2008. Activation of rho kinase by TNF-alpha is required for JNK activation in human pulmonary microvascular endothelial cells. *Journal of Immunology,* 180**,** 550-558.

MONTI, M., TERZUOLI, E., ZICHE, M. & MORBIDELLI, L. 2013. The sulphydryl containing ACE inhibitor Zofenoprilat protects coronary endothelium from Doxorubicin-induced apoptosis. *Pharmacol Res,* 76**,** 171-81.

MORDES, D. A. & CORTEZ, D. 2008. Activation of ATR and related PIKKs. *Cell Cycle,* 7**,** 2809-2812.

MOTZER, R., MICHAELSON, M., HUTSON, T., TOMCZAK, P., BUKOWSKI, R., RIXE, O., NEGRIER, S., KIM, S., CHEN, I. & FIGLIN, R. 2007. Sunitinib versus interferon (IFN)-alfa as first-line treatment of metastatic renal cell carcinoma (mRCC): updated efficacy and safety results and further analysis of prognostic factors. *Ejc Supplements,* 5**,** 301-301.

MULROONEY, D. A., YEAZEL, M. W., KAWASHIMA, T., MERTENS, A. C., MITBY, P., STOVALL, M., DONALDSON, S. S., GREEN, D. M., SKLAR, C. A., ROBISON, L. L. & LEISENRING, W. M. 2009. Cardiac outcomes in a cohort of adult survivors of childhood and adolescent cancer: retrospective analysis of the Childhood Cancer Survivor Study cohort. *BMJ :,* 339**,** b4606-b4606.

NADEL, G., MAIK-RACHLINE, G. & SEGER, R. 2023. JNK Cascade-Induced Apoptosis—A Unique Role in GqPCR Signaling. *International Journal of Molecular Sciences,* 24**,** 13527.

NAJAFI, M., MAJIDPOOR, J., TOOLEE, H. & MORTEZAEE, K. 2021. The current knowledge concerning solid cancer and therapy. *Journal of Biochemical and Molecular Toxicology,* 35.

NAREZKINA, A., NARAYAN, H. K. & ZEMLJIC-HARPF, A. E. 2021. Molecular mechanisms of anthracycline cardiovascular toxicity. *Clin Sci (Lond),* 135**,** 1311-1332.

NILSSON, M. & HEYMACH, J. V. 2006. Vascular Endothelial Growth Factor (VEGF) Pathway. *Journal of Thoracic Oncology,* 1**,** 768-770.

NITISS, J. 2009. Targeting DNA topoisomerase II in cancer chemotherapy. *Nature Reviews Cancer,* 9**,** 338-350.

NOONAN, J., BOBIK, A. & PETER, K. 2022. The tandem stenosis mouse model: Towards understanding, imaging, and preventing atherosclerotic plaque instability and rupture. *British Journal of Pharmacology,* 179**,** 979-997.

NOZAKI, N., SHISHIDO, T., TAKEISHI, Y. & KUBOTA, I. 2004. Modulation of doxorubicin-induced cardiac dysfunction in toll-like receptor-2-knockout mice. *Circulation,* 110**,** 2869-74.

NUVER, J., DE HAAS, E. C., VAN ZWEEDEN, M., GIETEMA, J. A. & MEIJER, C. 2010. Vascular damage in testicular cancer patients: a study on endothelial activation by bleomycin and cisplatin in vitro. *Oncol Rep,* 23**,** 247-53.

O'RIORDAN, E., CHEN, J., BRODSKY, S. V., SMIRNOVA, I., LI, H. & GOLIGORSKY, M. S. 2005. Endothelial cell dysfunction: The syndrome in making. *Kidney International,* 67**,** 1654-1658.

OBASI, M. A.-O., ABOVICH, A., VO, J. B., GAO, Y., PAPATHEODOROU, S. I., NOHRIA, A., ASNANI, A. & PARTRIDGE, A. H. 2021. Statins to mitigate cardiotoxicity in cancer patients treated with anthracyclines and/or trastuzumab: a systematic review and meta-analysis.

OZFILIZ KILBAS, P., SONMEZ, O., UYSAL-ONGANER, P., COKER GURKAN, A., OBAKAN YERLIKAYA, P. & ARISAN, E. D. 2020. Specific c-Jun N-Terminal Kinase Inhibitor, JNK-IN-8 Suppresses Mesenchymal Profile of PTX-Resistant MCF-7 Cells through Modulating PI3K/Akt, MAPK and Wnt Signaling Pathways. *Biology (Basel),* 9.

OZKOK, A., RAVICHANDRAN, K., WANG, Q., LJUBANOVIC, D. & EDELSTEIN, C. L. 2016. NF-κB transcriptional inhibition ameliorates cisplatin-induced acute kidney injury (AKI). *Toxicology Letters,* 240**,** 105-113.

PAECH, F., ABEGG, V., DUTHALER, U., TERRACCIANO, L., BOUITBIR, J. & KRAHENBUHL, S. 2018. Sunitinib induces hepatocyte mitochondrial damage and apoptosis in mice. *Toxicology,* 409**,** 13-23.

PALAZZO, A., CICCARESE, C., IACOVELLI, R., CANNIZZARO, M. C., STEFANI, A., SALVATORE, L., BRIA, E. & TORTORA, G. 2023. Major adverse cardiac events and cardiovascular toxicity with PARP inhibitors-based therapy for solid tumors: a systematic review and safety meta-analysis. *ESMO Open,* 8**,** 101154.

PALMER, R. M. J., ASHTON, D. S. & MONCADA, S. 1988. Vascular endothelial cells synthesize nitric oxide from L-arginine. *Nature,* 333**,** 664.

PAN, S. 2009. Molecular Mechanisms Responsible for the Atheroprotective Effects of Laminar Shear Stress. *Antioxidants & Redox Signaling,* 11**,** 1669-1682.

PAPA, S., BUBICI, C., ZAZZERONI, F., PHAM, C. G., KUNTZEN, C., KNABB, J. R., DEAN, K. & FRANZOSO, G. 2006. The NF-κB-mediated control of the JNK cascade in the antagonism of programmed cell death in health and disease. *Cell Death & Differentiation,* 13**,** 712-729.

PARK, H., IQBAL, S., HERNANDEZ, P., MORA, R., ZHENG, K., FENG, Y. & LOGRASSO, P. 2015. Structural Basis and Biological Consequences for JNK2/3 Isoform Selective Aminopyrazoles. *Scientific Reports,* 5**,** 8047.

PAUL, A., EDWARDS, J., PEPPER, C. & MACKAY, S. 2018. Inhibitory-κB Kinase (IKK) α and Nuclear Factor-κB (NFκB)-Inducing Kinase (NIK) as Anti-Cancer Drug Targets. *Cells,* 7**,** 176.

PENG, V., SUCHOWERSKA, N., ESTEVES, A. D. S., ROGERS, L., CLARIDGE MACKONIS, E., TOOHEY, J. & MCKENZIE, D. R. 2018. Models for the bystander effect in gradient radiation fields: Range and signalling type. *Journal of theoretical biology.,* 455**,** 16-25.

PICCO, V. & PAGES, G. 2013. Linking JNK Activity to the DNA Damage Response. *Genes & Cancer,* 4**,** 360-368.

PLANA, J., GALDERISI, M., BARAC, A., EWER, M., KY, B., SCHERRER-CROSBIE, M., GANAME, J., SEBAG, I., AGLER, D., BADANO, L., BANCHS, J., CARDINALE, D., CARVER, J., CERQUEIRA, M., DECARA, J., EDVARDSEN, T., FLAMM, S., FORCE, T., GRIFFIN, B., JERUSALEM, G., LIU, J., MAGALHAES, A., MARWICK, T., SANCHEZ, L., SICARI, R., VILLARRAGA, H. & LANCELLOTTI, P. 2014. Expert consensus for multimodality imaging evaluation of adult patients during and after cancer therapy: a report from the American Society of Echocardiography and the European Association of Cardiovascular Imaging. *Journal of the American Society of Echocardiography,* 27**,** 911-939.

QI, X., YANG, M., MA, L., SAUER, M., AVELLA, D., KAIFI, J. T., BRYAN, J., CHENG, K., STAVELEY-O'CARROLL, K. F., KIMCHI, E. T. & LI, G. 2020. Synergizing sunitinib and radiofrequency ablation to treat hepatocellular cancer by triggering the antitumor immune response. *Journal for ImmunoTherapy of Cancer,* 8**,** e001038.

QIAO, X.-R., WANG, L., LIU, M., TIAN, Y. & CHEN, T. 2020. MiR-210-3p attenuates lipid accumulation and inflammation in atherosclerosis by repressing IGF2. *Bioscience, Biotechnology, and Biochemistry,* 84**,** 321-329.

RAITOHARJU, E., LYYTIKAINEN, L., LEVULA, M., OKSALA, N., MENNANDER, A., TARKKA, M., KLOPP, N., ILLIG, T., KAHONEN, M., KARHUNEN, P., LAAKSONEN, R. & LEHTIMAKI, T. 2011. miR-21, miR-210, miR-34a, and miR-146a/b are up-regulated in human atherosclerotic plaques in the Tampere Vascular Study. *Atherosclerosis,* 219**,** 211-217.

RAJA, W., MIR, M. H., DAR, I., BANDAY, M. A. & AHMAD, I. 2013. Cisplatin induced paroxysmal supraventricular tachycardia. *Indian J Med Paediatr Oncol,* 34**,** 330-2.

RAJENDRAN, P., RENGARAJAN, T., THANGAVEL, J., NISHIGAKI, Y., SAKTHISEKARAN, D., SETHI, G. & NISHIGAKI, I. 2013. The Vascular Endothelium and Human Diseases. *International Journal of Biological Sciences,* 9**,** 1057-1069.

RAMER, R., SCHMIED, T., WAGNER, C., HAUSTEIN, M. & HINZ, B. 2018. The antiangiogenic action of cisplatin on endothelial cells is mediated through the release of tissue inhibitor of matrix metalloproteinases-1 from lung cancer cells. *Oncotarget,* 9.

RAMKUMAR, S., RAGHUNATH, A. & RAGHUNATH, S. 2016. Statin Therapy: Review of Safety and Potential Side Effects.

RAY, A., CH. MAHARANA, K., MEENAKSHI, S. & SINGH, S. 2023. Endothelial dysfunction and its relation in different disorders: Recent update. *Health Sciences Review,* 7**,** 100084.

RAYAMAJHI, M., ZHANG, Y. & MIAO, E. A. 2013. Detection of Pyroptosis by Measuring Released Lactate Dehydrogenase Activity. Humana Press.

RICCI, R., SUMARA, G., SUMARA, I., ROZENBERG, I., KURRER, M., AKHMEDOV, A., HERSBERGER, M., ERIKSSON, U., EBERLI, F. R., BECHER, B., BORÉN, J., CHEN, M., CYBULSKY, M. I., MOORE, K. J., FREEMAN, M. W., WAGNER, E. F., MATTER, C. M. & LÜSCHER, T. F. 2004. Requirement of JNK2 for Scavenger Receptor A: Mediated Foam Cell Formation in Atherogenesis. *Science,* 306**,** 1558-1561.

ROMBOUTS, C., AERTS, A., BECK, M., DE VOS, W. H., VAN OOSTVELDT, P., BENOTMANE, M. A. & BAATOUT, S. 2013. Differential response to acute low dose radiation in primary and immortalized endothelial cells. *International Journal of Radiation Biology,* 89**,** 841-850.

ROSKOSKI, R. 2007. Sunitinib: A VEGF and PDGF receptor protein kinase and angiogenesis inhibitor. *Biochemical and biophysical research communications.,* 356**,** 323-328.

RUBANYI, G. M. & VANHOUTTE, P. M. 1986. Superoxide anions and hyperoxia inactivate endothelium-derived relaxing factor. *American Journal of Physiology-Heart and Circulatory Physiology,* 250**,** H822-H827.

RUGGERI, C., GIOFFRE, S., CHIESA, M., BUZZETTI, M., MILANO, G., SCOPECE, A., CASTIGLIONI, L., PONTREMOLI, M., SIRONI, L., POMPILIO, G., COLOMBO, G. & D'ALESSANDRA, Y. 2018. A Specific Circulating MicroRNA Cluster Is

Associated to Late Differential Cardiac Response to Doxorubicin-Induced Cardiotoxicity In Vivo. *Disease Markers*.

RYAN, S.-L., BEARD, S., BARR, M. P., UMEZAWA, K., HEAVEY, S., GODWIN, P., GRAY, S. G., CORMICAN, D., FINN, S. P., GATELY, K. A., DAVIES, A. M., THOMPSON, E. W., RICHARD, D. J., O'BYRNE, K. J., ADAMS, M. N. & BAIRD, A.-M. 2019. Targeting NF-κB-mediated inflammatory pathways in cisplatin-resistant NSCLC. *Lung Cancer,* 135**,** 217-227.

SAAD, S. Y., NAJJAR, T. A. & ALASHARI, M. 2004. Role of non-selective adenosine receptor blockade and phosphodiesterase inhibition in cisplatin-induced nephrogonadal toxicity in rats. *Clinical and Experimental Pharmacology and Physiology,* 31**,** 862-867.

SABAPATHY, K., HOCHEDLINGER, K., NAM, S., BAUER, A., KARIN, M. & WAGNER, E. 2004. Distinct roles for JNK1 and JNK2 in regulating JNK activity and c-Jun-dependent cell proliferation. *Molecular Cell,* 15**,** 713-725.

SÁNCHEZ-PÉREZ, I., MARTÍNEZ-GOMARIZ, M., WILLIAMS, D., KEYSE, S. M. & PERONA, R. 2000. CL100/MKP-1 modulates JNK activation and apoptosis in response to cisplatin. *Oncogene,* 19**,** 5142-5152.

SÁNCHEZ-PEREZ, I., MURGUÍA, J. R. & PERONA, R. 1998. Cisplatin induces a persistent activation of JNK that is related to cell death. *Oncogene,* 16**,** 533-540.

SARKER, K. P., BISWAS, K. K., YAMAKUCHI, M., LEE, K.-Y., HAHIGUCHI, T., KRACHT, M., KITAJIMA, I. & MARUYAMA, I. 2003. ASK1-p38 MAPK/JNK signaling cascade mediates anandamide-induced PC12 cell death. 85**,** 50-61.

SAVITSKY, K., BAR-SHIRA, A., GILAD, S., ROTMAN, G., ZIV, Y., VANAGAITE, L., TAGLE, D., SMITH, S., UZIEL, T., SFEZ, S. & ET, A. 1995. A single ataxia telangiectasia gene with a product similar to PI-3 kinase. *Science,* 268**,** 1749-1753.

SAWYER, D., PENG, X., CHEN, B., PENTASSUGLIA, L. & LIM, C. 2010. Mechanisms of Anthracycline Cardiac Injury: Can We Identify Strategies for Cardioprotection? *Progress in Cardiovascular Diseases,* 53**,** 105-113.

SCHOCH, H. J. 2002. Hypoxia-induced vascular endothelial growth factor expression causes vascular leakage in the brain. *Brain,* 125**,** 2549-2557.

SCIOLI, M. G., STORTI, G., D'AMICO, F., RODRÍGUEZ GUZMÁN, R., CENTOFANTI, F., DOLDO, E., CÉSPEDES MIRANDA, E. M. & ORLANDI, A. 2020. Oxidative Stress and New Pathogenetic Mechanisms in Endothelial Dysfunction: Potential Diagnostic Biomarkers and Therapeutic Targets. *Journal of Clinical Medicine,* 9**,** 1995.

SEKIJIMA, T., TANABE, A., MARUOKA, R., FUJISHIRO, N., YU, S., FUJIWARA, S., YUGUCHI, H., YAMASHITA, Y., TERAI, Y. & OHMICHI, M. 2011. Impact of platinum-based chemotherapy on the progression of atherosclerosis. *Climacteric,* 14**,** 31-40.

SETERNES, O. M., KIDGER, A. M. & KEYSE, S. M. 2019. Dual-specificity MAP kinase phosphatases in health and disease. *Biochim Biophys Acta Mol Cell Res,* 1866**,** 124-143.

SHAH, R. R., MORGANROTH, J. & SHAH, D. R. 2013. Cardiovascular Safety of Tyrosine Kinase Inhibitors: With a Special Focus on Cardiac Repolarisation (QT Interval). *Drug Safety,* 36**,** 295-316.

SHEIBANI, M., AZIZI, Y., SHAYAN, M., NEZAMOLESLAMI, S., ESLAMI, F., FARJOO, M. H. & DEHPOUR, A. R. 2022. Doxorubicin-Induced Cardiotoxicity: An Overview on Pre-clinical Therapeutic Approaches. *Cardiovascular Toxicology,* 22**,** 292-310.

SHEN, H., PEREZ, R. E., DAVAADELGER, B. & MAKI, C. G. 2013. Two 4N Cell-Cycle Arrests Contribute to Cisplatin-Resistance. *PLoS ONE,* 8**,** e59848.

SHEN, X., WANG, H., WENG, C., JIANG, H. & CHEN, J. 2021. Caspase 3/GSDME-dependent pyroptosis contributes to chemotherapy drug-induced nephrotoxicity. *Cell Death & Disease,* 12.

SHI, S., CHEN, Y., LUO, Z., NIE, G. & DAI, Y. 2023. Role of oxidative stress and inflammation-related signaling pathways in doxorubicin-induced cardiomyopathy. *Cell Communication and Signaling,* 21**,** 61.

SHI, Y., NIKULENKOV, F., ZAWACKA-PANKAU, J., LI, H., GABDOULLINE, R., XU, J., ERIKSSON, S., HEDSTRÖM, E., ISSAEVA, N., KEL, A., ARNÉR, E. S. J. & SELIVANOVA, G. 2014. ROS-dependent activation of JNK converts p53 into an efficient inhibitor of oncogenes leading to robust apoptosis. *Cell Death & Differentiation,* 21**,** 612-623.

SHILOH, Y. 2003. ATM and related protein kinases: safeguarding genome integrity. *Nature Reviews Cancer,* 3**,** 155-168.

SHIN, C. & CHOI, D.-S. 2019. Essential Roles for the Non-Canonical IκB Kinases in Linking Inflammation to Cancer, Obesity, and Diabetes. *Cells,* 8**,** 178.

SHIN, H.-J., KWON, H.-K., LEE, J.-H., GUI, X., ACHEK, A., KIM, J.-H. & CHOI, S. 2015. Doxorubicin-induced necrosis is mediated by poly-(ADP-ribose) polymerase 1 (PARP1) but is independent of p53. *Scientific Reports,* 5**,** 15798.

SHINLAPAWITTAYATORN, K., CHATTIPAKORN, S. C. & CHATTIPAKORN, N. 2022. The effects of doxorubicin on cardiac calcium homeostasis and contractile function. *Journal of Cardiology,* 80**,** 125-132.

SHYAM SUNDER, S., SHARMA, U. C. & POKHAREL, S. 2023. Adverse effects of tyrosine kinase inhibitors in cancer therapy: pathophysiology, mechanisms and clinical management. *Signal Transduction and Targeted Therapy,* 8**,** 262.

SIARAVAS, K. C., KATSOURAS, C. S. & SIOKA, C. 2023. Radiation Treatment Mechanisms of Cardiotoxicity: A Systematic Review. *Int J Mol Sci,* 24.

SIEGEL, R., MILLER, K. & JEMAL, A. 2019. Cancer statistics, 2019. *Ca-a Cancer Journal For Clinicians,* 69**,** 7-34.

SINGH, M., CHAUDHRY, P., FABI, F. & ASSELIN, E. 2013. Cisplatin-induced caspase activation mediates PTEN cleavage in ovarian cancer cells: a potential mechanism of chemoresistance. *BMC Cancer,* 13**,** 233.

SIVEEN, K. S., PRABHU, K. S., ACHKAR, I. W., KUTTIKRISHNAN, S., SHYAM, S., KHAN, A. Q., MERHI, M., DERMIME, S. & UDDIN, S. 2018. Role of Non Receptor Tyrosine Kinases in Hematological Malignances and its Targeting by Natural Products. *Molecular Cancer,* 17.

SLOSS, C. M., CADALBERT, L., FINN, S. G., FULLER, S. J. & PLEVIN, R. 2005. Disruption of two putative nuclear localization sequences is required for cytosolic localization of mitogen-activated protein kinase phosphatase-2. *Cellular signalling.,* 17**,** 709-716.

SONG, J. J. & LEE, Y. J. 2007. Differential activation of the JNK signal pathway by UV irradiation and glucose deprivation. *Cell Signal,* 19**,** 563-572.

SONOWAL, H., PAL, P., SHUKLA, K., SAXENA, A., SRIVASTAVA, S. K. & RAMANA, K. V. 2018. Aldose reductase inhibitor, fidarestat prevents doxorubicin-induced endothelial cell death and dysfunction. *Biochemical Pharmacology,* 150**,** 181-190.

SPALLAROSSA, P., ALTIERI, P., BARISIONE, C., PASSALACQUA, M., ALOI, C., FUGAZZA, G., FRASSONI, F., PODESTA, M., CANEPA, M., GHIGLIOTTI, G. & BRUNELLI, C. 2010. p38 MAPK and JNK Antagonistically Control Senescence and Cytoplasmic p16INK4A Expression in Doxorubicin-Treated Endothelial Progenitor Cells. *Plos One,* 5.

STEBBINS, J. L., DE, S. K., MACHLEIDT, T., BECATTINI, B., VAZQUEZ, J., KUNTZEN, C., CHEN, L. H., CELLITTI, J. F., RIEL-MEHAN, M., EMDADI, A., SOLINAS, G., KARIN, M. & PELLECCHIA, M. 2008. Identification of a new JNK inhibitor targeting the JNK-JIP interaction site. 105**,** 16809-16813.

STÉEN, E. J. L., EDEM, P. E., NØRREGAARD, K., JØRGENSEN, J. T., SHALGUNOV, V., KJAER, A. & HERTH, M. M. 2018. Pretargeting in nuclear imaging and radionuclide therapy: Improving efficacy of theranostics and nanomedicines. *Biomaterials,* 179**,** 209-245.

STEINHERZ, L. J. 1991. Cardiac Toxicity 4 to 20 Years After Completing Anthracycline Therapy. *JAMA: The Journal of the American Medical Association,* 266**,** 1672.

STEWART, F., SEEMANN, I., HOVING, S. & RUSSELL, N. 2013. Understanding Radiation-induced Cardiovascular Damage and Strategies for Intervention. *Clinical Oncology,* 25**,** 617-624.

STRASSER, A. & VAUX, D. L. 2020. Cell Death in the Origin and Treatment of Cancer. *Molecular Cell,* 78**,** 1045-1054.

STULPINAS, A., TENKUTYTĖ, M., IMBRASAITĖ, A. & KALVELYTĖ, A. V. 2024. The Role and Efficacy of JNK Inhibition in Inducing Lung Cancer Cell Death Depend on the Concentration of Cisplatin. *ACS Omega,* 9**,** 28311-28322.

SWAIN, S. M., WHALEY, F. S. & EWER, M. S. 2003. Congestive heart failure in patients treated with doxorubicin. *Cancer,* 97**,** 2869-2879.

TAKEUCHI, K. 2004. Nitric oxide: inhibitory effects on endothelial cell calcium signaling, prostaglandin I2 production and nitric oxide synthase expression. *Cardiovascular Research,* 62**,** 194-201.

TAN, L. L. & LYON, A. R. 2018. Role of Biomarkers in Prediction of Cardiotoxicity During Cancer Treatment.

TERWOORD, J. D., BEYER, A. M. & GUTTERMAN, D. D. 2022. Endothelial dysfunction as a complication of anti-cancer therapy. *Pharmacology & therapeutics.,* 237**,** 108116.

THEODOSIOU, A. & ASHWORTH, A. 2002. *Genome Biology,* 3**,** reviews3009.1.

THIJS, A. M. J., VAN HERPEN, C. M. L., VERWEIJ, V., PERTIJS, J., VAN DEN BROEK, P. H. H., VAN DER GRAAF, W. T. A. & RONGEN, G. A. 2015. Impaired endothelium-dependent vasodilation does not initiate the development of sunitinib-associated hypertension. *Journal of Hypertension,* 33**,** 2075-2082.

THORN, C. F., OSHIRO, C., MARSH, S., HERNANDEZ-BOUSSARD, T., MCLEOD, H., KLEIN, T. E. & ALTMAN, R. B. 2011. Doxorubicin pathways. *Pharmacogenetics and Genomics,* 21**,** 440-446.

TICHY, L. & PARRY, T. L. 2023. The pathophysiology of cancer-mediated cardiac cachexia and novel treatment strategies: A narrative review. *Cancer Medicine,* 12**,** 17706-17717.

TILSED, C. M., FISHER, S. A., NOWAK, A. K., LAKE, R. A. & LESTERHUIS, W. J. 2022. Cancer chemotherapy: insights into cellular and tumor microenvironmental mechanisms of action. *Frontiers in Oncology,* 12.

TOBIUME, K., MATSUZAWA, A., TAKAHASHI, T., NISHITOH, H., MORITA, K. I., TAKEDA, K., MINOWA, O., MIYAZONO, K., NODA, T. & ICHIJO, H. 2001. ASK1 is required

for sustained activations of JNK/p38 MAP kinases and apoptosis. *EMBO reports,* 2**,** 222-228.

TOURNIER, C. 2013. The 2 Faces of JNK Signaling in Cancer. *Genes & Cancer,* 4**,** 397-400.

TOUYZ, R. M., LANG, N. N., HERRMANN, J., VAN DEN MEIRACKER, A. H. & DANSER, A. H. J. 2017. Recent Advances in Hypertension and Cardiovascular Toxicities With Vascular Endothelial Growth Factor Inhibition. *Hypertension,* 70**,** 220-226.

TRAN, N., GARCIA, T., ANIQA, M., ALI, S., ALLY, A. & NAULI, S. M. 2022. Endothelial Nitric Oxide Synthase (eNOS) and the Cardiovascular System: in Physiology and in Disease States. *Am J Biomed Sci Res,* 15**,** 153-177.

TRUITT, R., MU, A., CORBIN, E. A., VITE, A., BRANDIMARTO, J., KY, B. & MARGULIES, K. B. 2018 Increased Afterload Augments Sunitinib-Induced Cardiotoxicity in an Engineered Cardiac Microtissue Model. *JACC: Basic to Translational Science,* 3**,** 265-276.

TSVETKOVA, D. & IVANOVA, S. 2022. Application of Approved Cisplatin Derivatives in Combination Therapy against Different Cancer Diseases. *Molecules,* 27**,** 2466.

VAIDYA, J. S. 2021. Principles of cancer treatment by radiotherapy. *Surgery (Oxford),* 39**,** 193-201.

VAISHNAV, M., MACFARLANE, M. & DICKENS, M. 2011. Disassembly of the JIP1/JNK molecular scaffold by caspase-3-mediated cleavage of JIP1 during apoptosis. *EXP CELL RES,* 317**,** 1028-1039.

VALLABHAPURAPU, S. & KARIN, M. 2009. Regulation and Function of NF-κB Transcription Factors in the Immune System. *Annual Review of Immunology,* 27**,** 693-733.

VAN DEN BELT-DUSEBOUT, A., NUVER, J., DE WIT, R., GIETEMA, J., HUININK, W., RODRIGUS, P., SCHIMMEL, E., ALEMAN, B. & VAN LEEUWEN, F. 2006. Long-term risk of cardiovascular disease in 5-year survivors of testicular cancer. *Journal of Clinical Oncology,* 24**,** 467-475.

VANDE WALLE, L. & LAMKANFI, M. 2016. Pyroptosis. *Current Biology,* 26**,** R568-R572.

VÁSQUEZ-VIVAR, J., MARTASEK, P., HOGG, N., MASTERS, B. S. S., PRITCHARD, K. A. & KALYANARAMAN, B. 1997. Endothelial Nitric Oxide Synthase-Dependent Superoxide Generation from Adriamycin†. *Biochemistry,* 36**,** 11293-11297.

VILLALPANDO-RODRIGUEZ, G. E. & GIBSON, S. B. 2021. Reactive Oxygen Species (ROS) Regulates Different Types of Cell Death by Acting as a Rheostat. *Oxid Med Cell Longev,* 2021**,** 9912436.

VITALE, R., MARZOCCO, S. & POPOLO, A. 2024. Role of Oxidative Stress and Inflammation in Doxorubicin-Induced Cardiotoxicity: A Brief Account. *Int J Mol Sci,* 25.

VOLKOVA, M. & RUSSELL, R. 2011. Anthracycline Cardiotoxicity: Prevalence, Pathogenesis and Treatment. *Curr Cardiol Rev,* 7**,** 214-20.

VOLKOVA, M. & RUSSELL, R. 2012. Anthracycline Cardiotoxicity: Prevalence, Pathogenesis and Treatment. *Current Cardiology Reviews,* 7**,** 214-220.

VON HAEHLING, S., EBNER, N., DOS SANTOS, M. R., SPRINGER, J. & ANKER, S. D. 2017. Muscle wasting and cachexia in heart failure: mechanisms and therapies. *Nature Reviews Cardiology,* 14**,** 323-341.

VON HOFF, D. D., LAYARD, M. W., BASA, P., DAVIS, H. L., JR., VON HOFF, A. L., ROZENCWEIG, M. & MUGGIA, F. M. 1979. Risk factors for doxorubicin-induced congestive heart failure. *Ann Intern Med,* 91**,** 710-7.

VU, M., KASSOUF, N., OFILI, R., LUND, T., BELL, C. & APPIAH, S. 2020. Doxorubicin selectively induces apoptosis through the inhibition of a novel isoform of Bcl-2 in acute myeloid leukaemia MOLM-13 cells with reduced Beclin 1 expression. *International Journal of Oncology,* 57**,** 113-121.

WAGNER, E. F. & NEBREDA, A. R. 2009. Signal integration by JNK and p38 MAPK pathways in cancer development. *Nature reviews. Cancer,* 9**,** 537-549.

WANG, D., XIAO, F., FENG, Z., LI, M., KONG, L., HUANG, L., WEI, Y. G., LI, H., LIU, F., ZHANG, H. & ZHANG, W. 2020. Sunitinib facilitates metastatic breast cancer

spreading by inducing endothelial cell senescence. *Breast Cancer Research,* 22.

WANG, H., SHEEHAN, R. P., PALMER, A. C., EVERLEY, R. A., BOSWELL, S. A., RON-HAREL, N., RINGEL, A. E., HOLTON, K. M., JACOBSON, C. A., ERICKSON, A. R., MALISZEWSKI, L., HAIGIS, M. C. & SORGER, P. K. 2019. Adaptation of human iPSC-derived cardiomyocytes to tyrosine kinase inhibitors reduces acute cardiotoxicity via metabolic reprogramming. *bioRxiv*.

WANG, H., WANG, Y., LI, J., HE, Z., BOSWELL, S. A., CHUNG, M., YOU, F. & HAN, S. 2023. Three tyrosine kinase inhibitors cause cardiotoxicity by inducing endoplasmic reticulum stress and inflammation in cardiomyocytes. *BMC Medicine,* 21**,** 147.

WANG, H., YANG, Y., SHEN, H., GU, J., LI, T. & LI, X. 2012. ABT-737 Induces Bim Expression via JNK Signaling Pathway and Its Effect on the Radiation Sensitivity of HeLa Cells. *Plos One,* 7.

WANG, J. & XIA, Y. 2012. Assessing developmental roles of MKK4 and MKK7 in vitro. *Commun Integr Biol,* 5**,** 319-24.

WANG, P.-N., HUANG, J., DUAN, Y.-H., ZHOU, J.-M., HUANG, P.-Z., FAN, X.-J., HUANG, Y., WANG, L., LIU, H.-L., WANG, J.-P. & HUANG, M.-J. 2017a. Downregulation of phosphorylated MKK4 is associated with a poor prognosis in colorectal cancer patients. *Oncotarget,* 8**,** 34352-34361.

WANG, Q., CHEN, Y., CHANG, H., HU, T., WANG, J., XIE, Y. & CHENG, J. 2021. The Role and Mechanism of ATM-Mediated Autophagy in the Transition From Hyper-Radiosensitivity to Induced Radioresistance in Lung Cancer Under Low-Dose Radiation. *Front Cell Dev Biol,* 9**,** 650819.

WANG, S., KONOREV, E., KOTAMRAJU, S., JOSEPH, J., KALIVENDI, S. & KALYANARAMAN, B. 2004. Doxorubicin induces apoptosis in normal and tumor cells via distinctly different mechanisms - Intermediacy of H2O2- and p53-dependent pathways. *Journal of Biological Chemistry,* 279**,** 25535-25543.

WANG, S., KOTAMRAJU, S., KONOREV, E., KALIVENDI, S., JOSEPH, J. & KALYANARAMAN, B. 2002. Activation of nuclear factor-κB during doxorubicin-induced apoptosis in endothelial cells and myocytes is pro-apoptotic: the role of hydrogen peroxide. *Biochemical Journal,* 367**,** 729-740.

WANG, Y., GAO, W., SHI, X., DING, J., LIU, W., HE, H., WANG, K. & SHAO, F. 2017b. Chemotherapy drugs induce pyroptosis through caspase-3 cleavage of a gasdermin. *Nature,* 547**,** 99-103.

WANG, Y., JI, H.-X., XING, S.-H., PEI, D.-S. & GUAN, Q.-H. 2007. SP600125, a selective JNK inhibitor, protects ischemic renal injury via suppressing the extrinsic pathways of apoptosis. *Life Sci,* 80**,** 2067-2075.

WANG, Z., WANG, M., KAR, S. & CARR, B. I. 2009. Involvement of ATM-mediated Chk1/2 and JNK kinase signaling activation in HKH40A-induced cell growth inhibition. *Journal of Cellular Physiology,* 221**,** 213-220.

WATANABE, H., KUHNE, W., SPAHR, R., SCHWARTZ, P. & PIPER, H. 1991. Macromolecule Permeability of Coronary and Aortic Endothelial Monolayers Under Energy Depletion. *American Journal of Physiology,* 260**,** H1344-H1352.

WIGGS, M. P., BEAUDRY, A. G. & LAW, M. L. 2022. Cardiac Remodeling in Cancer-Induced Cachexia: Functional, Structural, and Metabolic Contributors. *Cells,* 11**,** 1931.

WILKINSON, E. L., SIDAWAY, J. E. & CROSS, M. J. 2018. Statin regulated ERK5 stimulates tight junction formation and reduces permeability in human cardiac endothelial cells. *J Cell Physiol,* 233**,** 186-200.

WILLOUGHBY, E. A. 2003. The JNK-interacting Protein-1 Scaffold Protein Targets MAPK Phosphatase-7 to Dephosphorylate JNK. 278**,** 10731-10736.

WILTSHIRE, C., MATSUSHITA, M., TSUKADA, S., GILLESPIE, D. A. F. & MAY, G. H. W. 2002. A new c-Jun N-terminal kinase (JNK)-interacting protein, Sab (SH3BP5), associates with mitochondria. *Biochemical Journal,* 367**,** 577-585.

WIN, S., THAN, T. & KAPLOWITZ, N. 2018. The Regulation of JNK Signaling Pathways in Cell Death through the Interplay with Mitochondrial SAB and Upstream

Post-Translational Effects. *International Journal of Molecular Sciences,* 19**,** 3657.

WIN, S., THAN, T. A., MIN, R. W. M., AGHAJAN, M. & KAPLOWITZ, N. 2016. c-Jun N-terminal kinase mediates mouse liver injury through a novel Sab (SH3BP5)-dependent pathway leading to inactivation of intramitochondrial Src. *Hepatology,* 63**,** 1987-2003.

WOJCIK, T., BUCZEK, E., MAJZNER, K., KOLODZIEJCZYK, A., MISZCZYK, J., KACZARA, P., KWIATEK, W., BARANSKA, M., SZYMONSKI, M. & CHLOPICKI, S. 2015. Comparative endothelial profiling of doxorubicin and daunorubicin in cultured endothelial cells. *Toxicology in Vitro,* 29**,** 512-521.

WOLF, M. B. & BAYNES, J. W. 2006. The anti-cancer drug, doxorubicin, causes oxidant stress-induced endothelial dysfunction. *Biochim Biophys Acta,* 1760**,** 267-71.

WONG, C. H., ISKANDAR, K. B., YADAV, S. K., HIRPARA, J. L., LOH, T. & PERVAIZ, S. 2010. Simultaneous Induction of Non-Canonical Autophagy and Apoptosis in Cancer Cells by ROS-Dependent ERK and JNK Activation. *PLoS ONE,* 5**,** e9996.

WOOD, R. A., BARBOUR, M. J., GOULD, G. W., CUNNINGHAM, M. R. & PLEVIN, R. J. 2018. Conflicting evidence for the role of JNK as a target in breast cancer cell proliferation: Comparisons between pharmacological inhibition and selective shRNA knockdown approaches. *Pharmacology Research & Perspectives,* 6**,** e00376.

WU, J., GAO, L., FAN, H., LIU, D., LIN, M., ZHU, M., DENG, T. & SONG, Y. 2022a. Calcium Overload or Underload? The Effects of Doxorubicin on the Calcium Dynamics in Guinea Pig Hearts. *Biomedicines,* 10.

WU, Q., WU, W., FU, B., SHI, L., WANG, X. & KUCA, K. 2019. JNK signaling in cancer cell survival. *Medicinal Research Reviews,* 39**,** 2082-2104.

WU, Q., WU, W., JACEVIC, V., FRANCA, T. C. C., WANG, X. & KUCA, K. 2020. Selective inhibitors for JNK signalling: a potential targeted therapy in cancer. *J Enzyme Inhib Med Chem,* 35**,** 574-583.

WU, Y., ZHANG, J., YU, S., LI, Y., ZHU, J., ZHANG, K. & ZHANG, R. 2022b. Cell pyroptosis in health and inflammatory diseases. *Cell Death Discov,* 8**,** 191-191.

WULLAERT, A., HEYNINCK, K. & BEYAERT, R. 2006. Mechanisms of crosstalk between TNF-induced NF-κB and JNK activation in hepatocytes. *Biochemical pharmacology,* 72**,** 1090-1101.

XIA, P., ZHANG, F., YUAN, Y., CHEN, C., HUANG, Y., LI, L., WANG, E., GUO, Q. & YE, Z. 2020. ALDH 2 conferred neuroprotection on cerebral ischemic injury by alleviating mitochondria-related apoptosis through JNK/caspase-3 signing pathway. *International Journal of Biological Sciences,* 16**,** 1303-1323.

XU, H., JIANG, S., YU, C., YUAN, Z. & SUN, L. 2022a. GSDMEa-mediated pyroptosis is bi-directionally regulated by caspase and required for effective bacterial clearance in teleost. *Cell Death & Disease,* 13**,** 491.

XU, J., QIN, X., CAI, X., YANG, L., XING, Y., LI, J., ZHANG, L., TANG, Y., LIU, J., ZHANG, X. & GAO, F. 2015. Mitochondrial JNK activation triggers autophagy and apoptosis and aggravates myocardial injury following ischemia/reperfusion. *Biochimica Et Biophysica Acta-Molecular Basis of Disease,* 1852**,** 262-270.

XU, Z., JIN, Y., GAO, Z., ZENG, Y., DU, J., YAN, H., CHEN, X., PING, L., LIN, N., YANG, B., HE, Q. & LUO, P. 2022b. Autophagic degradation of CCN2 (cellular communication network factor 2) causes cardiotoxicity of sunitinib. *Autophagy,* 18**,** 1152-1173.

YAN, D., AN, G. & KUO, M. T. 2016. C-Jun N-terminal kinase signalling pathway in response to cisplatin. *Journal of Cellular and Molecular Medicine,* 20**,** 2013-2019.

YAN, H., HE, L., LV, D., YANG, J. & YUAN, Z. 2024. The Role of the Dysregulated JNK Signaling Pathway in the Pathogenesis of Human Diseases and Its Potential Therapeutic Strategies: A Comprehensive Review. *Biomolecules,* 14.

YANG, D. D., KUAN, C.-Y., WHITMARSH, A. J., RINÓCN, M., ZHENG, T. S., DAVIS, R. J., RAKIC, P. & FLAVELL, R. A. 1997. Absence of excitotoxicity-induced apoptosis in the hippocampus of mice lacking the Jnk3 gene. *Nature,* 389**,** 865-870.

YANG, Z., SCHUMAKER, L., EGORIN, M., ZUHOWSKI, E., GUO, Z. & CULLEN, K. 2006. Cisplatin preferentially binds mitochondrial DNA and voltage-dependent anion channel protein in the mitochondrial membrane of head and neck squamous cell carcinoma: Possible role in apoptosis. *Clinical Cancer Research,* 12**,** 5817-5825.

YAU, J. W., TEOH, H. & VERMA, S. 2015. Endothelial cell control of thrombosis. *BMC Cardiovascular Disorders,* 15.

YAVAŞ, Ö., AYTEMIR, K. & CELIK, I. 2008. The prevalence of silent arrhythmia in patients receiving cisplatin-based chemotherapy. *Turkish Journal of Cancer,* 38**,** 12-15.

YEH, E. T. H. & BICKFORD, C. L. 2009. Cardiovascular Complications of Cancer Therapy. *Journal of the American College of Cardiology,* 53**,** 2231-2247.

YEN, H. C., OBERLEY, T. D., VICHITBANDHA, S., HO, Y. S. & ST CLAIR, D. K. 1996. The protective role of manganese superoxide dismutase against adriamycin-induced acute cardiac toxicity in transgenic mice. *Journal of Clinical Investigation,* 98**,** 1253-1260.

YIN, X., TIAN, W., WANG, L., WANG, J., ZHANG, S., CAO, J. & YANG, H. 2015. Radiation quality-dependence of bystander effect in unirradiated fibroblasts is associated with TGF-beta 1-Smad2 pathway and miR-21 in irradiated keratinocytes. *Scientific Reports,* 5.

YOSHIDA, M., SHIOJIMA, I., IKEDA, H. & KOMURO, I. 2009. Chronic doxorubicin cardiotoxicity is mediated by oxidative DNA damage-ATM-p53-apoptosis pathway and attenuated by pitavastatin through the inhibition of Rac1 activity. *J Mol Cell Cardiol,* 47**,** 698-705.

YOUSEF, M., SAAD, A. & EL-SHENNAWY, L. 2009. Protective effect of grape seed proanthocyanidin extract against oxidative stress induced by cisplatin in rats. *Food and Chemical Toxicology,* 47**,** 1176-1183.

YU, H., LIN, L., ZHANG, Z., ZHANG, H. & HU, H. 2020. Targeting NF-κB pathway for the therapy of diseases: mechanism and clinical study. *Signal Transduction and Targeted Therapy,* 5.

YU, H., WU, C.-L., WANG, X., BAN, Q., QUAN, C., LIU, M., DONG, H., LI, J., KIM, G.-Y., CHOI, Y. H., WANG, Z. & JIN, C.-Y. 2019a. SP600125 enhances C-2-induced cell death by the switch from autophagy to apoptosis in bladder cancer cells. *Journal of Experimental & Clinical Cancer Research,* 38.

YU, J., LI, S., QI, J., CHEN, Z., WU, Y., GUO, J., WANG, K., SUN, X. & ZHENG, J. 2019b. Cleavage of GSDME by caspase-3 determines lobaplatin-induced pyroptosis in colon cancer cells. *Cell Death & Disease,* 10.

YU, J., LI, S., QI, J., CHEN, Z., WU, Y., GUO, J., WANG, K., SUN, X. & ZHENG, J. 2019c. Cleavage of GSDME by caspase-3 determines lobaplatin-induced pyroptosis in colon cancer cells. *Cell Death Dis,* 10**,** 193.

YU, Y., GUO, Y., TIAN, Q., LAN, Y., YEH, H., ZHANG, M., TASAN, I., JAIN, S. & ZHAO, H. 2019d. An efficient gene knock-in strategy using 5'-modified double-stranded DNA donors with short homology arms. *Nature Chemical Biology*.

YU, Z., XU, C., SONG, B., ZHANG, S., CHEN, C., LI, C. & ZHANG, S. 2023. Tissue fibrosis induced by radiotherapy: current understanding of the molecular mechanisms, diagnosis and therapeutic advances. *Journal of Translational Medicine,* 21**,** 708.

ZEISSIG, M. N., HEWETT, D. R., MROZIK, K. M., PANAGOPOULOS, V., WALLINGTON-GATES, C. T., SPENCER, A., DOLD, S. M., ENGELHARDT, M., VANDYKE, K. & ZANNETTINO, A. C. W. 2024. Expression of the chemokine receptor CCR1 decreases sensitivity to bortezomib in multiple myeloma cell lines. *Leuk Res,* 139**,** 107469.

ZHAN, H., AIZAWA, K., SUN, J., TOMIDA, S., OTSU, K., CONWAY, S. J., MCKINNON, P. J., MANABE, I., KOMURO, I., MIYAGAWA, K., NAGAI, R. & SUZUKI, T. 2016. Ataxia telangiectasia mutated in cardiac fibroblasts regulates doxorubicin-induced cardiotoxicity. *Cardiovascular Research,* 110**,** 85-95.

ZHANG, C.-C., LI, C.-G., WANG, Y.-F., XU, L.-H., HE, X.-H., ZENG, Q.-Z., ZENG, C.-Y., MAI, F.-Y., HU, B. & OUYANG, D.-Y. 2019a. Chemotherapeutic paclitaxel and cisplatin differentially induce pyroptosis in A549 lung cancer cells via caspase-3/GSDME activation. *Apoptosis,* 24**,** 312-325.

ZHANG, J., GUO, L., ZHOU, X., DONG, F., LI, L., CHENG, Z., XU, Y., LIANG, J., XIE, Q. & LIU, J. 2016. Dihydroartemisinin induces endothelial cell anoikis through the activation of the JNK signaling pathway. *Oncol Lett,* 12**,** 1896-1900.

ZHANG, N. & ZHANG, S. W. 2019. Long-term effects of radiation prior to surgery and chemotherapy on survival of esophageal cancer undergoing surgery. *Medicine (Baltimore),* 98**,** e17617.

ZHANG, S., LIU, X., BAWA-KHALFE, T., LU, L., LYU, Y., LIU, L. & YEH, E. 2012a. Identification of the molecular basis of doxorubicin-induced cardiotoxicity. *Nature Medicine,* 18**,** 1639-+.

ZHANG, T., INESTA-VAQUERA, F., NIEPEL, M., ZHANG, J., FICARRO, SCOTT B., MACHLEIDT, T., XIE, T., MARTO, JARROD A., KIM, N., SIM, T., LAUGHLIN, JOHN D., PARK, H., LOGRASSO, PHILIP V., PATRICELLI, M., NOMANBHOY, TYZOON K., SORGER, PETER K., ALESSI, DARIO R. & GRAY, NATHANAEL S. 2012b. Discovery of Potent and Selective Covalent Inhibitors of JNK. *Chemistry & Biology,* 19**,** 140-154.

ZHANG, Y.-J., HUANG, H., LIU, Y., KONG, B. & WANG, G. 2019b. MD-1 Deficiency Accelerates Myocardial Inflammation and Apoptosis in Doxorubicin-Induced Cardiotoxicity by Activating the TLR4/MAPKs/Nuclear Factor kappa B (NF-κB) Signaling Pathway. *Medical Science Monitor,* 25**,** 7898-7907.

ZHANG, Y., LIU, X., BAI, X., LIN, Y., LI, Z., FU, J., LI, M., ZHAO, T., YANG, H., XU, R., LI, J., JU, J., CAI, B., XU, C. & YANG, B. 2018. Melatonin prevents endothelial cell pyroptosis via regulation of long noncoding RNA MEG3/miR-223/NLRP3 axis. *Journal of Pineal Research,* 64**,** e12449.

ZHANG, Z., ZHANG, H., LI, D., ZHOU, X., QIN, Q. & ZHANG, Q. 2021. Caspase-3-mediated GSDME induced Pyroptosis in breast cancer cells through the ROS/JNK signalling pathway. *Journal of Cellular and Molecular Medicine,* 25**,** 8159-8168.

ZHAO, S., GAO, N., QI, H., CHI, H., LIU, B., HE, B., WANG, J., JIN, Z., HE, X., ZHENG, H., WANG, Z., WANG, X. & JIN, G. 2019. Suppressive effects of sunitinib on a TLR

activation-induced cytokine storm. *European Journal of Pharmacology,* 854**,** 347-353.

ZHAOLIN, Z., GUOHUA, L., SHIYUAN, W. & ZUO, W. 2019. Role of pyroptosis in cardiovascular disease. *Cell Proliferation,* 52**,** e12563.

ZHENG, H., XU, N., ZHANG, Z., WANG, F., XIAO, J. & JI, X. 2022. Setanaxib (GKT137831) Ameliorates Doxorubicin-Induced Cardiotoxicity by Inhibiting the NOX1/NOX4/Reactive Oxygen Species/MAPK Pathway. *Front Pharmacol,* 13**,** 823975.

ZHENG, X., ZHONG, T., MA, Y., WAN, X., QIN, A., YAO, B., ZOU, H., SONG, Y. & YIN, D. 2020. Bnip3 mediates doxorubicin-induced cardiomyocyte pyroptosis via caspase-3/GSDME. *Life Sci,* 242**,** 117186.

ZHOU, Q., WANG, M., DU, Y., ZHANG, W., BAI, M., ZHANG, Z., LI, Z. & MIAO, J. 2015. Inhibition of c-Jun N-terminal kinase activation reverses Alzheimer disease phenotypes in APPswe/PS1dE9 mice. *Ann Neurol,* 77**,** 637-54.

ZHOU, W., XU, Y., ZHANG, J., ZHANG, P., YAO, Z., YAN, Z., WANG, H., CHU, J., YAO, S., ZHAO, S., YANG, S., GUO, Y., MIAO, J., LIU, K., CHAN, W. C., XIA, Q. & LIU, Y. 2022. MiRNA-363-3p/DUSP10/JNK axis mediates chemoresistance by enhancing DNA damage repair in diffuse large B-cell lymphoma. *Leukemia,* 36**,** 1861-1869.

ZIEGLER, V., DEUßEN, M., SCHUMACHER, L., ROOS, W. P. & FRITZ, G. 2020. Anticancer drug and ionizing radiation-induced DNA damage differently influences transcription activity and DDR-related stress responses of an endothelial monolayer. *Biochim Biophys Acta Mol Cell Res,* 1867**,** 118678.

ZYCHLINSKY, A., PREVOST, M. C. & SANSONETTI, P. J. 1992. Shigella flexneri induces apoptosis in infected macrophages. *Nature,* 358**,** 167-169.